






Universitat Autònoma de Barcelona

## Novel tools to study aggressive prostate cancer

Valentina Maggio

**ADVERTIMENT.** L'accés als continguts d'aquesta tesi queda condicionat a l'acceptació de les condicions d'ús establertes per la següent llicència Creative Commons:  [http://cat.creativecommons.org/?page\\_id=184](http://cat.creativecommons.org/?page_id=184)

**ADVERTENCIA.** El acceso a los contenidos de esta tesis queda condicionado a la aceptación de las condiciones de uso establecidas por la siguiente licencia Creative Commons:  <http://es.creativecommons.org/blog/licencias/>

**WARNING.** The access to the contents of this doctoral thesis it is limited to the acceptance of the use conditions set by the following Creative Commons license:  <https://creativecommons.org/licenses/?lang=en>



# **Novel tools to study aggressive prostate cancer**

By **Valentina Maggio**

For the title of PhD in Biochemistry, Molecular Biology and Biomedicine  
doctorate program

Universitat Autònoma de Barcelona

This work was carried out at the Biomedical Research in Urology group under the supervision of Dr. Rosanna Paciucci, Dr. Juan Morote with the tutorship of Dr. Anna Meseguer.

Director:  
Dr. Rosanna Paciucci

Tutor:  
Dr. Anna Meseguer

Co-director:  
Dr. Juan Morote

PhD student:  
Valentina Maggio

*A tutta la mia grande famiglia,  
fatta da parenti e amici,  
ma soprattutto ad Eli.*



# Index of contents

Index of figures.....	I
Index of tables .....	III
Abbreviations .....	IV
Summary.....	VII
Resumen .....	IX
Resum .....	XI
CHAPTER 1: INTRODUCTION.....	1
1. Anatomy of the prostate .....	3
2. Prostate cancer .....	5
2.1 Natural history of prostate cancer.....	5
2.2 Molecular alterations in prostate cancer.....	6
2.3 Prostate Cancer Stem Cells .....	11
2.4 Risk factors for prostate cancer .....	12
2.5 Diagnosis of prostate cancer.....	13
2.6 Therapies for prostate cancer.....	17
3. Models to study prostate cancer.....	18
3.1 In vivo models .....	18
3.2 In vitro models.....	20
4. Prostate Tumor OVer-expressed 1 (PTOV1).....	22
CHAPTER 2: HYPOTHESIS .....	24
CHAPTER 3: AIMS OF STUDY .....	28
CHAPTER 4: MATERIALS AND METHODS.....	32
1. Cellular cultures.....	34
1.1 Cell lines.....	34
1.2 Cell culture methods and reagents.....	35

1.3 Production of lentiviruses and cellular transduction .....	35
1.4 Cells transfection .....	37
1.5 Primary prostate tumors culture .....	37
2. Functional assays .....	38
2.1 Proliferation assay .....	38
2.2 Cytotoxicity assay .....	39
2.3 Spheres formation assay .....	39
3. RNA manipulation .....	40
3.1 Total RNA extraction .....	40
3.2 RNA extraction from frozen or FFPE tissue .....	40
3.3 Real time polymerase chain reaction (RT-PCR) .....	40
3.4 Primers.....	42
3.5 RNA interference.....	42
4. DNA manipulation.....	43
4.1 Chromatin immunoprecipitation.....	43
4.2 Vectors and constructions.....	46
4.3 Preparation of competent bacteria .....	46
4.4 Bacterial transformation, growth and plasmid DNA purification .....	47
4.5 Electrophoretic mobility shift assay (EMSA) .....	48
4.6 DNA sequencing .....	49
5. Protein manipulation.....	50
5.1 Protein extraction.....	50
5.2 Determination of protein concentration.....	51
5.3 Analysis by Sodium Dodecyl Sulfate Polyacrylamide Gel Electrophoresis (SDS-PAGE) and Western blot .....	51
5.4 Analysis of protein synthesis by Surface sensing of translation (SUnSET).....	53
6. In vivo tumorigenic assays .....	54

6.1 Immunohistochemistry .....	54
7. Bioinformatics analyses of data sets .....	54
8. Statistics .....	55
<b>CHAPTER 5: ESTABLISHMENT AND CHARACTERIZATION OF <i>ex vivo</i> CULTURES DERIVED FROM PRIMARY PROSTATE TUMORS .....</b>	<b>57</b>
1. Establishment of a protocol for ex vivo tumor growth.....	59
1.1 Ex vivo radical prostatectomy derived tumor cultures .....	59
1.2 Ex vivo primary tumor cultures established from needle biopsies.....	59
2. Phenotypic characterization of ex vivo primary tumor cultures.....	64
2.1 Clinical characteristics of the patients and expression of epithelial markers .....	64
2.2 Analysis of genomic alterations: TMPRSS2-ERG fusion, SPOP, PTEN and TP53 mutations. ....	65
2.3 Derivation of androgen Independent (AI) variant ex vivo tumor cultures .....	68
3. Functional characterization of androgen dependent and independent ex vivo primary tumor cultures. ....	71
3.1 Proliferation assays.....	71
3.2 Motility assays .....	73
3.3 Analysis of the epithelial and mesenchymal genes .....	74
3.4 Drug toxicity assays .....	76
3.5 Rate of protein synthesis .....	80
3.6 Analysis of the mTORC1 pathway in resistant prostate cancer cells.....	81
3.7 Analyses of expression of self-renewal genes.....	83
3.8 In vivo assays .....	84
4. Discussion.....	85
4.1 Development and characterization of new in vitro models from primary tumors.....	85
4.2 Phenotypic characterization of the ex vivo primary tumor cultures.....	86
4.3 Characterization of the androgen independent ex vivo cultures.....	89

CHAPTER 6: CANCER STEM CELLS AS A MODEL TO STUDY AGGRESSIVE PROSTATE CANCER.....	91
1. Enrichment and characterization of CSC populations from established prostate cancer cell lines and primary tumor ex vivo cultures. ....	93
2. Prostate spheres derived cells (CSCs) as in vitro models to test new anticancer drugs .....	101
2.1 Galiellalactone (GL).....	101
2.2 Chemotherapeutic drugs: Docetaxel and Cabazitaxel .....	103
2.3 Bozepinib analogues.....	105
3. Discussion.....	109
3.1 Development of new in vitro CSCs models to study cancer resistance .....	109
3.2 Targeting prostate tumor spheres .....	110
CHAPTER 7: A NOVEL DNA-BINDING MOTIF IN PROSTATE TUMOR OVEREXPRESSED-1 (PTOV1) REQUIRED FOR THE EXPRESSION OF <i>ALDH1A1</i> AND <i>CCNG2</i> IN CANCER CELLS .....	113
1. PTOV1 induces the expression of self-renewal genes in prostate cancer cells .....	115
2. PTOV1 directly induces the expression of <i>ALDH1A1</i> and <i>CCNG2</i> in PCa cells ..	116
3. PTOV1 directly binds to <i>ALDH1A1</i> and <i>CCNG2</i> promoters through a new motif in its A domain.....	119
4. The new PTOV1 AT-hook-like motif is necessary to modulate <i>ALDH1A1</i> and <i>CCNG2</i> expression. ....	120
5. PTOV1, <i>ALDH1A1</i> and <i>CCNG2</i> expression levels are associated with aggressiveness in prostate and colon carcinomas.....	122
6. Discussion.....	125
CHAPTER 8: GENERAL DISCUSSION.....	129
1. Novel tools to study primary prostate cancer .....	131
2. PTOV1 can directly regulate self-renewal genes like <i>ALDH1A1</i> and <i>CCNG2</i> .....	132
CHAPTER 9: CONCLUSIONS .....	135



CHAPTER 10: BIBLIOGRAPHY .....	139
ANNEX 1: PUBLICATIONS .....	159

# Index of figures

Figure 1. Anatomy of the prostate gland.....	4
Figure 2. Composition of the prostate epithelium. ....	5
Figure 3. Prostate cancer initiation and progression. ....	6
Figure 4. Clinical stages of prostate cancer.....	7
Figure 5. Scheme of the different types of <i>TMPRSS2-ERG</i> fusions.....	8
Figure 6. Schematic diagrams of prostate adenocarcinoma grading system.....	15
Figure 7. Schematic representation of the different phases of prostate cancer progression with associated therapies. ....	18
Figure 8. Protein structure of PTOV1.....	23
Figure 9. Set up of the protocol for <i>ex vivo</i> primary tumor cultures.....	61
Figure 10. Scheme of the protocol for the separation of fibroblasts from epithelial cells.....	62
Figure 11. Microscopy images of purified <i>ex vivo</i> primary tumor cultures.....	63
Figure 12. Expression of prostate epithelial markers and major driver proteins in <i>ex vivo</i> primary tumor cultures. ....	65
Figure 13. Molecular alterations found in <i>ex vivo</i> primary tumor cultures and their corresponding original tumor tissues. ....	68
Figure 14. The effect of ADT on AR signaling in AI and AD LNCaP cells and <i>ex vivo</i> primary tumor cultures. ....	70
Figure 15. The effects of ADT on the growth of <i>ex vivo</i> primary tumor cultures. ....	72
Figure 16. Motility of AI and AD <i>ex vivo</i> primary tumor cultures.....	74
Figure 17. ADT induce EMT in AI LNCaP cells and in three <i>ex vivo</i> primary tumor cultures. ....	75
Figure 18. EMT signaling in <i>ex vivo</i> primary cultures from 6 to 9 is not induced by ADT.....	76
Figure 19. The resistance to androgen deprivation in AI and AD <i>ex vivo</i> primary tumor cultures increases their resistance to Docetaxel. ....	77
Figure 20. The resistance to androgen deprivation in <i>ex vivo</i> primary tumor cultures increases their resistance to Cabazitaxel.....	79
Figure 21. The effects of ADT or chemotherapy on the protein synthesis ratio in PCa cell lines and <i>ex vivo</i> primary tumor cultures. ....	81
Figure 22. The effects of ADT on the protein synthesis ratio in AD and AI LNCaP cells and <i>ex vivo</i> primary tumor cultures. ....	82
Figure 23. Expression of self renewal markers in <i>ex vivo</i> primary tumor cultures. ....	84
Figure 24. <i>Ex vivo</i> primary tumor cultures are tumorigenic <i>in vivo</i> .....	85
Figure 25. Spheres formed with cell lines and <i>ex vivo</i> primary tumor cultures are enriched in CSCs. ....	95
Figure 26. Spheres forming efficiency of prostate cancer cell lines and <i>ex vivo</i> primary tumor cultures.....	97
Figure 27. Characterization of docetaxel-resistant spheres and <i>ex vivo</i> primary tumor cultures-derived spheres. ....	99
Figure 28. Tumors formed <i>in vivo</i> by LNCaP cells. ....	101

<b>Figure 29. Galiellalactone toxicity on Du145 spheres and <i>ex vivo</i> primary tumors spheres.</b> .....	103
<b>Figure 30. Docetaxel toxicity on LNCaP and Du145 spheres.</b> .....	105
<b>Figure 31. Bozepinib analogues toxicity using the Du145 cell model and <i>ex vivo</i> primary tumor cultures.</b> .....	107
<b>Figure 32. Effects of bozepinib analogues on genes involved in angiogenesis and EMT in Du145 cells.</b> .....	108
<b>Figure 33. The ectopic expression of PTOV1 in prostate cancer cells promotes ALDH1A1 and CCNG2 expression.</b> .....	116
<b>Figure 34. Wnt and JNK pathways regulate PTOV1 action.</b> .....	117
<b>Figure 35. PTOV1 is associated to the chromatin of ALDH1A1 and CCNG2 promoters.</b> .....	118
<b>Figure 36. EMSA identify a new AT-hook-like motif in the A domain of PTOV1.</b> ..	120
<b>Figure 37. Mutation of the newly discovered AT-hook-like ‘core’ motif of PTOV1.</b>	121
<b>Figure 38. The expression of PTOV1, ALDH1A1 and CCNG2 is significantly associated with the Gleason score in prostate carcinomas.</b> .....	123
<b>Figure 39. PTOV1 accumulates in the nuclei of mitotic colon carcinoma cells.</b> .....	124
<b>Figure 40. PTOV1 accumulates in the nuclei of mitotic bladder carcinoma and breast carcinoma cells.</b> .....	125

# Index of tables

<b>Table 1. The new classification of tumor stages in prostate carcinomas.</b> .....	16
<b>Table 2. Principal genetic and phenotypic features of cell lines.</b> .....	34
<b>Table 3. Cycling conditions for RT-PCR.</b> .....	41
<b>Table 4. Primers used in RT-PCR.</b> .....	42
<b>Table 5. Short hairpins used to inhibit PTOV1 expression.</b> .....	43
<b>Table 6. Primers from the regions of the indicated genes used for Chromatin Immunoprecipitation (ChIP).</b> .....	45
<b>Table 7. Preparation of acrylamide gel for ChIP assays.</b> .....	46
<b>Table 8. Primers used in sequencing.</b> .....	50
<b>Table 9. Primary antibodies list.</b> .....	52
<b>Table 10. Secondary antibodies.</b> .....	53
<b>Table 11. Summary of the clinical characteristics of the 10 patients selected for this study.</b> .....	64
<b>Table 12. Scheme of the alterations found in tissues and corresponding ex vivo primary tumor cultures.</b> .....	67
<b>Table 13. The doubling time of AD and AI ex vivo primary tumor cultures LNCaP culture.</b> .....	73
<b>Table 14. The half maximal inhibitory concentration (IC50) of AD and AI ex vivo primary tumor cultures and LNCaP cells in response to taxanes.</b> .....	80
<b>Table 15. Co-occurrence of DNA alterations in PCa.</b> .....	122

# Abbreviations

---

## **4**

4EBP1	
eIF4E binding protein 1	67

---

## **A**

AAH	
atypical adenomatous hyperplasia	17
ABC	
ATP-binding cassette	30
AD	
androgen dependent	45
ADT	
androgen deprivation therapy	26
Ago	
Argonaute protein	54
AI	
androgen independent	45
<i>ALDH1A1</i>	
aldehyde dehydrogenase 1 family member A1	38
AR	
Androgen Receptor	15, 20, 23, 24, 31, 32, 33, 35, 44, 53, 86, 87
ATCC	
American Type Culture Collection	44
<i>ATM</i>	
Ataxia Telangiectasia Mutated	24

---

## **B**

BPH	
benign prostate hyperplasia	14, 17
BRCA	
breast cancer DNA repair associated	18

---

## **C**

<i>CCNG2</i>	
Cyclin G2	38
CDH1	
cadherin 1	54
CDKN1B	
Cyclin-dependent kinase inhibitor 1B	23

---

## **Ch**

<i>CHDI</i>	
chromodomain helicase DNA-binding protein 120	

CHGA	
chromogranin A	67
ChIP	
chromatin immunoprecipitation	55

---

## **C**

CK14	
Cytokeratin 14	15, 90
CK18	
Cytokeratin 18	15
CK5	
Cytokeratin 5	15, 32, 75, 90
CK8	
Cytokeratin 8	15, 32
CNAs	
copy number alterations	20
COPA	
cancer outlier profile analysis	20
CRPC	
castration resistant prostate cancer	24
CSCs	
cancer stem cells	34
Ct	
Threshold cycle	53
CYP17	
Cytochrome P450 17	31
CZ	
central zone	14

---

## **D**

DDR	
DNA damage repair	18
DHT	
dihydrotestosterone	17
DKK1	
Dickkopf wnt signaling pathway inhibitor 1	38
DMSO	
Dimethyl sulfoxide	44
DR	
docetaxel-resistant	44
DRE	
digital rectal examination	24

---

## **E**

EAU	
European Association of Urology	25
EGF	
epidermal growth factor	50
EMSA	
Electrophoretic mobility shift assay	61

EMT	
epithelial-mesenchymal transition	23
<i>ERG</i>	
ETS related gene	20
Erk	
extracellular signal-regulated kinases	67
<i>ETS</i>	
erythroblast transformation-specific	20
<i>ETVI</i>	
ETS variant 1	20

---

## F

FBS	
fetal bovine serum	46
FFPE	
Formalin-fixed paraffin-embedded	51
FGF	
fibroblast growth factor	50
<i>FOXA1</i>	
forkhead box A1	20

---

## G

GEM	
genetically engineered mice	36

---

## H

HBS	
Hepes Buffered Saline	47
<i>HES1</i>	
hes family bHLH transcription factor1	38
<i>HEY1</i>	
hes related family bHLH transcription factor with YRPW motif1	38
HGPIN	
High grade PIN	18
HIV	
human immunodeficiency virus	46
hK2	
kallikrein-related peptide 2	26
HMBS	
hydroxymethylbilane synthase	54

---

## I

iCRT14	
inhibitor of $\beta$ -catenin-responsive transcription (CRT)	45
IPO8	
Importin 8	54

---

## J

JNK	
c-Jun NH2-terminal kinase	22

---

## K

<i>KLK3</i>	
kallikrein 3	25

---

## L

LADY	
Long probasin Promoter	36
LEF1	
Lymphoid enhancer-binding factor 1	54
LHRH	
luteinizing hormone-releasing hormone	30
LNA	
Locked Nucleic Acids	52
LTRs	
long terminal repeats	46
LV	
Lentiviral vectors	46

---

## M

mCRPC	
metastatic castration resistant prostate cancer	31
MRI	
magnetic resonance imaging	26

---

## N

NCAM	
neural cell adhesion molecule	16
NEPC	
Neuroendocrine Prostate Cancer	16
NHEJ	
non-homologous end joining	23
NSE	
neuronal specific enolase	16

---

## P

p-AKT	
phosphorylated RAC-alpha serine/threonine-protein kinase	67
PBS	
Phosphate-buffered saline	49
Pca	
prostate cancer	16
PDCD4	
Programmed cell death protein 4	67
PDX	
Patient derived xenograft	37
PHI	
prostate health index	25
PI3K	
phosphatidylinositol 3-kinase	22
PIN	
prostatic intraepithelial neoplasia	17

---

## V

POU5F1	
Putative POU domain, class 5, transcription factor	
1	54
PSA	
prostate-specific antigen	15
<i>PTEN</i>	
phosphatase and tensin homolog	20
<b>PTOV1</b>	
Prostate Tumor OVer-expressed 1	37
PZ	
peripheral zone	14

---

## R

RACK1	
receptor of activated protein C kinase 1	37
RB1	
Retinoblastoma	67
RISC	
RNA-induced silencing complex	54
RT	
room temperature	47
RT-qPCR	
Quantitative real time polymerase chain reaction	52

---

## S

SFE	
Sphere Forming Efficiency	50
SHARP	
SMRT/HDAC1-associated repressor protein	38
shRNAs	
short hairpin RNAs	54
SNAI1	
Zinc finger protein SNAIL	54
SOX2	
SRY (sex determining region Y)-box 2	54
<i>SPINK1</i>	
serine peptidase inhibitor, Kazal type 1	20
<i>SPOP</i>	
speckle type BTB/POZ protein	20

---

## T

TBP	
TATA-box binding protein	54
TICs	
tumor initiating cells	34
<i>TMPRSS2</i>	
transmembrane protease serine 2	20
TNM	
Tumor Node Metastasis	29
TRAMP	
Transgenic adenocarcinoma of the mouse prostate	36
TRUS	
transrectal ultrasound-guided needle biopsy	26
TZ	
transition zone	14

## VI

---

## U

UPL	
Universal Probe Library of Roche	52

## Summary

Metastatic prostate cancer (PCa) is the third leading cause of death for cancer in Europe and North American men. Gold standard therapy is the androgen deprivation therapy (ADT), although taxanes and newly developed drugs to Androgen Receptor can temporarily bypass the resistance to castration, the Castration Resistant Prostate Cancer (CRPC) is a mortal disease and remains the greatest clinical challenge of prostate cancer. Significant effort has been devoted to discover efficient treatments for these patients and a number of specific inhibitors to some signaling pathways have been identified. However, one important limitation is the very low number of suitable models that reproduce the aggressive disease. In fact, *in vivo* models able to recapitulate the heterogeneity of prostate tumors are scarce and have several setbacks. Similarly, most *in vitro* models are derived from metastasis, thus poorly represent the heterogeneity of human prostate tumors. A growing body of evidence suggests that within tumors resides a small population with stem cell-like properties. We hypothesized that ADT can enrich tumors for cancer stem cells (CSCs). Additionally, a successful therapy for PCa would need to be applied at early stages and new markers for the prompt identification of aggressive tumors, or to predict CRPC, together with more specific therapeutic targets are prerequisites. Our previous studies suggested that PTOV1 is a good discriminating marker for HGPIN associated to PCa, that is overexpressed in more aggressive metastatic disease. Furthermore, our functional studies on the role of this protein in resistant tumors suggest that PTOV1 is a good target to eliminate more aggressive cancer cells. The main objective of this thesis is to obtain a simple *in vitro* model to reproduce the characteristics and behavior of primary prostate tumors to be used in *in vitro* drug screenings. A second objective is to analyze the mechanisms of the oncogenic protein PTOV1 in the promotion of cancer resistance to chemotherapy. In this work, we established 16 new *ex vivo* primary prostate tumor cultures from needle biopsies of untreated patients with aggressive cancer. These cultures were characterized for their phenotypes and functional characteristics. In addition, each culture was in parallel treated to derive corresponding Androgen Independent (AI) cultures. These AI primary tumor cultures exhibited in general a reduction of proliferation rate, increase of motility, and resistance to chemotherapy, suggesting that AI cultures are highly plastic and able to overcome the stress caused by chemotherapies. Of note, the treatment with ADT *in vitro* was associated with an increment of expression of self-renewal markers, suggesting an increase of stemness capacities in the resistant AI cell



populations. To establish a model to study CSCs resistance, cells were efficiently selected through a functional protocol based in their ability to form spheres. These spheres were characterized, validated and used to test new drugs.

Finally, we discovered a new AT-hook *like* motif within the A domain of the protein PTOV1 with higher affinity to DNA rather than RNA. We have shown that this AT-hook-*like* motif, through which PTOV1 directly binds to *ALDH1A1* and *CCNG2* promoters, is necessary to activate the expression of these genes in androgens sensitive cells. *PTOV1*, *ALDH1A1* and *CCNG2* high levels are significantly correlated with aggressive metastatic prostate tumors and worst outcome, suggesting that PTOV1 represents a potential target for the treatment of these tumors. These results provide novel tools to targets aggressive prostate tumors.

## Resumen

El cáncer de próstata (PCa) metastásico es la tercera causa de muerte por cáncer en hombres en el mundo occidental. La terapia estándar es la privación de andrógenos (ADT), aunque los taxanos y los medicamentos recientemente desarrollados para el receptor de andrógenos pueden evitar temporalmente la resistencia a la castración. El cáncer de próstata resistente a la castración (CRPC) es una enfermedad mortal y sigue siendo el mayor desafío clínico del PCa. Se ha dedicado un esfuerzo significativo para descubrir tratamientos eficientes y se han identificado varios inhibidores específicos de algunas vías de señalización. Sin embargo, una limitación importante es el muy bajo número de modelos adecuados que reproducen la enfermedad. De hecho, los modelos *in vivo* capaces de recapitular la heterogeneidad de los tumores de próstata son escasos. De manera similar, la mayoría de los modelos *in vitro* se derivan de metástasis, por lo que representan de manera deficiente la heterogeneidad del PCa. Numerosos estudios sugieren que dentro de los tumores reside una pequeña población con propiedades similares a las células madre. Presumimos que el ADT puede enriquecer las células tumorales de células madre cancerosas (CSCs). Entonces, una terapia eficaz tendría que ser aplicada en etapas tempranas. Otros desafíos son encontrar nuevos marcadores para la pronta identificación de tumores, o poder predecir CRPC. Nuestros estudios anteriores sugirieron que PTOV1 es un buen marcador discriminatorio para HGPIN asociado a PCa, que se sobre expresa en la enfermedad metastásica. Además, nuestros estudios funcionales sobre el papel de esta proteína en tumores resistentes sugieren que PTOV1 es una buena diana para eliminar las células cancerosas más agresivas.

El objetivo principal de esta tesis es obtener un modelo *in vitro* simple para reproducir las características y el comportamiento del PCa primario y para testar nuevas drogas. Un segundo objetivo es analizar los mecanismos de la proteína oncogénica PTOV1 en la promoción de la resistencia al cáncer a la quimioterapia. En este trabajo, establecimos 16 nuevos cultivos primarios tumorales *ex vivo* a partir de biopsias de pacientes con PCa no tratados, derivando el cultivo independiente de andrógenos (AI) correspondiente. Después de la ADT *in vitro*, los cultivos primarios mostraron en general una reducción de la tasa de proliferación, un aumento de la motilidad y la resistencia a la quimioterapia, lo que sugiere que las poblaciones de AI son altamente plásticas y capaces de superar el estrés causado por las quimioterapias.

El ADT *in vitro* se asoció con un aumento de la expresión de marcadores de auto-renovación, lo que sugiere un aumento de las capacidades de células madres en las poblaciones de células

AI resistentes. Para establecer un modelo dirigido a estudiar la resistencia de las CSCs, las células se seleccionaron de manera eficiente a través de un protocolo funcional basado en la capacidad para formar esferas. Las esferas fueron caracterizadas, validadas y utilizadas para probar nuevos medicamentos.

Finalmente, descubrimos un nuevo motivo tipo AT-hook dentro del dominio A de la proteína PTOV1 con una mayor afinidad por el ADN en lugar del ARN. Hemos demostrado que este motivo tipo AT-hook, a través del cual PTOV1 se une directamente a los promotores *ALDH1A1* y *CCNG2*, es necesario para activar la expresión de estos genes en las células sensibles a los andrógenos. Los niveles altos de *PTOV1*, *ALDH1A1* y *CCNG2* se correlacionan significativamente con PCa agresivos y mal pronóstico, lo que sugiere que PTOV1 podría ser una diana potencial para el tratamiento del PCa que responde a los andrógenos. En conjunto, estos resultados proporcionan herramientas novedosas para estudiar el PCa.

## Resum

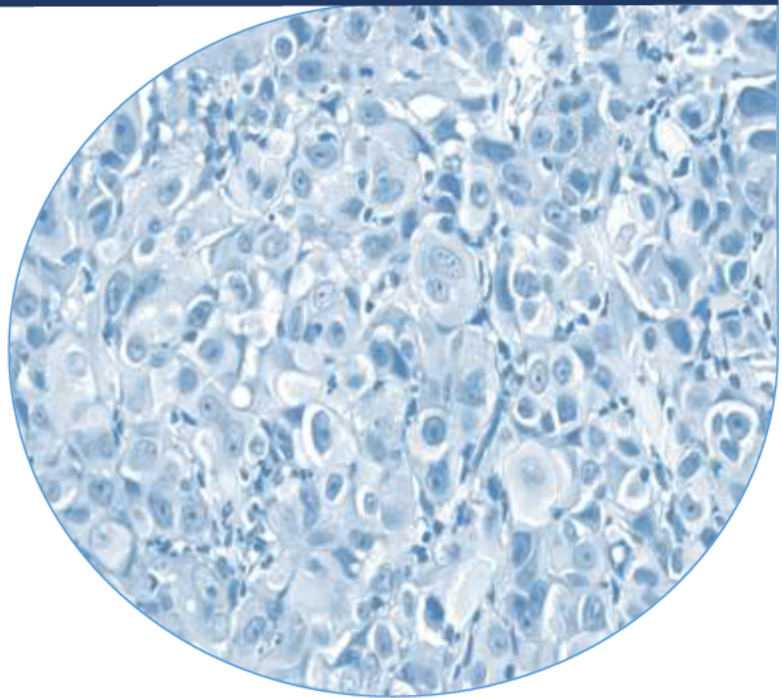
El càncer de pròstata (PCa) metastàtic és la tercera causa de mort per càncer en homes en el món occidental. La teràpia estàndard és la privació d'andrògens (ADT), encara que els taxans i els fàrmacs anti receptor d'androgen recentment desenvolupats poden escapar temporalment la resistència a la castració. El càncer de pròstata resistent a la castració (CRPC) és una malaltia mortal i segueix sent el major desafiament clínic del càncer de pròstata. S'ha dedicat un esforç significatiu per descobrir tractaments eficients i s'han identificat diversos inhibidors específics d'algunes vies de senyalització. No obstant això, una limitació important és el molt baix nombre de models adequats disponibles. De fet, els models *in vivo* capaços de recapitular l'heterogeneïtat dels tumors de pròstata són escassos. De manera similar, la majoria dels models *in vitro* es deriven de metàstasi, pel que representen de manera deficient l'heterogeneïtat del PCa. Nombrosos estudis suggereixen que dins dels tumors resideix una petita població amb propietats similars a les cèl·lules mare. Pressuposant que l'ADT pot enriquir les cèl·lules tumorals de cèl·lules mare canceroses (CSCs). Així doncs, una teràpia eficaç hauria de ser aplicada en etapes primerenques. Altres desafiaments són trobar nous marcadors per a la ràpida identificació de tumors, o poder predir CRPC, disminuiria el nombre de defuncions. Els nostres estudis funcionals sobre el paper de PTOV1 en tumors CRPC suggereixen que PTOV1 és un bona diana per eliminar les cèl·lules canceroses més agressives. L'objectiu principal d'aquesta tesi és obtenir un model *in vitro* simple per reproduir les característiques i el comportament del càncer de pròstata primari i per testar noves drogues. Un segon objectiu és analitzar els mecanismes de la proteïna oncogènica PTOV1 en la promoció de la resistència al càncer a la quimioteràpia. En aquest treball, vam establir 16 nous cultius primaris tumorals *ex vivo* a partir de biòpsies de pacients amb càncer de pròstata no tractats, derivant el cultiu independent d'andrògens (AI) corresponent. Després de l'ADT *in vitro*, els cultius primaris van mostrar en general una reducció de la taxa de proliferació, un augment de la motilitat i la resistència a la quimioteràpia, el que suggereix que les poblacions d'AI són altament plàstiques i capaces de superar no només l'ADT sinó també altres teràpies farmacològiques i condicions d'estrès.

L'ADT *in vitro* es va associar amb un augment de l'expressió de marcadors d'auto-renovació, el que suggereix un augment de les propietats de cèl·lules mares en les poblacions de cèl·lules AI. Per establir un model dirigit a estudiar la resistència de les CSCs, les cèl·lules es van seleccionar de manera eficient a través d'un protocol funcional basat en la capacitat

per formar esferes. Les esferes van ser caracteritzades, validades i utilitzades per provar nous medicaments. Finalment, vam descobrir que PTOV1 posseeix un altre motiu similar a l'AT-hook dins el domini A que té més afinitat amb l'ADN que amb l'ARN. A través d'aquest domini, PTOV1 s'uneix directament als promotors dels gens *ALDH1A1* i *CCNG2* per activar la seva expressió en cèl·lules dependents d'andrògens. Els nivells alts de *PTOV1*, *ALDH1A1* i *CCNG2* es correlacionen amb PCa agressius i de mal pronòstic, el que suggereix que PTOV1 podria ser una diana potencial per al tractament del PCa que respon als andrògens. En conjunt, aquests resultats proporcionen noves eines per l'estudi del PCa.

# CHAPTER 1: INTRODUCTION

---





## **1. Anatomy of the prostate**

The prostate gland plays a key role in male reproduction. Its main function is to secrete a fluid containing enzymes, lipids, amines and metal ions essential for the normal activity of spermatozoa. The development, differentiation and maintenance of the prostate gland depend on steroid and peptide hormones<sup>1</sup>. The prostate is a large pyramidal gland located between the bladder and the penis, in front of the rectum. The base of the prostate is in continuity with the bladder to which is connected by the urethra, that runs through the center of the prostate from the bladder to the penis, letting urine flow out of the body.

Embryologically, the prostate, seminal vesicles, and ductus (vas) deferens originate from 2 separate structures. The prostate arises from a budding collection of tissue in the urogenital sinus. The seminal vesicles and the ductus deferens are formed from the mesonephric duct. The prostate develops from epithelial outgrowths from the prostatic segment of the urethra that grows into the surrounding mesenchyme.

The prostate gland is enclosed by a capsule composed of collagen, elastin and large amounts of smooth muscle. The gland has been classically recognized as composed of different areas or zones<sup>2</sup>:

- 1- The transition zone (TZ), located in the inner part, next to the urethra, it occupies 10% of the prostatic glandular tissue and it is the location where 20% of the adenocarcinomas of the prostate arise. The epithelium consists of transitional cells similar to the bladder epithelium. The benign prostate hyperplasia (BPH) arises in this area.
- 2- The central zone (CZ), a triangular area surrounding the ejaculatory ducts, it represents about 25% of the glandular tissue. Only a small proportion of adenocarcinomas develop in this region.
- 3- The peripheral zone (PZ), located in the posterior and lateral area of the gland, it represents 70% of the glandular tissue of the prostate. It is the area that is palpated on digital rectal examination (DRE) and it is the most frequent site where prostate cancer arises<sup>3</sup>.



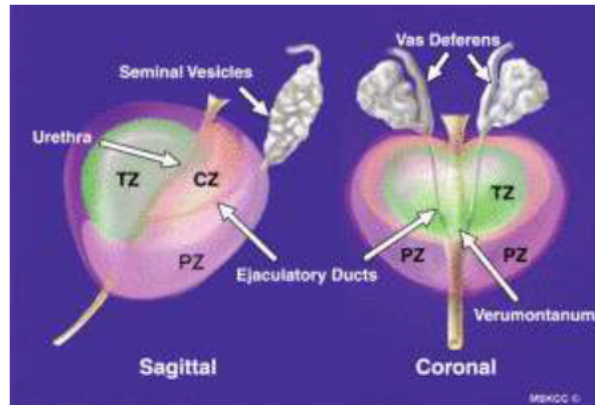


**Figure 1. Anatomy of the prostate gland.** From Geneva foundation of Medical Education and Research.

The glandular and stromal parts of the prostate are strongly fused in a capsule of smooth muscle covered by collagen. The prostate epithelium is composed by different cellular types: basal, luminal and rare neuroendocrine cells<sup>4</sup> (**Figure 2**). The basal epithelial cells, smoothed cuboidal cells forming one continuous layer below the luminal cell layer, are attached to the basal membrane, forming one or two continuous layers. Basal cells express cytokeratins (CK) 5, CK14, p63 (an homologue of p53 tumor suppressor gene that can act as a dominant negative or activator of p53<sup>5</sup> and low levels of the androgen receptor (AR). The luminal epithelial cells are exposed to the gland lumen, express CK8, CK18, and AR. These cells represent the major part of the prostate epithelium and, in response to androgens, are able to secrete a variety of products, including the prostate-specific antigen (PSA), that contributes to the formation of the seminal fluid.

Neuroendocrine cells are rare cells interspersed within the luminal layer and express characteristic markers of neuronal cells like synaptophysin, the neural cell adhesion molecule (NCAM), neuronal specific enolase (NSE) and chromogranin A, but not AR or PSA<sup>6</sup>. These cells are implicated in the development of the prostate and the regulation of both secretory and basal cells through the release of different molecules as calcitonin or survivin<sup>7</sup>. Neuroendocrine cells are abundant in the most aggressive subtype of PCa, called Neuroendocrine Prostate Cancer (NEPC), characterized by the absence of AR, PSA but expression of neuronal markers<sup>8</sup>.

Finally, a subpopulation of cells called transit amplifying, or intermediate cells, that co-express both types of CKs, was also described within the two epithelial layers. These cells have been suggested as the prostatic progenitor/stem cell population<sup>9-11</sup>.

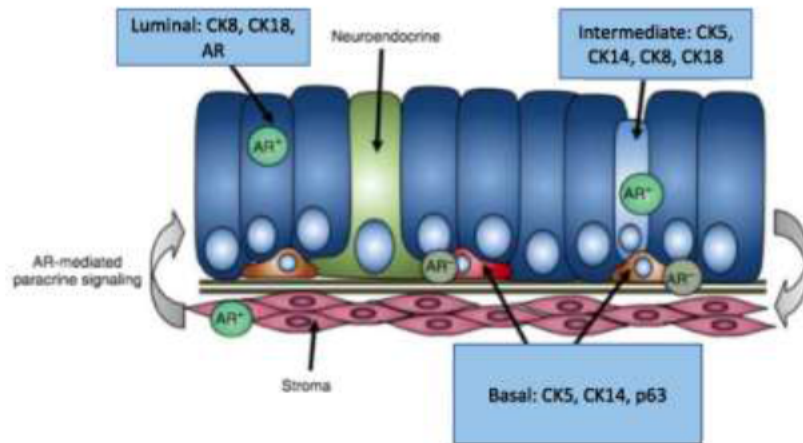


**Figure 2. Composition of the prostate epithelium.** Adapted from Taylor R.A. et al.<sup>11</sup>

The prostatic fluid contains kallikreins, a family of serine proteases that include the PSA, and citrate, an intermediate metabolite of the Krebs cycle and  $Zn^{2+}$ , a key element accumulated in the luminal cells. This fluid contributes to male fertility. Intraprostatic accumulation of  $Zn^{2+}$  and citrate, inhibition of the Krebs cycle and prostatic fluid release are regulated by male sex steroids *via* their main intracellular effector, the AR. Indeed, within the prostate, testosterone is converted by the enzyme  $5\alpha$ -reductase into the more potent (in terms of binding affinity for the AR) androgen,  $5\alpha$ -dihydrotestosterone (DHT). Hundreds of genes have been discovered to be regulated by DHT within the prostate epithelium<sup>12-14</sup>.

## 2. Prostate cancer

### 2.1 Natural history of prostate cancer

Prostate cancer (PCa) is the most frequent neoplasia in men and the third leading cause of death for cancer in western countries<sup>15,16</sup>. PCa develops generally as acinar adenocarcinoma expressing AR<sup>16</sup>. One malignant precursor lesion has been described for PCa: the prostatic intraepithelial neoplasia (PIN). PIN appears as lesions with atypical epithelial proliferation arising in the tubular glands of the prostate where cells have nuclear atypia. Bostwick and Brawer first graded PIN lesions into three categories<sup>17</sup>: they showed a progressive loss of basal cells was accompanying increasing grades of PIN, with loss of more than one third of the basal cell layer in 52% of PIN compared with less than 2% in lower grades of PIN (**Figure 3**).

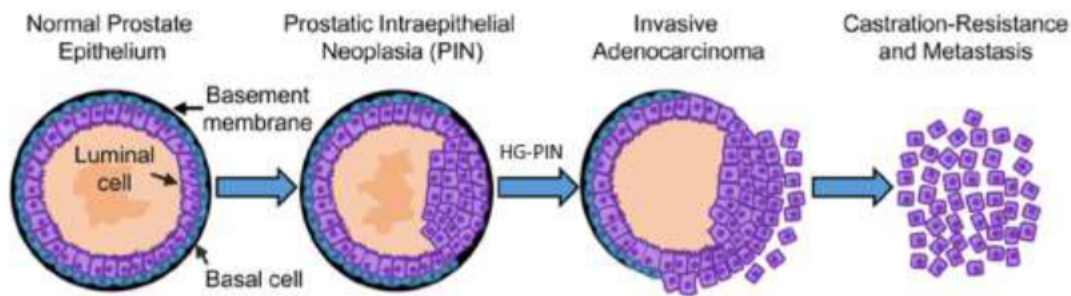


**Figure 3. Prostate cancer initiation and progression.** Adapted from Rybak et al.<sup>18</sup>

High grade PIN (HGPIN) lesions are associated genotypically and phenotypically to invasive carcinoma<sup>17</sup>. They consist of large cytologic lesions with enlarged nuclei, prominent nucleoli, and increased levels of several proliferation markers in the majority of the affected duct and acini cells. Many molecular alterations encountered in HGPIN are observed in advanced PCa, supporting the link of this lesion with cancer<sup>19</sup>. Another lesion that in some cases has been associated with PCa is the AAH (AAH) that arises only in the Transition Zone and it is frequently linked with benign prostate hyperplasia (BPH). It is characterized by the proliferation of small acini or glands<sup>20</sup>.

### *2.2 Molecular alterations in prostate cancer*

Prostate cancer progression can be divided into three main stages: localized, metastatic and castration resistant. Each phase of the disease is characterized by the occurrence of distinct genomic alterations, often mutually exclusive. Each phase of the disease is characterized by the occurrence of distinct genomic mutations, often mutually exclusive, that contribute to the molecular heterogeneity of PCa and to the aggressive stages of castration resistance (**Figure 4**).

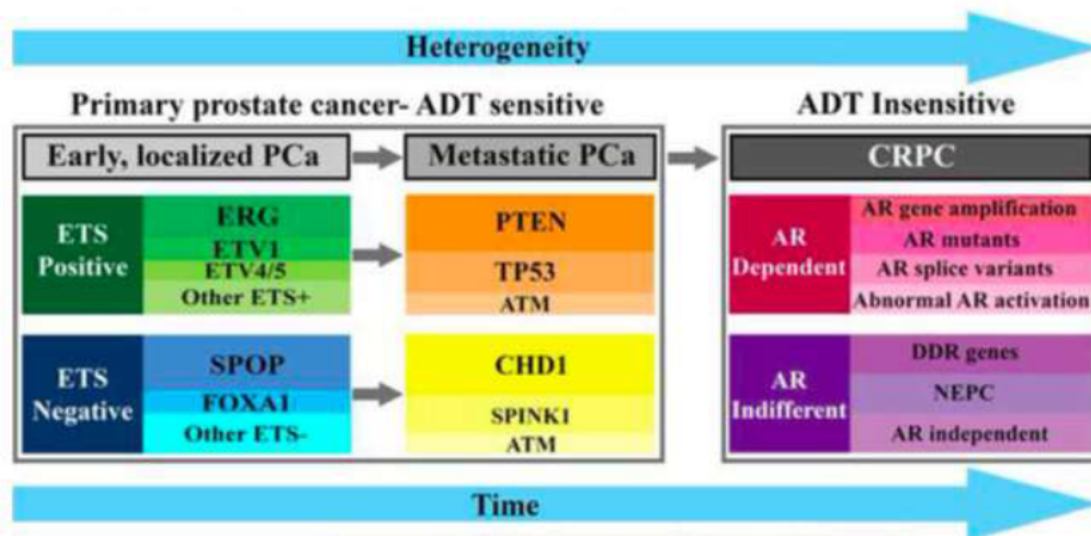


Figure 4. Clinical stages of prostate cancer. From Arora K, Barbieri C.E.<sup>21</sup>

During cancer progression, DNA copy number alterations (CNAs) occur more frequently than somatic point mutations<sup>21</sup>. Mutations have been observed in specific genes, for example in *ETS*, *PTEN*, *TP53*, *SPOP*, *FOXA1*, *CHD1*, *SPINK1*, *ATM*, *AR* and others.

#### *ETS* genes

Chromosomal translocations involving the *ETS* family of genes with androgens regulated genes have been observed with a frequency of 50%<sup>22</sup>. *ETS* genes are a family of transcription factors important for development, differentiation, proliferation, apoptosis, migration, tissue remodeling, invasion and angiogenesis in many types of cells<sup>23</sup>. Tomlins and colleagues developed a method termed cancer outlier profile analysis (COPA) able to identify recurrent rearrangements or high-level amplifications in several data sets<sup>22</sup>. This method consistently identified translocation of *TMPRSS2* mostly with two *ETS* genes, *ERG* and *ETV1*. The *ETS* were already discovered because of their involvement in others chromosomal translocations in Ewing's sarcoma and myeloid leukemias<sup>24,25</sup>. *TMPRSS2*, a gene coding for a serine protease located in chromosome 21, is expressed in normal prostate tissue and it is strongly regulated by androgens and functionally *TMPRSS2-ETS* fusions are androgen-dependent. Fusions between *TMPRSS2* and *ERG* genes constitute the most common translocation described in PCa<sup>22</sup>. The resulting transcript generally leads to high levels of ETS expression that initiate the neoplasia and in some cases promote progression of PCa<sup>21</sup>. Among the eight isoforms of the fusion gene, two groups are distinguished: one containing the *TMPRSS2*

## Chapter 1: Introduction

exon 1 fused with *ERG* and one where *TMPRSS2* exon 2 and 3 are fused with *ERG*<sup>26</sup> (Figure 5).

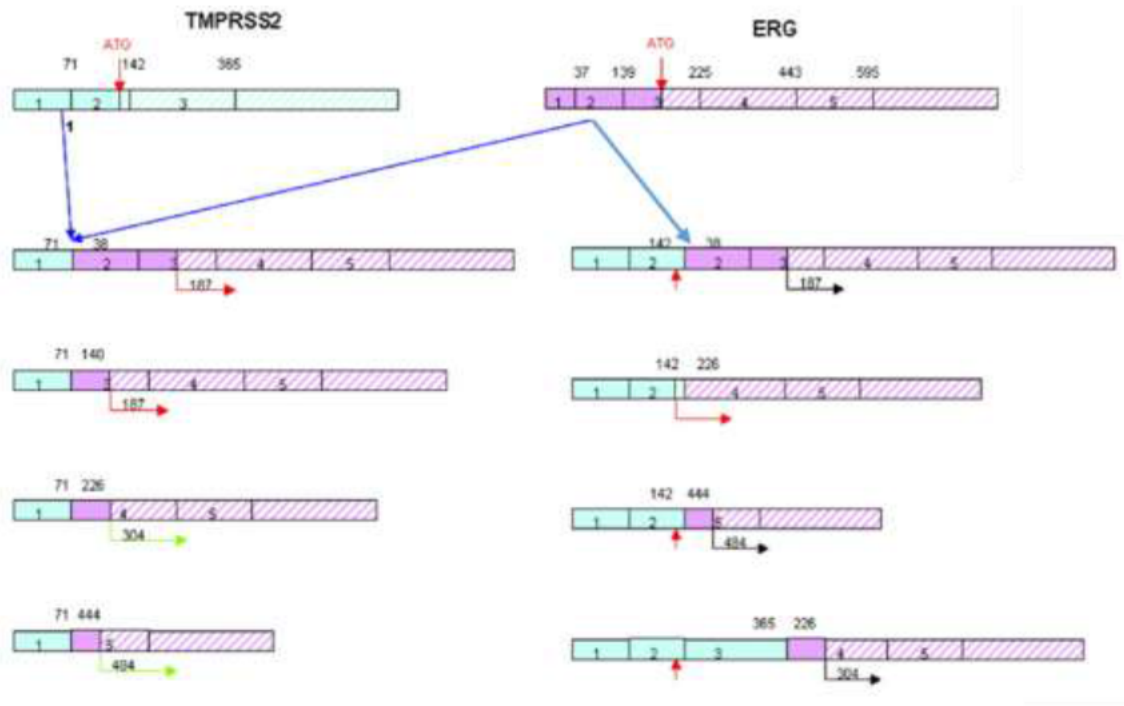


Figure 5. Scheme of the different types of *TMPRSS2-ERG* fusions. Adapted from Wang et al.<sup>27</sup>

For still unknown reasons, the expression of the fusions *TMPRSS2* exon 1 with *ERG* exon 4 or with *ERG* exon 6 is strongly linked with aggressive PCa<sup>27</sup>.

### *PTEN*

ETS transcription factors negatively regulates *PTEN* transcription in a direct manner<sup>28</sup>. *PTEN* is located in chromosome 10 and encodes for a dual- specificity protein phosphatase that negatively regulates the phosphatidylinositol 3-kinase (PI3K) signaling pathway. The PI3K pathway is a driver of cell proliferation and survival in many tumors<sup>29,30</sup>. When PI3K is active, the second messenger phosphatidylinositol 4,5-bisphosphate PIP<sub>2</sub> is phosphorylated to phosphatidylinositol (3,4,5) triphosphate (PIP<sub>3</sub>). PIP<sub>3</sub> activates a signaling cascade that leads to inhibition of apoptosis and induction of cell proliferation. *PTEN* dephosphorylates PIP<sub>3</sub>, converting it to its inactive form PIP<sub>2</sub><sup>31</sup>. *PTEN* loss, partial deletion, or inactivating mutations result in the constitutive activity of PI3K pathway and also in the activation of c-Jun NH<sub>2</sub>-terminal kinase (JNK)<sup>32</sup>. *PTEN* deletions occur in 20%-30% of primary prostate tumors and are correlated with worst outcome<sup>33,34</sup>.

### *TP53*

Mutations in the tumor suppressor gene *TP53* are generally early events in PCa and lead the primary tumor to a faster development of drug resistance<sup>35</sup>. *TP53* is reported deleted in approximately 30% of PCa clinically localized tumors and point mutations occur in 5-40% of the cases<sup>36,37</sup>. A common polymorphism that affects the codon 72, encoding either proline or arginine, alters p53 functions. In fact, P72 variant leads p53 to activate more p21 inducing growth arrest, while R72 induces apoptosis<sup>38</sup>. It has been demonstrated that the R72 variant is positively associated with type II diabetes and obesity<sup>39</sup>. Although there are minor evidences about the R72 involvement in cancer risk, at least three links have been observed between obesity and cancer, such as cytokines, the insulin-IGF-1 axis and sex hormones<sup>40</sup>.

### *SPOP*

The *SPOP* gene encodes for the substrate-recognition component of a Cullin3-based E3-ubiquitin ligase<sup>36</sup>. This gene is found mutated in 13% of prostate tumors, and in mutual exclusivity with the chromosomal translocation *TMPRSS2-ERG*<sup>41</sup>. The mutated *SPOP* protein is not able to promote the degradation of SRC-3, thus resulting in over activation of the androgen receptor pathway<sup>42</sup>. *SPOP* mutations are mainly distributed in the substrate binding motif present in the MATH domain of the protein, producing gain of function modifications or altered substrate binding specificity<sup>41</sup>. Recently, it has been reported that *SPOP* mutations also lead to genomic instability, increased sensibility to DNA damaging agents and PARP inhibitors like Olaparib or Velaparib. In particular, *SPOP* mutants F133V deregulate DSB repair by promoting the error-prone NHEJ pathway<sup>43</sup>.

### *FOXA1*

The Forkhead transcription factor A1 (*FOXA1*) is required for the transcription of the *AR* gene and the activation of *CDKN1B*<sup>44</sup>. *FOXA1* is mutated in 4% of prostate tumors not affected by the *TMPRSS2-ERG* fusion<sup>37</sup>. Some missense mutations at the winged helix domain lead to an increased cell motility and genomic aberrations<sup>21</sup>. Indeed, these mutations reduces the PCa cell dependency on AR signaling through increasing *FOXA1* binding to a subset of AR-independent enhancers that regulates transcription of genes mediating EMT and metastasis<sup>45</sup>.

### *CHD1*

The chromodomain helicase DNA-binding protein 1 (*CHD1*) is a tumor suppressor gene, involved in chromatin assembly and activation of transcription<sup>46</sup>. Loss of *CHD1* in PCa exposes cells to DNA damage because it enhances the non-homologous end joining (NHEJ) activity and down-regulates the error free homologous recombination repair machinery<sup>47</sup>. Prostate cancer cells depleted for *CHD1* have a higher sensitivity to DNA damage agents as the topoisomerase inhibitor irinotecan and PARP inhibition<sup>48</sup>. Deletions of *CHD1* has been detected in about 10%–25% of both primary and advanced prostate tumors<sup>36</sup>.

### *SPINK1*

*SPINK1* is a serine protease inhibitor of digestive trypsins<sup>49</sup>. *SPINK1* has subsequently been found to be secreted into the blood and urine by a variety of other tumor types<sup>50</sup>. This protein is involved in the induction of the epithelial-mesenchymal transition (EMT) in prostate tissue, which is associated to a higher cell motility and invasion<sup>51</sup>. *SPINK1* is commonly altered by overexpression in 5-10% of prostate cancers and its overexpression is correlated with the aggressivity of tumors<sup>21</sup>.

### *ATM*

The Ataxia Telangiectasia Mutated (*ATM*) is a tumor suppressor gene that encodes a guardian protein responsible for the DNA-damage alert. In normal cells, ATM is an inactive dimer but, after a DNA damage, it is recruited in the DSB break and induced by the MRN (Mre11-Rad50-Nbs1) complex to transit in an active auto phosphorylated monomer<sup>52</sup>. In a phase II clinical trial, ATM mutated patients had a high response rate to the PARP inhibitor Olaparib<sup>53</sup>. ATM mutated cells show alterations in the cell cycle and p53 functions<sup>54</sup>. Mutations in *ATM* are found in 19% of the prostate cancers<sup>55</sup>.

### *AR*

The Androgen Receptor (*AR*) is the most altered gene in PCa. Indeed, when amplified, it is able to drive localized PCa to metastatic castration resistant prostate cancer (CRPC)<sup>56</sup>. Although tumors might be starved of androgens when androgen depletion therapies are applied, the increased expression of AR maintains stable the androgen activity, because it

hyper-sensitizes cells to the fewer level of hormones<sup>21</sup>. The *AR* is also frequently reported to be mutated in the ligand binding domain that allows the promiscuous binding of other hormones<sup>57</sup>. Moreover, the gene undergoes to alternative splicing producing variants that lack a ligand binding domain and result in cancer cells having a constitutive active signaling of the AR signaling that drives cells to drug resistance<sup>58</sup>.

### 2.3 Prostate Cancer Stem Cells

During cancer progression, several genetic and epigenetic alterations occur to promote the transition of cancer cells to a more malignant phenotype. In this transition, cancer cells acquire plasticity and are able to switch from a differentiated to a non-differentiated state<sup>59</sup>. In addition to these observations, rare populations of cells with properties of stem-like cells, namely cancer stem cells (CSCs) or tumor initiating cells (TICs), have been detected in the bulk of tumor cells<sup>60</sup>. The initial identification of CSCs was based on the presence of surface markers also reported overexpressed in adult stem cells, like CD44 and CD133 among others<sup>61</sup>. CSCs were identified for the first time in tumors of the breast as CD44<sup>+</sup>CD24<sup>-</sup> cells that were characterized by a high *in vivo* tumorigenic capacity<sup>62</sup>. Following that study, populations of CSCs have been identified in different solid tumors, *e.g.* brain<sup>63</sup>, skin<sup>64</sup>, colon<sup>65</sup>, head and neck<sup>66</sup>, pancreas<sup>67</sup>, lung<sup>68</sup>, bladder<sup>69</sup> and also prostate<sup>70</sup>. In prostate tumors, CSCs were first detected by the presence of high expression of CD133 and integrin  $\alpha_2\beta_1$ <sup>70</sup>. In addition, a population of CSCs was identified in xenografted tissues of human prostate tumors by the expression of the stemness marker *ABCG2*, a member of ABC transporter family, implicated in drug expulsion<sup>71</sup>. This small population of cells represents about 30% of the tumor bulk and possesses intrinsic abilities of stem cells, namely self-renewal and plasticity, was shown to alternate in different cycles of expression of high or low levels of *ABCG2*<sup>72</sup>. Since the identification of CSCs in PCA, three principal models of differentiation have been proposed. The first model states that CSCs originate from basal prostate cells, according to their self-renewal and regeneration capacities, as observed in other tissues like skin, intestine epithelium, and bone marrow<sup>11</sup>. The second model rebuts the previous linear one, establishing that transit-amplifying cells are the progenitor of CSCs because of their bi-directionality that allows the development of both basal or luminal cells derived CSCs<sup>9</sup>. Finally, CSCs were identified in the luminal portion of the prostate epithelium, suggesting the CSCs may derive also from both basal and luminal cell types<sup>10</sup>.



Prostate CSCs form niches and are regulated by growth factors and cytokines released by the tumor microenvironment, stromal cells or cancer associated fibroblasts (CAFs)<sup>73</sup>. It has been observed that prostate CSCs are negative for AR expression despite, as described above, tumor resistance to androgen deprivation therapy (ADT) is generally acquired by the amplification of *AR*<sup>74</sup>. This apparent contradiction might be explained by the action of ADT that would kill the majority of AR<sup>+</sup> cancer cells but not CSCs that are AR<sup>-</sup>. The ADT would also cause the generation of an intermediate cell stage of CSCs that gives rise to the androgen independent population. As an alternative explanation, survivor AR<sup>-</sup> CSCs would be fed by growth factors released by CAFs that allow their survival in the absence of androgens<sup>75</sup>. An additional possibility comes from the observations that CSCs plasticity confers to an ABCG2<sup>+</sup>/AR<sup>+</sup> population the ability to convert into ABCG2<sup>-</sup>/AR<sup>-</sup> in certain conditions<sup>76</sup>. Furthermore, the absence of AR during the ADT activates a STAT3-dependent inflammatory pathway that contributes to the development of castration resistance of prostate CSCs populations<sup>77</sup>.

### *2.4 Risk factors for prostate cancer*

Of the several known prostate cancer risk factors, the most important are age, ethnicity, genetic factors, and possibly, dietary factors.

1. Age. Detection of PCa increases with advanced age: 64% of PCa cases in USA are diagnosed in men older than 65 years, and 23% in men older than 75 years<sup>78</sup>.
2. Ethnicity. African American men or from the Caribbean with west African ancestry, and South American men have a higher incidence rate compared to European or North American. The lowest incidence is detected in the Asian population, where this neoplasia appears associated not only with genetic susceptibility but also with the diet, lifestyle and environmental factors<sup>79</sup>.
3. Genetic factors. Prostate cancer is among the most heritable tumors<sup>80</sup>. About 7 out of 10 PCa cases are supposed to be caused by susceptible inherited genes and this risk is increased in men with family history of breast cancer, especially those involving BRCA-1 BRCA-1 and BRCA-2 mutations that cause early alterations of the DNA damage repair (DDR) pathway (DDR)<sup>81</sup>.
4. Dietary factors. Different meta analyses studies with large cohort of men demonstrated that smoking<sup>82</sup>, diet<sup>83</sup>, obesity<sup>84</sup> and alcohol consumption<sup>85</sup> have a positive link with PCa risk and progression.

### 2.5 Diagnosis of prostate cancer

Presently, the diagnosis of PCa is based on the results obtained from serum PSA levels, digital rectal examination (DRE) and prostate biopsy. First, the serum levels of PSA are screened and, if levels are  $>10$  ng/mL, the physician performs a DRE examination. If DRE is positive, a prostate biopsy is usually performed. The diagnosis of prostate cancer is finally made by the pathologist when cancer lesions are observed in the biopsy. Additionally, the Gleason score given in the biopsy is a useful marker of prognosis. If no cancer is detected, the suggestion is to re-biopsy after 6 months<sup>86</sup>.

#### Serum PSA

Diagnosis of PCa has significantly increased since the establishment of the test for the prostate specific antigen (PSA) serum levels. PSA is encoded by *KLK3* gene and belongs to the kallikeins family, a group of serine protease genes located in chromosome 19q13.33 expressed in prostatic epithelial cells<sup>87</sup>. PSA function is to proteolyze semigelin and fibronectin, two components of the semen gel. In men's blood, PSA is present in a complexed form with the  $\alpha$ 1-antichymotrypsin and in a minor fraction as free PSA<sup>88</sup>. According to the EAU guidelines, when serum PSA levels are lower than 10 ng/mL, patients have a low risk of PCa, between 10 and 20 ng/mL the risk is medium, and if levels are above 20 ng/mL the risk is high<sup>89</sup>. Although this classification associates with an increased survival rate of patients with PCa, PSA is not an ideal cancer biomarker because its levels also increase in benign diseases, such as hyperplasia or prostatitis, generating false positives for the diagnosis of PCa<sup>86</sup>. One controversy has been shown in a trial where 15% of men with PSA levels below 10 ng/mL were at risk for PCa, and another 15% of these men at risk had high-grade disease<sup>90</sup>. The PSA levels were calculated considering the total PSA in blood, complexed and free. For the early detection of PCa, the use of the percentage of free PSA was considered reliable when total PSA levels were between 4 and 10 ng/mL. Recently, it has been discovered that within the free PSA different forms can be distinguished, among them the -2proPSA, a truncated precursor form of the proPSA. The -2proPSA was the most abundant in PCa extracts and so it has been included in a new test called the *prostate health index (phi)*, a mathematical formula that combines total PSA, free PSA and [-2]proPSA ( $[-2]proPSA/free\ PSA) \times \sqrt{PSA}$ ) and gives a single score that can be used to aid in clinical decision-making. The *phi* score suggests that men with a higher total PSA and [-2]proPSA

with a lower free PSA are more likely to have a clinically significant prostate cancer<sup>91,92</sup>. The Food and Drug Administration (FDA) has approved the use of *phi* for men with PSA levels between 4 and 10 ng/mL<sup>93</sup>.

Additionally, a similar prebiopsy test is the 4Kscore that, through an algorithm, performs a combined analysis of total, free, intact PSA and kallikrein-related peptide 2 (hK2), with age, natural history of the patient, prior DRE to predict the probability of aggressive PCa on biopsy<sup>94</sup>. An important advantage of this test is the prediction with good accuracy of PCa without performing a biopsy<sup>95</sup>, although presently the cost might discourage the use of the 4Kscore test in clinical practice<sup>93</sup>. Notwithstanding the debate about the use of PSA as a diagnostic marker, its blood determination remains a solid biomarker for the prognosis of PCa and for the response to the androgen deprivation therapy, ADT<sup>96</sup>.

### Digital rectal examination

The digital rectal examination (DRE) was the first tool applied for detection of PCa, before the development of PSA serum levels detection<sup>97</sup>. In this test the urologist analyzes the peripheral zone of the prostate by palpation and it is a widely used clinical tool. An abnormal result in the DRE increases between the 5 and 30% the PCa risk<sup>89</sup>.

### Prostate biopsy

The official diagnosis of PCa is confirmed by a transrectal ultrasound-guided needle biopsy (TRUS)<sup>98</sup>. Usually the TRUS is performed using an 18G needle and about 10-12 cores are taken from both parts of the gland starting from the apex to base<sup>89</sup>. TRUS-guided biopsy is recommended when PSA levels are elevated and/or DRE is suspicious<sup>98</sup>. If the first biopsy is negative, the guidelines suggest to re-biopsy a patient after the rising of the PSA serum levels, abnormal DRE, a positive magnetic resonance imaging (MRI), atypical small acinar proliferation or multifocal high-grade prostatic intraepithelial neoplasia<sup>99</sup>.

### Gleason grade

The Gleason grading system classifies prostate cancers based on the tumor histologic patterns. According to this system, tumors were classified with a score that ranged from 2 to 10<sup>100</sup>, where men with tumors presenting a higher Gleason score showed increased mortality rates<sup>101</sup>. The original and revised Gleason grading system with the identification of the 5

different patterns, are shown in **Figure 6A**<sup>101</sup> (Gleason 1964):

Pattern 1 consists in well differentiated uniform single glands, closely packed in masses with relatively circumscribed boundaries;

Pattern 2 was characterized by well-differentiated but more variable single glands, slightly spaced apart, boundaries of tumor less well circumscribed;

Pattern 3 presented moderately differentiated glands that may range from small to large, growing in spaced-out infiltrative patterns, may be papillary or cribriform;

Pattern 4 was raggedly infiltrating, fused-glandular tumor frequently with pale cells, may resemble hypernephroma of kidney;

Pattern 5 was an anaplastic carcinoma with minimal glandular differentiation, diffusely infiltrating prostatic stroma.

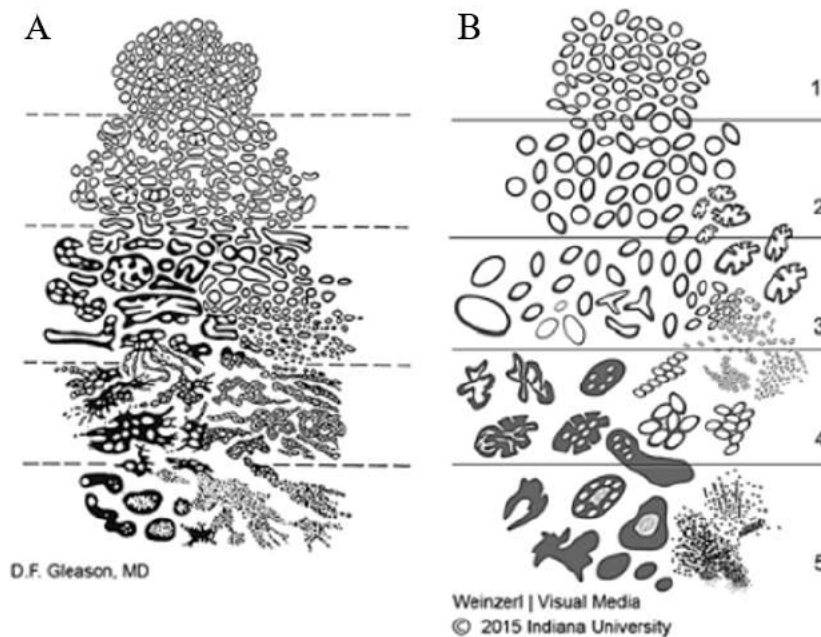


**Figure 6. Schematic diagrams of prostate adenocarcinoma grading system.** (A) Original, (B) updated schematic diagrams of prostate adenocarcinoma grading system, from Epstein et al.<sup>102</sup>

Prostate tumors show a very heterogenic phenotype, thus the Gleason score attempts to represent this heterogeneity. The score, given by the pathologist, results from the addition of the most frequent pattern observed and the second most frequent one: for example, Gleason score  $4+3=7$ . Although the actual version of this grading system differs significantly from

the original, the Gleason score is still a used prognostic tool in PCa<sup>103</sup> (**Figure 6B**). The new system, revised in 2014 by the International Society of Urological Pathology (ISUP), established five groups, group 1 to 5, adjusting PCa grading with other carcinomas grading system, as indicated in **Table 1**<sup>102</sup>.

**Table 1.** The new classification of tumor stages in prostate carcinomas.

Gleason score	Group
6 (3+3 or 3+2 or 2+3 or 2+2)	1
7 (3 + 4)	2
7 (4 + 3)	3
8 (4+4 or 3+5 or 5+3)	4
9-10	5

As shown in **Table 1**, in the new classification the score 7 is divided into 2 groups, depending on whether the most frequent pattern is 3 or 4. According to the original grading, cribriform glands were considered with histological pattern 3, however it was demonstrated that this histology was linked with a more aggressive PCa in 84% of the cases. Nowadays, cribriform glands are included in Gleason pattern 4 instead of 3, in order to clarify the prognosis<sup>102</sup>.

### Clinical stage

The clinical stage is based on the Tumor Node Metastasis (TNM) classification, recently updated in the European Association of Urology Guidelines<sup>89</sup>. The T value ranges from 1 to 4 with a more accurate definition of the phenotype within each category. N indicates tumor invasion in the lymph nodes (N1) or not (N0). Finally, M1 is consistent with the presence of metastasis and that can be to the lymph nodes (M1a), the bone (M1b) or other organs (M1c)<sup>104</sup>.

### 2.6 Therapies for prostate cancer

Men with localized tumors have a low or very-low risk for PCa and are selected for active surveillance, which is monitored with serum PSA tests and prostate biopsies. If the risk increases, standard treatments are radical prostatectomy, external-beam radiotherapy and brachytherapy<sup>105</sup>. These patients have a very good survival rate (>95%)<sup>15</sup>. However, for men experiencing recurrence after radical prostatectomy or when metastases are detected at diagnosis, chemical castration (ADT) is applied. Patients with metastatic disease have a survival rate of 29%<sup>15</sup>. ADT can be achieved by suppression of luteinizing hormone-releasing hormone (LHRH) production, through the administration of anti-androgens, or adrenal androgen inhibitors or estrogens<sup>106</sup>. These treatments result in a significant decrease in testosterone and PSA levels in blood and tumor mass<sup>107</sup>. However, after 1 to 5 years, up to 40% of patients eventually develop a castration resistance disease and metastasis<sup>108</sup>. Before 2010, the mainstay treatment for CRPC was docetaxel, a taxane, that prevents the depolymerization of microtubules and blocks mitosis, in combination with prednisone, an anti-inflammatory corticoid that prevents DNA synthesis (**Figure 7**)<sup>109</sup>. This therapy inhibits cancer growth for a few months, after which tumors develop resistance to docetaxel<sup>110</sup>. Resistant tumor cells show associated upregulation of several members of the ATP-binding cassette (ABC) transporters and expression of alternative isoforms of tubulins<sup>111,112</sup>. Three trials compared the action of ADT alone or in combination with docetaxel in men with metastatic aggressive prostate cancer: patients treated with the combined therapy showed significantly improved overall survival<sup>113</sup>. This combination is currently being applied in patients with naïve metastatic prostate cancer.

More recently, alternative drugs have been developed in order to target more specifically prostate tumors subtypes and bypass docetaxel acquired resistance. FDA approved new second generation of taxanes, as cabazitaxel, selected for its poor affinity to the ABCB1 transporter P-glycoprotein (P-gp), an adenosine triphosphate (ATP)-dependent drug efflux pump, known to decrease anticancer drugs accumulation<sup>114-116</sup>.

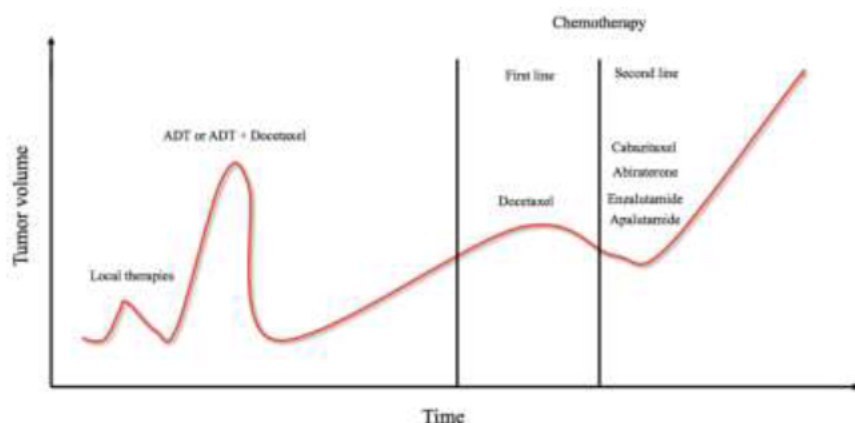


**Figure 7.** Schematic representation of the different phases of prostate cancer progression with associated therapies.

Interestingly, CRPC patients have been shown to be androgens and AR-dependent, with increased AR levels and activity, and increased conversion of steroid precursors<sup>117</sup>. Therefore, a third line of new drugs approved by FDA includes compounds that target androgens or AR, such as abiraterone, enzalutamide and apalutamide.

Abiraterone is a CYP17 inhibitor that represses the production of androgens from prostate cells, testes, and adrenal glands<sup>118</sup>. In the phase III trial LATITUDE, results show that the addition of abiraterone in men with mCRPC, treated with prednisone and ADT, improved the overall survival<sup>119</sup>.

On the other hand, enzalutamide and apalutamide directly and specifically inhibit the AR, preventing its translocation to the nucleus and its binding to androgen response elements. This class of compounds is generally well-tolerated and contributes to increase overall survival and decrease metastasis risk. Nowadays, they are administrated both to naïve-patients and docetaxel pre-treated men<sup>120</sup>.

### 3. Models to study prostate cancer

#### 3.1 *In vivo* models

Among the animal models available, those that spontaneously develop PCa are dogs, but due to expensive price and ethical concerns, researchers have preferred mice as models to study prostate cancer<sup>121</sup>. Mice prostate substantially differs from human prostate in its at macroscopic level but also for the lower content of basal cells and stroma. In fact, the murine prostate is not a unique organ as in men, but there are four lobes are paired right and left and each has a distinct anatomy and histology<sup>122,123</sup>. The most important histological difference

between the prostate of both species lies in the stromal component, which in mice it is sparse with minimal smooth muscle cells<sup>124</sup>.

However, genetic manipulation techniques allowed the development of a number of genetically engineered mice (GEM) transgenic models for PCa<sup>125</sup>. Important GEMs are the TRAMP mice (Transgenic adenocarcinoma of the mouse prostate) and LADY mice (Long probasin Promoter) that overexpress the oncogenic T protein of the virus SV40 under direction of the probasin promoter, and are widely selected to study tumor progression of the prostate. Mice develop PCa at 18-24 weeks of age in the TRAMP model, and at 33 weeks in the LADY model with metastasis in lymph nodes, liver and lung. These models have an important limitation because, unlike human tumors, tumorigenesis is driven by the overexpression of the viral oncogenic T protein that leads to the formation of androgen independent tumors, preventing the study of tumorigenesis and the development of hormone resistance disease<sup>126</sup>. One reliable transgenic model to study PCa progression targets the *PTEN* gene (*PTEN*<sup>+</sup>/*PTEN*<sup>-</sup> mouse), because the loss of this gene is an early event present in more than 50% of PCa patients. However, the *PTEN*<sup>+</sup>/*PTEN*<sup>-</sup> mouse fails to develop metastasis in the majority of the cases, while the *PTEN*/*PTEN* knockout is lethal at embryonic stage<sup>126</sup>. This model has been used in combination with other genetic lesions that are frequent in prostate tumors to obtain the development of adenocarcinoma and metastasis, for example loss of *Nkx3.1*, *TP53*, or *SMAD4*<sup>123</sup>.

An additional powerful very useful mouse model is the xeno-transplantation of human PCa cell lines into immunosuppressed mice. The subcutaneous xenografts are the easiest to perform and allow the introduction of almost a limitless amount of cancer cells. However, the reported take rate is low, from 3% to a maximum of 58% and mostly without formation of metastasis<sup>127</sup>. The orthotopic xenograft model was developed, and widely used, in order to study the factors implicated in tumor development and metastasis progression, despite the technical problems for cell implantations and the limited amount of tumor cells that can be introduced<sup>128</sup>. Finally, the xenograft of tumor cell lines into the sub-renal capsule is also successfully developed in PCa, with the principal advantage of recovery more than the 93% different phenotypes occurring in PCa, even though these models are not suitable for the study of oncogenic drivers and metastatic genes<sup>129</sup>.

More recently, the xenografted mice models have been expanded by direct transplant into mice of human tissues or cells derived from patients<sup>130</sup>. This model of patient derived xenograft (PDX) allows to recapitulate the heterogeneity of human tumors, maintaining gene



expression patterns and it represents one of the most used *in vivo* models to study the effects of new drugs<sup>131</sup>. PDX models have been developed in many cancer types, including colon<sup>132</sup>, breast<sup>133</sup>, and cervical cancer<sup>134</sup>. In prostate cancer they are not extensively used because of their described long latency period, ranging from 12 months up to 3 years, among other problems, including difficult management, the requirement of a substantial amount of tissue from the patient, great difficulty to be grown *in vitro*, and costs<sup>127,135</sup>.

### 3.2 *In vitro* models

*In vitro* models are a powerful tool to analyze the molecular alterations that occur in cancer cells that dictate their behavior in cancer progression and the acquisition of resistance to therapeutic drugs. Reliable *in vitro* models are crucial, especially for high throughput screenings to test and define the efficacy of newly developed compounds. However, despite the numerous cell lines presently available to study major types of human cancers, the establishment of cell lines from prostate tumors has proven particularly difficult to obtain, and the few existing cell lines lack many of the characteristic genetic lesions commonly observed in human prostate tumors<sup>136-138</sup>.

As mentioned, the majority of patients develop a CRPC disease, after 1-3 years. Once patients' tumors are castration resistant, their ability to resist to second-line therapies increases. Therefore, the identification of more effective and specific treatments continues as one major challenge in research in prostate cancer<sup>121</sup>.

The most widely used cell lines are the LNCaP, Du145 and PC3 prostate cancer cells, all derived from metastatic nodules to different organs and therefore poorly representative of the primary tumor heterogeneity<sup>139-141</sup>. Thus, cell lines established from primary tumors would be very useful models to study the progression of prostate cancer to metastasis and to androgen resistance<sup>142-146</sup>.

Recently, few new PCa cell lines have been developed, both from metastasis and primary tumors and improve the representation of the heterogeneity of PCa<sup>147</sup>. In the following lines, a short description of the most used cellular models and their phenotypes is presented.

#### LNCaP

This human prostate epithelial cell line was obtained in 1977 through a needle biopsy of a left supraclavicular lymph node from a Caucasian patient with metastatic prostate

carcinoma. LNCaP cells show a slow growth ratio with a doubling time around 60-72 hours. *In vivo* they display an engraftment of 50% and a tumor doubling time of 86 hours<sup>121</sup>. They have a karyotype of 33 to 91 chromosomes and are androgen sensitive because of the positive expression for the androgen receptor (AR), estrogen receptor (ER) and prostate specific antigen (PSA). LNCaP cells present a peculiar mutation in the AR, T877A, that increases the promiscuous affinity between AR and several steroids. In addition, they express luminal cytokeratins, a wild type p53 while PTEN is inactive.

### Du145

Du145 cells were derived in 1975 from a brain metastasis from a Caucasian male with mPCa. The rate of growth is higher than LNCaP cells with a doubling time of 34 hours. *In vivo*, Du145 cells are able to form an adenocarcinoma of grade II and metastasis to several organs<sup>121</sup>. This cell line is androgen resistant and negative for the expression of PSA. Du145 present the mutations P223L/V274F in *TP53*,<sup>148</sup> an heterozygous *PTEN*<sup>149</sup> and homozygous for C2143A in *RBI*, that leads to a loss of function<sup>150</sup>. They are an hypotriploid cell line with a karyotype of 58 to 63 chromosomes with rearrangements in the 70% of the 22 chromosomes. The Y chromosome is abnormal through translocation to an unidentified chromosomal segment. The X chromosome is present in single copy<sup>121</sup>.

### PC3

These cells derived from a bone metastasis of a grade IV prostatic adenocarcinoma from a Caucasian man. PC3 cells have a similar doubling time of Du145, of about 33 hours. They are castration resistant and do not express AR or PSA. These cells show a transit amplifying epithelial phenotype co-expressing CK5, CK8 and CK18. They contain molecular alterations in *PTEN* (deletion) and a frameshift mutation in *TP53* that provokes a premature stop codon<sup>121</sup>. Recent studies highlighted that PC3 cells are more similar to neuroendocrine or small prostate carcinoma cells, rare but very aggressive subtypes of prostate cancer<sup>151</sup>. PC3 cells are a triploid cell line with a modal number of 62 chromosomes.

### VCaP

These cells, derived from a vertebral metastasis, are of epithelial origin with high AR and PSA expression. Cells are androgen sensitive *in vitro* and *in vivo*. Their almost triploid genome is characterized by the presence of the gene fusion *TMPRSS2-ERG*<sup>152</sup>. Although

these cells are very difficult to grow *in vitro*, they have been used in some studies of castration resistance mechanisms<sup>153-155</sup>.

### NCI-H660

This cell line is derived from a lymph node metastasis of small cell cancer originated in the prostate. It is composed of androgen independent luminal epithelial cells and of neuroendocrine cells, that resemble small cell lung carcinoma<sup>156</sup>.

### MDA PCa 1, 2a and 2b

These cells derived from bone metastasis, are good androgens responders and share many features with LNCaP<sup>157</sup>. The bone is the most frequent site of PCa metastasis and this model, although not widely used, has been exploited to study the role of AR signaling in the metastatic process to bone.

### 22Rv1

22Rv1 cells were derived from a xenograft that was serially propagated in mice after castration-induced regression and relapse of the parental, androgen-dependent CWR22 xenograft. As the contamination of stromal mouse cells dominated the culture, 22Rv1 were obtained after sorting for CD44 marker and co-culture with irradiated feeder cells. They express luminal prostate markers, PSA and are androgen dependent<sup>158</sup>.

## **4. Prostate Tumor Over-expressed 1 (PTOV1)**

The gene *PTOV1*, discovered in our laboratory, encodes for a protein with oncogenic functions. The gene is located in chromosome 19 and encodes for a protein structured into two highly homologous sequence domains arranged in tandem, named PTOV-A and PTOV-B domains<sup>159</sup>. High levels of PTOV1 have been found associated with areas of malignant carcinoma, HG-PIN and AAH, while in normal prostate tissue and benign prostate hyperplasia its expression is low or undetectable<sup>160,161</sup>. After its discovery, several studies identified a correlation between its overexpression and cancer progression not only in the prostate but also in breast, liver, laryngeal, urothelial, ovary, colon and bladder cancers<sup>162-167</sup>. The functions of PTOV1 have been recently reviewed<sup>168</sup>. Basically, PTOV1 is able to shuttle between nucleus and cytoplasm, its over-expression induces cell proliferation, tumor growth, and increases the motility of PCa and breast cancer cells *in vitro*, and metastasis *in*

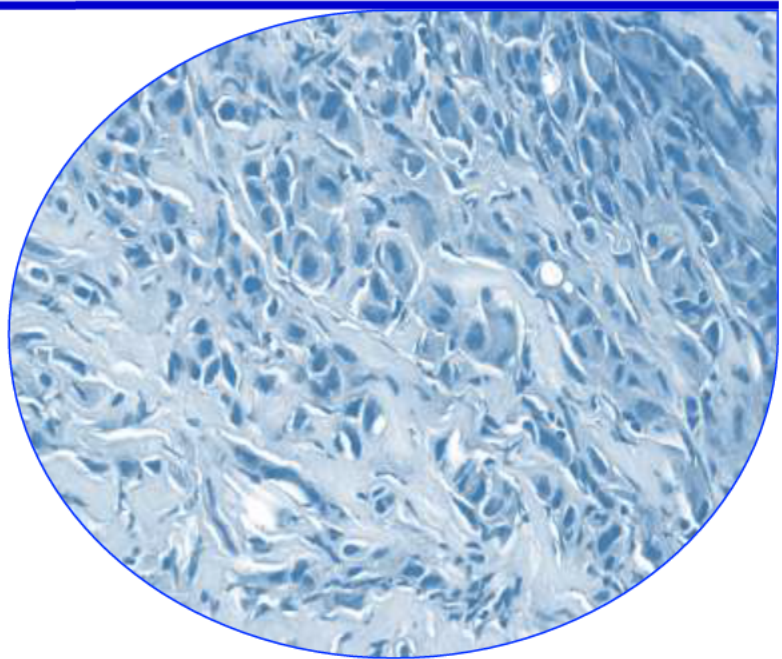
*in vivo*<sup>169,170</sup>. Mechanistically in the cytoplasm, PTOV1 was shown to interact with the receptor of activated protein C kinase 1 (RACK1) and positively regulate protein synthesis, in particular the translation and activity of the JUN transcription factor required for the induction of cell invasion<sup>169</sup>. Moreover, it has been demonstrated that PTOV1 favors the lipid-rafts protein flotillin-1 shuttling from the cytoplasm to the nucleus during the cell cycle. This action is associated to increased proliferation<sup>172,173</sup>. In the nucleus, PTOV1 was shown to decrease Notch signaling in metastatic prostate tumors by repressing the transcription of two major Notch target genes *HES1* and *HEY1*, an action that was associated to active histone deacetylases<sup>171</sup>. Recently, PTOV1 expression was shown to confer docetaxel resistance in prostate cancer cells through the direct activation of expression of *ABCB1*, *CCNG2*, *ALDH1A1* and epithelial-mesenchymal transition (EMT) factors<sup>167,174</sup>. In breast cancer cells, PTOV1 was found to repress Dickkopf 1 (DKK1) expression, a major secreted Wnt signaling antagonist that resulted in the activation of downstream Wnt/ $\beta$  catenin signaling and cancer progression<sup>170</sup>. The protein (416 amino acids) contains two nuclear localization signals, one in each domain<sup>168</sup>. In addition, PTOV1 was described to contain a nucleic acids binding region was described in the 43 amino acids sequence at the N-terminal identified as a new type of AT-hook motif, or extended AT-hook (eAT-hook). This eAT-hook is 10–15 amino acids longer and differs from the canonical motif<sup>175</sup> (**Figure 8**).



**Figure 8. Protein structure of PTOV1.** From Maggio V., Canovas V. et al.<sup>167</sup>

The protein structure of PTOV1 shares similarities with other proteins that interact with nucleic acids, like the  $\beta$ -barrel sequence present in Ku (Ku70/Ku80) heterodimers and the SMRT/HDAC1-associated repressor protein (SHARP). These proteins have a key role in mechanisms such as double-stranded DNA break repair and transcriptional regulation, respectively<sup>168</sup>. These similarities suggest that PTOV1 may function as an epigenetic factor that triggers the recruitment of chromatin regulators and transcription factors that regulate gene expression<sup>167</sup>.

## **CHAPTER 2: HYPOTHESIS**





Metastatic prostate cancer is the third leading cause of death for cancer in Europe and North American men<sup>15</sup>. Gold standard therapy is the androgen deprivation, although taxanes and newly developed anti AR drugs can temporarily bypass the resistance to castration, the CRPC is a mortal disease and remains the greatest clinical challenge of prostate cancer<sup>176</sup>. Significant effort has been devoted to discover efficient treatments for these patients and a number of specific inhibitors to some signaling pathways have been identified. However, one important limitation to the challenge of curing the CRPC disease is the very low number of suitable models available. In fact, *in vivo* models able to recapitulate the heterogeneity of prostate tumors are scarce and have several setbacks<sup>137</sup>. Similarly, most *in vitro* models are derived from metastasis, thus poorly represent the heterogeneity of human prostate tumors. Additionally, a successful therapy for PCa would need to be applied at early stages and new markers for the prompt identification of tumors, or able to predict CRPC, together with more specific therapeutic targets are prerequisites. Our own previous studies toward the identification of early diagnostic markers for prostate cancer suggested that PTOV1 is a good discriminating marker for HGPIN associated to PCa, that is overexpressed in more aggressive and metastatic disease. Furthermore, our functional studies on the role of this protein in tumors resistant to treatments suggest that PTOV1 is a good target to eliminate more aggressive cancer cells.

In the present thesis, we formulated the following hypotheses:

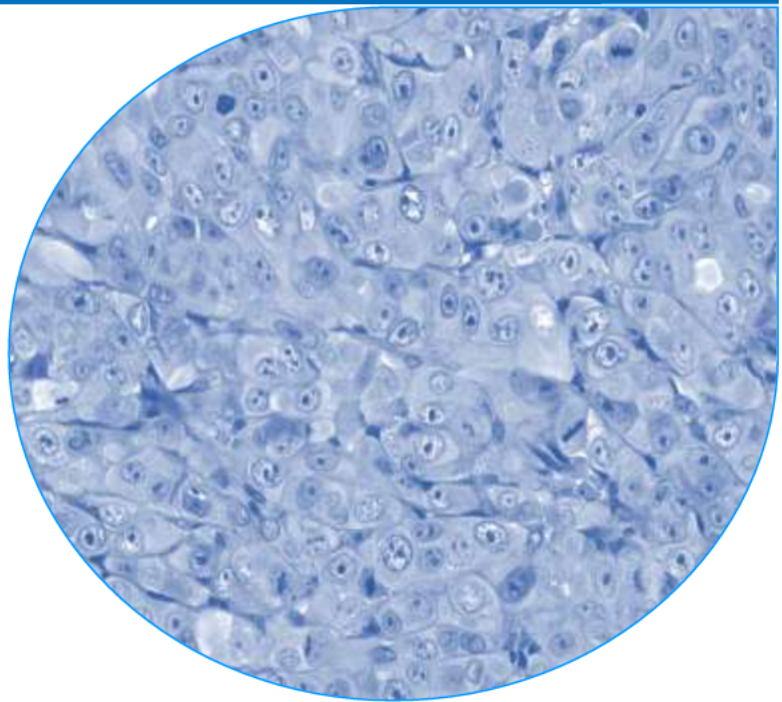
- 1) *Ex vivo* cultures derived from primary hormone-naïve tumors may better represent the heterogeneity of prostate tumors, be useful models to study their biology, and be used to discover and study new more efficient therapies.
- 2) The original untreated tumor contains rare subpopulations of CSCs, responsible for tumor progression and resistance. These cells may be present in a representative small tissue biopsy of the primary tumor and maintained and expanded when cultured *ex vivo*.
- 3) PTOV1 promotes the resistance of prostate cancer cells to chemotherapy by direct binding to regulatory regions of key genes whose expression is required for cells growth in the presence of the drug.





## **CHAPTER 3: AIMS OF STUDY**

---





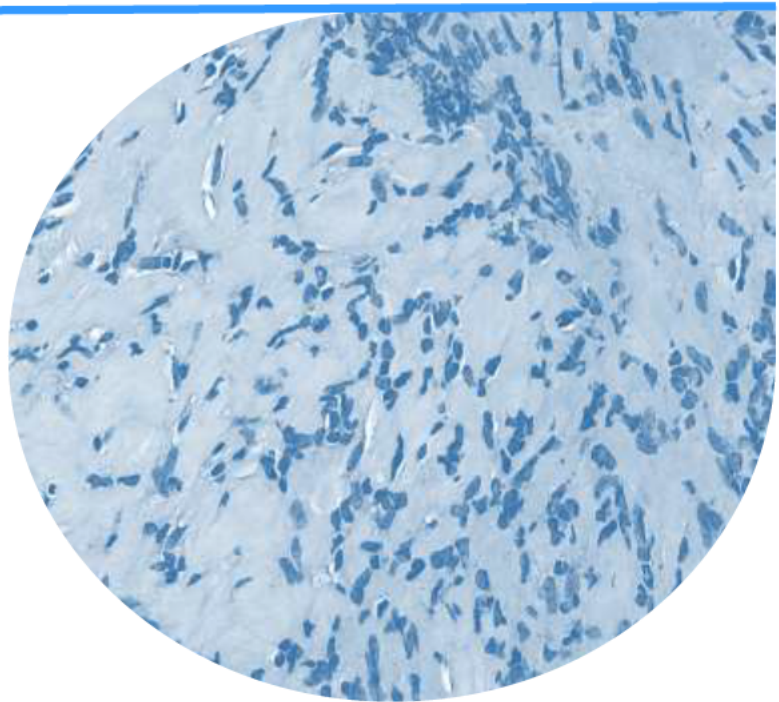
The main objective of this thesis is to obtain a simple *in vitro* model to reproduce the characteristics and behavior of prostate cancer, its progression and recurrence, to be used in molecular studies and *in vitro* drug screenings. A second objective is to analyze the mechanisms of the oncogenic protein PTOV1 in the promotion of cancer resistance to chemotherapy.

Specific objectives:

1. Establishment of *ex vivo* cultures from primary human prostate tumor tissues (radical prostatectomy or needle biopsy) to obtain models representing *in vitro* the PCa heterogeneity.
2. Validation of these *in vitro* models as representative of the primary tumor tissues by analysis of the genomic lesions in the original tumor tissue and the corresponding *ex vivo* tumor cultures.
3. Demonstration of the usefulness of these cultures to study the characteristics of the primary tumors, determining their: phenotypic characterization, abilities to proliferate, invade, and develop resistance to androgen deprivation. Finally, their response to new anti-cancer drugs and combination thereof will also be tested.
4. Analyses of the CSCs populations present in prostate cancer cell lines and explant tumor cultures for their response to drugs directed to eliminate the resistant cells.
5. Analysis of the role of PTOV1 in the induction of resistance to chemotherapy in prostate cancer cells by studying the mechanisms by which it regulates the *ALDH1A1* and *CCNG2* expression.



# **CHAPTER 4: MATERIALS AND METHODS**





## 1. Cellular cultures

### 1.1 Cell lines

All cells lines were purchased from the American Type Culture Collection (ATCC) repository. The principal characteristics of these cell lines are reported in **Table 2**.

**Table 2. Principal genetic and phenotypic features of cell lines.**

Cell line	Race	Source	Disease	AR response	<i>PTEN</i>	<i>TP53</i>	<i>RB1</i>	karyotype	Doubling time (hours)
HEK293T	Unknown	Kidney	-	-	-			-	24
LNCaP	Caucasian	Lymph node	Metastatic prostate carcinoma	+	-	wt	wt	76-91	60-72
Du145	Caucasian	Brain	Metastatic prostate carcinoma	-	wt	mut	-	64	34

LNCaP androgen independent (AI) and androgen dependent (AD) cells were obtained from Anna C. Ferrari's laboratory (Division of Neoplastic Diseases department, Mount Sinai School of Medicine in New York, USA). After a continuous culture in a medium deprived of androgens for 6 months (RPMI-1640 and 10% charcoal stripped heat-inactivated FBS), the AI subline was obtained.

The docetaxel-resistant cellular models Du145 was kindly provided by Dr. Begoña Mellado (Laboratory and Medical Oncology Department, Hospital Clínic in Barcelona, Spain). DR-Du145 cells were selected starting at 5 nM of docetaxel with a gradual increase of the dose every 72 hours for 1 year. Selected cells were cultured with a scale of docetaxel concentration from 10 to 250 nM. As control, parental Du145 cells were exposed to the same dose scale of vehicle, DMSO.

### *1.2 Cell culture methods and reagents*

All cells were cultured at 37°C in an atmosphere of 5% CO<sub>2</sub>. HEK293T cells were cultured in DMEM, while LNCaP and Du145 cells were cultured in RPMI-1640. All media contained 10% fetal bovine serum (FBS), 2 mM L-glutamine, 100 U of penicillin/mL, 100 µg of streptomycin/mL, and 0.1 mM non-essential amino acids (all from BioWest). LNCaP AI subline was cultured in RPMI-1640 containing 10% charcoal-stripped (Sigma Aldrich), heat-inactivated FBS plus the above supplements, whereas docetaxel resistant cell lines were maintained with 2.5 nM of docetaxel. To study PTOV1 effects on Wnt signaling, activation of this pathway was achieved by Wnt3a conditioned medium, kindly provided by Diego Arango (Biomedical Research in Digestive tract tumors laboratory, Vall d'Hebron Institute of Research in Barcelona, Spain). Wnt3a medium was originally obtained from mouse L1-Wnt3a (ATCC® CRL2647TM) cells, cultured in DMEM supplemented with 10% FBS and 0.4 mg/mL G418. After 4 days, medium was collected, filtered and store at 4°C. Fresh medium was added to cells and cultured for another 3 days. Medium was collected, filtered and mixed with the first batch of medium. For long storage, Wnt3a-conditioned medium was store in aliquots at -20°C. Du145 cells were cultured for 24 h with Wnt3a-conditioned medium diluted 1:1 with supplemented RPMI medium. The JNK inhibitor II (Calbiochem) and iCRT14 (Tocris Bioscience) inhibitor of Wnt signaling were also used.

For cryopreservation, two million cells were frozen slowly in 1 mL of cold FBS plus 10% DMSO and they were immediately placed on ice. Cells were stored 1 day at -20°C, then stored at -80°C for a few days and for long storage, vials were transferred to a liquid-nitrogen freezer. For the recovery of cryopreserved cells, frozen vials were thawed rapidly in a 37°C water bath and immediately diluted in pre-warmed complete culture medium. Cells were centrifuged at 400 xG for 5 min, suspended in complete culture medium and seeded into an appropriate flask.

### *1.3 Production of lentiviruses and cellular transduction*

Lentiviruses have become increasingly tools for the integration of transgenes or for stable RNA interference, using sequence-specific degradation (RNAi). We have used stable RNAi to knockdown the expression of PTOV1 in different prostate cancer cell lines. Lentiviral vectors (LV) belong to the family of retroviruses derived from immunodeficiency virus (HIV). Lentiviruses are composed of a single positive-sense strand. After the entry into a



cell, they undergo a reverse transcription into double-stranded DNA able to integrate into the host genome. Using the HEK293T model, it is possible to produce the lentiviral particles through a transient transfection of the LV of interest together with two vectors encoding for the envelope and the packaging proteins. The vector encoding the insert of interest is flanked by long terminal repeats (LTRs) that favor the integration in the host genome. To improve safety, transfer vectors are all replication incompetent. The envelope vector (*env*) encodes for the envelope glycoprotein. The most used glycoprotein is the G protein of the Vesicular Stomatitis Virus. The packaging plasmid contains the genes for the internal structural and enzymatic protein (*gag* and *pol*, respectively). Briefly,  $4 \times 10^6$  of HEK293T cells were seeded in four 10 cm culture dishes in complete DMEM medium. After 24 hours, cells were transfected using CaPO<sub>4</sub> precipitation method. Two tubes were prepared:

Tube A: Lentiviral plasmid (12 µg), packaging plasmid (8 µg), envelope plasmid (4 µg), 60 µL 2.5 M CaCl<sub>2</sub>, and sterile water were added to complete a final volume 500 µL.

Tube B: 500 µL of 2 times concentrated (2X) Hepes Buffered Saline (HBS) solution pH=7 (280 mM NaCl, 1.5 mM PO<sub>4</sub>, 50 mM HEPES) were added to a 50 mL falcon tube.

The content of tube A was added to tube B, drop wise and slowly while constantly bubbling the solution in tube B. The mixture was incubated 20 minutes at room temperature (RT). One mL of the transfection mix was added to cells in drops. Plates were incubated six hours at 37°C. Then the medium was removed, 10 mL fresh complete medium were added, and plates were incubated O/N at 37°C. We collected three times the medium containing lentiviral particles, at 24, 48 and 72 hours. The first supernatant was collected and replaced with 6 mL of fresh complete medium for the second and the third collection. To transduce the lentiviral particles supernatants were filtered through a 0.22 µm strainer and ultracentrifuged 1.5 hour at 89,000 xG at 4°C. The pellets obtained were resuspended in 1 mL of medium and stored at -80°C.  $7 \times 10^5$  cells were seeded in a 10 cm culture dish. After 24 hours, 1 mL of lentiviral particles was added to 7 mL of complete medium supplemented with 10 µg/mL of polybrene, to facilitate transduction. This medium was added to cells for 24 hours, then replaced with complete fresh medium. 1 µg/mL of puromycin was used to select the transduced cells for at least 4 days.

### *1.4 Cells transfection*

The transfection is a wide used method to deliver sequences of DNA or RNA into cells for the study of gene expression. With a transient transfection, it is possible to introduce many copies of the exogenous gene of interest between 24 and 96 hours. Cells were seeded in an appropriate concentration to reach 80% confluence the day of transfection. For transient transfections, we used the CaPO<sub>4</sub> precipitation method preparing two tubes:

Tube A: Transfer plasmid (3 µg), 60 µL 2.5 M CaCl<sub>2</sub>, and sterile water were added to complete a final volume 500 µL and mixed well.

Tube B: 500 µL of 2 times concentrated (2X) Hepes Buffered Saline (HBS) solution pH=7 were added to a 50 mL falcon tube.

The following procedure was the same reported for the lentivirus production, described above. Plates were swirled and incubated 6 hours at 37°C. Then the medium was removed, 10 mL fresh complete medium were added, and plates were incubated O/N at 37°C for 72 hours.

### *1.5 Primary prostate tumors culture*

#### **From Radical Prostatectomy tissues**

Radical prostatectomies were resected from the Unit of Urology of Vall d'Hebron Hospital in Barcelona, Spain. Tissues were collected in medium DMEM-F12 (Biowest) plus 250 ng/mL of Amphotericin B and 10 ng/mL of Gentamicin (Sigma Aldrich) (named Basic Medium). With the collaboration of the Unit of Pathological Anatomy of Vall d'Hebron Hospital, a tumor focus was cut. Then, half of the tissue was deep-frozen at 80°C for the extraction of RNA while the other part was used for the culture. Tissue was minced with a scalpel in DMEM-F12 medium supplemented with enzymes (collagenase I and hyaluronidase). Thus, tissue was incubated at 37°C in a shaker for 30 minutes to allow the enzymatic digestion. Then, tissue was washed for 10 minutes at 240 xG, filtered with a 40 µm strainer to enrich for single cells and remove the undigested pieces. Single cells were plated on top of collagen coated dishes in a complete medium. The complete medium was prepared with DMEM-F12 containing 2 mM of l-glutamine, 100 U of penicillin/mL, 100 µg

of streptomycin/mL, 0.1 mM of non-essential amino acids, 7% of FBS, 6 mg/mL glucose, 1  $\mu$ M hydrocortisone, 0.97  $\mu$ g/mL putrescine, 10  $\mu$ g/mL transferrin, 3  $\mu$ M sodium selenite, 2.5  $\mu$ g/mL insulin. 200 ng/mL of vitamin A, 200 ng/mL of vitamin E (all from Sigma-Aldrich), 20 ng/mL of epidermal growth factor (EGF) and 10 ng/mL of basic fibroblast growth factor (bFGF) (both from Tebu-bio) were complemented fresh to the medium. After the first passages, in order to eliminate the fibroblasts component, cultures were treated for 10 days with 1 mg/mL Geneticin (G418) (Sigma Aldrich).

### **From needle biopsy tissues**

Fresh needle biopsies were obtained at the Unit of Urology of Vall d'Hebron hospital in Barcelona (Spain) from naïve patients with positive DRE and PSA higher than 50 ng/mL. From each patient, 5 biopsies were selected for the culture and 2 to further extraction of RNA. Biopsies for RNA were collected in RNA later (Quiagen), stored for 24 hours at 4°C. Then, RNA later was removed, and tissue were deep-frozen at 80°C. Biopsies for culture were collected in Basic Medium and cut into pieces lower than 1 mm<sup>3</sup> with a scalpel. Thus, tissue was centrifuged for 10 minutes at 240 xG and cut pieces were seeded with half of the complete medium on p6 well dishes or t25 cm<sup>2</sup> flask to facilitate the adhesion. Both types of dishes were pre-treated for 1 hour at 37°C with collagen I and with Poly-D-lysine 1x for another hour. After 24 hours, complete medium was added to the dishes to reach the final volume. Finally, cells were allowed to come out the pieces and fill the dish. In the first passage, pieces were trypsinized and seeded again to allow the eventual adhesion of cells. After the first passage, the purification of epithelial cells from fibroblasts started adapting a protocol of a differential trypsinization<sup>177</sup>. The first trypsinization was performed with TRYPLE (Biowest) 0.5% in PBS 1x at room temperature until fibroblasts, which have a lower adhesion than epithelial cells, detached and could be collected. The second trypsinization, to collect the epithelial cells, was performed with TRYPLE at 37°C. After the collection, epithelial cells were centrifuged at 135xG for 5 minutes and seeded in complete medium.

## **2. Functional assays**

### *2.1 Proliferation assay*

To analyze the cellular rate of growth, we stained adherent cells with crystal violet dye, that

binds to proteins and DNA. Died cells are not stained because of their loss of adhesion. For these assays, cells ( $2 \times 10^3$  cells/well) were seeded on 96-wells plates in octuplicates. At the indicated time points, cells were fixed in 4% formaldehyde solution, washed with PBS 1X and stained with 0.5% crystal violet. Crystals were dissolved with 15% acetic acid and optical density was read at 590 nm.

### 2.2 Cytotoxicity assay

Cells ( $5 \times 10^3$  cells/well) were seeded on collagen-coated 96-well plates in sextuplicates. After 24 hours, cells were treated with vehicle (control) or the drug at different concentrations for 72 hours. At the indicated time points, cells were fixed and processed as described for proliferation assays. Docetaxel (Sigma-Aldrich) and Cabazitaxel were diluted in DMSO at 1 mg/mL and aliquots were stored at  $-20^\circ\text{C}$ , Galiellalactone at 0,5 M in PBS 1x, MDN-90 and MEGR756B at 20  $\mu\text{M}$  in distilled sterile water. As docetaxel and cabazitaxel are thermo labile, complete medium with the drug was replaced every day.

### 2.3 Spheres formation assay

Cancer stem cells (CSCs) or tumor initiating cells (TICs) are able to form, under specific conditions, a characteristic tumor sphere. For their identification and analysis, we set up a protocol of spheres formation culturing cells in serum-free medium and non-adherent conditions. In particular, cells were seeded ( $4.5 \times 10^6$  Du145 cells/dish or  $2 \times 10^6$  LNCaP AD cells/dish or  $1 \times 10^6$  LNCaP AI cells/dish) in 150 cm culture dish pre-treated with poly-HEMA 1.2% (poly2hydroxyethyl methacrylate) in 20 mL of stem cells enrichment medium. Poly-HEMA provide the ultra-low attachment to the dish. Poly-HEMA (Gibco) was dissolved in 95% ethanol at  $50^\circ\text{C}$  and filtered with 0.2  $\mu\text{m}$  strainer. Dishes were treated twice with poly-HEMA, dried and washed with PBS 1x before the use. The medium was prepared from DMEM-F12 containing 1% methyl cellulose, 60  $\mu\text{g/mL}$  glucose, 1  $\mu\text{M}$  hydrocortisone, 1  $\mu\text{g/mL}$  putrescine, 10  $\mu\text{g/mL}$  transferrin, 3 nM sodium selenite, 2.5  $\mu\text{g/mL}$  insulin, 10 ng/mL  $\beta$ - FGF, 20 ng/ml EGF 5 U/mL, heparin (Sigma Aldrich), and 0.4% B27 (Invitrogen). Cells were fed with fresh media every three days and allowed to grow for 7 days. The number of spheres were then counted and expressed as ratio of spheres/1000 plated cells (Sphere Forming Efficiency, SFE).

### 3. RNA manipulation

#### 3.1 Total RNA extraction

Total RNA was extracted with the RNeasy mini kit (Qiagen) according to manufacturer's instructions. This kit allows the purification of total RNA from small amounts of starting material. Through a silica-gel based filter and a high salt buffer, it is possible to purify up to 100 µg of RNA longer than 200 bases. Briefly, cells or tissue are lysed and homogenized in a high guanidine isothiocyanate buffer that provides the RNase inactivation. 70% Ethanol RNase free is added to the lysate to facilitate the binding of RNA in the mini spin column and contaminants are efficiently washed away. Finally, RNA is eluted in 30-50 µL of RNase-free water.

#### 3.2 RNA extraction from frozen or FFPE tissue

Total RNA was extracted with the AllPrep DNA/RNA mini kit or FFPE kit (Quiagen), according to manufacturer's information. After the homogenization, as describe above, the lysate is firstly passed through a DNA spin column. This column, in combination with the high-salt buffer, allows selective and efficient binding of genomic DNA. The column is washed, and pure DNA is then eluted. Ethanol is added to the flow-through from the AllPrep DNA spin column to provide appropriate binding conditions for RNA, and the sample is then applied to an RNA spin column, where total RNA binds to the membrane and contaminants are efficiently washed away. High-quality RNA is then eluted in 30 µl, or more, of RNase-free water. For the extraction of DNA/RNA from FFPE tissue sections, freshly cut FFPE tissue sections were incubated in an optimized lysis buffer that contained proteinase K. Under these conditions, RNA was released into solution, while genomic DNA and other insoluble material were precipitated. The sample was then centrifuged to give an RNA containing supernatant and a DNA-containing pellet, which then underwent separate purification procedures, as described above.

#### 3.3 Real time polymerase chain reaction (RT-PCR).

RT-PCR is a sensitive technique for mRNA detection and quantification of changes in gene expression. In this method, RNA is first transcribed into complementary DNA (cDNA) by reverse transcriptase from total RNA or messenger RNA (mRNA). Then, the cDNA is used

as the template for the qPCR. For retrotranscription, the cDNA Reverse Transcription Kit (NZY Tech) was used following the manufacturer's protocol in a final volume of 20  $\mu\text{L}$ . Samples were incubated for 10 min at 25°C, 1 hours at 37°C and 5 min at 85°C. cDNA was diluted 1:5 in water and kept at -20°C. RT-PCR was performed using the Universal Probe Library (UPL) System (Roche) on a LightCycler 480 instrument (Roche). The UPL System is based on only 165 short hydrolysis probes, labeled at the 5' end with fluorescein (FAM) and at the 3' end with a dark quencher dye. The sequences of the 165 UPL probes detect 8- and 9-mer motifs that are highly prevalent in the transcriptomes, ensuring optimal coverage of all transcripts in a given transcriptome. In order to maintain the specificity and melting temperature that hybridizing qPCR probes require, Locked Nucleic Acids (LNA, DNA nucleotide analogues with increased binding strengths compared to standard DNA nucleotides) are incorporated into the sequence of each UPL probe. Each PCR reaction was performed as follows: 2.5  $\mu\text{L}$  cDNA, 1  $\mu\text{L}$  UPL-probe, 0.1  $\mu\text{L}$  forward primer (20  $\mu\text{M}$ ), 0.1  $\mu\text{L}$  reverse primer (20  $\mu\text{M}$ ), 5  $\mu\text{L}$  UPL Master Mix and 2.2  $\mu\text{L}$  water. The thermocycler PCR conditions are described in **Table 3**.

**Table 3.** Cycling conditions for RT-PCR.

	Cycles	Temperature	Hold	Ramp rate °C/s
<b>Preincubation</b>	1	95	5 min	4.4
<b>Amplification</b>	40	95	10 sec	4.4
		60	30 sec	2.2
		72	1 sec	4.4
<b>Cooling</b>	1	40	10 sec	1.5

Data were analyzed with the LightCycler 480 SW 1.5 software. To estimate relative transcript levels, we used the comparative Threshold cycle (Ct) method. The Ct (Ct) is the cycle number at which the fluorescence signal crosses the threshold. The Ct value is obtained by comparing the samples of interest with a control, or calibrator, such as a non-treated sample or RNA from normal tissue. The Ct values of both the calibrator and the samples of interest are normalized to an appropriate endogenous housekeeping gene:

$$\Delta\Delta\text{Ct} = \Delta\text{Ct}_{\text{sample}} - \Delta\text{Ct}_{\text{reference}}$$

where  $\Delta\text{Ct}_{\text{sample}}$  is the Ct value for any sample normalized to the endogenous housekeeping gene and  $\Delta\text{Ct}_{\text{reference}}$  is the Ct value for the calibrator also normalized to the endogenous housekeeping gene. To calculate the expression change in fold, it is

necessary to calculate the value of  $2^{-\Delta\Delta Ct}$ .

### 3.4 Primers

Primers (Table 4) were designed using the UPL Assay design center (<https://qpcr.probefinder.com/organism.jsp>).

**Table 4. Primers used in RT-PCR.**

Gene	UPL Probe	Forward 5'-3'	Reverse 5'-3'
ALDH1A1	#34 (AGAGGCAG)	GCTCTCCACGTGGCATCT	GCCCCATAACCAGGAACAAT
AR	#14	GCCTTGCTCTCTAGCCTCAA	GGTCGTCCACGTGTAAGTTG
CCNG2	#55 (GGAGAGGA)	GGGGGTTGTTTTGA TGAAAGT	TTGATCACTGGGAGGAGAGC
CD133	#86 (GCAGTGGA)	GGAAACTAAGAAGTATGGGAGAAC A	CGATGCCACTTTCTCACTGA T
CD44	#41	CAAGCAGGAAGAAGGATGGAT	AACCTGTGTTTGGATTTGCA G
CDH1	#35 (AGAAGAGGA)	CCCGGGACAACGTTTATTAC	GCTGGCTCAAGTCAAAGTCC
HMBS	#26 (CAGCCAG)	TGTGGTGGGAACCAGCTC	TGTTGAGGTTTCCCCGAAT
IPO8	#18	CAAATGTGGCAGCTTCTAGGT	ATGCAGGAGAGGCATCATGT
JUN	#19 (CTCCAGCC)	CCAAAGGATAGTGCATGTTT	CTGTCCCTCTCCACTGCAAC
KLK2	#75	GTTGGGAATGCTTCTCACACT	TTCTCTCCATCGCCTTGCT
KLK3	#44	CAGCAAGATCACGCTTTTGT	GTGCTTGTGGCCTCTCGT
CK14	#28	CCTCTCCTCCTCCAGTTCT	ATCGTGCACATCCATGACC
CK18	#85 (GACCTGGA)	GAGGTTGGAGCTGCTGAGAC	ACCTCCCTCAGGCTGTCTC
CK5	#81	GGCTGCTGCGTGAGTACC	TGGTCCAACCTCTCTCCAC
LEF1	#31	TGAATCAGGTACAGGTCCAA	CGTTGGGAATGAGCTTCG
NANOG	#69 (CTTCCTCC)	ATGCCTCACACGGAGACTGT	AGGGCTGTCCTGAATAAGCA GGCACAAACTCCAGGTTTT T
POU5F1	#52 (GGGAGGAG)	GTGCCTGCCCTTCTAGGAAT	
PTOV1	#9 (CATCACCA)	GCTTCGTACGTGCCATCC	TGAGTTGACACCACCAGGTC
SNAI1	#11 (CTTCAGC)	GCTGCAGGACTCTAATCCAGA	ATCTCCGGAGGTGGGATG GGAGGAAGAGGTAACACAG G
SOX2	#19 (CTCCAGCC)	ATGGGGTTCGGTGGTCAAGT	
TBP	#87 (CTGCCACC)	GAACATCATGGATCAGAACAACA	ATAGGGATTCCGGGAGTCAT AGCCTCAGAGAGGTCAGCA A
VIMENTIN	#16 (GGAGGCAG)	AAAGTGTGGCTGCCAAGAAC	

### 3.5 RNA interference

The mechanism of RNA interference (RNAi) is based on the sequence-specific degradation of host mRNA through the cytoplasmic delivery of double-stranded RNA (dsRNA) complementary to the target sequence. Degradation of target gene expression involves the endogenous RNA-induced silencing complex (RISC) with the assistance of Argonaute (Ago) proteins. One method used to produce RNAi involves the use of short hairpin RNAs

(shRNAs) that are synthesized inside the cell after transfection of DNA vectors bearing the specific sequences to be produced. shRNAs are transcribed by RNA Pol III or modified Pol II promoters but can also be delivered into mammalian cells through transduction of viral vectors. shRNAs can integrate in the host DNA. They consist of two complementary 19–22 bp RNA sequences linked by a short loop of 4–11 nucleotides similar to the hairpin found in naturally occurring miRNA. Following transcription, the shRNA sequence is exported to the cytosol where it is recognized by an endogenous enzyme, Dicer, which processes the shRNA into short interfering RNA (siRNA) duplexes. Lentiviral vectors carrying short-hairpin RNA specific to PTOV1 were obtained from Sigma’s MISSION shRNA Library (Table 5).

**Table 5. Short hairpins used to inhibit PTOV1 expression.**

shRNA	ID	Sequence
PTOV1	TRCN0000143905	CCGGCCTGTACTCTTCAGAGAAG AACTCGAGTTCTTCTCTGAAGAG TACAGGTTTTTTG
PTOV1	TRCN0000139737	CCGGCCTGTACTCGTCCAAGAAG AACTCGAGTTCTTCTTGGACGAG TACAGGTTTTTTG

## 4. DNA manipulation

### 4.1 Chromatin immunoprecipitation

The chromatin immunoprecipitation (ChIP) assay is a powerful method for studying interactions between specific proteins and a genomic DNA region. This assay can be used to determine whether a transcription factor interacts with a candidate target gene sequence. ChIP was performed using EZ ChIP™ Kit (Millipore) following manufacturer’s instructions. Briefly,  $3 \times 10^6$  cells were seeded on 15 cm diameter plates. Two plates were used for ChIP. The following day, cells were fixed with 1% formaldehyde and incubated 10 minutes at room temperature to crosslink proteins and DNA. Next, 1 mL of 1.25 M glycine was added to quench unreacted formaldehyde and cells were incubated for 5 min at room temperature. Cells were washed in PBS 1x and centrifuged at 700 xG for 5 minutes. Cell



pellets were resuspended in 1 mL SDS Lysis Buffer (1% SDS, 10 mM EDTA, 50 mM Tris pH=8.1) containing protease inhibitor cocktail II. Supernatant was aliquoted (400  $\mu$ L) and cross-linked chromatin was sonicated to generate smaller DNA fragments. These aliquots containing sheered chromatin were kept frozen until use. In a typical immunoprecipitation (IP), 20  $\mu$ L of protein G coupled to magnetic beads (Invitrogen) were used for each immunoprecipitation. Magnetic protein G beads were pre-washed in dilution buffer before incubation overnight with the desired primary antibody. For PTOV1 immunoprecipitation, the rabbit in-house produced antibody (4  $\mu$ g) was used. Positive controls were antibodies to total RNA-Polymerase II (1  $\mu$ g) and phosphorylated RNA- Polymerase II (1  $\mu$ g). Negative controls were mouse IgG and rabbit IgG (1  $\mu$ g each). Extra beads bound to unspecific antibodies (IgG mouse or IgG rabbit) were also prepared. Supernatants containing sheered chromatin were incubated with IgG mouse/rabbit coated beads for 3 hours at 4°C for pre-washing. Then, 1% of this chromatin was taken as input and stored at -20°C. Chromatin was incubated with appropriate antibody-coated beads O/N at 4°C with rotation. DNA sequences associated with the target protein will co-precipitate as part of the cross-linked chromatin/antibody complex. After IP, beads were washed twice in each of the following buffers:

1. Low salt immune complex wash buffer (0.1% SDS, 1% Triton X-100, 2 mM EDTA, 20 mM Tris-HCl pH=8.1, 150 mM NaCl)
2. High salt immune complex wash buffer (0.1% SDS, 1% Triton X-100, 2 mM EDTA, 20 mM Tris-HCl pH=8.1, 500 mM NaCl)
3. LiCl immune complex wash buffer (0.25M LiCl, 1% IGEPAL-CA630, 1% deoxycholic acid (sodium salt), 1 mM EDTA, 10 mM Tris-HCl pH=8.1)
4. TE buffer (10 mM Tris-HCl, 1mM EDTA pH 8.0).

To elute protein/DNA complexes 100  $\mu$ L of Elution buffer (EB) (10  $\mu$ L 20% SDS, 20  $\mu$ L 1M NaHCO<sub>3</sub> and 170  $\mu$ L distilled H<sub>2</sub>O) was added to antibody/beads complex. For input tubes, 200  $\mu$ L of EB were added. Samples were incubated for 15 minutes at room temperature. 100  $\mu$ L of EB was added again to antibody/beads complexes and samples were incubated 15 minutes. To reverse crosslinking and free the DNA, samples were added with 8  $\mu$ L 5 M NaCl followed by O/N incubation at 65°C. Next, all samples were added with 1

$\mu\text{L}$  of RNase A (10 mg/mL) and incubated for 30 minutes at 37°C. Then, 4  $\mu\text{L}$  0.5 M EDTA, 8  $\mu\text{L}$  1 M Tris-HCl and 1  $\mu\text{L}$  Proteinase K (10 mg/mL) were added to digest the protein component and samples were incubated at 45°C for 2 hours. Finally, the DNA was purified using Illusta GFX PCR DNA Purification kit and eluted in 50  $\mu\text{L}$  of EB and stored at -20°C for further use. This DNA was used as template for PCR reactions with specific primers (**Table 6**) using the Hot-Start Taq polymerase (Platinum PCR master mix, Invitrogen). Reactions were as follows: 25  $\mu\text{L}$  Platinum mix, 1  $\mu\text{L}$  Forward primer (10  $\mu\text{M}$ ), 1  $\mu\text{L}$  Reverse primer (10  $\mu\text{M}$ ) and 2  $\mu\text{L}$  of desired DNA. The amplification cycles were as follows:

Initial denaturation 94°C 5 min

Denaturation 94°C 20 sec

Annealing 57°C 30 sec

Extension 72°C 30 sec

repeat for 37 cycles

Final extension 72°C 2 min

**Table 6.** Primers from the regions of the indicated genes used for Chromatin Immunoprecipitation (ChIP).

Gene	Forward primer 5'-3'	Reverse primer 5'-3'
ABCB1	CTCTGCCTTCGTGGAGATGC	CGGTCCCCTTCAAGATCCAT
ALDH1A1	TGGAGCGTGCCGTCCTTTAT	TAACCCAAAACCTCCGCTCACC
CCNG2	GAGCGTGACATTCGCCCAA	AAAGTCCGCCCAAAGTAGCC
HES1	TACCTCTCCTTGGTCCTGGACC	CAGATGCTGTCTTTGGTTTATCCG

Samples were loaded in an acrylamide gel prepared as shown in **Table 7**.

Table 7. Preparation of acrylamide gel for ChIP assays.

Reagent	Volume (mL)
30% Acrylamide mix	2
TBE buffer	2
ddH2O	6
APS 10%	0.060
TEMED	0.0075

Gel was stained with SYBR SAFE and visualized with a Molecular Imager Gel Doc<sup>TM</sup> XR system (BioRad).

#### 4.2 Vectors and constructions

All plasmid vectors employed in this thesis are listed below:

##### **pE-GFP**

##### **GFP-PTOV1**

Constructs for the expression of chimeric GFP-PTOV1 were generated in pEGFP-N1 (Clontech) by placing the full-length PTOV1 cDNA in frame and downstream of GFP<sup>159</sup>.

##### **GFP-PTOV1 MUT**

The PTOV1 mutant at amino acids 98–100 (the sequence KRRP was changed to EGGP) was obtained with the plasmid GFP-PTOV1 using the QuikChange<sup>TM</sup> Site-Directed Mutagenesis kit (Stratagene) according to the manufacturer's instructions. The primers used for mutagenesis were:

5'-GAGTGGCAGGAGGAGGGCGGACCCTAGTCTGAC-3' (Forward) and

5'-GTCAGAGTAGGGTCCGCCCTCCTCCTGCCACTC-3' (Reverse).

#### 4.3 Preparation of competent bacteria

To increase the transformation efficiency of bacteria we generated competent cells. We used a protocol based in the alkali metal halid rubidium chloride (RbCl). *E. coli*, streak Sbt13, were treated with a hypotonic solution containing RbCl expand. As a result of this treatment, the expulsion of membrane proteins from the bacteria allows negatively charged DNA to

bind. The protocol used is detailed as follows:

Preparation of competent bacteria. Cell strains were seeded on LB-agar plates without antibiotics and incubated O/N at 37°C. A single colony was picked from the plate and inoculated in 30 mL of Luria Bertani (LB) buffer with 300 µL Mg<sup>++</sup> (MgCl<sub>2</sub> 1 M + MgSO<sub>4</sub> 1 M). Flasks were shaken O/N at 37°C. The O/N culture (8 mL) was inoculated into a flask containing 200 mL of LB plus 2 mL of Mg<sup>++</sup>. The flask was shaken at 37°C until an OD<sub>550</sub> of about 0.45-0.55 (about 2 hours). The culture was collected into four sterile 50 mL conical tubes and chilled rapidly on ice for 15 minutes. Then, cells were pelleted by centrifugation at 2,700 xG for 10 minutes at 4°C. The supernatant was discarded, and pellets were resuspended gently in 16 mL of Transformation Buffer 1 (100 mM RbCl, 50 mM MnCl<sub>2</sub>·4 H<sub>2</sub>O, 30 mM KAc pH 7.5, 10 mM CaCl<sub>2</sub>·2 H<sub>2</sub>O, 15% Glycerol 99% v/v) and incubated on ice for 15 minutes. After a second centrifugation at 2,700 xG, the supernatant was discarded and cells were resuspended in 4 mL of Transformation Buffer 2 (10 mM MOPS, 10 mM RbCl, 75 mM CaCl<sub>2</sub>·2 H<sub>2</sub>O, 15% Glycerol). Cells were collected into one conical tube and incubated in RF2 on ice for 15 minutes. Then, cells were aliquoted (100 µL each) into chilled 1.5 mL eppendorf tubes, frozen on dry ice, and stored at -80°C.

#### *4.4 Bacterial transformation, growth and plasmid DNA purification*

We used a standard heat-shock transformation method of chemically competent bacteria. The protocol details are below:

One µL of DNA (usually 10 pg to 100 ng) was added to 50 µL of competent bacteria prepared as above in a microcentrifuge tube, gently mixed and placed on ice for 30 minutes. The tube was placed at 42°C for 60 seconds and put back on ice. Two hundred 200 µL of LB media without antibiotic were added, then the tube was placed at 37°C in a shaking incubator for 60 min. 30 µL of the transformation were plated onto a 10 cm LB agar plate containing the appropriate antibiotic and plates were incubated O/N at 37°C upside-down. An isolated colony was scraped from the dish with a sterile pipette tip, immersed in a sterile culture tube containing LB media (3 mL) supplemented with the appropriate antibiotic (100 µg/mL) and shaken in an orbital shaker at 37°C for 2 hours. For plasmid DNA preparation, 3 mL of culture were placed into a sterile flask (500 mL) containing approximately 100 mL of LB media plus the appropriate antibiotic and shake in an orbital shaker overnight at 37°C (no

more than 17h). On the next day, for plasmid DNA isolation we used the Nucleobond AX PC 100 kit (Macherey-Nagel GmbH), following the manufacturer's instructions. Briefly, the bacterial cells were lysed by buffers based on the NaOH/SDS alkaline lysis. After equilibration of the column, the entire lysate was loaded by gravity flow and simultaneously cleared by column filters. The silica resin consists of hydrophilic, macropores silica beads functionalized with methyl-amino-ethanol that provides a high overall positive charge density under acidic pH conditions that permits the negatively charged phosphate backbone of plasmid DNA to bind with high specificity. Plasmid DNA was bound to the silica resin and after an efficient washing step with ethanol 70% the DNA was eluted, precipitated with isopropanol and dissolved in water and stored at -20°C for further use.

### 4.5 Electrophoretic mobility shift assay (EMSA)

EMSA allows to study the direct binding of a protein of interest to a specific nucleic acid sequence. We used double-stranded DNAs sequences corresponding to regions of the *ALDH1A1* promoter (from -395- to -363), the *CCNG2* promoter (from -269 - to -239) and the *HES1* promoter (from +45 to +69) as a negative control. The dsDNA probes were formed by mixing 20 µg of each single-stranded oligodeoxynucleotide in a 150 mM NaCl solution. After incubation at 90°C for 5 min, solutions were allowed to cool down slowly to room temperature. The duplexes were purified in a non- denaturing 20% polyacrylamide gel electrophoresis and DNA concentration was determined by measuring its absorbance (260 nm) at 25 °C in a Nanodrop ND-1000 spectrophotometer (Thermo Fisher Scientific). Duplexes were 5'-end-labeled with [ $\gamma$ -<sup>32</sup>P]-ATP (Perkin Elmer) by T4 polynucleotide kinase (New England BioLabs) in a 10 µL reaction mixture, according to the manufacturer's protocol. After incubation at 37°C for 1 hour, 90 µL of Tris-EDTA buffer (1 mM EDTA and 10 mM Tris, pH 8.0) were added to the reaction mixture, which was subsequently filtered through a Sephadex G-25 (Sigma Aldrich) spin-column to eliminate the no-incorporated [ $\gamma$ -<sup>32</sup>P]-ATP. Radio-labeled probes (100,000 cpm, [ $\gamma$ -<sup>32</sup>P]-ATP) were placed on ice for 30 min with 10 µg of PTOV1 domains or 0.3 µg of peptides using either 5 µg or 0.15 µg poly (dI:dC), respectively, as unspecific competitor, in the presence of the binding buffer (5% Glycerol, 0.5 mM DTT, 4 mM MgCl<sub>2</sub>, 36 mM KCl, 0.5 mM EDTA, 25 mM Tris-HCl pH=8.0). All reagents were purchased from Sigma-Aldrich. The products of these binding reactions were electrophoretically resolved in 5% polyacrylamide and 5% glycerol native gels at a fixed voltage of 220 V and 4°C. Gels were dried at 80°C and visualized on a Storm 840

PhosphorImager (Molecular Dynamics, GE Healthcare Life Sciences). ImageQuant software v5.2 was used to visualize the results.

#### 4.6 DNA sequencing

Frederick Sanger received a Nobel prize for discovering a method for sequencing DNA using a primer-extension strategy to develop more rapid DNA sequencing methods. This method consists of a selective incorporation of chain-terminating dideoxynucleotides by DNA polymerase during *in vitro* DNA replication<sup>178</sup>. Sequencing begins with denaturation of the double-stranded DNA. The single-stranded DNA is then annealed to oligonucleotide primers and elongated using a mixture of deoxynucleotide triphosphates (dNTPs), which provide the needed adenine (A), cytosine (C), thymine (T), and guanine (G) nucleotides to build the new double-stranded structure. In addition, a small quantity of chain-terminating dideoxynucleotide triphosphates (ddNTPs) for each nucleotide is included. The sequence will continue to extend with dNTPs until a ddNTP attaches. As the dNTPs and ddNTPs have an equal chance of attaching to the sequence, each sequence will terminate at varying lengths.

Each ddNTP (ddATP, ddGTP, ddCTP, ddTTP) also includes a fluorescent marker. When a ddNTP is attached to the elongating sequence, the base will fluoresce based on the associated nucleotide. By convention, A is indicated by green fluorescence, T by red, G by black, and C by blue. A laser within the automated machine used to read the sequence detects a fluorescent intensity that is translated into a “peak.” When a heterozygous variant occurs within a sequence, loci will be captured by two fluorescent dyes of equal intensity. When a homozygous variant is present, the expected fluorescent color is replaced completely by the new base pair’s color.

We analyzed mutations in expressed genes in tumor tissues and *ex vivo* cultures, by studying their RNA reverse transcribed to DNA. The DNA was then sequenced by the Sanger’s method. The step of reverse transcription to generate DNA was performed using NZY M-MuLV First-Strand cDNA Synthesis Kit (NZY Tech) using 2720 Thermocycler (Applied Biosystems). In the first step, the solution that contains RNA is incubated at 65°C for 5 minutes together with the annealing buffer and random primers. The second incubation, performed after the addition of NZYRT 2x Master Mix and NZYM-MuLV RT Enzyme Mix, is at 37°C for 50 minutes and then at 85°C for 5 minutes to inactivate the enzyme. The third

incubation is at 37°C for 20 minutes with RNase H. cDNAs were amplified with the kit Supreme NZY Taq II 2x Green Mastermix and the specific primers indicated in **Table 8** in a 2720 Thermocycler. Amplified products were run into a 1% agarose gel for 1 h at 100 V. Then, we performed a shadowing with a UV lamp to cut with a scalpel blade collect the corresponding band and purify the DNA with the GelPure kit (NZY Tech).

**Table 8. Primers used in sequencing.**

Gene	Forward primer 5'-3'	Reverse primer 5'-3'
SPOP	CGTAGCTGAGAGTTGGTGC	ATTCTCCCACAGTCCTCCTAAC
PTEN I	CAGAGCCATTTCATCCTGC	GAACTGTCTTCCCGTCGTG
PTEN II	GCGGAACTTGCAATCCTCAG	AACTGGTAATCTGACACAATGTCC
TP53 I	GACACGCTTCCCTGGATTG	TAGGGCACCACCACACTATG
TP53 II	GACATAGTGTGGTGGTGCC	CAGTGGGGAACAAGAAGTGG

The kit was equipped with a silica-gel based membrane which selectively adsorbs up to 20 µg of DNA fragments in the presence of specialized binding buffers. Soluble agarose, nucleotides, oligos (<30-mer), primer dimers, enzymes, mineral oil and other impurities do not bind to the membrane and are washed away. DNA fragments were then eluted off the column for 20 minutes in Elution Buffer. To obtain an appropriate amount of DNA for sequencing, the PCR for each sample was done in triplicate.

## 5. Protein manipulation

### 5.1 Protein extraction

Cells and tissues were lysed in a lysis buffer containing 50 mM Tris pH=7.5; 200 mM NaCl; 5 mM EDTA; 0.1% Triton X-100, proteases inhibitors (Sigma Aldrich; 1:200) and phosphatases inhibitors (1 mM Sodium Fluoride). Briefly, cells were washed twice with cold PBS and ice-cold lysis buffer was added (approximately 100 µL per  $1 \times 10^6$  cells in 10 cm dish). Adherent cells were collected using a cell scraper, transferred into a pre-cooled microfuge tube, vortexed and kept on ice for 30 minutes. Lysates were centrifuged 15 minutes at 12,000 xG at 4°C. Supernatant was collected in a new tube kept on ice and it was stored at -20°C for later use.

### 5.2 Determination of protein concentration

To determine protein concentration, we used the Bradford method. Bovine serum albumin (BSA) was used as standard. This method can determine the total protein concentrations in solutions depending on the change in absorbance based on the bound dye Coomassie Blue G-250 to proteins. A set of BSA standards (Panreac) was created from a stock of 2 mg/mL (0, 0.25, 0.5, 0.75, 1, 1.5, 1.75 and 2 mg/ml). Five  $\mu\text{L}$  of standards, or sample, were added to a 96 well plate. Then, 200  $\mu\text{L}$  of Bradford solution (Panreac) was added and plate was incubated for 15 minutes at room temperature. Absorbance was measured at 595 nm in an Epoch<sup>TM</sup> Microplate Spectrophotometer (BioTek). The values obtained for the BSA standards were used to construct a standard curve used to compare the samples values to know their concentration.

### 5.3 Analysis by Sodium Dodecyl Sulfate Polyacrylamide Gel Electrophoresis (SDS-PAGE) and Western blot

Western blot is a widely used analysis to separate and identify proteins from different samples. In denaturing SDS-PAGE, a mixture of proteins is separated based on molecular weight, and not by intrinsic electrical charge of the polypeptide, through gel electrophoresis. These results are then transferred to a membrane producing a band for each protein. Later, the membrane is incubated with labels antibodies specific to the protein of interest. Protein samples were denatured in loading buffer (*Laemmli buffer*: 250 mM Tris pH=6.8; 10% SDS; 0.5% Bromophenol blue; 50% Glycerol; 500 nM DTT) and boiled at 95°C for 5 minutes. Generally, at least 30  $\mu\text{g}$  of protein lysate per lane were loaded per gel and included one lane with molecular weight markers for identification of protein sizes and electrophoretic monitoring. The electrophoresis was run in running buffer (25 mM Tris base; 190 mM glycine; 0.1% SDS; pH=8.3) for approximately 1.5 hours or until the migration front reached the bottom of the gel. After the electrophoresis, the separated proteins were transferred onto a solid support matrix. Electrophoretic wet transfer was used to immobilize proteins onto polyvinylidene difluoride (PVDF) membranes, previously activated with methanol, in transfer buffer (25 mM Tris-HCl pH 8.3; 192 mM glycine; 20% (v:v) methanol). The gel and PVDF membrane were submerged in transfer buffer in tanks where they were sandwiched between buffer-wetted filter papers that were in direct contact with flat-plate electrodes. The electric field strength makes negatively charged proteins travel towards the



positively charged electrode, so most proteins are transferred to the membrane. The electrophoresis conditions for transference were the following:

- For large proteins (>100 kD) the transference was performed slowly overnight at 60 mA/hour for a total of approximately 1000-1200 mA.
- For small proteins (<100 kD) the transference was run for 2 hours at 400 mA/hour. To visualize the transferred proteins, membranes were stained with Naftol Blue for 5 minutes. Specific proteins in the membranes were detected by incubation with antibodies.

First, membranes were blocked to prevent non-specific binding of the antibodies. Blocking solution was 5% not-fat milk or BSA solution prepared in Tris Buffer Saline Tween (TBST) buffer (50 mM Tris-Cl pH 7.5; 150 mM NaCl; 0.1% Tween) for 30 minutes incubation. Primary antibodies (**Table 9**), prepared in the same solution, were prepared at 1 µg/mL and incubated overnight at 4°C.

**Table 9. Primary antibodies list.**

Antibody	Origen	Reference
Actin I-19	Goat	Santa Cruz Biotechnology
4EBP1	Rabbit	Cell Signaling Technology
CHGA A	Mouse	NeoMarkers
Erk	Rabbit	Cell Signaling Technology
Keratin 18 (CD10)	Mouse	NeoMarkers
Keratin 5	Mouse	Santa Cruz Biotechnology
p-AKT (Ser473)	Rabbit	Cell Signaling Technology
P63	Mouse	Ventana
PDCD4	Rabbit	Cell Signaling Technology
phospho-E4-BP1 (Thr37/46)	Rabbit	Cell Signaling Technology
phospho-Erk 1/2	Mouse	Promega
phospho-Ribosomal Protein S6	Rabbit	Cell Signaling Technology
PTEN	Rabbit	Cell Signaling Technology
PTOV1	Rabbit	home made
Puromycin (12D10)	Mouse	Millipore
RB1	Rabbit	Santa Cruz Biotechnology
Ribosomal Protein S6 (5G10)	Rabbit	Cell Signaling Technology
p53 (DO-1)	Mouse	Santa Cruz Biotechnology
Vinculin	Mouse	Cell Signaling Technology

Membranes were washed several times in TBST and incubated with secondary antibodies 1 hour at room temperature. Horseradish peroxidase (HRP)-conjugated secondary antibodies (Dako) diluted in blocking buffer were used as indicated in **Table 10**.

**Table 10. Secondary antibodies.**

Antibody	Origen	Dilution
Anti-goat immunoglobulins/HRP	Polyclonal Rabbit	1:2000
Anti-rabbit immunoglobulins/HRP	Polyclonal Goat	1:2000
Anti-mouse immunoglobulins/HRP	Polyclonal Rabbit	1:2000

Finally, the ECL Western Blotting Detection reagent (GE Healthcare) was used to reveal the specific proteins on the membranes. This is a luminescence emitting nonradioactive method for detection of immobilized specific antigens with HRP-labeled antibodies.

#### *5.4 Analysis of protein synthesis by Surface sensing of translation (SUnSET)*

SUnSET is a nonradioactive method to monitor protein synthesis<sup>179</sup>. It is based in the use of low amounts of puromycin, a structural analog of aminoacyl tRNAs, which is incorporated into the nascent polypeptide chain preventing elongation. mRNA translation can be analyzed by Western blotting using a monoclonal antibody to puromycin. Briefly, the protocol is:

Cells ( $3 \times 10^5$ ) were seeded in 6 well plates. Twenty-four hours later cells were treated with 10  $\mu\text{g}/\text{mL}$  puromycin for 10 minutes. Non treated cells were the negative control. Positive control cells were treated with 10  $\mu\text{g}/\text{mL}$  puromycin and 10  $\mu\text{g}/\text{mL}$  cycloheximide for 10 minutes, in order to inhibit protein synthesis. Cell lysates were collected and analyzed by Western blotting. Monoclonal puromycin antibody was prepared 1:10,000 in 5% BSA in TBST.

## 6. In vivo tumorigenic assays

LNCaP cells ( $1 \times 10^6$  or  $5 \times 10^5$ ), G2 LNCaP spheres ( $1 \times 10^6$  or  $5 \times 10^5$ ), or primary tumor ex vivo AD/AI cultures 1 ( $5 \times 10^6$ ), in 100  $\mu$ L mix of PBS and Matrigel (mix 1:1), were inoculated subcutaneously in the right flank of 6-week-old male mice (Rj:NMRI-Foxn1<sup>nu/nu</sup>, n = 6) (Charles River Laboratories). All animal experimental procedures were approved by the Vall d'Hebron Hospital Animal Experimentation Ethics Committee. After tumors reached 1 cm in diameter, mice were euthanized, and tumors excised. Tumors were fixed in formol, embedded in paraffin and processed for histopathology. Hematoxylin & eosin staining to verify the histopathological findings were performed.

### 6.1 Immunohistochemistry

For this technique, the avidin-biotin peroxidase method was used. Briefly, four-micron sections from human and mice tumors were used for antigen retrieval in citrate buffer, as described<sup>171</sup>. After blocking endogenous peroxidase activities and non-specific labeling, sections were labeled with PTOV1 antibody in blocking buffer for 2 hours at room temperature. As a negative control, primary antibody was omitted or replaced with non-specific rabbit IgGs, obtaining clean negative results in all cases (data not shown). Reaction was revealed by the avidin-biotin complex and staining with diaminobenzidine (ABC Elite kit, Burlingame). Nuclei were counterstained with Hematoxylin.

## 7. Bioinformatics analyses of data sets

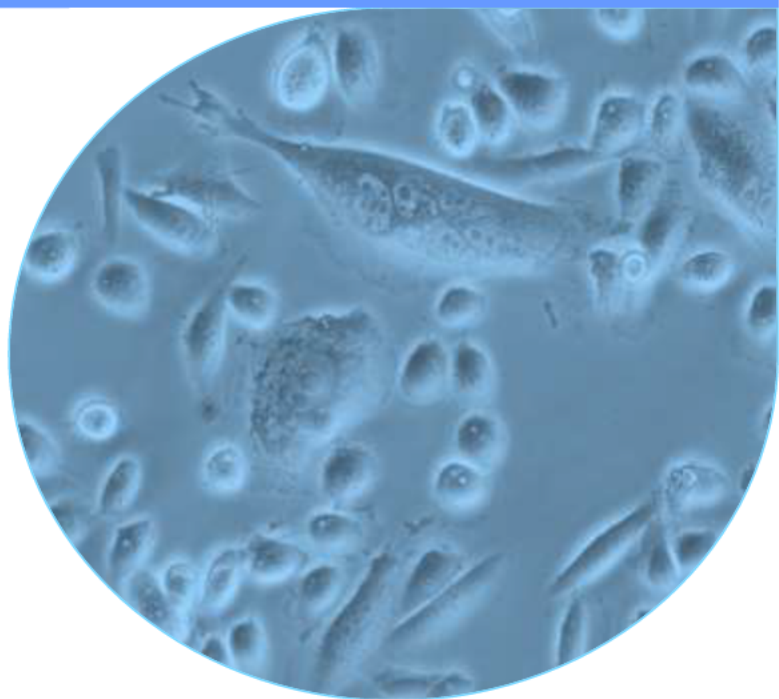
The mRNA expression of *PTOV1*, *ALDH1A1* and *CCNG2* genes was analyzed using publicly available data set from human prostate tumors (GSE97284 n = 188) using the R2 bioinformatics platform (<http://r2.amc.nl>). The most informative probe set, according to its average present signal (APS) and average value (Avg) was selected for each gene. The presence of DNA amplification, point mutations and deletions in the genes of interest were analyzed from publicly available datasets of human prostate tumors using the cBioPortal platform<sup>136,180</sup>. Correlations between *PTOV1*, *ALDH1A1*, and *CCNG2* genes and survival of patients with colon carcinoma were obtained using the dataset GSE14333 (n=290).

## 8. Statistics

Results are expressed as the average + standard deviation of the mean. IC50 values for docetaxel treatments were determined by non-linear regression. For statistical analysis, depending on whether data were sampled from a Gaussian distribution or not, the unpaired t-test or Mann-Whitney U test were used to compare two groups. For multiple comparisons, ANOVA followed by the Dunnett method or the alternative non- parametric method (Kruskal-Wallis followed by Dunn method) were employed. To quantify the association between two quantitative variables, the Spearman correlation was used for statistical analysis. The Fisher's exact test was employed to determine whether a non-random association of co-occurrence between two categorical variables was significant. A *p* value lower than 0.05 was taken as the level of significance. These analyses were performed using GraphPad Prism 6 software.



**CHAPTER 5: ESTABLISHMENT AND  
CHARACTERIZATION OF *ex vivo*  
CULTURES DERIVED FROM PRIMARY  
PROSTATE TUMORS**





### 1. Establishment of a protocol for *ex vivo* tumor growth

PCa is a hormone-dependent neoplasia and the gold standard treatment is the androgen deprivation therapy (ADT), very effective in reducing the tumor volume. However, approximately 40% of tumors develop resistance to this therapy, turning PCa into a mortal disease. As mentioned above, the study of the mechanisms implicated in PCa resistance is hindered mostly by the small number of proper cellular models and the striving to establish Patient Derived Xenograft (PDX) models. In fact, the few PCa cell lines available fail to represent the heterogeneity of prostate tumor<sup>181,182</sup>, while PDX from prostatectomy have a small rate of engraftment (2%-50%) with have a long latency, from 2 months up to 3 years. Presently, most of the mechanisms of PCa progression have been using three cell lines, *i.e.* LNCaP, Du145 and PC3. However, these cell lines were derived from metastatic nodules to different organs, therefore are poorly representatives of the heterogeneity of the cancer cells in the primary tumor<sup>139-141</sup>. The establishment of more reliable *in vitro* models from a needle biopsy of aggressive tumors might be useful not only to represent the tumors heterogeneity of different patients, but also to predict patients' response to ADT and recurrence. Finally, such cellular models might allow reproducing *in vitro* the patient's treatment, thus predicting the tumor response *in vivo*.

#### 1.1 *Ex vivo* radical prostatectomy derived tumor cultures

Radical prostatectomy is rarely performed in patients with aggressive prostate cancer, and although this procedure allows the obtention of a large amount of cancer tissue, this rarely contains aggressive cancer cells. The protocol to establish *ex vivo* tumor cultures from a radical prostatectomy included tissue mincing with a scalpel, digestion with enzymes (collagenase I and hyaluronidase), filtration to enrich for single cells, and plating on top of collagen coated dishes (please see full methodology in CHAPTER 4 p.37). We obtained few *ex vivo* primary tumor cultures although fibroblasts overgrew the cultures. Cells efficiently attached and grew especially from small tissue pieces, although fibroblast cells prevailed in the majority of the cultures. The use of geneticin to prevent fibroblast growth was insufficient (**Figure 9A**).

#### 1.2 *Ex vivo* primary tumor cultures established from needle biopsies



Patients with a suspicious PSA and/or DRE analyses are screened for the presence of prostate cancer by a needle biopsy<sup>183</sup>. In collaboration with the Urology Service at the Vall d'Hebron Hospital, starting in January 2017, we initiated a collection of aggressive prostate tumors from needle biopsy cores of patients with PSA levels > 50 ng/mL and positive DRE. The latter were processed (please see CHAPTER 4, p.38) without enzymatic digestion. The suspension was filtered with a 40 µm filter and seeded in a 24-wells dish coated with matrigel (**Figure 9B**). This method was slightly simplified from previously described methods in order to grow structures with abilities to form *in vitro* prostatic acinar glands<sup>136</sup>. A small percentage of cells assumed a spherical shape, but these structures did not survive past 72 hours.

After further adjustments of the protocol, including the use of an increased number of initial biopsy cores (up to five), very fine mincing of the tissue to small pieces (smaller than 1 mm), elimination of the enzymatic digestion and filtration steps, the seeding of the tissue pieces with half of the medium for the first 24 hours to facilitate the adhesion, cells were able to emerge from the small pieces of tissues seeded in the plate, as shown in **Figure 9C**.

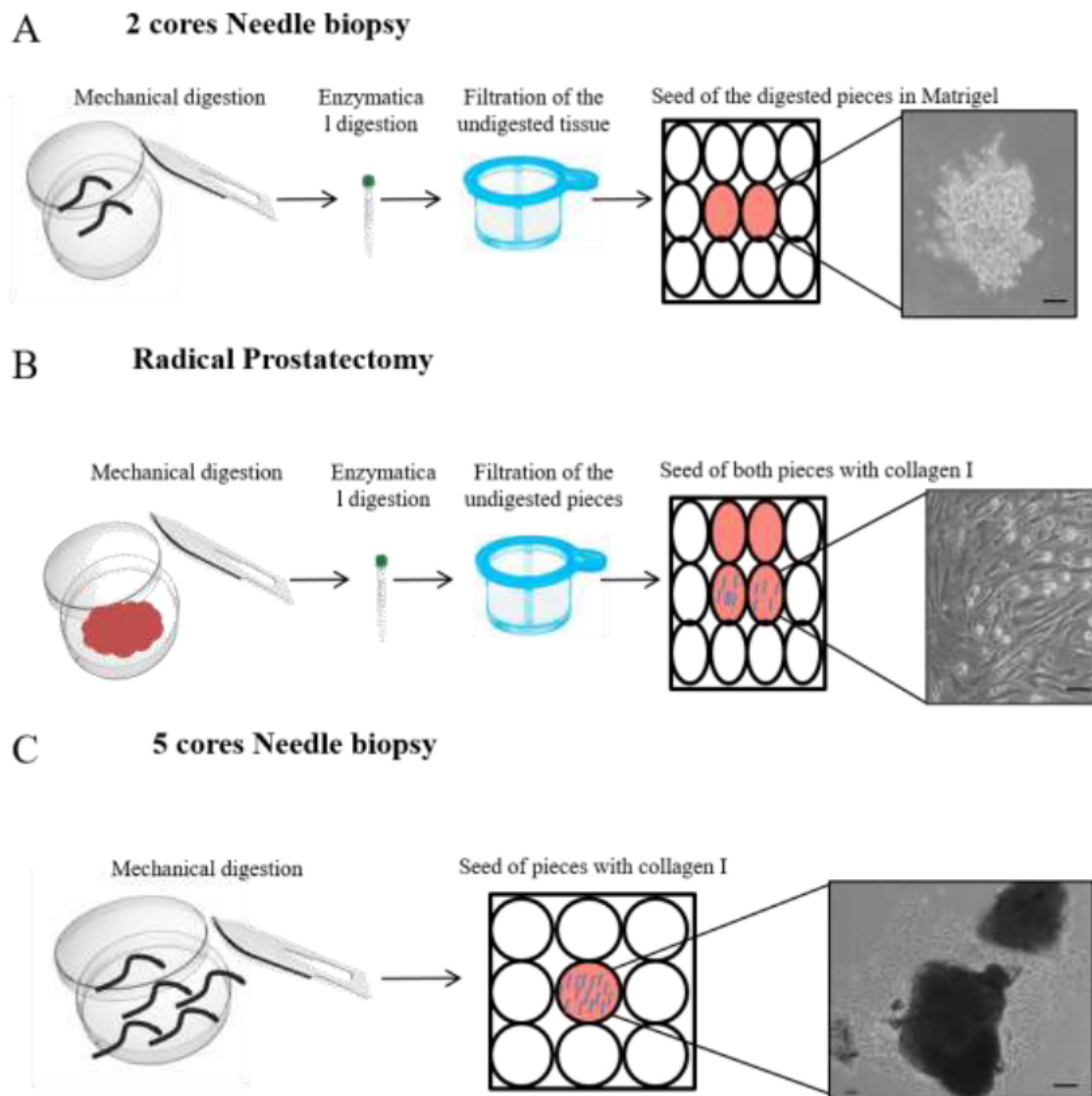


**Figure 9.** Set up of the protocol for *ex vivo* primary tumor cultures. (A) Scheme of the protocol with radical prostatectomy as starting tissue. (B) Scheme of the protocol using 2 cores of prostate cancer biopsy. (C) Scheme of the optimized protocol using 5 cores of needle biopsy. Scale bar: 100  $\mu\text{m}$ .

Once cells started to attach to the plate, fibroblasts cells were efficiently separated through a differential trypsinization treatment. During the first, second or -third passages, these cultures were treated with a diluted solution of TRYPLE to remove the majority of fibroblasts (**Figure 10**). Then, with a standard solution of TRYPLE for five minutes at 37°C, the epithelial cells were detached and purified (please, see the details in CHAPTER 4, p.38).

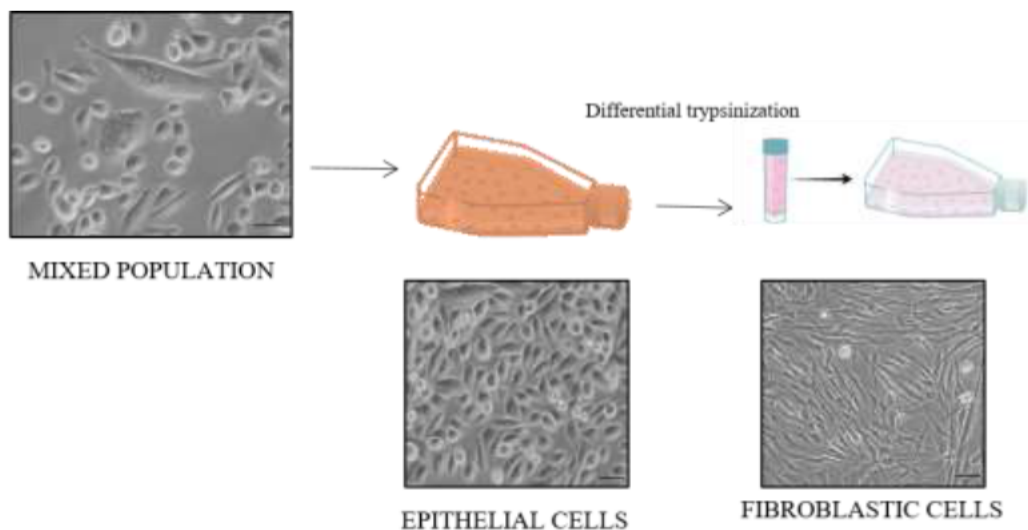


**Figure 10.** Scheme of the protocol for the separation of fibroblasts from epithelial cells. The mixed population of attached cells was firstly treated for with a diluted TRYPLE solution (0.5% in PBS 1X) and the majority of the fibroblasts were collected. Then, a standard TRYPLE solution was added to the mixed population, to recover the majority of the epithelial cells. Scale bar: 100  $\mu\text{m}$ .

This optimized protocol let to the collection of 16 *ex vivo* primary tumor cultures among a total 80 collected tissues. Two of 16 cultures were derived from CRPC patients, while 14 belonged to untreated patients with aggressive prostate cancer (**Figure 11**). From these 14 cultures, we selected 10 for further analyses.

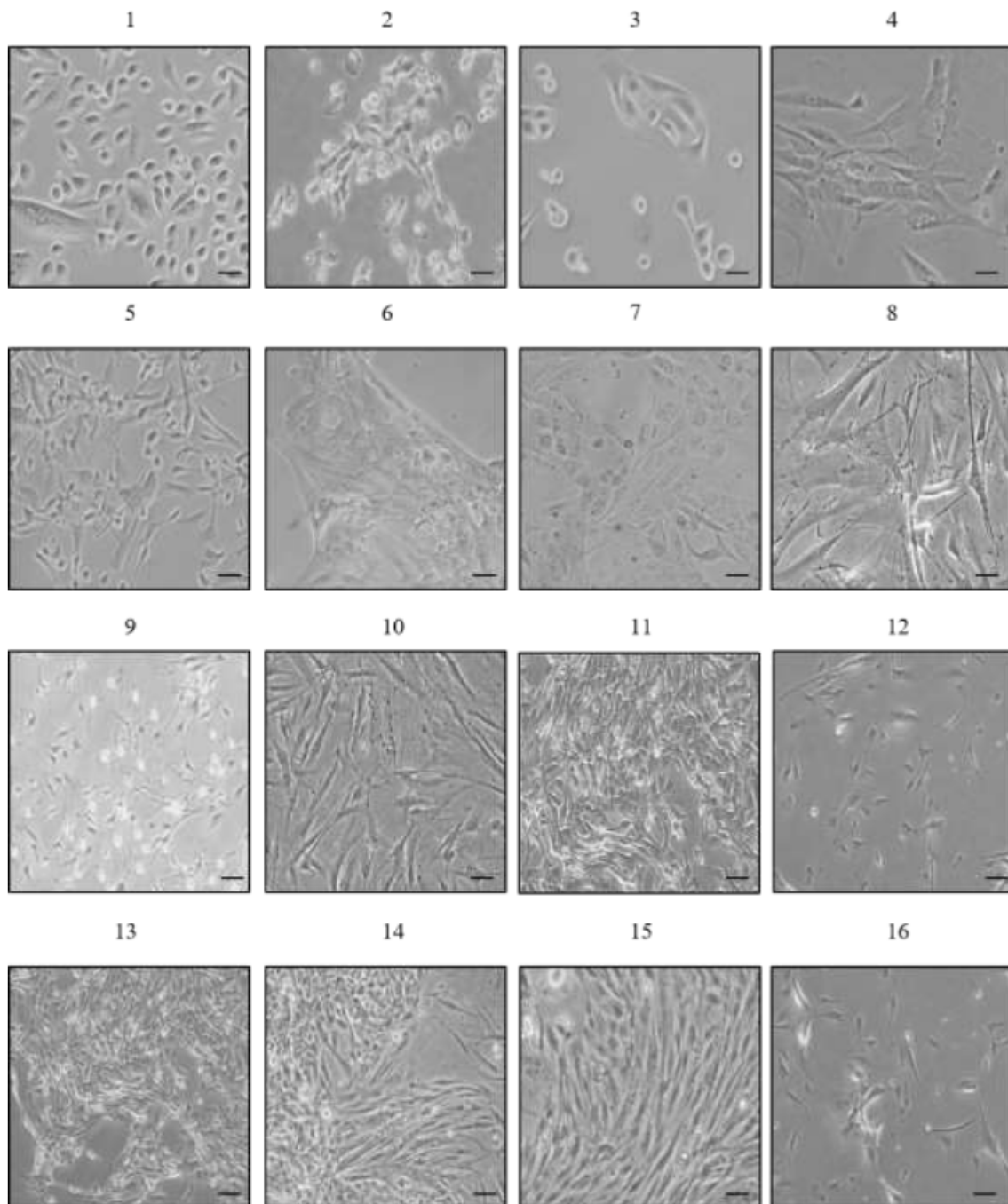


**Figure 11. Microscopy images of purified *ex vivo* primary tumor cultures.** *Ex vivo* primary tumor cultures shown were established after a mechanic digestion of five needle biopsies into pieces of 1 mm<sup>3</sup>, then seeded in half of the complete medium for the first 24 hours in poly-D-lysine plus collagen I pre-coated plates. These cultures were also treated to eliminate the presence of fibroblasts. Scale bar: 100  $\mu$ m.

## 2. Phenotypic characterization of *ex vivo* primary tumor cultures

### 2.1 Clinical characteristics of the patients and expression of epithelial markers

The clinical characteristics of the patients from which 10 *ex vivo* primary tumor cultures were generated, are described in **Table 11**. All patients from whom successful establishment of tumor culture was obtained, had a high-grade tumor, ( $\geq 8$ ), and 8 patients out of 10, were positive for metastasis at the time of biopsy. All patients were treated with ADT, and four of them received ADT in combination with docetaxel. The follow up was up to July 2019 (31 months). During this time, one patient became castration resistant and one died. These 10 *ex vivo* primary tumor cultures were selected for characterization, performed by studying the expression of prostate epithelial markers, and genetic alterations in relevant driver genes (oncogenes and tumor suppressor) previously described in primary naïve prostate tumors (**Table 11**)<sup>21</sup>.

**Table 11. Summary of the clinical characteristics of the 10 patients selected for this study.**

PSA: Prostate specific antigen.

ADT: Androgen deprivation therapy

CT: Chemotherapy

CRPC: Castration resistant prostate cancer

PATIENT	PSA	GLEASON	METASTASIS	ADT	CT	CRPC	EXITUS
1	1106	9 (5 + 4)	YES	YES	NO	YES	NO
2	60	8 (4 + 4)	YES	YES	NO	NO	NO
3	85	8 (4 + 4)	NO	YES	YES	NO	YES
4	222	8 (4 + 4)	YES	YES	NO	NO	NO
5	107	8 (4 + 4)	NO	YES	YES	NO	NO
6	90	8 (4 + 4)	YES	YES	YES	NO	NO
7	83	10 (5 + 5)	YES	YES	YES	NO	NO
8	103	8 (4 + 4)	YES	YES	YES	NO	NO
9	50	9 (4 + 5)	YES	YES	NO	NO	NO
10	98	10 (5 + 5)	YES	YES	NO	NO	NO

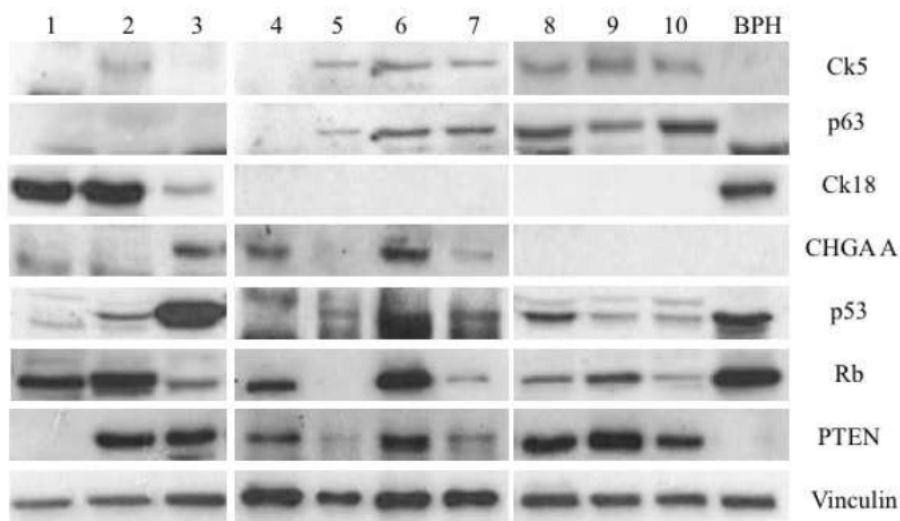


**Figure 12. Expression of prostate epithelial markers and major driver proteins in *ex vivo* primary tumor cultures.** Representative immunoblots showing the expression of endogenous levels of the indicated proteins from the 10 selected *ex vivo* primary tumor cultures (androgen sensitive) using specific antibodies. Numbers identified the patient tissue from which the culture was derived. Signals were revealed by secondary antibodies coupled to HRP using a chemiluminescent substrate (ECL). Vinculin signal was used as control of protein loading. BPH, benign prostate hyperplasia.

Results from these analyses show that cultures 1, 2, and 3 expressed the epithelial luminal marker CK18 but did not express basal cells markers CK5 and p63, suggesting the presence of cancer epithelial cells with luminal characteristics (**Figure 12**). In contrast, cultures 5 to 10 showed moderate expression of CK5 and p63 and no expression of CK18, suggesting the presence of cells with a basal epithelial phenotype. Interestingly, cultures 3, 4, and 6 are possible mixed populations of cells positive for the expression of chromogranin A (CHGA A), a neuroendocrine marker that identifies a very aggressive type of prostate cancer that in culture 3 is mixed with a luminal epithelial type, and in culture 6 is mixed with basal epithelial cells. Culture 4 did not express any of these epithelial markers (**Figure 12**). Regarding the status of activation expression of gene drivers of tumorigenesis, we examined the expression of p53, Rb and PTEN proteins. p53 was not expressed in cultures 1 and 4 but overexpressed in cultures 3 and 6, possibly indicating the presence of a stabilizing mutation. Rb was not expressed in culture 5 and significantly decreased in cultures 3, 7 and 10. Finally, PTEN was not found in culture 1 and very low levels were detected in cultures 5 and 7. Culture derived from patient 1 did not express p53 or PTEN, suggesting a complete loss of function.

*2.2 Analysis of genomic alterations: TMPRSS2-ERG fusion, SPOP, PTEN and TP53 mutations.*

To further characterize the *ex vivo* primary tumor cultures, we studied the more frequent genomic alterations described in primary naïve prostate tumors<sup>36</sup>. In addition, to verify whether these cultures may be useful models of the tumor from which they derived, the corresponding tumor tissues were also studied. Results are presented in **Table 12**, where each alteration found is compared in the tissue and in the corresponding *ex vivo* primary tumor culture from the same patient. Using mRNA from these samples and Real Time PCR, we studied the chromosomal translocation *TMPRSS2-ERG*, while PCR and DNA sequencing was used to detect mutations in *SPOP*, *PTEN* and *TP53* genes. Although *RBI* is another important gene frequently mutated in PCa, we could not evaluate the status of alterations in the selected tissues and corresponding cultures. **Figure 13** shows the percentage of the lesions reported for each gene in the *ex vivo* primary tumor cultures (**Figure 13A**) and the original tissues (**Figure 13B**). All *ex vivo* primary tumor cultures and original tumor tissues were negative for the presence of *SPOP* mutations. In contrast, different types of mutations were found in *TP53*, both in *ex vivo* primary tumor cultures and tumor tissues. In particular, we detected two missense mutations in the *ex vivo* tumor cultures. A deletion of one cytosine in tumor culture 1, provokes a shift in the ORF at residue 139 (K139R) that leads to a premature stop codon at residue 169 (**Figure 13B-C**), with the translation of a truncated p53 product for culture 1, in agreement with the absence of signal for this protein observed in the western blot (**Figure 12**). The second mutation found in *TP53* is a common nonsynonymous substitution P72R, detected in cultures 2, 3, 4, 5, 8, 9, 10 and primary tumor tissues 2, 3 and 8 (**Figure 13D-E**). The alteration P72R is described as a frequent allele variant and causes an alteration in the p53 functions. Indeed, when p53 undergoes to this alteration, apoptosis is enhanced<sup>38</sup>. These two polymorphic variants of *TP53* confer different functions and for this, they have been implicated in susceptibility and predisposition to solid tumors, inflammation, type II diabetes<sup>184 38 39</sup>.

Finally, *PTEN* was found no mutated in all prostate tumor tissues. However, *ex vivo* primary tumor culture 1 presented a mutation (T to G) in the first codon that caused the missense mutation M1R, and resulted in the formation of a non-functional protein (**Figure 13F-G**).

We then analyzed the chromosomal translocation *TMPRSS2-ERG*, described to be as frequent as up to 50% of primary naïve prostate tumors<sup>185</sup>. The gene fusion was detected in three original tissues (1, 3 and 5), however the corresponding *ex vivo* cultures were negative for the presence of *TMPRSS2-ERG* (**Figure 13A**).

**Table 12. Scheme of the alterations found in tissues and corresponding *ex vivo* primary tumor cultures.**  
n.d. : not detected.

PATIENT	<i>TMPRSS2-ERG</i> +		<i>TP53</i> mut		<i>PTEN</i> mut	
	TISSUE	CULTURE	TISSUE	CULTURE	TISSUE	CULTURE
1	YES	NO	N.D.	DEL	NO	M1R
2	NO	NO	P72R	P72R	NO	NO
3	YES	NO	P72R	P72R	NO	NO
4	NO	NO	N.D.	P72R	NO	NO
5	YES	NO	N.D.	P72R	NO	NO
6	NO	NO	N.D.	N.D.	NO	NO
7	NO	NO	N.D.	N.D.	NO	NO
8	NO	NO	P72R	P72R	NO	NO
9	NO	NO	N.D.	P72R	NO	NO
10	NO	NO	N.D.	P72R	NO	NO



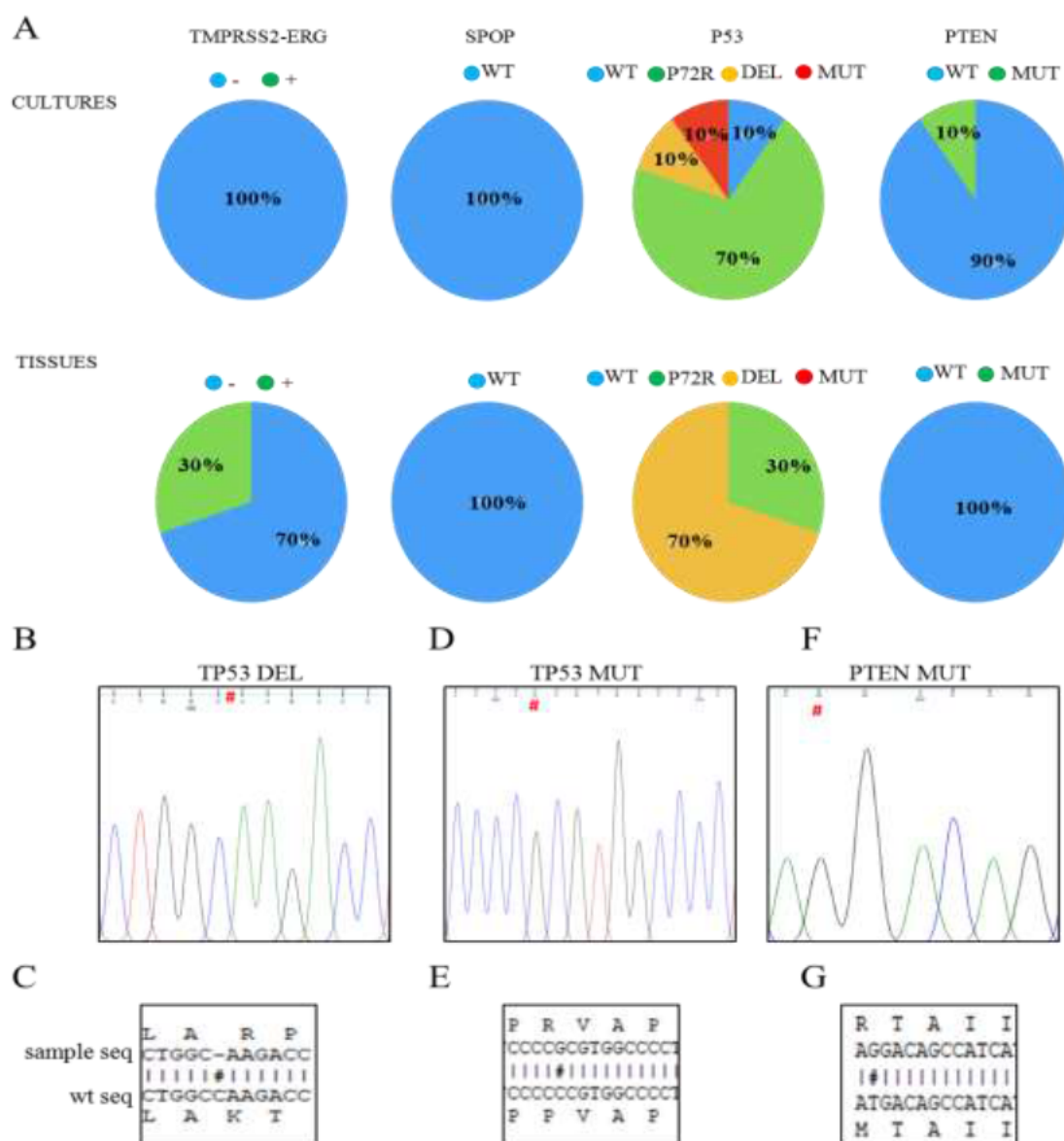


**Figure 13. Molecular alterations found in *ex vivo* primary tumor cultures and their corresponding original tumor tissues.** (A) Representative pie charts of the genetic alterations in *TMPRSS2-ERG*, *SPOP*, *TP53* and *PTEN* genes in *ex vivo* cultures and in corresponding original tissues. (B) Chromatogram showing the point mutation in the nucleotide 610 of *TP53* and (C) the consequent missense mutation K139R and a premature stop codon in the residue 169. (D) Chromatogram showing the point mutation in nucleotide 413 of *TP53* and (E) the consequent missense mutation P72R. (F) Chromatogram showing the point mutation in the nucleotide 846 of *PTEN* and (G) the consequent missense mutation M1R.

### 2.3 Derivation of androgen Independent (AI) variant *ex vivo* tumor cultures

The deprivation of androgens, ADT, is the first line therapy in tumors that show extra capsule invasion or metastasis at the time of diagnosis<sup>107,186</sup>. To reflect the treatment given to the patient, the *ex vivo* primary tumor cultures were treated with medium lacking steroid hormones and androgen independent (AI) cultures were derived by selection of cells able to grow in these conditions for at least seven days. Surviving cells were trypsinized and replated at the same conditions (without hormones) and expanded for further analysis.

The androgen receptor (AR) has a crucial role in PCa progression, activating a variety of downstream pathways that regulate proliferation, invasion and metastasis. The AR induces the expression of many genes, including the *KLKs* family of genes that comprises PSA, encoded by the *KLK3* gene, and the protease *KLK2*, responsible for cleaving and activating the pro-prostate-specific antigen (PSA)<sup>187</sup>. We analyzed the mRNA relative levels of *AR* and both *KLK2* and *KLK3* in LNCaP AI cells in comparison to LNCaP AD as reference cell line. In LNCaP AI cells, AR expression is maintained high, although they are resistant to androgens. In contrast, both *KLKs* had significantly decreased levels compared to parental AD cells (**Figure 14**). The same analysis performed in *ex vivo* primary tumor cultures showed a high heterogeneity. Three categories of response to androgen independence can be observed in comparison to AD cultures: (i) AI cultures with very low or undetectable expression of *AR*, *KLK2* and *KLK3* genes, (ii) AI cultures showing similarities with LNCaP AI cells, and (iii) AI *ex vivo* primary tumor cultures showing increased levels of *KLK3*. AI *ex vivo* primary tumor cultures 4, 5 and 6 can be part of the first category (i) showing very low expression of both *KLKs*. *AR* levels were increased 2-fold in AI *ex vivo* primary tumor culture 4, while they were slightly decreased in AI cultures 5 and 6 (**Figure 14**). In contrast, *ex vivo* AI primary tumor cultures 9 and 10 shared analogies with LNCaP AI cells, expressing small increased levels of *AR*, although, unlike LNCaP AI cells, maintained the expression of *KLKs* (**Figure 14**). Finally, AI *ex vivo* primary tumor cultures 1, 7 and 8 shared significant increased levels of *KLK3*. However, in AI *ex vivo* primary tumor culture 1, the *AR* and *KLK2* levels were undetectable. In AI *ex vivo* primary tumor culture 7, the *AR* was present and *KLK2* was strongly increased, and in AI *ex vivo* primary tumor culture 8, the *AR* and *KLK2* were expressed at comparable levels as in AD cells (**Figure 14**). In summary, the acquisition of the androgen independence in the *ex vivo* primary tumor cultures did not in general affect the expression of *KLK3*, that it was also found significantly increased in three of the AI cultures, suggesting that this gene might be a good marker to identify androgen independent cells<sup>188</sup>.

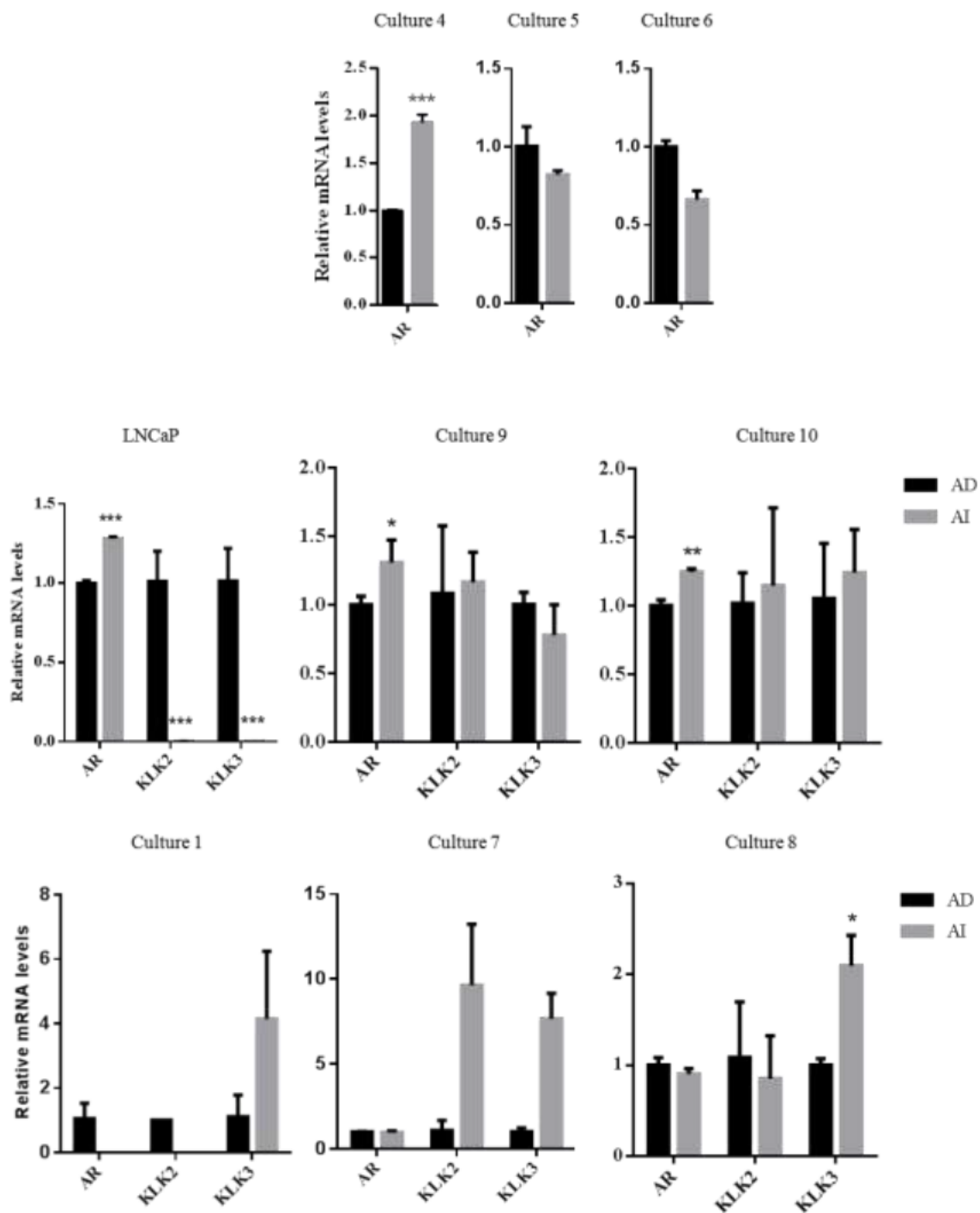


**Figure 14.** The effect of ADT on AR signaling in AI and AD LNCaP cells and *ex vivo* primary tumor cultures. Relative mRNA levels of *AR*, *KLK2* and *KLK3* on AI and AD LNCaP cells and *ex vivo* primary tumor cultures 1, 4, 5, 6, 7, 8, 9 and 10. *TBP* and *IPO8* were used as housekeeping genes. Data are the mean of 2 experiments (n=2), each performed in sextuplicate. *p* value < 0.05 \*, < 0.01 \*\*, < 0.001 \*\*\*.

### 3. Functional characterization of androgen dependent and independent *ex vivo* primary tumor cultures.

#### 3.1 Proliferation assays

The proliferation rate of androgen dependent (AD) and independent (AI) *ex vivo* primary tumor cultures was analyzed. The LNCaP AD and AI cultures were used as reference. When comparing the proliferation of parental AD cultures to AI cultures, different behaviors were observed in the nine *ex vivo* cultures analyzed. One group of *ex vivo* primary tumor cultures (1, 3, 4, and 6) behaved similarly to the LNCaP cell model (**Figure 15**). Culture 2 had the slowest growth rate, the majority of cells were senescent and we could not further evaluate this primary culture (data not shown). For the remaining *ex vivo* primary tumor cultures, the parental AD cells replicated faster compared to AI variant cells, although in cultures 5 and 7 no significant differences were observed between AD and AI cultures proliferation rates. Accordingly, the duplication time of these AD cultures was lower compared to the corresponding AI variants (**Table 13**), for example the LNCaP AD parental cells showed duplication time of 43 hours, while the AI variant cells duplicated in 50 hours (**Table 13**). In turn, in *ex vivo* tumor cultures 8, 9, 10, the AI variant cells grew at a faster rate compared to their parental AD cells (**Figure 15**), although this difference was statistically significant only for culture 8. Accordingly, the duplication time of parental AD cultures 8, 9, 10 were longer compared to the AI variants (**Table 13**). In summary, the results show a high heterogeneity of behaviors in AI *ex vivo* primary tumor cultures, with four examples in agreement with LNCaP AI cells (AI *ex vivo* primary tumor cultures 1, 3, 4 and 6).

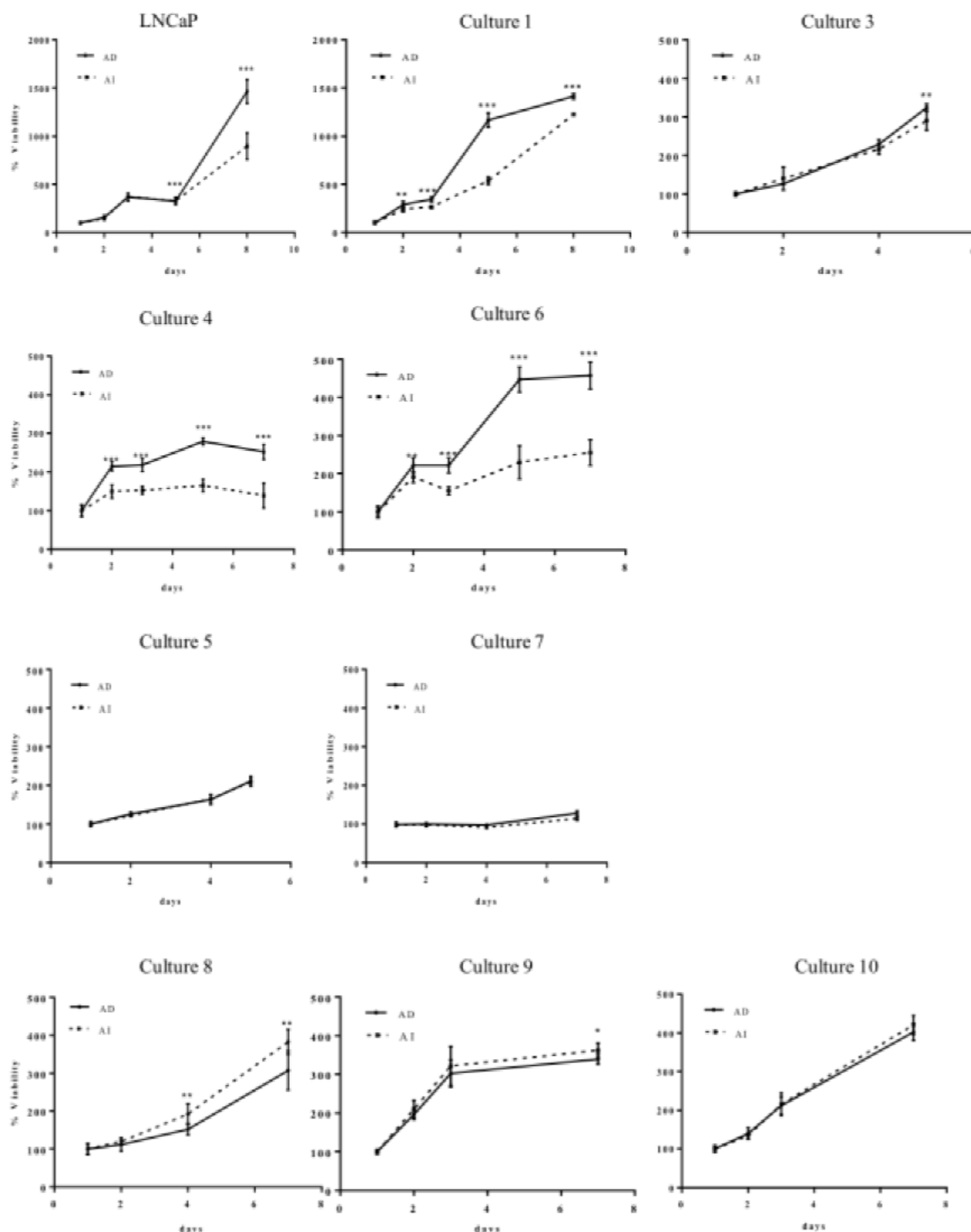


**Figure 15. The effects of ADT on the growth of *ex vivo* primary tumor cultures.** Proliferation curves of androgen dependent (AD) and androgen independent LNCaP cells, *ex vivo* primary tumor cultures 1, 3, 4 and 6 showing significant differences in their growth rate with respect to AD cells. AD and AI *ex vivo* primary tumor cultures 5 and 7 did not show differences in their proliferation rate. AI *ex vivo* primary tumor cultures 8, 9 and 10 grew faster than the AD variant. Cells plated in 96 well dishes, were grown for 7 days with (AD) or without (AI) androgens in the culture medium. The growth rate was measured at day 1, 2, 3, 5 and 7. Data are the mean  $\pm$  s.d. of three independent experiments (n=3), each performed in octuplicate. *p* value < 0.05 \*, < 0.01 \*\*, < 0.001 \*\*\*.

**Table 13. The doubling time of AD and AI *ex vivo* primary tumor cultures LNCaP culture.**

ID: identification; AD: Androgen Dependent; AI: Androgen Independent; h: hours; Doubling time was calculated using the formula:  $\text{duration} \times \log(2) / \log(\text{final concentration}) - \log(\text{initial concentration})$ , adapted from Zhang et al.<sup>189</sup>.

Culture ID	AD (h)	AI (h)
LNCaP	43	50
1	50	53
3	71	78
4	44	83
5	111	113
6	76	124
7	134	253
8	103	86
9	49	45
10	83	81

### 3.2 Motility assays

The above results have shown that most AI cultures that acquired abilities to overcome the stress of the lack of androgens have reduced their doubling time. In order to characterize whether the androgen independent state is associated to a more aggressive invasive phenotype, we studied cell motility *in vitro*. For these analyses, we tested the cell capacities to recover from an inflicted wound (wound healing assay), where cells show their ability to close a scratch made in the monolayer. To be able to compare the capacity of migration of each cell culture, we expressed the motility as the time required by each culture to completely close the wound. The results showed that *ex vivo* AI primary tumor cultures 1, 4, 5, and 6 showed increased motilities than their parental AD cultures, and in cultures 4, 5, and 6 this difference was statistically significant (**Figure 16**). However, AI culture 3 had a significantly decreased motility with respect to AD parental cells (**Figure 16**). This data suggests that the majority of AI *ex vivo* cultures (three among five tested) developed a higher motility than AD cells, that may be associated to invasion and progression to aggressive PCa.

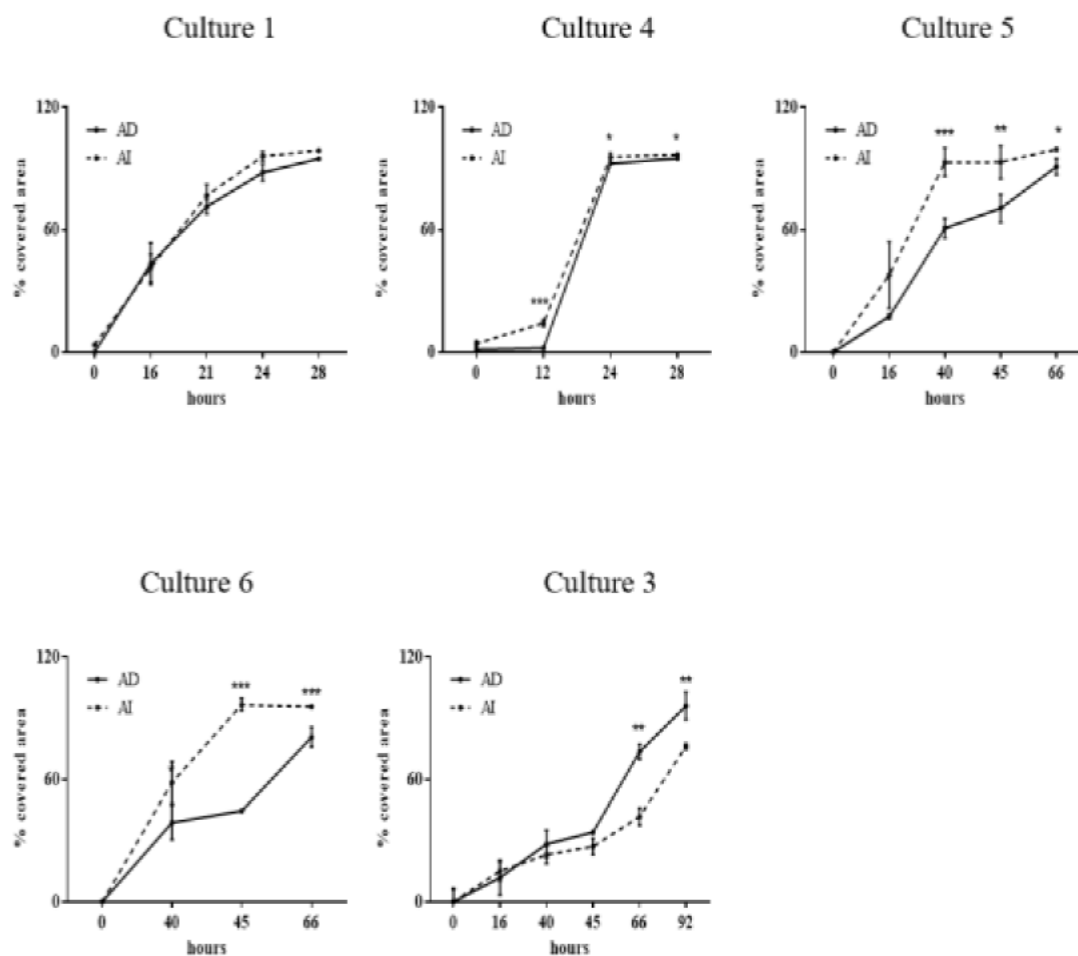


**Figure 16. Motility of AI and AD ex vivo primary tumor cultures.** Quantitative measurements of cell migration of the AD and AI ex vivo primary tumor cultures were performed at different time points and are represented in the graphs as the percentage of closure of the wound. Data are from cultures grown in triplicates.  $p$  value  $< 0.05$  \*,  $< 0.01$  \*\*,  $< 0.001$  \*\*\*.

### 3.3 Analysis of the epithelial and mesenchymal genes

We next investigated whether the increased motility of AI cultured cells was attributable to the induction of an epithelial-mesenchymal transition (EMT). Thus, we analysed the mRNA expression of markers of EMT (*CDH1*, *Vimentin*, *SNAI1*) in parental AD and AI LNCaP cells. Results showed that AI cells had increased expression of *Vimentin* and *SNAI1* and decreased levels of epithelial markers *CDH1*, *CK5*, *CK14* and *CK18* (Figure 17). Similar results were observed in AI ex vivo primary tumor cultures 4, 5 and 10, where *Vimentin* and/or *SNAI1* levels were significantly increased compared to AD cells, while *CDH1* decreased or did not significantly change (Figure 17). In contrast, the other AI ex vivo primary tumor cultures did not show changes in the levels of EMT markers (Figure 17-Figure 18). Of notice, the primary AI cultures 1, 3, 8 and 10 showed an up-regulation of the prostate basal marker *CK14*, suggesting an enrichment of basal epithelial cells in the AI

population. In particular, AI *ex vivo* primary tumor culture 3 showed the so-called transit amplifying phenotype with co-occurrence of basal and luminal *CK5*, *CK14*, and *CK18* expression (**Figure 17**), while the AI *ex vivo* primary tumor culture 8 was mostly composed by basal cells *CK5*<sup>+</sup>/*CK14*<sup>+</sup>. These analyses demonstrate that in ADT induces the expression of EMT signalling pathway actors and consequently an increased motility of at least 2 AI *ex vivo* primary tumor cultures.

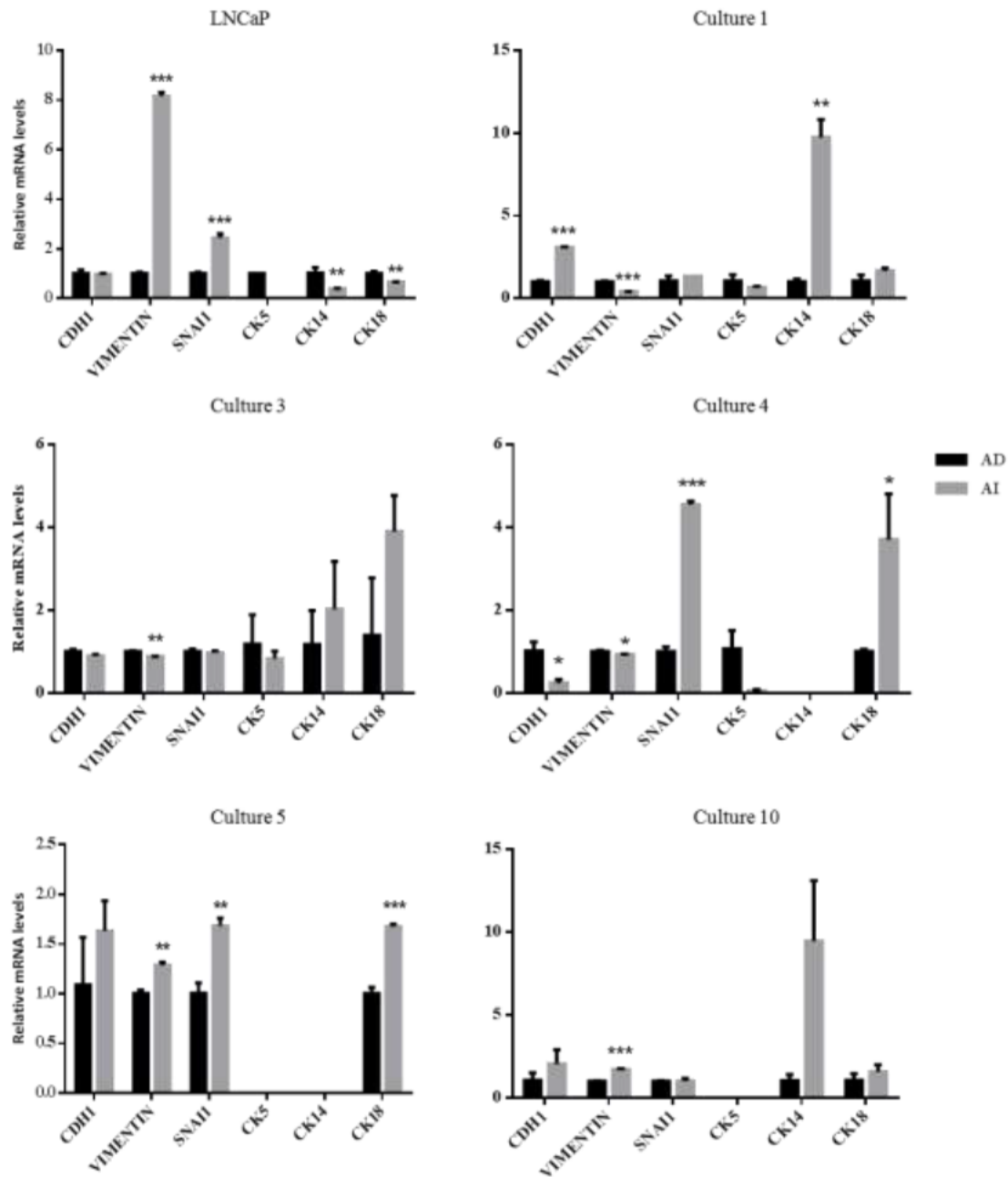


**Figure 17.** ADT induce EMT in AI LNCaP cells and in three *ex vivo* primary tumor cultures. Relative mRNA levels of indicated genes on AI and AD LNCaP cells and *ex vivo* primary tumor cultures 1, 2, 3, 4, 5 and 10. *TBP* and *IPO8* were used as housekeeping genes. Data are the mean  $\pm$  s.d. of 2 experiments (n=2), each performed in sextuplicate. *p* value < 0.05 \*, < 0.01 \*\*, < 0.001 \*\*\*.



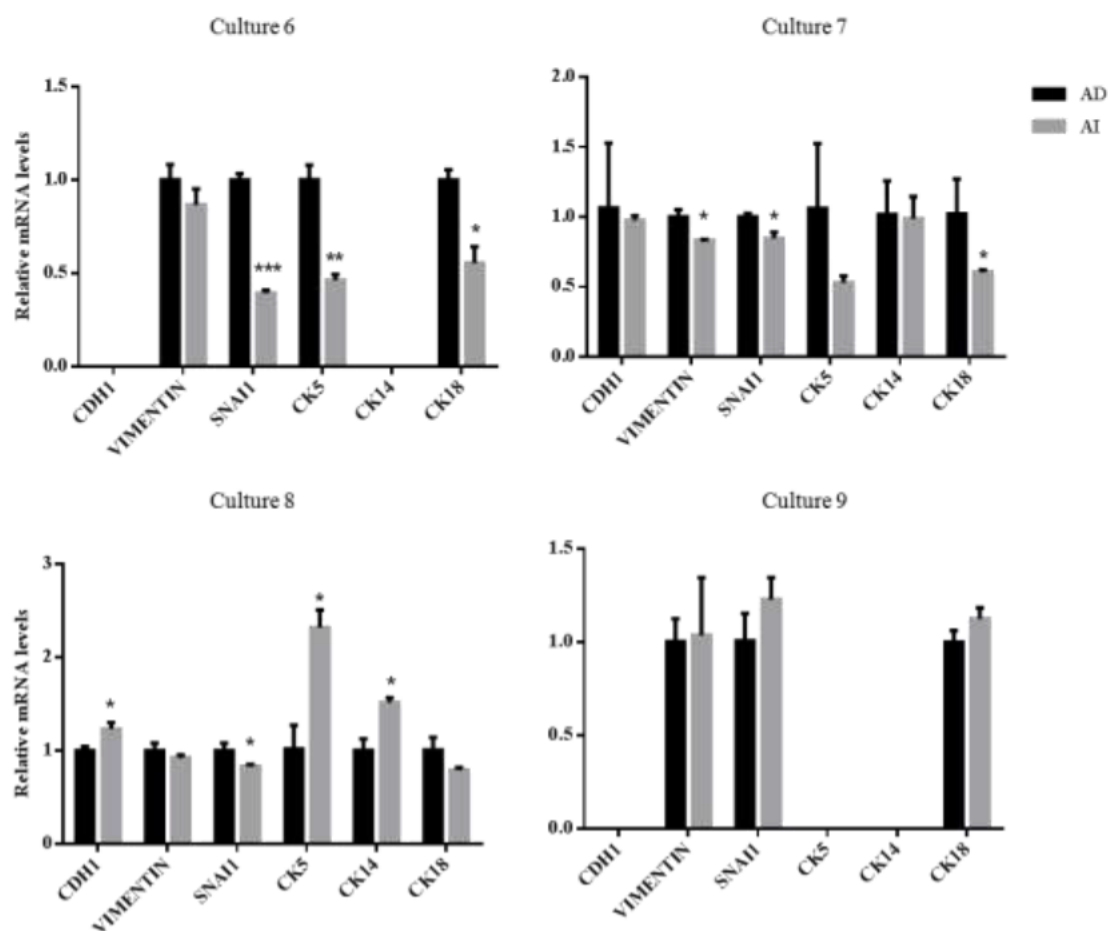


**Figure 18.** EMT signaling in *ex vivo* primary tumor cultures from 6 to 9 is not induced by ADT. Relative mRNA levels of indicated genes on AI and AD *ex vivo* primary tumor cultures 6, 7, 8 and 9. *TBP* and *IPO8* were used as housekeeping genes. Data are the mean  $\pm$  s.d. of 2 experiments (n=2), each performed in sextuplicate. *p* value < 0.05 \*, < 0.01 \*\*, < 0.001 \*\*\*.

### 3.4 Drug toxicity assays

It has been proposed that resistance to one therapeutic treatment confers tumor cells resistance to other drugs<sup>190</sup>. Therefore, we analyzed the viability of the AI *ex vivo* primary tumor cultures resistant to ADT to cross-resist to docetaxel and cabazitaxel. As shown in **Figure 19** AI *ex vivo* primary tumor cultures from patients 1, 3, 5, and 6 including the LNCaP AI cells, showed a significantly increased resistance (higher half maximal inhibitory concentration IC<sub>50</sub>) to docetaxel compared to their corresponding AD cells, while for culture 4 it was not possible to calculate the IC<sub>50</sub>.

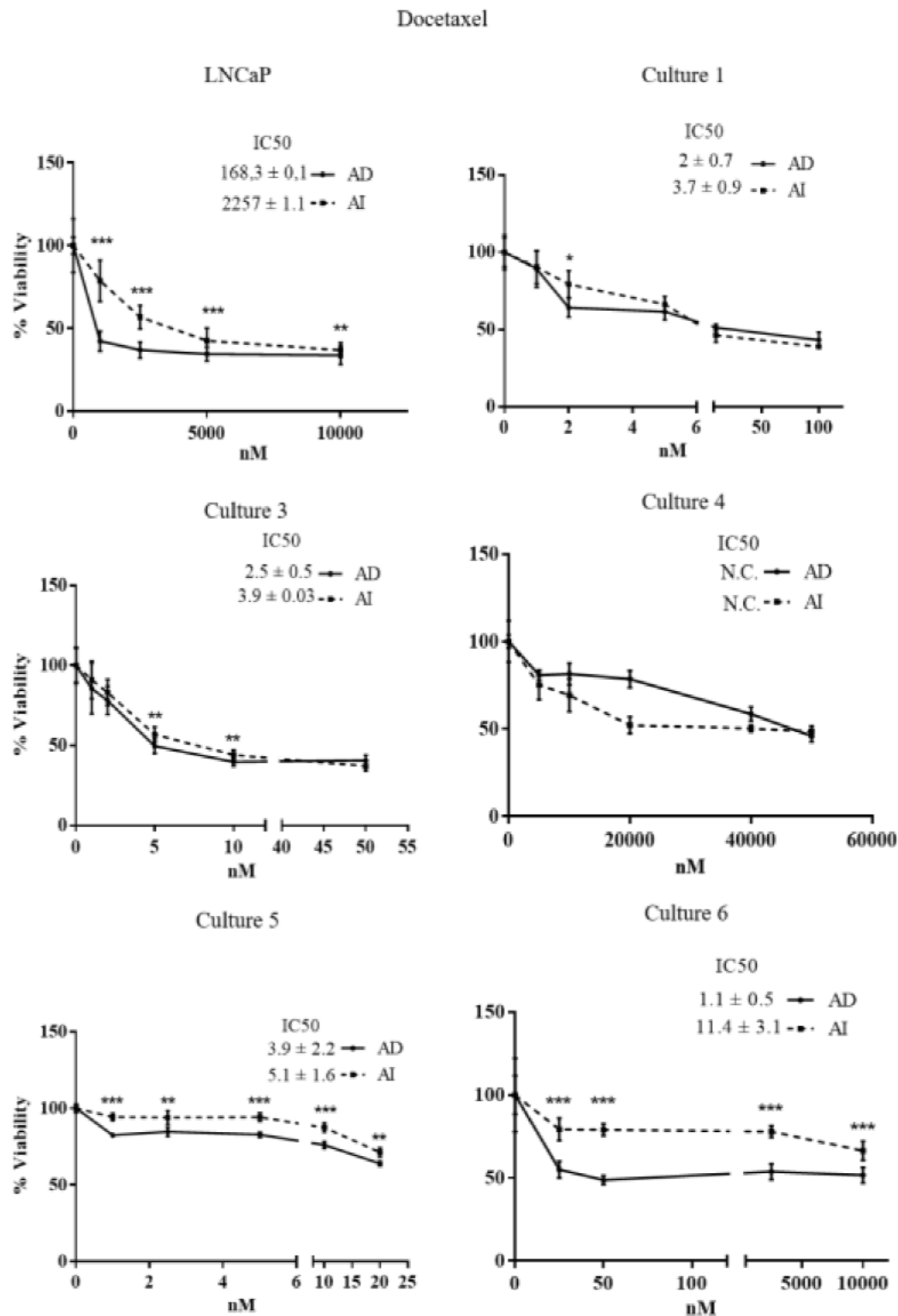


**Figure 19.** The resistance to androgen deprivation in AI and AD *ex vivo* primary tumor cultures increases their resistance to docetaxel. Drug toxicity curves from AD and AI LNCaP cells and *ex vivo* primary tumor cultures 1, 3, 4, 5 and 6 in presence of docetaxel. Cells were treated with vehicle (DMSO) or serial concentration of drug for 72 h. Results represent the mean  $\pm$  s.d. of three ( $n = 3$ ) independent experiments, each performed in quintuplicate.  $p$  value  $< 0.05$  \*,  $< 0.01$  \*\*,  $< 0.001$  \*\*\*.

In addition, LNCaP AI cells and AI *ex vivo* primary tumor cultures from patients 1, 3, and 6 also showed significantly increased IC50 values to cabazitaxel compared to their corresponding AD cultures (**Figure 20**). AI *ex vivo* primary tumor cultures 4 and 5, showed a strong resistance to cabazitaxel (the IC50 could not be calculated). These results are

summarized in **Table 14** and suggest that ADT may induce resistance also to chemotherapy.

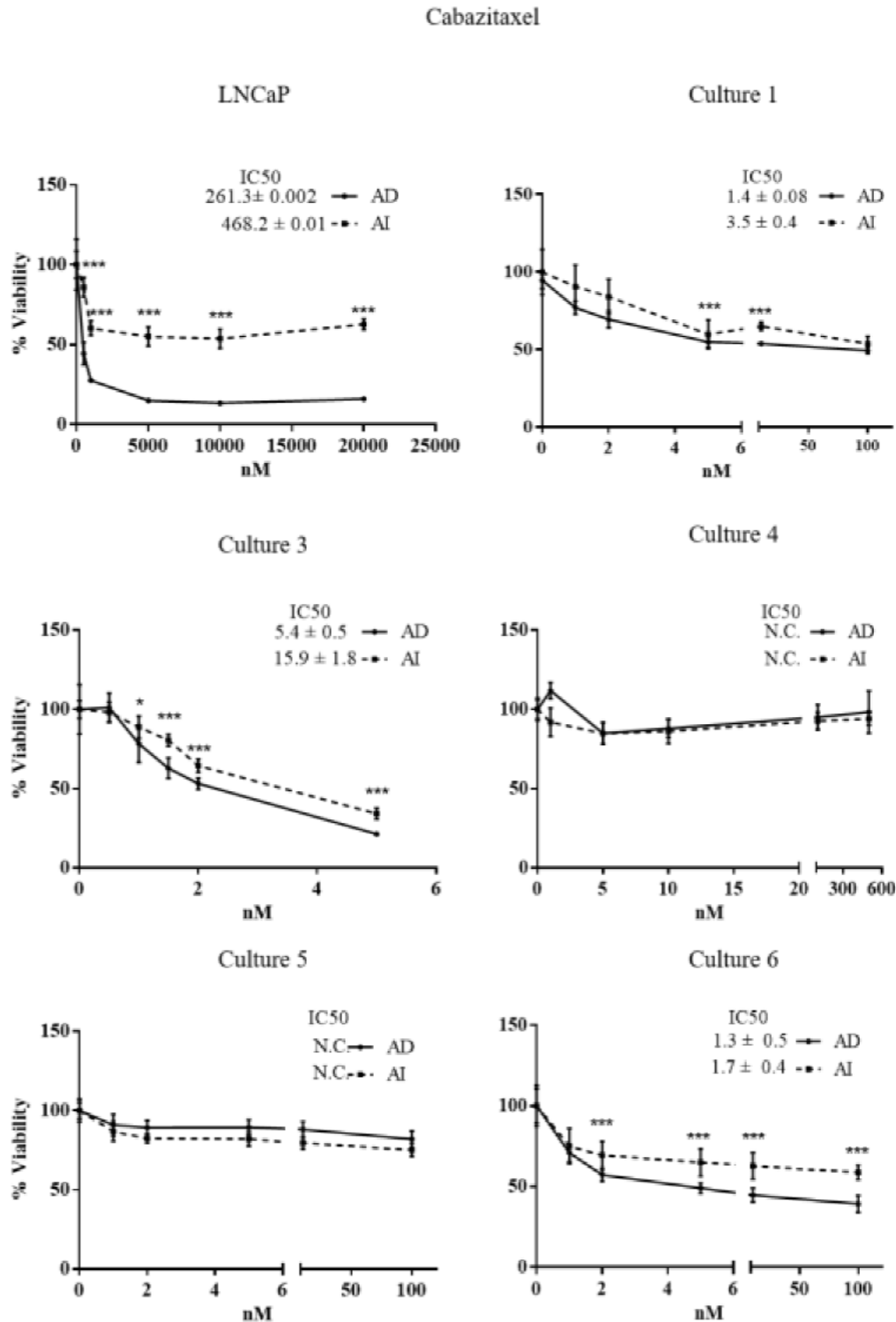


**Figure 20. The resistance to androgen deprivation in *ex vivo* primary tumor cultures increases their resistance to cabazitaxel.** Drug toxicity curves from AD and AI LNCaP cells and *ex vivo* primary tumor cultures 1, 3, 4, 5 and 6 in presence of cabazitaxel. Cells were treated with vehicle (DMSO) or serial concentration of drug for 72 h. Results represent the mean ± s.d. of three (n = 3) independent experiments, each performed in quintuplicate. *p* value < 0.05 \*, < 0.01 \*\*, < 0.001 \*\*\*.

**Table 14. The half maximal inhibitory concentration (IC50) of AD and AI ex vivo primary tumor cultures and LNCaP cells in response to taxanes.**

ID: identification; AD: Androgen Dependent; AI: Androgen Independent. The IC50 is expressed in  $\mu\text{M}$ . ID: identification; AD: Androgen Dependent; AI: Androgen Independent; IC50: inhibitory concentration of the 50% of the culture expressed in  $\mu\text{M}$ .

Culture ID	AD	AI	AD	AI
	IC50 Docetaxel		IC50 Cabazitaxel	
LNCaP	168.3	2257	261.3	468.2
1	2.1	3.7	1.4	3.5
3	2.4	3.7	5.4	15.9
4	N.C.	N.C.	N.C.	N.C.
5	3.9	5.1	N.C.	N.C.
6	1.1	11.4	1.3	1.7

### 3.5 Rate of protein synthesis

Many evidences show that cancer progression is significantly linked to alteration of the transcriptome and the traslatome<sup>191</sup>. It has been shown in different types of cancer cells that anticancer therapies affect the protein synthesis process. Thus, in order to survive, cancer cells under the therapeutic stress modulate the translation of mRNAs to select those that encode for proteins critical for their proliferation and survival<sup>192</sup>. For these experiments, we used the LNCaP model, sensitive and resistant to androgen deprivation, but we used also the Du145 and PC3 cell models sensitive and resistant to docetaxel, as previous results demonstrated a high resistance of AI cultures also to chemotherapy. We investigated whether resistant cell variant cultures (*e.g.* AI and DR) showed a decreased protein synthesis compared to their corresponding parental cultures. Using the non-radioactive SUnSET method, we could estimate the rate of mRNA translation efficiency<sup>179</sup>. Cells were treated with puromycin, a structural analog of aminoacyl tRNAs, which was incorporated in the new polypeptides for 10 minutes, preventing elongation. As positive control, cells were treated with the protein synthesis inhibitor cycloheximide in order to obtain a decrease in the amount of newly synthesized proteins. Results with the PCa cell lines showed that LNCaP and Du145 translation efficiency is not significantly affected by androgen starvation or docetaxel, whereas DR PC3 cells clearly decreased their protein synthesis ratio. *Ex vivo* primary tumor cultures 1, 3, and 5 did not highlight differences in protein synthesis between sensitive and

resistant cells, however AI variant cells 4 and 6 showed clear decreased translation rate (**Figure 21**).

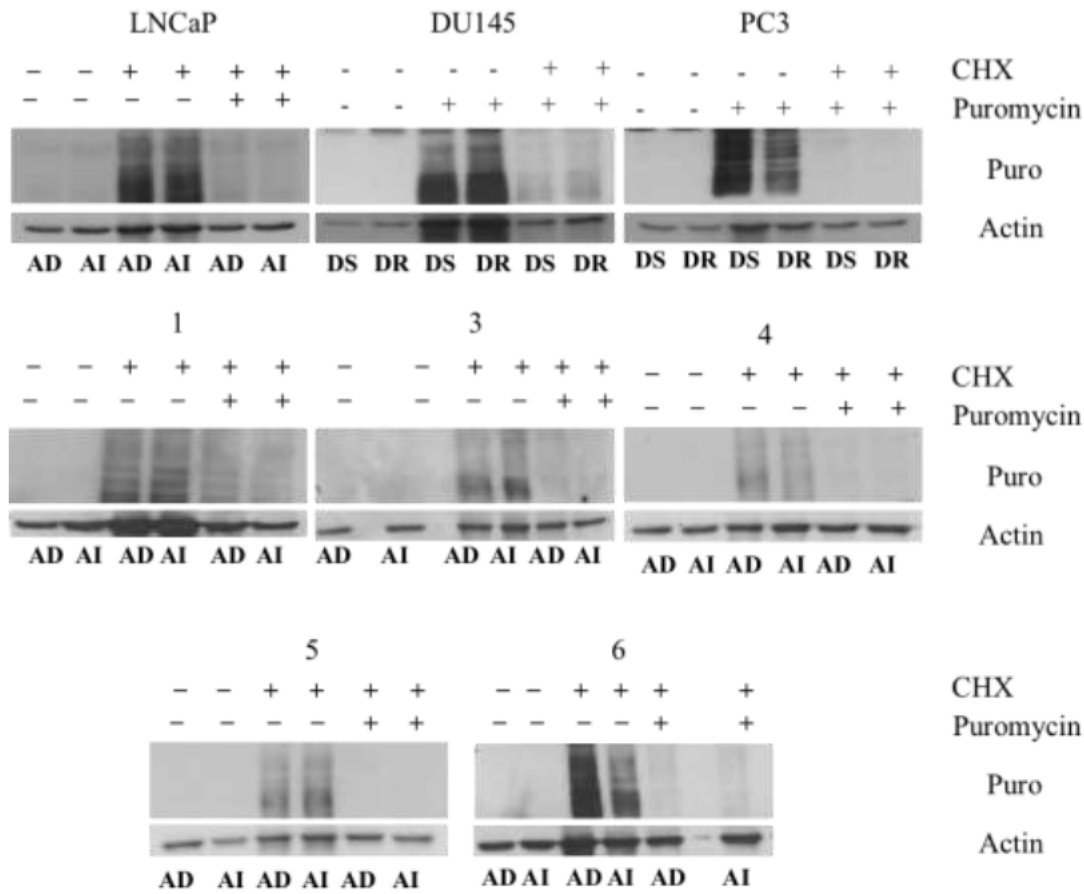


**Figure 21. The effects of ADT or chemotherapy on the protein synthesis ratio in PCa cell lines and *ex vivo* primary tumor cultures.** Representative immunoblots of protein synthesis ratio in LNCaP AI and AD cells, DS and DR Du145 and PC3 cells and *ex vivo* primary tumor cultures 1, 3, 4, 5 and 6. Cells were treated during 10 minutes with 10 µg/mL Puromycin. Negative control are untreated cells. Positive controls are cells treated with 10 µg/mL Puromycin and 10 µg/mL Cycloheximide. Signals were revealed by secondary antibodies coupled to HRP using a chemiluminescent substrate (ECL). Actin signal was used as control of protein loading.

### 3.6 Analysis of the mTORC1 pathway in resistant prostate cancer cells

Cancer cells use a variety of signaling pathway to activate proliferation and motility<sup>193</sup>. The mammalian target of rapamycin complex 1 (mTORC1), a major responsible for the regulation of protein synthesis, homeostasis and proliferation, is one of the most altered pathways in cancer, including prostate cancer<sup>194</sup>. We analyzed this pathway using the LNCaP model, sensitive and resistant to androgen deprivation, and the Du145 and PC3 cell models sensitive and resistant to docetaxel (**Figure 22**). To determine the activity of mTOR signaling, keys proteins were analyzed for their status (activation by phosphorylation) using western blotting and specific antibodies. Resistant LNCaP AI cells, showed an accumulation

of 4EBP1 protein that was not phosphorylated. The 4EBPs unphosphorylated proteins are inhibitors of the eIF4E, the eukaryotic translation initiation factor involved in directing ribosomes to the cap structure of mRNA. When 4EBPs are bound to eIF4E its action is blocked and mRNA translation is inhibited<sup>195</sup>. Thus, the increased levels of unphosphorylated 4EBPs suggest a decreased (or inactive) translation. On the other hand, the drug resistant models Du145 and PC3 cells resistant to docetaxel (DR) showed very low expression of 4EBPs, possibly indicating activation of translation. However, both DR cell lines showed significantly decreased phosphorylation of Ribosomal Protein S6 (RPS6), indicating that mTOR is not active. In addition, Du145 and PC3 DR cells expressed higher levels of programmed cell death 4 (PDCD4), an inhibitor of protein synthesis that is an mTORC1/S6K1 substrate. These observations would indicate that in resistant Du145 and PC3 DR cells the mTOR pathway is not active.

In *ex vivo* primary tumor AI cultures, mTOR signaling was found affected in cultures 4, 5 and 6. AI culture 4 behaved similarly to LNCaP AI cells, showing higher levels of total 4EBP1, although AI culture 4 also expressed higher levels of PDCD4. In contrast, AI cultures 5 and 6 showed decreased levels of p-RPS6, resembling DR cells lines **Figure 22B**). In addition, similarly to resistant PC3 DR cells, AI culture 5 showed increased pERKs signal. Taken together, these results would suggest that in comparison with the parental cells, the resistant cultures studied (androgen independent and docetaxel resistant) show in general decreased proliferation activities, increased motility, and increased resistance to drugs (taxanes). In addition, the mTOR pathway appears affected in several of the AI *ex vivo* primary tumor cultures and in the cell lines models resistant to docetaxel.

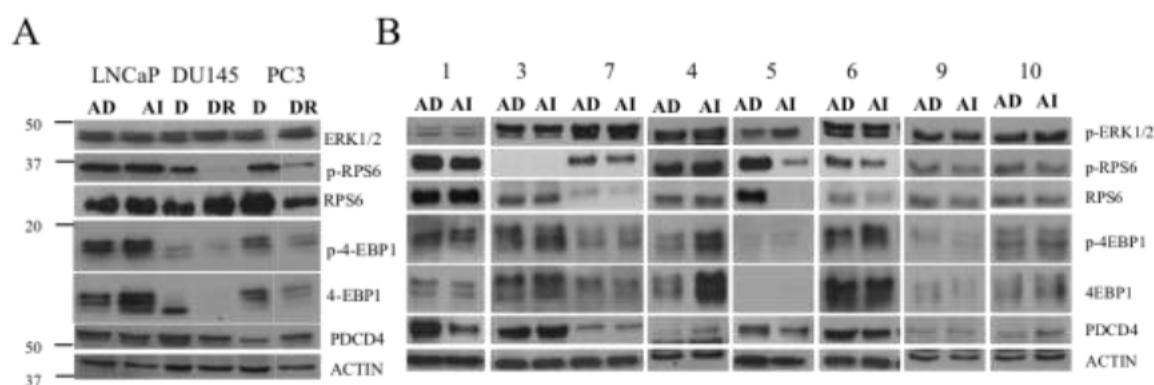


**Figure 22.** The effects of ADT on the protein synthesis ratio in AD and AI LNCaP cells and *ex vivo* primary tumor cultures. Western blot showing the levels for the indicated proteins in AD and AI LNCaP cells, DS and DR Du145 and PC3 cells (left panel), and *ex vivo* primary tumors cultures 1, 3, 7, 4, 5, 6, 9 and 10 (right panel). Signals were revealed by secondary antibodies coupled to HRP using a chemiluminescent substrate (ECL). Actin signal was used as control of protein loading.

### 3.7 Analyses of expression of self-renewal genes

It has been proposed that small subpopulations of cells with intrinsic resistance to drugs and self-renewal properties, identified as CSCs or TICs are present within a tumor mass<sup>196</sup>. CSCs have been described to have high plasticity and abilities to undergo reversible changes in their cellular properties by stochastic transition among states that differ in their capacity to contribute to tumor growth<sup>197</sup>. Drugs resistance is acquired through genetic alterations that affect a variety of processes, including the activation of epigenetic mechanisms that create a transient chromatin state that helps to mediate the emergence of drug tolerance<sup>198</sup>. Androgen Independent cultures have survived to the ADT, therefore might be enriched with populations of cells with abilities to self-renew. Here we studied the expression of self-renewal markers to assess whether AI *ex vivo* primary tumor cultures are enriched in CSCs. The LNCaP AI cells were used for comparison. AI cells with respect to parental AD cells, showed significantly higher levels of four stem cells markers (*SOX2*, *CD44* and *ALDH1A1*) (**Figure 23**). The results in AI *ex vivo* primary tumor cultures showed heterogeneous phenotypes: similarly to the LNCaP model, AI *ex vivo* primary tumor cultures 1, 4, 7 and 10 showed increased levels of several CSC markers (**Figure 23**). However, AI *ex vivo* primary tumor cultures 3, 5, 8 and 9 showed smaller differences in the expression of the markers analyzed compared to AD cells (**Figure 23**). The above observations indicated an association of the resistance to androgen deprivation with an increase in the expression of self-renewal genes in one established cell line model (LNCaP cells) and three different AI *ex vivo* primary tumor cultures.



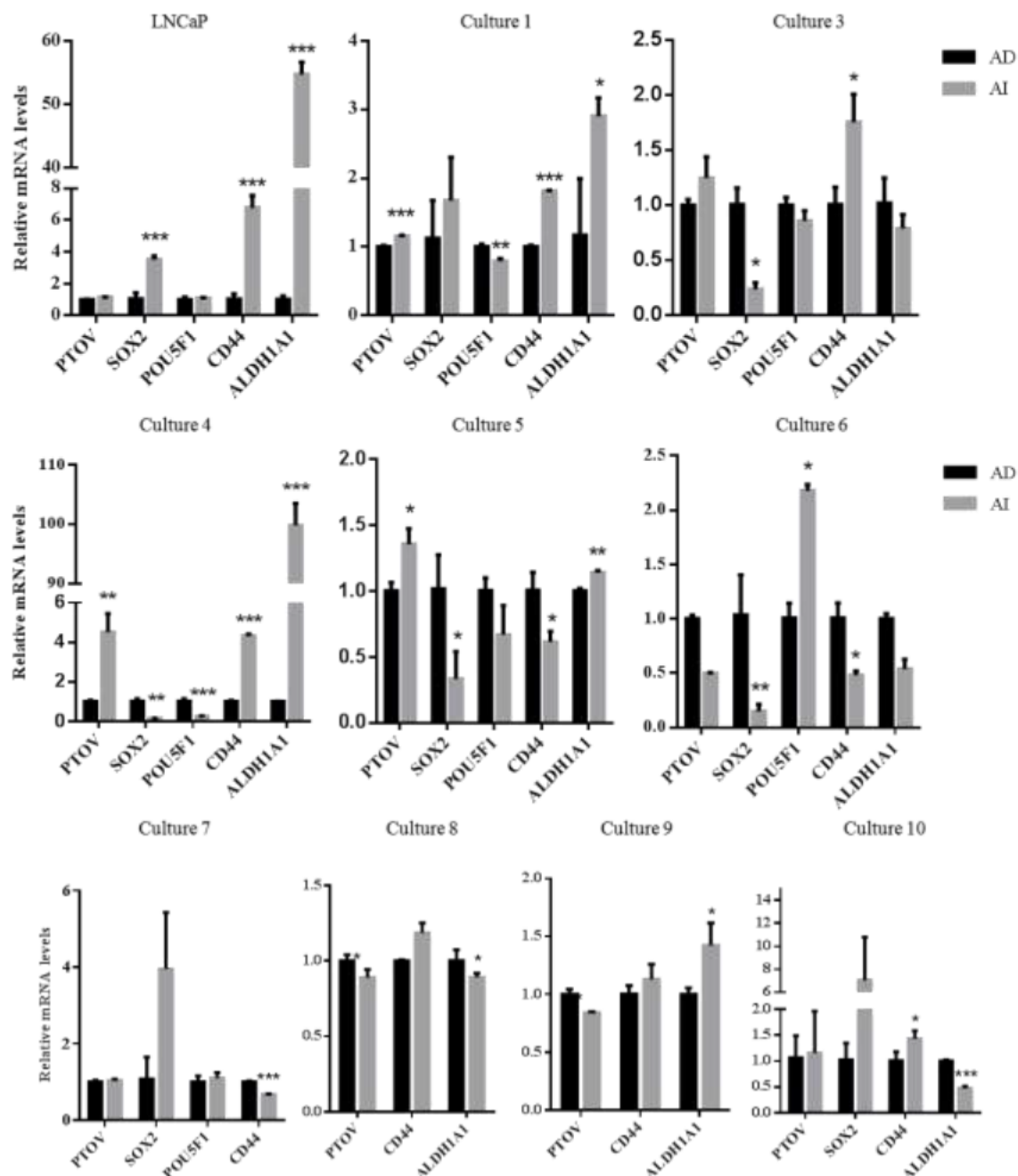


**Figure 23. Expression of self-renewal markers in AD and AI *ex vivo* primary tumor cultures.** Relative mRNA levels of indicated genes in AD and AI LNCaP cells and *ex vivo* primary tumor cultures 1, 3, 4, 5, 6, 7, 8, 9 and 10. *TBP* and *IPO8* were used as housekeeping genes. Data are the mean  $\pm$  s.d. of 2 experiments (n=2), each performed in sextuplicate. *p* value < 0.05 \*, < 0.01 \*\*, < 0.001 \*\*\*.

### 3.8 *In vivo* assays

To analyze the tumor generating ability of AD and AI *ex vivo* primary tumor cultures, we used xenotransplants in immunosuppressed mice. For these experiments, we chose *ex vivo* primary tumor culture 1. The same number of AD and AI cells ( $5 \times 10^6$ ) was injected subcutaneously into nude mice (please see detail in CHAPTER 4 p.54). The formation of

tumors was monitored weekly using a Vernier caliper. AD *ex vivo* primary tumor cultures were able to form a visible tumor after 20 days post-injection while AI tumor cultured cells formed a visible tumor after 35 days (**Figure 24**). In addition, tumors formed by AD *ex vivo* primary cultures showed a higher ability to grow than AI one, probably because the environment was more favorable to AD cells than AI population, as used mice were not castrated (**Figure 24B**). Immunohistochemistry revealed that AD tumors were anaplastic, composed mostly by undifferentiated cells with high index of mitosis, while AI tumors were desmoplastic, formed by fibrous connective tissue (**Figure 24A**).

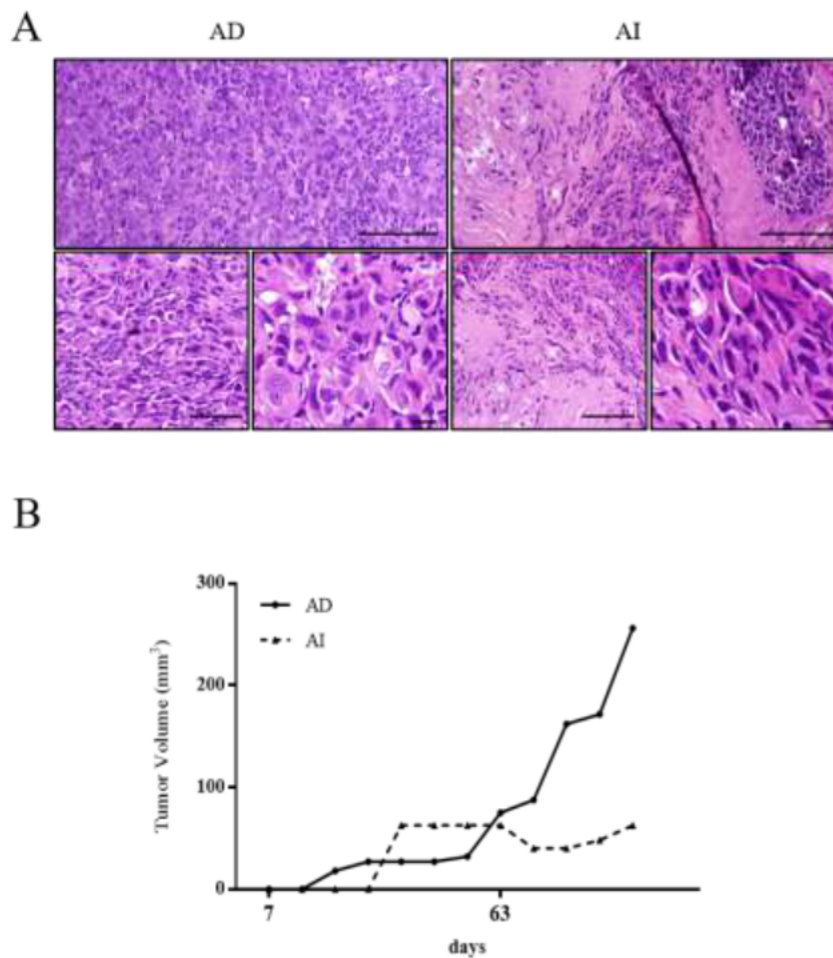


**Figure 24.** *Ex vivo* primary tumor cultures are tumorigenic *in vivo*. (A) Hematoxylin and eosin staining of tumors formed in nude mice by AD or AI *ex vivo* primary cultures 1. Scale bar: 100  $\mu$ m. (B) Tumor volume measured the growth of the tumors in mice.  $5 \times 10^6$  AD or AI cells were injected subcutaneously in each flank of the mice. Tumors were measured weekly by a caliper and allowed to grow until they reached 1 cm in diameter.

## 4. Discussion

### 4.1 Development and characterization of new *in vitro* models from primary tumors.

Historically, *in vitro* cultures derived from human prostate have been limited in availability compared with those from other organs<sup>199</sup>. The need for representative *in vitro* models of different stages of prostate cancer has produced numerous attempts to establish cell lines from human carcinomas<sup>200</sup>. The most widely used cell lines, LNCaP, Du145 and PC3, are all derived from metastatic nodules<sup>139,140,151</sup>. With the advances of technology, additional prostate cancer cell lines have become available, although recently some of these cultures have been reported cross-contaminated with the three aforementioned cell lines or other non-prostatic lines<sup>200</sup>. Presently, the repertoire of available prostate cancer cell lines mostly consist of cells derived from metastases, and therefore does not represent the heterogeneity of primary prostate tumors<sup>201-203</sup>. In addition, it is still at debate how extensively long-term culture alters the biological properties of cultured cell lines. For these reasons, cells freshly established from primary prostate tumors and from normal tissues are sought<sup>204</sup>. The amount of tissue and the optimization of the protocol are critical to generate new *in vitro* prostate cell lines. Several primary tumor cell lines were derived from radical prostatectomies, that ensure an abundant quantity of initial tissue<sup>205,206</sup>. However, radical prostatectomies are performed for small and localized tumors rather than in larger aggressive ones and these circumstances limit the frequency of times they are performed. Furthermore, patients undergoing a radical prostatectomy show a very high (95%) survival rate, whereas the challenge of the scientific community is to find new therapies for patients with aggressive and recurrent PCa<sup>207</sup>. For this reason, as starting tissue we used needle biopsies from aggressive tumors<sup>208</sup>. Because the amount of tissues is very small, different approaches were used to maximize of the recovery of cells. For example, with respect to previously described protocols, several steps were avoided (enzymatic digestion and filtration)<sup>209</sup>. Moreover, we added a poly-D-lysine coating and prolonged the cell adhesion phase (**Figure 9**). The medium was adapted to improve the selection of epithelial and stem-*like* cells present in the tissue, and disfavoring fibroblasts growth using differential trypsinization<sup>209,210</sup> (**Figure 10**). These conditions allowed the generation of a total of 16 *ex vivo* primary prostate cancer cultures starting from needle biopsies from 40 patients (rate of 40%), that could represent the heterogeneity of human primary prostate tumors.

### 4.2 Phenotypic characterization of the *ex vivo* primary tumor cultures

These cultures differed for the morphology and composition of cells (**Figure 11**). Eight *ex vivo* primary tumor cultures showed an epithelial phenotype, mostly composed of CK5<sup>+</sup>/p63<sup>+</sup>

basal cells (cultures 5, 6, 7, 8, 9 and 10), and CK18<sup>+</sup> luminal cells (cultures 1 and 2). Three tumor cultures were CHGA<sup>+</sup>, suggesting a NEPC phenotype (culture 3, 4 and 6) that was mixed to CK18<sup>+</sup> cells in culture 3, and with CK5<sup>+</sup>/p63<sup>+</sup> in culture 6 (**Figure 12**). These results are in contrast to other protocols that resulted in tumor cultures phenotype of transit-amplifying cells<sup>211</sup>.

Molecular characterization using Sanger sequencing was used to compare the genetic lesions present in biopsies and the corresponding *ex vivo* primary tumor cultures. Indeed, the molecular characterization represents a fundamental analysis to test the purity of the cultures and the presence of eventual cross-contamination between cultures<sup>212-215</sup>. One limitation of this characterization is the selection of just a few genes, that included the chromosomal translocation *TMPRSS2-ERG*, and the genes *SPOP*, *PTEN* and *TP53*, all described as the most altered genes in primary prostate tumors<sup>36</sup>.

The gene fusion *TMPRSS2:ERG*, described in approximately 50% of prostate tumors<sup>216</sup>, was suggested to mediate the development of prostate cancer from PIN lesions<sup>217</sup>. We found this translocation in three biopsies but not in their derived *ex vivo* cultures (cultures 1, 3 and 5). In particular, by Real Time PCR, tissue 1 presented two types of translocations, one involving the most frequent fusion (exon I of *TMPRSS2* and exon IV of *ERG*) and one composed by exon I of *TMPRSS2* and exon VI of *ERG*, while tissues 3 and 5 only showed the most frequent fusion product (data not shown). Previous studies also reported that from 56 spheres cultures established from *TMPRSS2-ERG*<sup>+</sup> prostate tumors, 39 (70%) did not contain the gene fusion, suggested to be derived from a preferential enrichment of prostate CSCs within cultures that lack this gene rearrangement<sup>218</sup>. On the other side, it is possible that the culture conditions we optimized, sustain the proliferation of the cancer stem cells but not of more differentiated progeny, in agree with works that highlighted that serum free medium composition selects for growth of normal prostate epithelial stem and transit-amplifying cells<sup>219</sup>. Mutations in the MATH domain of *SPOP* (Speckle-type POZ protein) occur in around 10% of prostate cancers and mutually exclusive with the chromosomal translocation<sup>41</sup>. No mutations were detected in the tissues and corresponding *ex vivo* primary tumor cultures for *SPOP*, possibly because of the small size of our group ( $n=10$ ).

*PTEN* is described altered in 20-30% of primary *ETS* positive tumors, and this frequency is significantly higher in metastatic tumors<sup>21</sup>. In culture 1, we found a point mutation in the first codon of *PTEN* that altered the whole transcript product, leading to protein absence. Consistent with other studies, the original tissue for culture 1 belonged is *ETS*-fusion

positive<sup>55,220</sup>. In contrast, cultures 5 and 7 showed low protein levels although they expressed a *wild type* *PTEN*. One hypothesis of this possible contradiction is that *PTEN* undergoes to a complex regulation where many actors are involved, *e.g.* transcription factors, microRNAs, pseudogenes and other competitive endogenous RNAs<sup>221-222</sup>. In *de novo* diffuse large B cell lymphoma, for instance, the *PTEN* protein levels were not corresponding to the *PTEN* transcript levels because several *PTEN*-targeting miRNAs were overexpressed, suggesting a key role for the post-transcriptional regulation of *PTEN*<sup>223</sup>. Thus, *PTEN* levels are decreased in the 30% of the selected cultures, although no alterations were detected in the transcripts of the original tissues. It may be important to evaluate the protein status in the tissues and analyze whether also in the patients *PTEN* is de-regulated at a post-transcriptional level.

Regarding *TP53* in primary prostate tumors but especially in aggressive cancer, 50% of the cases are reported to have loss of function mutations<sup>21</sup>. In culture 1, *TP53* has a point mutation at residue 139 that leads to a premature stop codon and a non-functional protein. This result was confirmed by Western blot where no signal is detected for p53. This alteration was not detected in the corresponding tissue, suggesting that cells p53 K129R<sup>+</sup> are positively selected.

Interestingly, seven cultures and three tissues had a polymorphism in residue 72, resulting in the R72 variant. The high frequency of this variant in the cultures may suggest that the alteration is specifically linked to tumor cells and provides them with a selective advantage for *in vitro* growth. However, R72 variant confers to p53 decreased ability to interact with inflammation related proteins and the immunity system<sup>38</sup>, and was described to localize preferentially in mitochondria, harboring a stronger apoptotic potential<sup>224</sup>. In addition, previous studies in breast, lung or head and neck cancers reported that patients with the R72 variant were more sensitive to chemotherapy<sup>225-227</sup>.

Others studies, supporting our findings, linked this variant to type 2 diabetes, one important cancer risk factor<sup>228,229</sup>. In addition, it is reported that the biochemical activity of p53 R72 variant has an enhanced pathological role in some tumors<sup>230</sup>, increasing the affinity with p73. Possibly, this explains the stabilization of expression in lung cancer<sup>231</sup>. All together, these results suggest that the *in vitro* culture process may cause a stress in the cells dis-aggregated from the fresh tissue that may result in a selection/survival of specific cell populations in culture (p53 R72<sup>+</sup>, p53 K139R) and *PTEN* null/ or with lower expression with respect to the cancer cell populations present in the tumor biopsy.

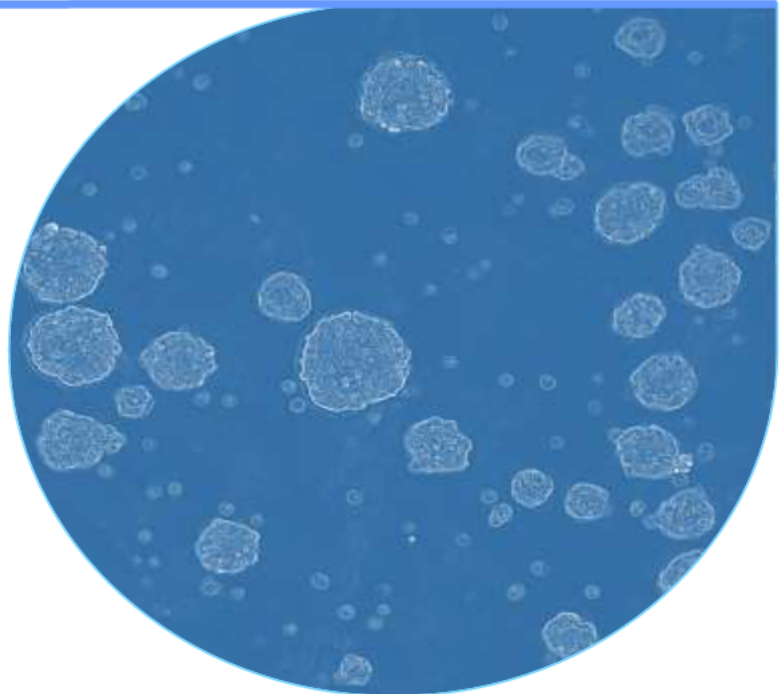
### 4.3 Characterization of the androgen independent *ex vivo* cultures

The first line therapy in patients with advanced prostate cancer is the depletion of androgen, a potent treatment that blocks cancer growth and provokes an intense stress for cancer cells<sup>232</sup>. However, small subpopulations of cancer cells may survive and lead to recurrence<sup>59,61,233</sup>. These cells with high plasticity have the ability to adapt to new stressful environments and have been recognized as CSCs<sup>234,235</sup>. They generally present a relative quiescence state, resistance to drugs, overexpress drug transporters and self-renewal genes, and are negative for AR expression<sup>74,236</sup>. According to these characteristics, several of the *ex vivo* primary tumor cultures established here, present features of CSCs: the Androgen Independent (AI) *ex vivo* primary tumor cultures 1, 3, 4, 5, 6 and 7, displayed a significant slower growth rate (**Figure 15**), together with lower protein synthesis ratio in AI cultures 4 and 6 (**Figure 21**), a higher resistance to drugs (cultures 1, 3, 4, 5 and 6) (**Figure 19** and **Figure 20**), and overexpression of self-renewal genes (cultures 1, 3, 4 and 6) (**Figure 23**). In addition, cultures 1, 5 and 6, also showed low levels of *AR* and *AR*-targets (**Figure 14**). Furthermore, primary cultures 1, 4, 5 and 6 showed a more aggressive phenotype, which was enhanced in the cases of cultures 4 and 5 by the induction of EMT genes, as *Vimentin* and *SNAIL* and the down-regulation of epithelial markers like *CDH1*, *cytokeratins*<sup>237</sup>. However, we also observed some apparent incongruence with the above described characteristics of CSCs, such as the overexpression of *AR* in AI cultures 3, 4, 7, 8, 9 and 10. The AR in fact, is a driver of chemotherapy resistance and a hallmark of metastatic PCa at the terminal stage where the AR is aberrantly expressed<sup>238,239</sup>. Additionally, in AI *ex vivo* primary tumor cultures 3, 5, 6, 7, 8 and 9 no differences in expression of stemness or EMT genes were detected, although functionally AI cultures 3, 5 and 6 showed significantly dissimilarity. For these cultures, differences were detected at translational level in the ratio of protein synthesis (**Figure 21**), and/or the activity of mTOR pathway (**Figure 22**). Although the translation machinery is strongly involved and finely regulated in the progression to metastatic phenotypes<sup>169,240</sup> the translational rate of AI cultures 3 and 5 was not affected, as shown by the SUNSET assay. These data need to be confirmed by additional experiments (*e.g.* incorporation of <sup>35</sup>S-methionine and polyribosomes profiling)<sup>241,242</sup>. In *in vivo* assays performed with *ex vivo* primary culture 1, and contrary to what expected according to the increased aggressiveness of culture 1 AI population, AD culture form faster a tumor culture compared to AI culture<sup>243</sup>. This pilot experiment was performed in non-

castrated nude mice, and this may at least partially explain the unexpected result. It has been shown that androgen independent cells engrafted in castrated mice were able to form a tumors, but still needed *AR* to be silenced by shRNA, confirming again the importance of *AR* presence production for the development of PCa<sup>244</sup>.

In summary, these results highlighted the heterogeneity of *ex vivo* primary tumor cultures and their utility to be used as models to study aggressive and metastatic prostate cancer. Cells in primary cultures have compensatory signaling pathways that are lost in commercial cell lines, and so even if a cell line is significantly sensitive to a drug, the same compound may be less effective or ineffective in primary cultures<sup>245</sup>. Additional studies have demonstrated that using a panel of cell lines including primary cultures provided a strong improvement in the drug discovery and screening fields<sup>246</sup>.

# CHAPTER 6: CANCER STEM CELLS AS A MODEL TO STUDY AGGRESSIVE PROSTATE CANCER



Parts of the data presented in this chapter have been submitted for publication in the article: **STAT3 inhibition with Galiellalactone effectively targets the prostate cancer stem-like cell population**. Canesin G., **Maggio V.**, Collins A. T., Contreras H.R., Castellón E.A., Morote J., Paciucci R., Maitland N. J., Bjartell A. and Hellsten R. (sent in June 2019).





## 1. Enrichment and characterization of CSC populations from established prostate cancer cell lines and primary tumor *ex vivo* cultures.

CSCs are intrinsically resistant to treatments with radiation and chemotherapy<sup>247</sup>. The results shown in the previous chapter suggested that *ex vivo* primary tumor cultures sensitive and resistant to the androgen deprivation might contain different proportions of CSC sub-populations that are enriched by consecutive growth in 3D-dimension conditions (**Figure 23**). Thus, to confirm the above results, we evaluated the efficiency of each cell line and *ex vivo* primary tumor culture to form spheres (SFE) by counting the number of spheres generated in each generation. Results with the LNCaP cell model and *ex vivo* primary tumor cultures 1 and 318 confirmed that AI cells had increased ability to form spheres compared to parental AD cells (**Figure 26A**). Results with the Du145 cell model also showed a higher SFE of DR cells in comparison to DS cells. These results suggest that cells derived from spheres can be considered as cultures enriched in CSCs populations. We have shown in the previous chapter that androgen independent LNCaP AI cells and *ex vivo* AI primary tumor cultures 1 and 4, overexpressed several stemness markers, *e.g.* *SOX2*, *CD133*, *CD44*, and *ALDH1A1*, in comparison to parental AD cultures (**Figure 23**). One additional AI *ex vivo* culture 318 (developed from a prostate primary tumor culture established by Dr. H. Contreras' laboratory, University of Santiago, Chile) was found to significantly overexpress various self-renewal genes (data not shown). To confirm that the androgen independence promoted an enrichment of CSCs populations in the AI cultures, CSCs were selected functionally based in their abilities to grow as spheres without attachment to the substrate and then analysed the resulting cultures for the expression of self-renewal genes (please see details in CHAPTER 4 p.39). Spheres formed by LNCaP AI cells expressed significant higher levels of *NANOG*, *OCT3/4* and *ALDH1A1* genes when compared to parental AD spheres grown in the same conditions (**Figure 25A**), confirming that the resistance to androgen deprivation is associated to an increase in self-renewal gene expression and stemness capacity. To avoid co-selection of non-CSCs that, in order to survive, aggregated together with CSCs, spheres were trypsinized, washed and replated every 7 days and new generations of spheres were identified as Generation 2 (G2) and G3. The expression of self-renewal markers was monitored in G1, G2 and G3 spheres in LNCaP and Du145 cell models of resistance and in *ex vivo* primary tumor cultures 1 and 318 (**Figure 25**). When grown as spheres and, in comparison to growth in adherent conditions, LNCaP AD cells showed increased the expression of self-renewal genes at G2, and significant differences were found

for the expression of *NANOG*, *OCT3/4*, *CD133*, *CD144* and *ALDH1A1* genes at G3 (**Figure 25A**). Similar results were observed with the LNCaP AI cells: although adherent cultures of AI cells expressed higher levels of these genes when compared to adherent AD cells (**Figure 23**), spheres G2 and G3 expressed progressive increasing levels of self-renewal genes (**Figure 25C**). The Du145 cell model of docetaxel sensitive (DS) and docetaxel resistant (DR) cells behaved in a similar manner, and sphere G2 and G3 in general expressed higher levels of self-renewal genes compared to G1 and to adherent parental cells, although *NANOG*, *CD44*, and *ALDH1A1* did not increase in G3 of DR cells (**Figure 25B-D**). Finally, when the AD and AI *ex vivo* primary tumors cultures 1 and 318 were grown to allow the formation of spheres, very similar results were observed and showed increased levels of

several self-renewal markers in G1 and G2 compared to the adherent parental cultures.

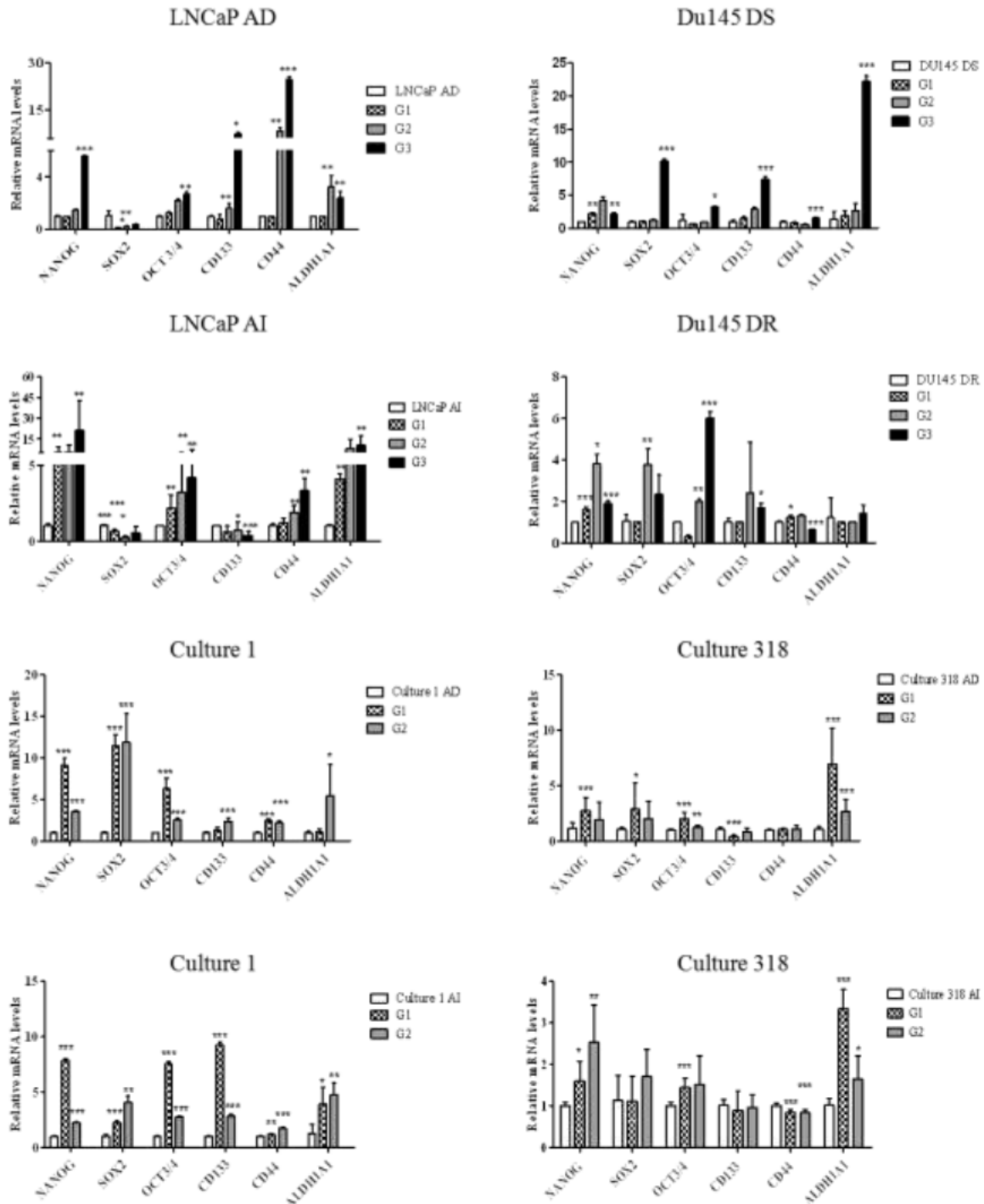


**Figure 25. Spheres formed with cell lines and *ex vivo* primary tumor cultures are enriched in CSCs.** Histograms representing the relative mRNA levels of the indicated genes analyzed by RT-PCR in LNCaP AD and AI cells, Du145 DS and DR cells, AD and AI *ex vivo* primary tumor culture 1 and 318. (G) Adherent *ex vivo* AI primary tumor culture 1 is compared to G1, G2, G3 spheres from AI culture 1. Adherent cells are compared to their corresponding G1, G2, G3 spheres. *TBP* and *IPO8* were used as housekeeping genes. Data are the mean  $\pm$  s.d. of 3 experiments (n=3), each performed in sextuplicate. *p* value < 0.05 \*, < 0.01 \*\*, < 0.001 \*\*\*.

The morphology of the spheres formed by these cell lines were different, as it is shown in

**Figure 26.** The spheres formation efficiency (SFE) confirmed that LNCaP AI cells had increased ability to grow in non-adherent conditions compared to parental AD cells. In a similar way, Du145 DR compared to DS cells, and AI *ex vivo* cultures in comparison with

AD cultures did show significant differences in SFE (Figure 26).

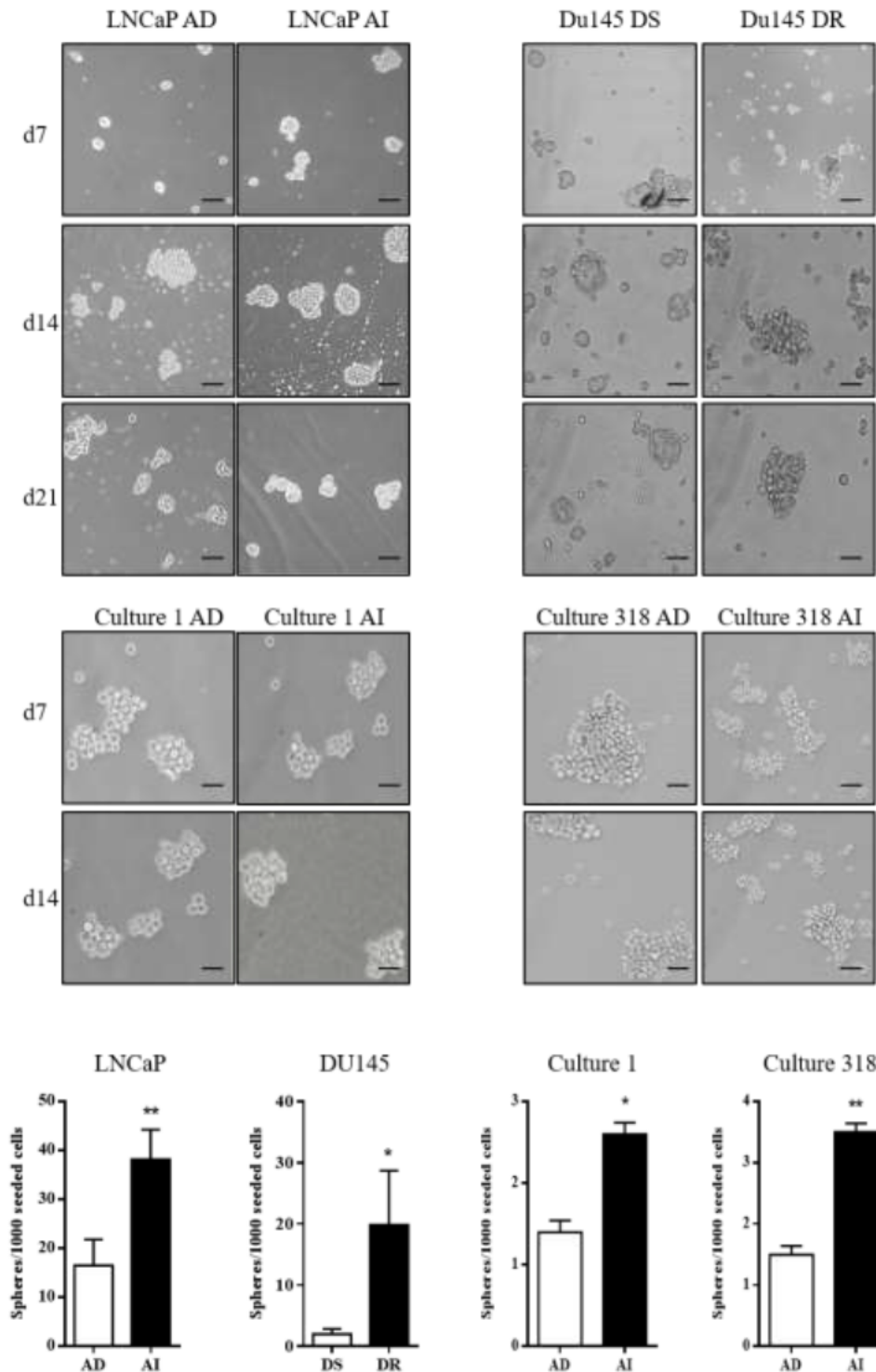


**Figure 26. Spheres forming efficiency of prostate cancer cell lines and *ex vivo* primary tumor cultures.** Upper panels: Images of G1, G2 and G3 spheres derived from LNCaP AD and AI cells, Du145 DS and DR cells, and AD and AI *ex vivo* primary tumor cultures 1 and 318. Images were acquired with an inverted microscope (BX61, Olympus). Scale bar: 100  $\mu$ m. Lower graphs: Histograms representing the SFE as the number of spheres formed /1000 seeded cells, in LNCaP, Du145 cells, and *ex vivo* primary tumor cultures 1 and 318 after 14 days of culture in non-adherent conditions.  $p$  value < 0.05 \*, < 0.01 \*\*, < 0.001 \*\*\*.

CSCs within tumors have been defined as subpopulations of cells with a significantly lower replication and diminished protein translation rates, features that favour cancer cell survival to chemotherapy, which is targeting highly proliferative cancer cells<sup>248</sup>. Thus, to further confirm that cells with higher SFE were enriched in CSCs, we analysed CSCs derived from Du145 DS cells and AD *ex vivo* primary tumor cultures for proliferation rates and translational efficiency. In agreement with previous evidences, results from these experiments showed that Du145 DS cells from G2 spheres had a significantly lower rate of proliferation than their adherent DS control cells (**Figure 27**). Similarly, cells from G2 spheres of Du145 DR cells and AI *ex vivo* primary tumor cultures 1 and 318, showed significant diminished proliferative activity (**Figure 27**)<sup>210</sup>. The rate of protein synthesis of cells from G2 spheres was compared to adherent control cells in Du145 DS, DR and *ex vivo* primary tumor cultures 1 and 318 using the SUNSET assay. Cells from G2 spheres and adherent cells were treated with puromycin, as described in CHAPTER 4 p.53. G2 spheres from each cell line and *ex vivo* primary tumor cultures showed a visible reduction in the efficiency of translation in comparison with their adherent control cells, confirming that G2 spheres were enriched in CSCs.

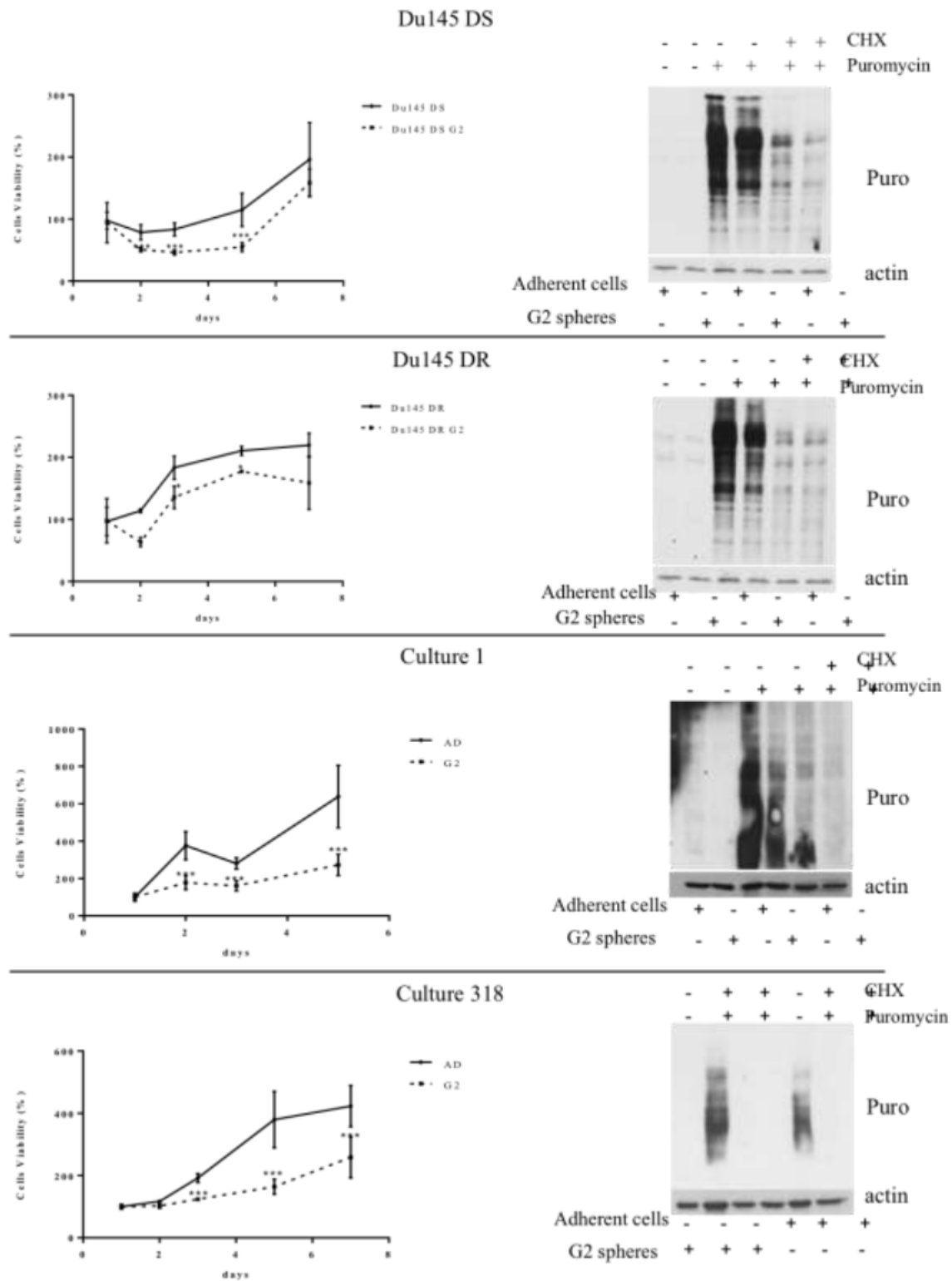


**Figure 27. Characterization of docetaxel-resistant spheres and *ex vivo* primary tumor cultures-derived spheres.** Left panel: Growth curves of adherent cells and spheres (G2) cells grown in adherent conditions for 7 days. Cells were derived from Du145-DS and DR adherent cells and spheres, from AD *ex vivo* primary tumor culture 1, and 318. Results represent the mean  $\pm$  s.d. of n=3 independent experiments, each performed in octuplicate. Statistical significance was determined using two-way ANOVA. *p* value < 0.05 \*, < 0.01 \*\*, < 0.001 \*\*\*. Right panel: Evaluation of global protein synthesis by puromycin SUNSET assays for Du145-DS adherent cells and spheres, Du145-DR adherent cells and spheres spheres, adherent cells from AD *ex vivo* culture 1 and AD culture 318. Cells were treated during 10 minutes with 10  $\mu$ g/mL



Puromycin. Negative control are untreated cells. Positive controls are cells treated with 10  $\mu\text{g}/\text{mL}$  Puromycin and 10  $\mu\text{g}/\text{mL}$  Cycloheximide. Signals were revealed by secondary antibodies coupled to HRP using a chemiluminescent substrate (ECL). Actin signal was used as control of protein loading.

CSCs are also identified as Tumor Initiating Cells (TICs). Thus, we tested CSCs derived from spheres of LNCaP AD cells and compared to AD cells grown in adherent conditions for their abilities to generate tumors in immunosuppressed *nude* mice. Two concentration of cells ( $1 \times 10^6$  or  $5 \times 10^5$ ) from G2 spheres and adherent cultures were injected subcutaneously, as described in CHAPTER 4 p.54). Tumors appeared in both groups after 5 weeks and their growth was measured weekly until the maximal size of 1 cm was obtained. As shown in **Figure 28**, two tumors formed by cells derived from spheres were large and 4 had smaller sizes. In turn, adherent AD cells formed four tumors of large size, and two of small size. Histologically these tumors showed similar features: they were highly undifferentiated with large necrotic areas and high indexes of mitosis (**Figure 28A**). No evidences for metastasis were detected in the principal organs examined (**Figure 28B**). Therefore, contrary to what expected, no significant differences were found in the TIC of LNCaP AD cells when the total cell population was compared to the cell populations with sphere forming capacity.

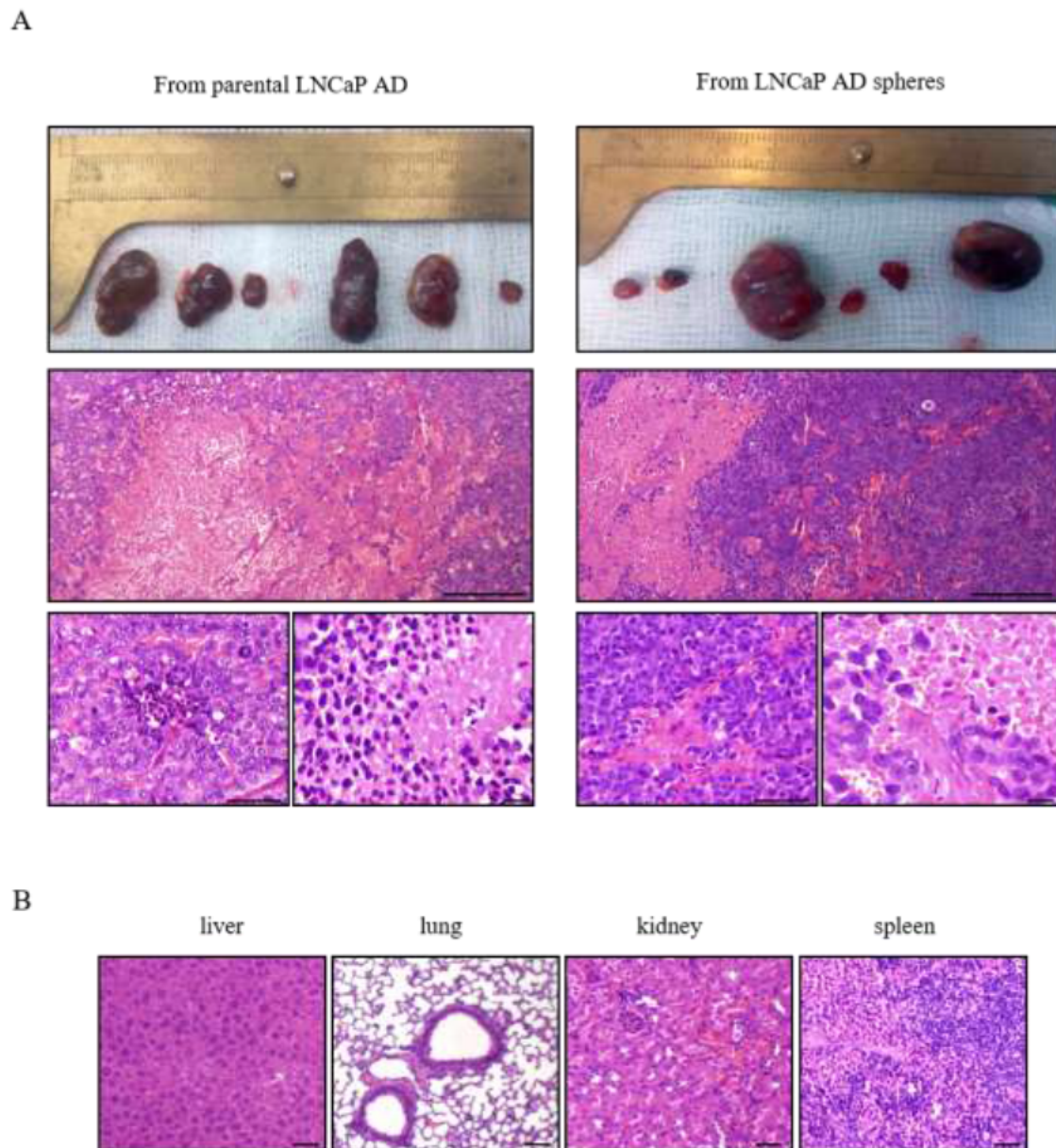


**Figure 28. Tumors formed *in vivo* by LNCaP cells.** (A) Hematoxylin and eosin staining of tumors formed *in vivo* after the subcutaneous injection of LNCaP AD adherent or spheres cells in two different concentration ( $1 \times 10^6$  in 3 mice or  $5 \times 10^5$  in 3 mice) and (B) representative images of liver, lung, kidney or spleen. Scale bar: 100 $\mu$ m.

## 2. Prostate spheres derived cells (CSCs) as *in vitro* models to test new anticancer drugs

### 2.1 Galiellalactone (GL)

Due to their resistance to conventional therapies, CSCs are considered responsible for tumor recurrence after chemo- and radiotherapy and their targeting has been suggested as a potential novel therapy to suppress PCa metastasis<sup>249</sup>. Activation of signaling by the

transcription factor signal transducer and activator of transcription 3 (STAT3) has been implicated in prostate carcinogenesis by regulating the cancer stem cell niche: it is therefore a valid strategy to selectively target prostate cancer-CSCs by STAT3 inhibition<sup>250</sup>. Galiellalactone (GL) is a direct STAT3 inhibitor that binds to STAT3 and prevents transcription of target genes without interfering with its upstream activation<sup>251</sup>. Previous works from Dr. Hellsten et al. have shown that STAT3 blockade by GL not only reduces proliferation and induces apoptosis of PCa cells and *ALDH1A1* expressing stem cell-like PCa cells *in vitro*<sup>252</sup> but it also inhibits the growth of prostate tumors and the metastatic spread to regional and distal lymph nodes *in vivo*<sup>253</sup>. In collaboration with Dr. Bjartell's group, we investigated the therapeutic effect of GL for patients with prostate cancer using the models that we established of CSCs (spheres) derived from primary tumor *ex vivo* cultures AD and AI, and of CSCs derived from Du145 DS and DR cells. As shown in **Figure 29A**, GL significantly decreased the viability of CSCs derived from DS and DR Du145 cells in a concentration-dependent manner. We reported that the IC<sub>50</sub> of G2 spheres from DS spheres was 10.1  $\mu\text{M}$  while the IC<sub>50</sub> of adherent cells was 8.5  $\mu\text{M}$ . A similar effect was detected in the DR G2 spheres (IC<sub>50</sub> of 6.8  $\mu\text{M}$ ) in comparison with the DR Du145 adherent cells, which had an IC<sub>50</sub> of 5  $\mu\text{M}$ . Similarly to what observed with Du145 cells, spheres derived from AD *ex vivo* primary tumor culture 1 responded very well to GL, showing a significant decrease in their viability with an IC<sub>50</sub> of 4.3  $\mu\text{M}$  while the AD *ex vivo* adherent culture had an IC<sub>50</sub> of 3.1  $\mu\text{M}$  (**Figure 29A**). G2 spheres from the AD primary tumor *ex vivo* culture 285 (an *ex vivo* prostate tumor culture established in Dr. H. Contreras' laboratory, University of Santiago, Chile) showed a high sensibility to GL, with an IC<sub>50</sub> of 1.2  $\mu\text{M}$ , almost the same as the adherent *ex vivo* culture that displayed an IC<sub>50</sub> of 1  $\mu\text{M}$  (**Figure 29A**). Finally, we tested the effect of GL in G2 spheres from the *ex vivo* primary tumor cultures 318 (AD and AI). We found that GL significantly affected the growth of both AD and AI spheres, that showed IC<sub>50</sub> of 7.4  $\mu\text{M}$  and 9.7  $\mu\text{M}$ , respectively, in contrast to the resistance shown by the parental adherent cultures (IC<sub>50</sub> = 2.7  $\mu\text{M}$ ) (**Figure 29A**).

To explore the functionality of GL, the expression of one of its target *STAT3* was analyzed by RT-PCR in G2 spheres and parental adherent cells from DS and DR Du145 cultures. Cells were treated during 24 hours with concentrations of GL corresponding to their IC<sub>50</sub>. Previous evidences pointed out that CSCs had higher levels of STAT3 than the bulk of cancer cells<sup>252</sup>. In agreement with this study, our results showed that cells derived from both DS and DR G2 spheres significantly overexpressed STAT3 compared to the adherent

control. In addition, GL treated cells showed a significant reduction in the levels of *STAT3* in comparison with untreated control cultures, confirming the specificity of GL (Figure 29B).

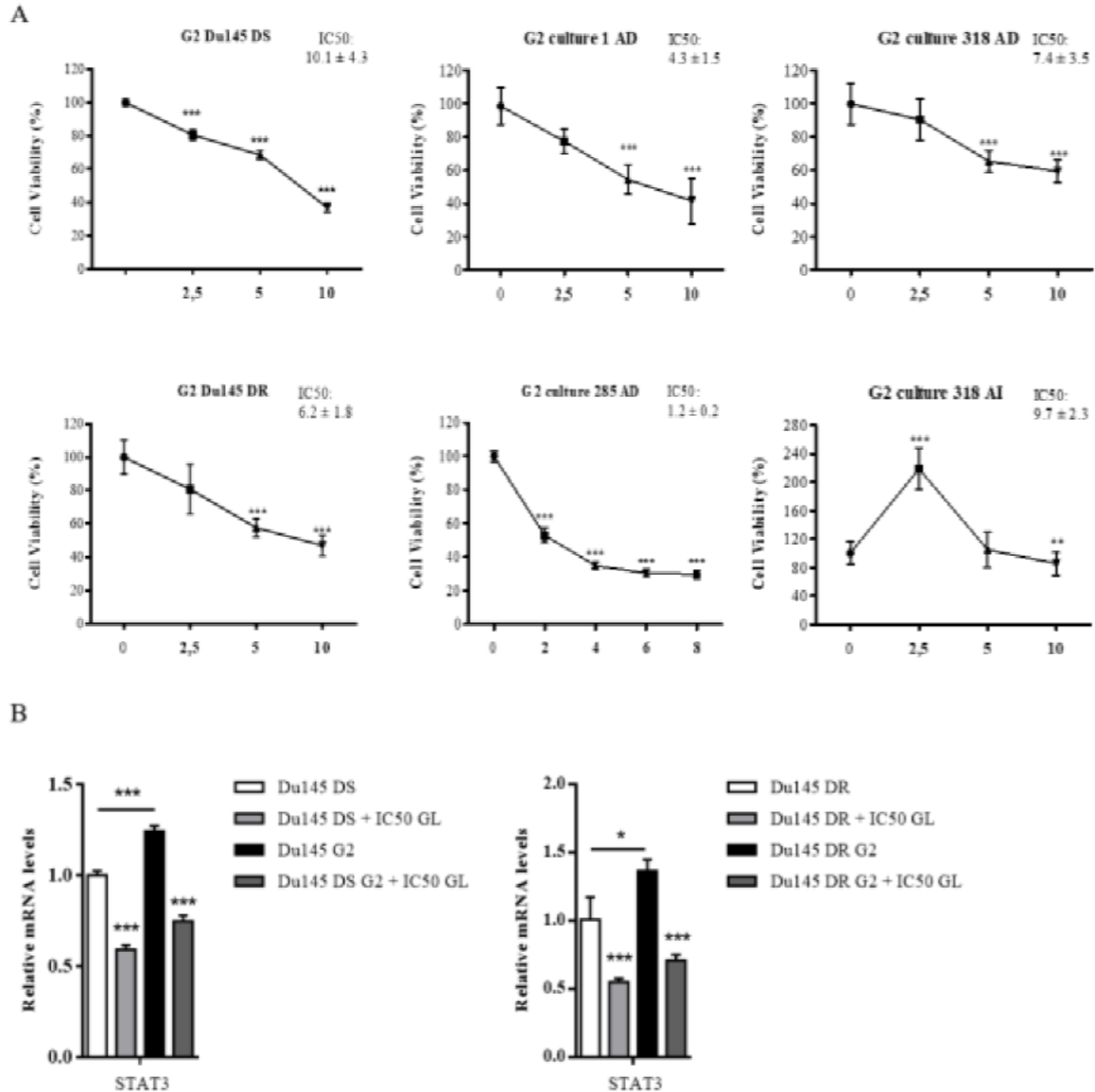


**Figure 29. Galiellalactone toxicity on Du145 spheres and *ex vivo* primary tumors spheres.** (A) Viability assay on spheres derived from AD *ex vivo* primary tumor culture 318, 285 and 1, AI *ex vivo* primary tumor culture 318 and 1, DS and DR Du145, grown in the presence of vehicle or 2,5–10 µM GL for 72 h. Results represent the mean ± s.d. of three (n=3) independent experiments, each performed in quintuplicate. Statistical significance was determined using one-way ANOVA with Bonferroni post hoc test. (B) Relative mRNA levels of *STAT3* in DS and DR Du145 adherent cells or spheres untreated or treated for 24 hours with the respective GL IC50. *TBP* and *IPO8* were used as housekeeping genes. Data are the mean ± s.d. of 2 experiments (n=2), each performed in sextuplicate p value < 0.05 \*, < 0.01 \*\*, < 0.001 \*\*\*.

### 2.2 Chemotherapeutic drugs: Docetaxel and Cabazitaxel

Docetaxel is presently a first line chemotherapeutic agent applied in combination with androgen deprivation in the clinics. We previously reported that PCa AI cell lines and *ex*

*in vivo* primary tumor AI cultures, had a significant higher resistance to docetaxel (**Figure 19**). Therefore, because we also showed that AI cells are more enriched in CSCs subpopulations, we evaluated docetaxel effects using the models of CSCs spheres established in the present thesis. G2 spheres derived from AD and AI LNCaP cells, and from DS and DR Du145 cells were treated with increasing concentrations of docetaxel for 72 hours. As shown in **Figure 30A**, docetaxel did not affect the viability of G2 spheres, confirming the higher resistance of CSCs populations to common drugs. The IC<sub>50</sub> could not be calculated for G2 spheres derived from AD and AI LNCaP cells (**Figure 30A**) while, as reported in **Figure 19**, AD and AI LNCaP adherent cells showed an IC<sub>50</sub> of 168.3 nM and 2.3 μM, respectively. Similar results were obtained with G2 spheres derived from DR Du145 for which the IC<sub>50</sub> could not be determined. However, DR Du145 adherent cells showed an IC<sub>50</sub> of 8.7 nM. Finally, G2 spheres from DS cells appeared more sensitive to Docetaxel, with an IC<sub>50</sub> of 2 nM while the IC<sub>50</sub> of adherent DS Du145 cells was 5.6 nM (**Figure 30A**).

Cabazitaxel is a taxol derivative synthesized to overcome cancer resistance to docetaxel and it is used as a second line therapy in PCa. We firstly tested its toxicity using AD and AI LNCaP cell line and primary tumor *ex vivo* AD and AI cultures derived spheres, showing a significant higher resistance of AI LNCaP cells and AI *ex vivo* cultures (**Figure 30B**). These results were confirmed in G2 spheres derived from DS and DR Du145 cells. Results showed that DS Du145 G2 spheres were more resistant to cabazitaxel (IC<sub>50</sub> = 167 pM), compared to DS Du145 adherent cells (IC<sub>50</sub> = 152.5 pM). Similar results were obtained with DR Du145 cells derived from G2 spheres and DR Du145 adherent control cells (IC<sub>50</sub> of 2 nM and 0.4 nM, respectively).

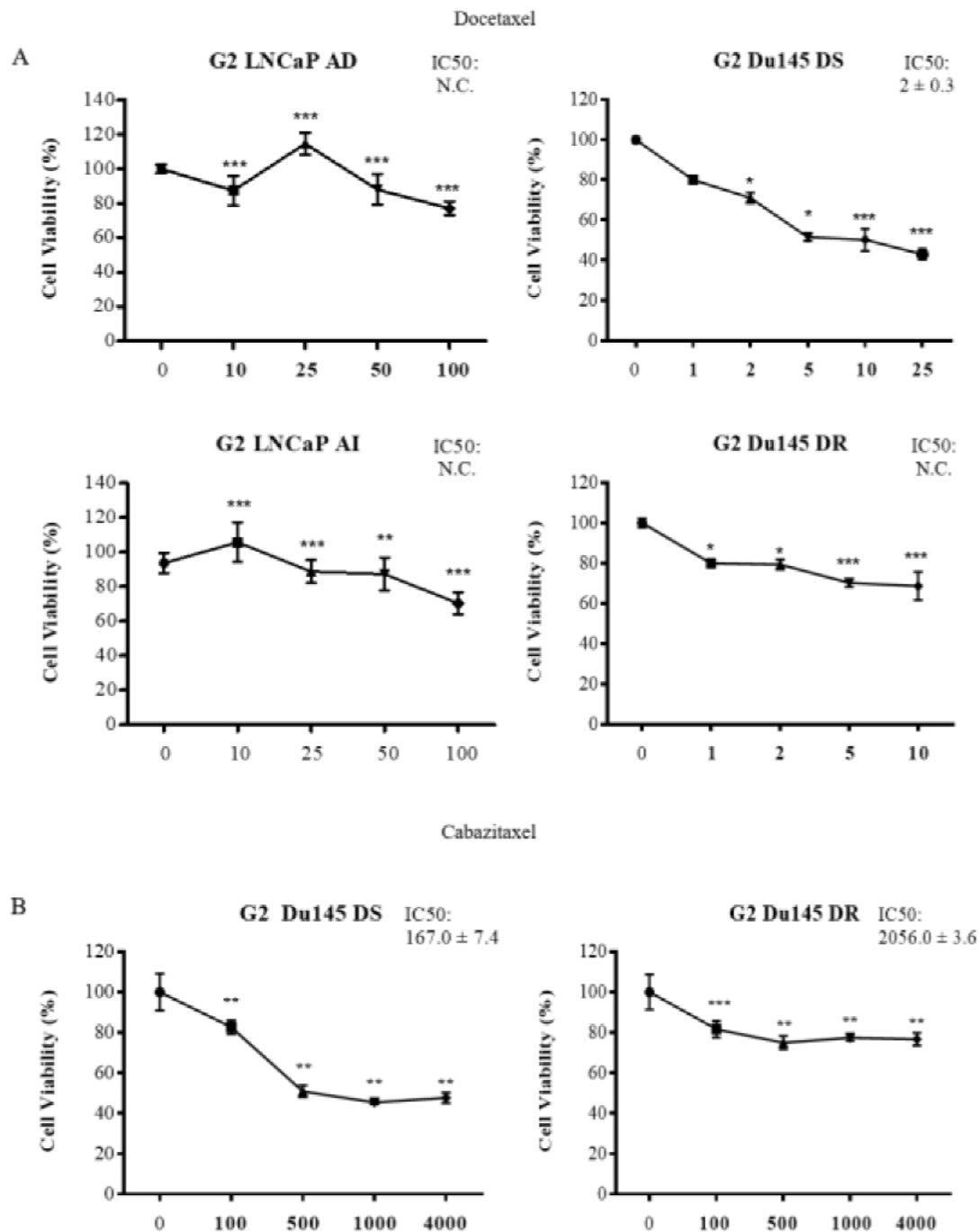


**Figure 30. LNCaP and Du145 spheres are highly resistant to chemotherapy.** (A) Viability assay on spheres derived from AD and AI LNCaP, DS and DR Du145, in the presence of vehicle or different concentration of docetaxel for 72 hours. (B) Viability assay on spheres derived from DS and DR Du145 in the presence of vehicle or different concentrations of cabazitaxel for 72 hours. Results represent the mean  $\pm$  s.d. of three ( $n = 3$ ) independent experiments, each performed in quintuplicate. Statistical significance was determined using one-way ANOVA with Bonferroni post hoc test.  $p$  value  $< 0.05$  \*,  $< 0.01$  \*\*,  $< 0.001$  \*\*\*.

### 2.3 Bozepinib analogues

Bozepinib is a new potent compound described to target CSCs<sup>254</sup>. It has been developed by

the group of Juan Antonio Marchal who reported a strong apoptotic effect on cancer cells from colon and breast at low dosage<sup>255</sup>. Recently, this Group developed two more stable formulation of Bozepinib, namely MDN-90 and MEGR756B. In collaboration with his Group, we tested these new compounds using our CSCs models derived from the Du145 cells and from AD and AI *ex vivo* primary tumor 318 cultures. In **Figure 31A**, we observed a significant effect of MDN-90 in cells derived from G2 spheres of DS and DR Du145 cells (IC<sub>50</sub>=10.1  $\mu$ M and IC<sub>50</sub>=7.3  $\mu$ M, respectively). A similar significant action was observed in cells of G2 spheres from AD and AI *ex vivo* tumor culture 318 (IC<sub>50</sub> = 7.0  $\mu$ M and IC<sub>50</sub> = 7.1  $\mu$ M, respectively) (**Figure 31A**).

The second formulation, MEGR756B, was tested at similar concentrations as for MDN-90 in cells derived from G2 spheres of DS and DR Du145 cells. These cells showed a strong resistance at all concentrations tested and IC<sub>50</sub> could not be calculated (**Figure 31B**). Of note, cells derived from G2 spheres of AD *ex vivo* primary tumor cultures 318 were more resistant (IC<sub>50</sub>=31.3  $\mu$ M) compared to cells from AI G2 spheres (IC<sub>50</sub> =14.3  $\mu$ M).

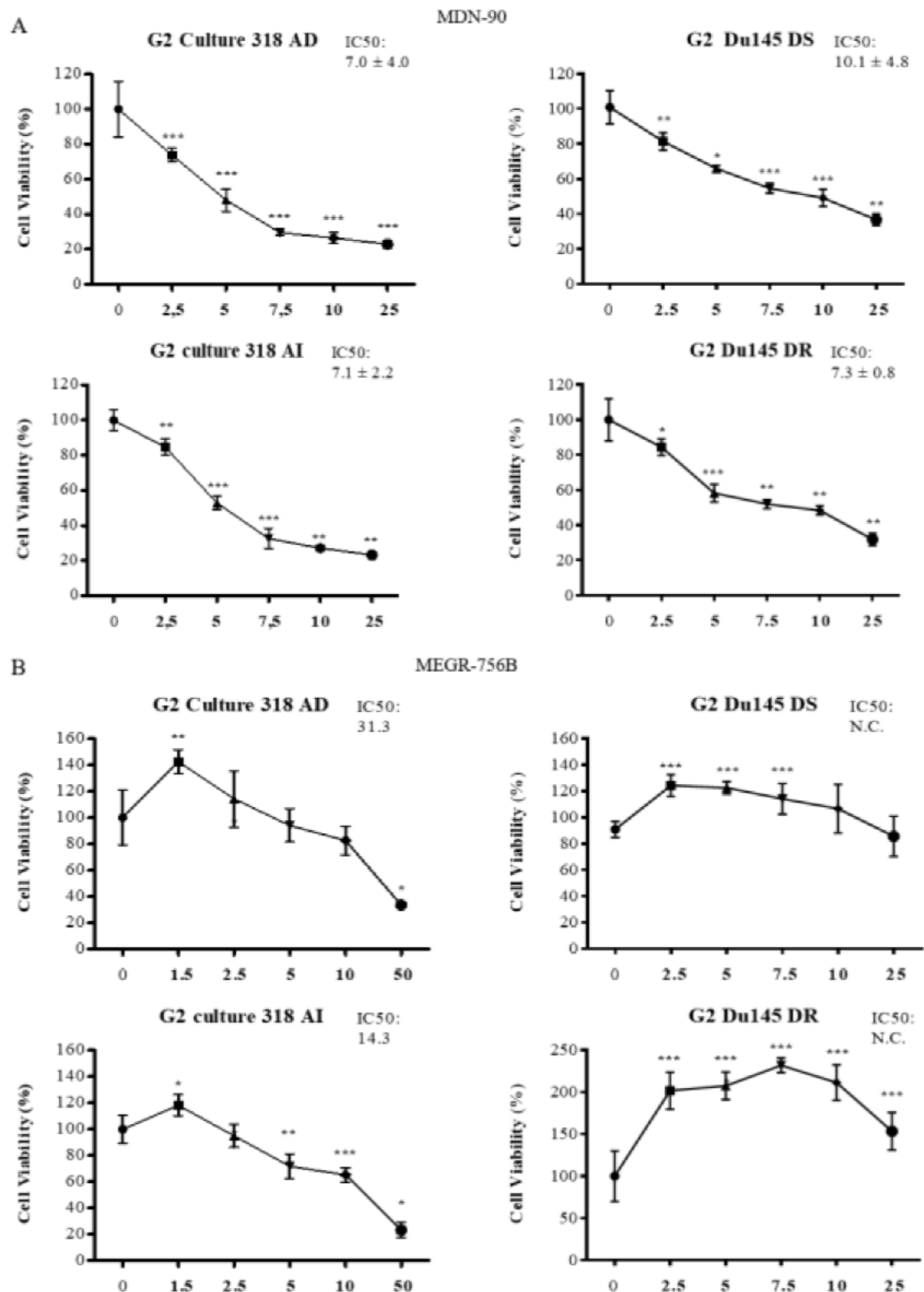


**Figure 31.** Bozepinib analogues toxicity using the Du145 cell model and *ex vivo* primary tumor cultures. (A) Viability assay using cells derived from spheres of (A) DS and DR Du145, AD and AI *ex vivo* primary tumor culture 318. Cells were treated in the presence of vehicle or different concentration of MDN90 for 72 hours. (B) Viability assay using the same cell models were repeated with different concentration of MEGR756B for 72 h. Results represent the mean  $\pm$  s.d. of three ( $n = 3$ ) independent experiments, each performed in quintuplicate. Statistical significance was determined using one-way ANOVA with Bonferroni post hoc test.  $p$  value  $< 0.05$  \*,  $< 0.01$  \*\*,  $< 0.001$  \*\*\*.



The targets of these compounds have not been identified, although modulation of genes involved in proliferation, EMT, and angiogenesis processes, like *c-fos* and *VEGF* has been observed in treated breast cancer cells. As an attempt to confirm these potential candidate genes for MDN-90, we have analyzed their expression levels after treating Du145 cells with this compound. **Figure 32** shows that the levels of *VEGF* in DS Du145 cells are not affected, however higher levels of *c-fos* were detected in DS spheres. In contrast, in DR Du145 cells, an increase in the expression of both genes was observed. Although it belongs from the same family of compounds, preliminary experiments from Marchal's group suggested that MEGR756B may regulate genes involved in EMT, inhibiting the process. Therefore, we studied the expression of *CDH1*, *VIMENTIN*, *SNAI1*, *TWIST1* and *PTOV1*, known to be implicated in the regulation of EMT in prostate cancer<sup>169,256,257</sup>. However, we could not evaluate these genes because we could not identify an IC50 for the Du145 cell line.

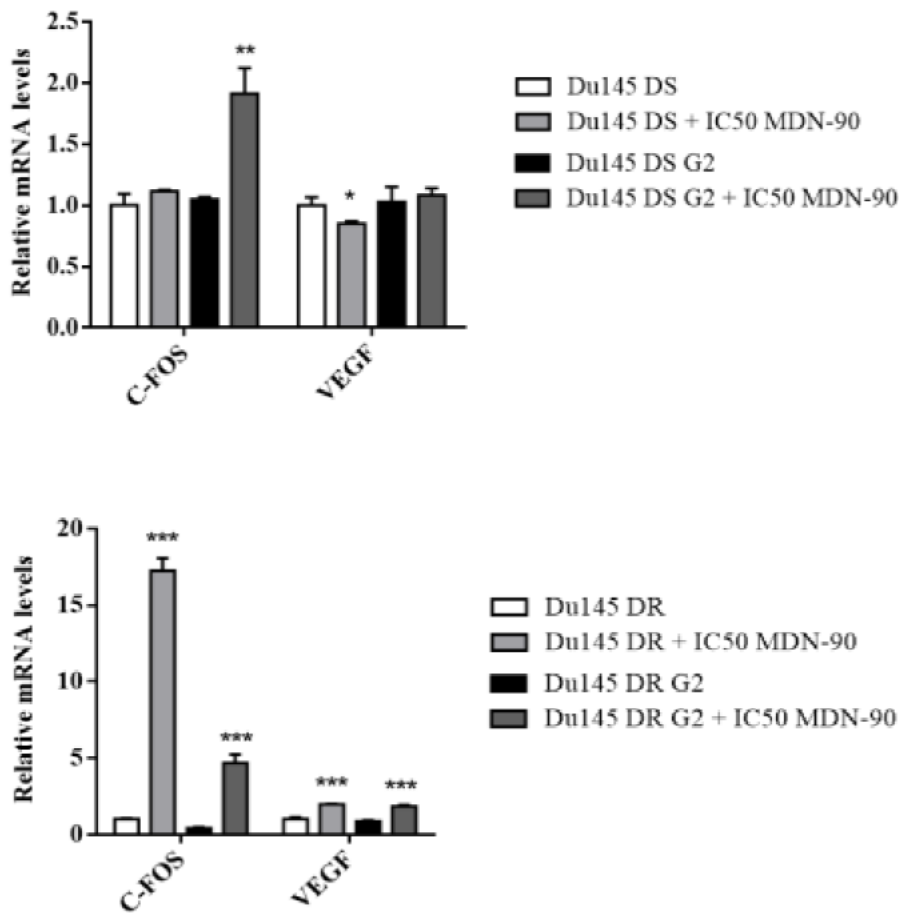


**Figure 32. Effects of MDN-90 on genes involved in angiogenesis and EMT in Du145 cells.** Relative mRNA levels of *c-fos* and *VEGF* in DS and DR Du145 adherent cells or cells derived from G2 spheres untreated or treated for 24 h with

MDN-90 (5  $\mu$ M). *TBP* and *IPO8* were used as housekeeping genes. Data are the mean  $\pm$  s.d. of 2 experiments (n=2), each performed in sextuplicate. *p* value < 0.05 \*, < 0.01 \*\*, < 0.001 \*\*\*.

### 3. Discussion

#### 3.1 Development of new *in vitro* CSCs models to study cancer resistance

CSCs have been described as small subpopulations of mostly quiescent cells that reside within tumors and have the potential to differentiate into recognizable, replicating tumor cells. They are considered to play a major role in tumor initiation, maintenance, progression to metastasis, and tumor heterogeneity<sup>258</sup>. Several studies indicate that CSCs in prostate cancer are characterized by the expression of CD133 and CD44 cell surface markers (CD133<sup>+</sup>/CD44<sup>+</sup>) and are less differentiated than transient-amplifying (TA) or committed-basal (CB) cells<sup>259,260</sup>. However, a strong marker of CSCs from the prostate has not yet been identified, and a debate is open about the irregular levels of CD133 and CD44 during CSCs life<sup>261,262</sup>. Because CSCs are resistant to conventional therapies, they have been associated to tumor reappearance after chemo- and radiation therapy. Thus, targeting CSCs has been suggested as a potential novel therapy to suppress PCa metastasis and recurrence<sup>249</sup>. To this aim, a protocol to enrich CSCs, both from prostate cancer cell lines and *ex vivo* primary tumor cultures, was established<sup>210</sup>. Using this functional model we have shown that cells resistant to androgen deprivation, or to docetaxel, shared common features with CSCs (**Figure 23**). Thus, we successfully enriched CSCs-like cells from 3D spheres, as shown by the significant expression of several self-renewal markers (Figure 23), also in agreement with other studies (**Figure 25**)<sup>262,263</sup>. On the other hand, drug resistant cells showed a greater ability to form spheres (**Figure 26**), confirming their higher content of CSCs. We additionally showed that cells derived from spheres in general also had slow growth rates, lower translational efficiency, and higher resistance to chemotherapy, all features in common with normal stem cells<sup>74,236</sup>. Another important hallmark of CSCs resides in their ability to form a tumor *in vivo*<sup>218,264,265</sup>. We confirmed the ability of the LNCaP AD cells derived from spheres (enriched for TICs) to form a tumor in a nude mouse model. However, in contrast to other studies, an increase of tumor formation in cells derived from spheres in comparison to control adherent LNCaP AD cells, was not observed<sup>266</sup>. Nevertheless, it should be considered that subcutaneous injections of tumorigenic cells have shown a dramatic low rate of engraftment and tumorigenic potential when compared to orthotopic injection<sup>121</sup>, and immunosuppressed mouse models have shown an extraordinary heterogeneity in TICs

assays<sup>65,267-271</sup>.

### 3.2 Targeting prostate tumor spheres

Targeting the CSCs may lead to the eradication of the tumor<sup>272</sup>. One important challenge for this aim is to find suitable CSCs models that allow to discover new molecular targets and test novel compounds<sup>273</sup>. A number of known molecules overexpressed in CSCs have been addressed as targets, such as *ALDH1A1* and *ABCG2*<sup>274,275</sup>. However, the complexity of CSCs regulatory networks is high, so a target strategy should be multimodal, such that target drugs should be able to block drug transporters and exert a cytotoxic activity toward both CSCs and the bulk of the tumor cells<sup>276</sup>. In this work, three different drugs that target CSCs have been tested using the CSCs functional culture models developed.

#### 3.2.1 Galiellalactone efficiently affect drug resistant and androgen resistant spheres viability

Galiellalactone (GL) is a direct STAT3 inhibitor that binds to the STAT3 protein and prevents transcription of target genes without interfering with its upstream activation<sup>251</sup>. Previous studies showed that STAT3 blockade by GL not only reduces proliferation and induces apoptosis of PCa cells and ALDH expressing stem cell-like PCa cells *in vitro* but it also inhibits the growth of prostate tumors and the metastatic spread to regional and distal lymph nodes *in vivo*<sup>252,253</sup>. GL significantly decreased the mRNA levels of STAT3 and the viability of spheres derived from DS and DR Du145 cells in a concentration-dependent manner as well as the spheres derived from *ex vivo* primary tumor cultures that showed a high sensibility to GL. Of note, DR Du145 cells were more sensitive to GL than DS cells (IC<sub>50</sub>=6.8 μM and IC<sub>50</sub>=10.1 μM, respectively), suggesting that GL is a potential drug to be used in combination with a second line therapy of PCa. In turn, AI *ex vivo* primary culture 318 resulted more resistant to GL than parental AD culture (IC<sub>50</sub>=9.7 μM and IC<sub>50</sub>= 7.4 μM, respectively). Results from AD *ex vivo* primary cultures 1 and 285 highlighted lower IC<sub>50</sub> (4.3 μM and 1.2 μM, respectively) than *ex vivo* primary AD culture 318 (IC<sub>50</sub>= 7.4 μM). The clinical features suggest that maybe the efficacy of GL is correlated with the aggressiveness of the carcinoma. Taken together, our data confirm that PCa-CSCs are dependent on STAT3 signaling for survival, and that blocking this pathway with GL effectively impairs their viability. Our findings here provide the first evidence that GL can target the CSCs in patient-derived primary prostate tumor cultures. This is particularly

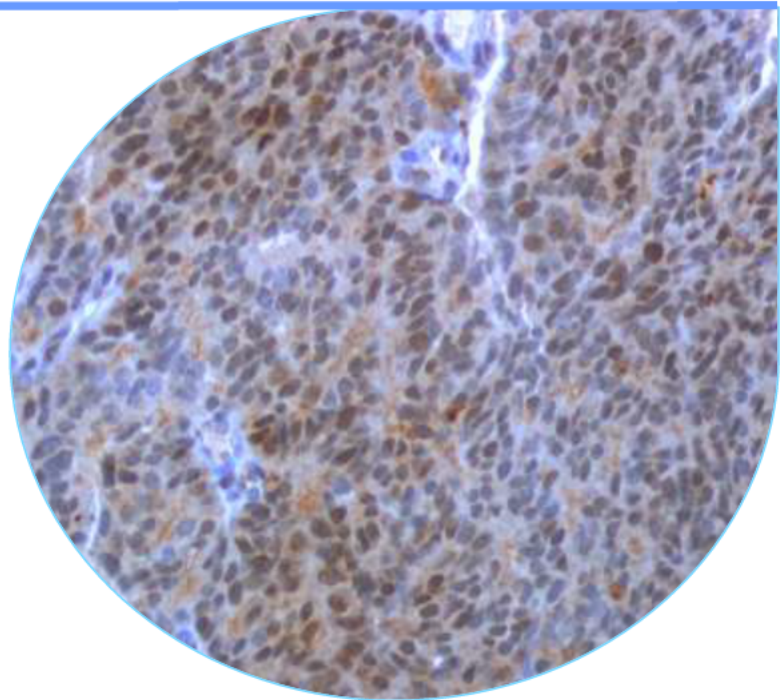
relevant, considering that the majority of current therapies effectively eliminates the non-CSC bulk of the tumor, but fails to eliminate CSCs. For a more effective treatment it may be necessary to target both cell populations. Thus, we propose the use of GL in association with current therapies to achieve a reduction of viability of in both CSCs and non-CSC populations<sup>252,253,277</sup>.

3.2.2. Bozepinib analogues differentially affect Du145 cells and ex vivo primary cultures viability

Bozepinib is another example of drug described to target CSCs<sup>254</sup>. Two new formulations, named MDN-90 and MEGR756B, were tested. DR Du145 cells resulted more sensitive to MDN-90 (IC<sub>50</sub>=7.3 μM) compared to DS cells (IC<sub>50</sub>=10.1 μM). In contrast, both DS and DR Du145 cells resulted, according to the recommended concentration, strongly resistant to MEGR756B. At a molecular level using Du145 cells, we investigated possible targets of MDN-90 that comprise *c-fos* and *VEGF*. The results showed that MDN-90 efficiently down-regulated *VEGF* in both adherent cells and spheres from DS cells. However, the opposite was observed in DR cells where, higher levels of both genes were observed. Possibly, the treatment of 24 hours in DR cells was not sufficient to activate the cascade signaling, like in DS Du145 cells. In addition, DR Du145 cells could express *VEGF* by activation of other pathways that are MDN-90-independent, thus could circumvent the action of the drug<sup>278,279</sup>. The AD and AI *ex vivo* primary cultures 318 are quite different from the Du145 drug resistant model: they did not show differences in the sensitivity to MDN-90 (IC<sub>50</sub>=7.4 μM), however, MEGR756B was significantly more effective in AI culture compared to parental AD (IC<sub>50</sub>=31 μM in AD cells versus IC<sub>50</sub>=14 μM in AI). These data highlight the need of new *in vitro* models that can represent the vast heterogeneity of prostate tumors to allow improvement of personalized medicine<sup>280,281</sup>.



**CHAPTER 7: A NOVEL DNA-BINDING  
MOTIF IN PROSTATE TUMOR  
OVEREXPRESSED-1 (PTOV1) REQUIRED  
FOR THE EXPRESSION OF *ALDH1A1* AND  
*CCNG2* IN CANCER CELLS**



These data have been published in the article: **A novel DNA-binding motif in Prostate Tumor Overexpressed-1 (PTOV1) required for the expression of *ALDH1A1* and *CCNG2* in cancer cells.** **Maggio V., Canovas V., Félix A.J., Gomez V., de Torres I., Semidey M.E., Morote J., Noe V., Ciudad C.J., and Paciucci R.** *Cancer Letters*. 2019 Jun 28;452:158-167.



## 1. PTOV1 induces the expression of self-renewal genes in prostate cancer cells

Our prior studies identified *PTOV1*, *ALDH1A1* and *CCNG2* genes as potential significant markers of metastasis and poor prognosis when overexpressed in primary androgen dependent prostate tumors<sup>174</sup>. *ALDH1A1* is a hallmark of both normal and cancer stem cells (CSCs) and an enabler of drug resistance in different types of cancers<sup>282,283</sup>, while *CCNG2* is a promoter of G2/M cell cycle arrest that contributes to thiopurine and doxorubicin resistance<sup>284,285</sup>. In metastatic CRPC Du145 and PC3 cells, the overexpression of *PTOV1* provoked an increase in the expression of these genes (**Figure 33A**)<sup>174</sup>. Additionally, in androgen dependent LNCaP cells *PTOV1* also significantly induced the expression of *ALDH1A1* and *CCNG2* (**Figure 33B** and **C**). On the other hand, knockdown of *PTOV1* by short hairpin RNAs provoked a significant reduction of endogenous *PTOV1* levels and a parallel significant decrease in *ALDH1A1* and *CCNG2* mRNA expression with respect to a control shRNA (**Figure 33B** and **C**).



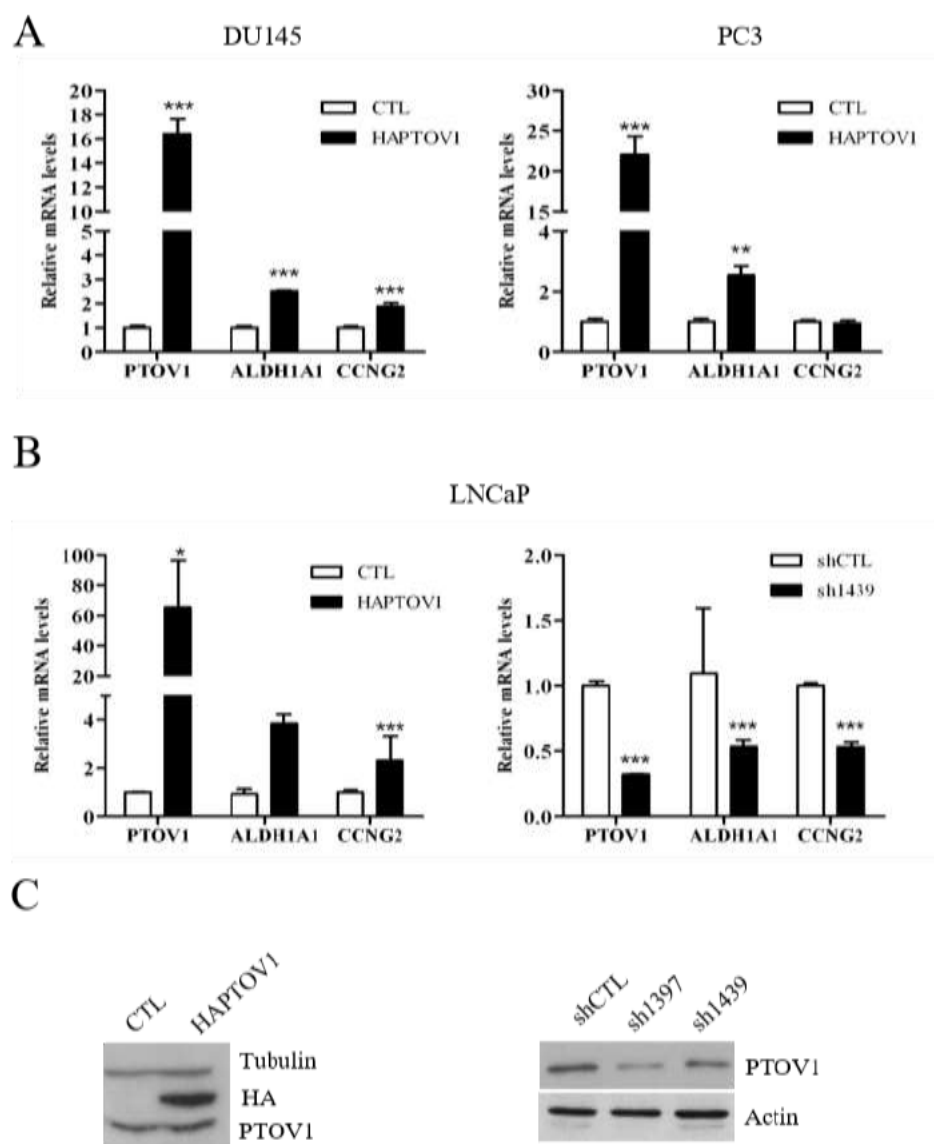


**Figure 33. The ectopic expression of PTOV1 in prostate cancer cells promotes *ALDH1A1* and *CCNG2* expression.** (A) CRPC Du145 and PC3 cells transduced with a lentiviral vector HAPTOV1-ires-GFP, or a control lentivirus (GFP), were analyzed by real time PCR for *ALDH1A1* and *CCNG2* expression. (B) Left, LNCaP cells transduced with the lentiviral vector HAPTOV1, or the control lentivirus (GFP), were analysed by real time qPCR for *gene* expression. Right, LNCaP cells transduced with lentiviral vectors bearing shRNA sequences (sh1397 or sh1439) and a control shRNA (shCTL) for PTOV1 knockdown, were analyzed by real time qPCR. Bottom: immunoblots with anti PTOV1 antibodies showing the levels of the protein in each case. *p*-value: \* < 0.05; \*\* < 0.01; \*\*\* < 0.001.

## 2. PTOV1 directly induces the expression of *ALDH1A1* and *CCNG2* in PCa cells

We next interrogated the mechanisms by which PTOV1 drives the transcription of *ALDH1A1* and *CCNG2*. Prior work had shown that the engagement of two signaling networks, Wnt/ $\beta$ -catenin and Jun kinase (JNK), activate PTOV1-mediated functions<sup>169,170</sup>. Upon inhibition of these pathways by iCRT14 or JNK inhibitor II, specific inhibitors of Wnt

and JNK signaling, respectively, the expression of *ABCB1*, driven by PTOV1, was abrogated (Figure 34C). In contrast, the PTOV1-dependent expression of *ALDH1A1* and *CCNG2* was not affected, suggesting that PTOV1 induced their transcription independently from these pathways (Figure 34)<sup>169,170</sup>.

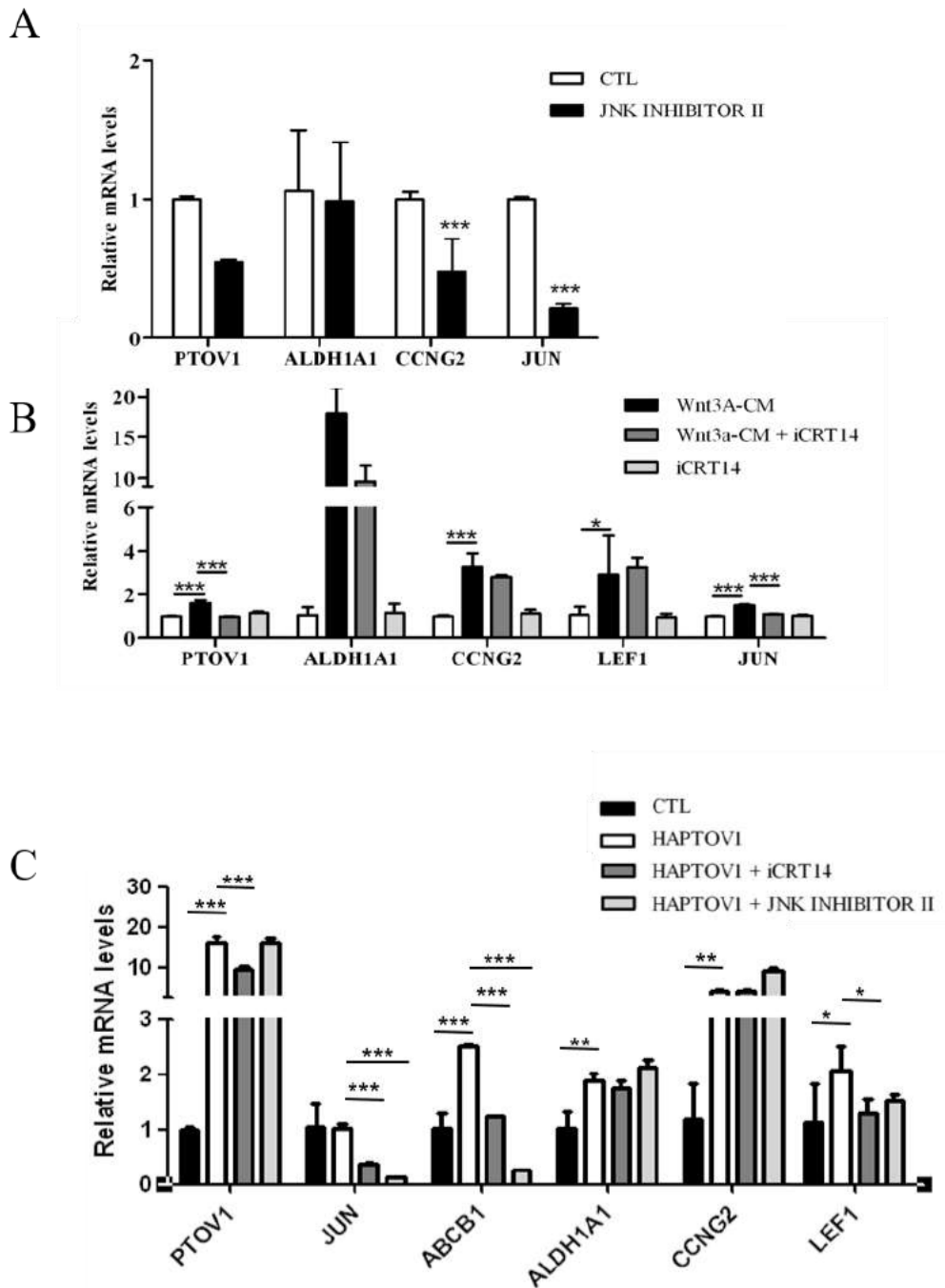


**Figure 34. Wnt and JNK pathways regulate PTOV1 action.** (A) The JNK inhibitor II on gene expression was determined by qRT-PCR in Du145 cells after 24 hours of treatment. CTL cells are treated with dilution buffer. (B) Gene expression in Du145 cells analyzed after the addition of conditioned medium with Wnt3a (Wnt3a-CM), activator of Wnt signaling, without and with a Wnt inhibitor (iCRT14), or control cells treated only with iCRT14. (C) Gene expression was determined

by qRT-PCR in Du145 cells transfected with HAPTOV1 in the presence of Wnt inhibitor (iCRT14) or JNK inhibitor II. *LEF1* and *JUN* levels indicate the activity of the respective pathway, Wnt and JNK, respectively. *p*-value: \* < 0.05; \*\* < 0.01; \*\*\* < 0.001.

Based on these observations, we hypothesized that PTOV1 mediates the transcription of *ALDH1A1* and *CCNG2* genes by direct association with their promoters. We thus performed chromatin immunoprecipitation (ChIP) in LNCaP cells, observing a specific binding of PTOV1 to the *ALDH1A1* and *CCNG2* promoter sequences (Figure 35A and B). In contrast, no specific binding of PTOV1 was observed to promoter sequences of other genes, including *ABCBI* or *HES1* (Figure 35D and E).

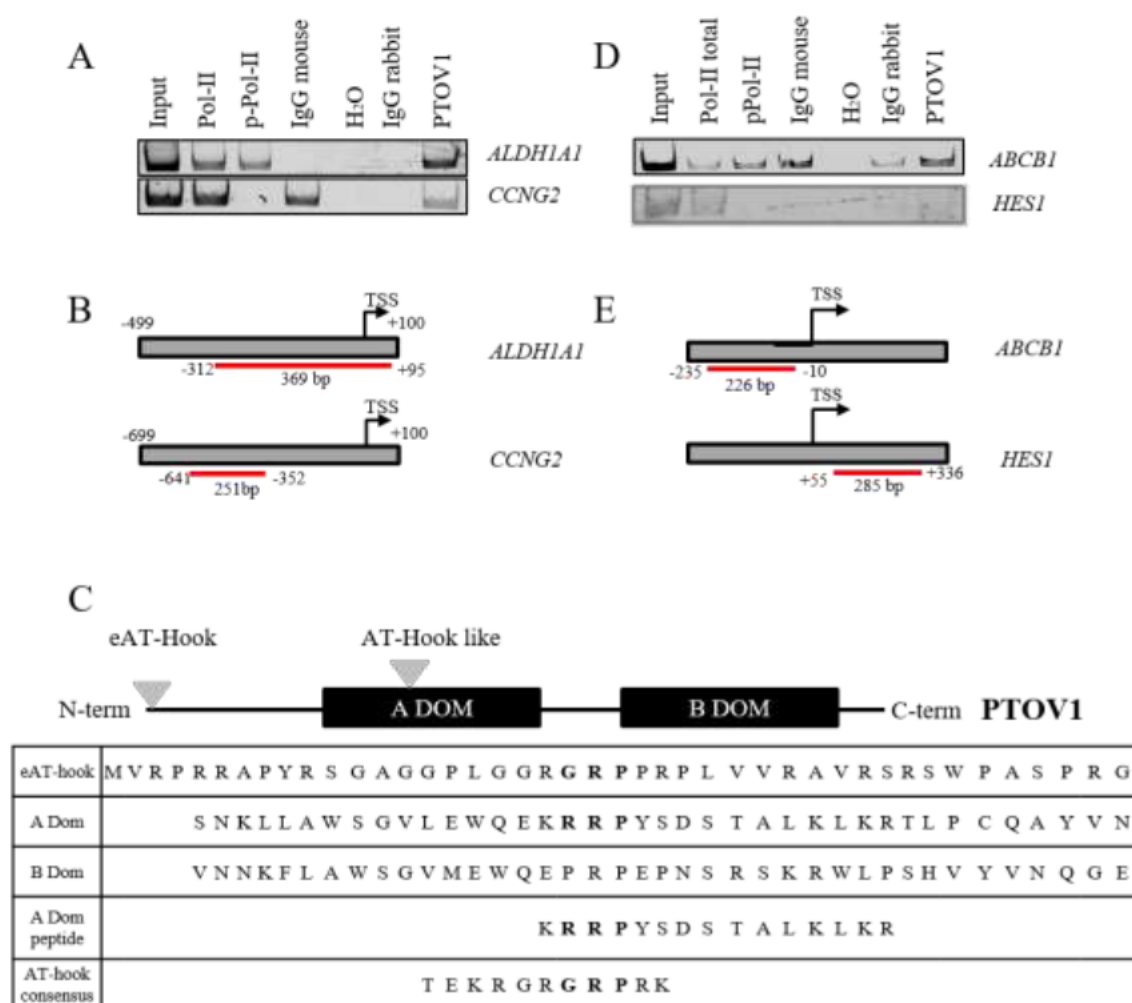


**Figure 35. PTOV1 is associated to the chromatin of *ALDH1A1* and *CCNG2* promoters.** (A) Sheered chromatin from LNCaP cells transfected with a lentivirus encoding the fusion protein HAPTOV1 was immunoprecipitated with rabbit antibodies to PTOV1, total and phosphorylated polymerase II, and rabbit or mouse IgGs as controls. Co-immunoprecipitated DNA fragments were analyzed by PCR with specific primers for *ALDH1A1* and *CCNG2* promoter regions. (B) Graphical representation of primers localization and length of the amplified sequences on the promoters. TSS: transcription start site. (C) Schematic of the protein structure of PTOV1 identifying the AT-hook domains present at the N-terminal (eAT-hook) and inside the A domain (AT-hook-like) (not in scale). Bottom, eAT-hook, the first 43 amino acids from the N-terminal of PTOV1; A domain, the partial amino acid sequence (85 to 125) in the A domain; B domain, the partial amino acid sequence from the B domain (amino acid 249 to 292); A domain AT-hook-like, the amino acid sequence used for EMSA assays (amino acid 100 to 114); AT-hook consensus, the described AT-hook- of HGMA1 (amino acid 21

to 31). Bold identify amino acids in the ‘core’ of AT-hook motifs. (D) Sheered chromatin from LNCaP cells transduced with a lentivirus encoding the fusion protein HAPTOV1 was immunoprecipitated with antibodies to PTOV1, total and phosphorylated polymerase II, and control specie IgGs. Associated DNA fragments were analysed by PCR with primers specific for *ABCBI* and *HES1* sequences. ChIP promoter primers location and length of amplified promoter sequences are indicated on the bottom panel. TSS: transcription start site.

### 3. PTOV1 directly binds to *ALDH1A1* and *CCNG2* promoters through a new motif in its A domain.

Previously, the N-terminal region of PTOV1 was identified to contain an extended AT-hook (eAT-hook) motif<sup>175</sup>. AT-hook amino acid motifs confer proteins the ability to bind DNA or RNA. To study the mechanisms of direct binding of PTOV1 to the promoter sequences of the genes above identified, we analyzed different regions of the protein, including the eAT-hook motif, the A domain, and the B domain for their ability to bind small DNA sequences derived from the *ALDH1A1* and *CCNG2* promoters by means of electrophoretic mobility shift assays (EMSA). We synthesized small DNA probes (32 nucleotides) from the *ALDH1A1* and *CCNG2* promoters containing putative AT-hook target sequences (**Figure 36**), and from the *HES1* intron-1 as negative control. These probes were labeled with [<sup>32</sup>P] and used in binding reactions with recombinant glutathione-S-transferase (GST) full-length protein (GST-PTOV1), A domain (GST-A), B domain (GST-B) or two short peptides containing wild-type or mutated eAT-hook motifs<sup>175</sup> (**Figure 35C**). A specific shifted band is detected when recombinant GST-PTOV1 is incubated with either *ALDH1A1* or *CCNG2* probes (**Figure 36A**). Surprisingly, the GST-A domain of PTOV1, but not the GST-B domain, showed a strong binding activity with both *ALDH1A1* and *CCNG2* probes. No shifted band was visible with the *HES1* negative control probe. Wild type and mutated eAT-hook did not produce shifts of the probes (**Figure 36A**).

A more detailed sequence analysis of the A domain revealed a motif with similarities to a ‘classic AT-hook’ (**Figure 35C**)<sup>286</sup>. This sequence is not conserved in the corresponding homologous B domain of PTOV1. Therefore, we synthesized a short peptide of 15 amino acids of this newly unveiled motif that includes the KRRP residues present in the A domain (**Figure 35C**). Interestingly, labeled probes from both *ALDH1A1* and *CCNG2* were specifically shifted in the presence of this peptide (**Figure 36A**). This result indicates that PTOV1 binds to these promoters through a new AT-hook-like motif present only in the A domain of the protein, rather than through the previously described eAT-hook.

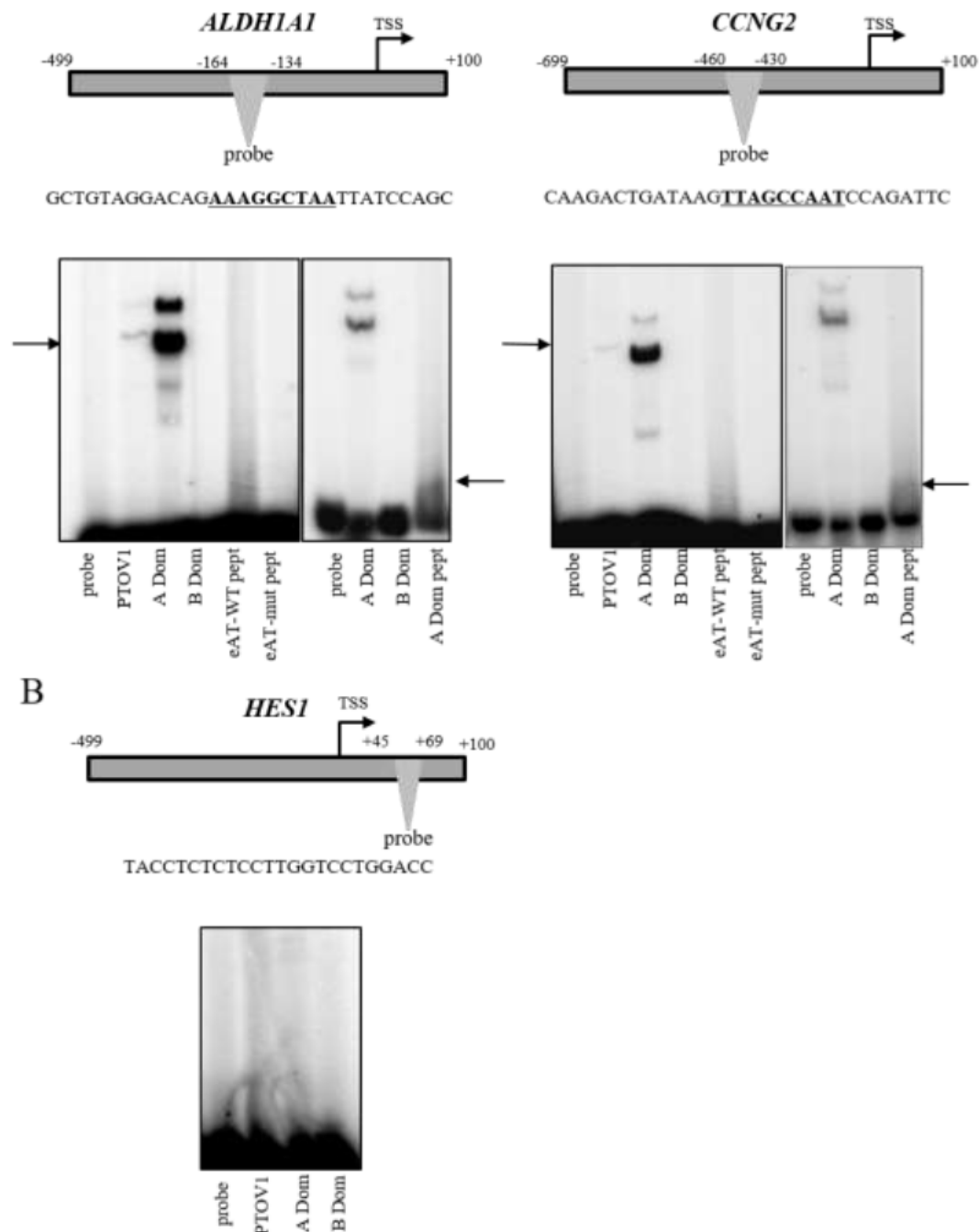


**Figure 36. EMSA identify a new AT-hook-like motif in the A domain of PTOV1.** (A) Drawings show the localization of the DNA sequence probes with respect to the transcription start sites (TSS). Two gel shift assays are shown for each *ALDH1A1* and *CCNG2* probe. In the left *ALDH1A1* gels, labeled sequences were incubated with recombinant GST-PTOV1 (PTOV1), GST-A domain (A dom), GST-B domain (B dom), eAT-hook wild type peptide (eAT-WT pept) and mutated eAT-hook peptide (eAT-mut pept). In the right *CCNG2* gels, labeled sequences were incubated with the GST-A domain (A dom), GST-B domain (B dom), and the A domain AT-hook-like peptide (A dom pept). (B) Gel shift assay performed with the *HES1* probe.

#### 4. The new PTOV1 AT-hook-like motif is necessary to modulate *ALDH1A1* and *CCNG2* expression.

In order to study the functional relevance of the KRRP sequence resembling the core AT-hook (Figure 35C) present in the peptide that binds to *ALDH1A1* and *CCNG2* promoters

(Figure 36), we changed the motif to EGGP, by means of site-directed mutagenesis. This mutant was created in the frame of full-length PTOV1, so as to study its function as a transcription activator. As shown in Figure 37A, both wild-type and EGGP mutant PTOV1 were efficiently expressed in transfected cells. Importantly, the expression of the EGGP mutant caused a moderate but significant decrease of *ALDH1A1* and *CCNG2* transcript levels relative to wild-type PTOV1 (Figure 37B). The fused GFP-PTOV1 plasmids express comparable levels of the exogenous protein, indicating similar levels of transfection in these experiments (Figure 37C). Together with the above demonstration of direct binding to *ALDH1A1* and *CCNG2* promoter sequences, these results lend support to the hypothesis that the AT-hook-like motif in the A domain of PTOV1 is critical for the PTOV1 promoted activation of transcription of these genes.

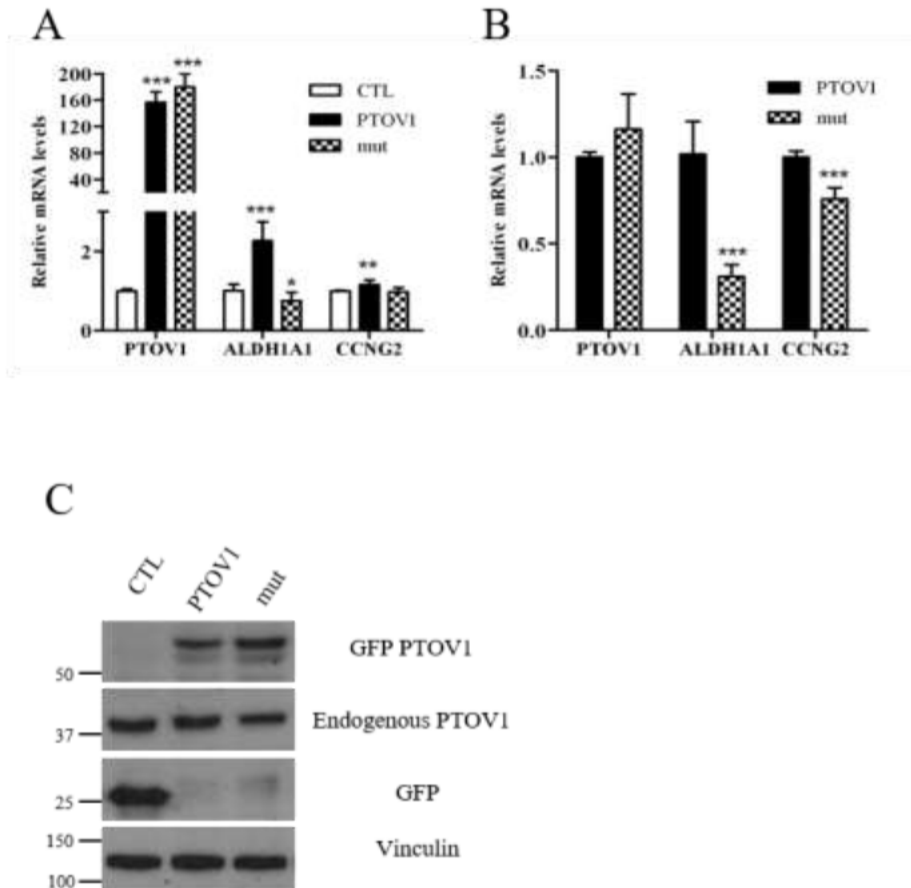


**Figure 37. Mutation of the newly discovered AT-hook-like 'core' motif of PTOV1.** (A) and (B) The plasmid containing the full-length PTOV1 mutated at the AT-hook (EGGP) or wild-type plasmid were transfected in HEK293T cells. After 72 hours, cells were analysed by real-time PCR for gene expression. (C) Western blot analysis of cells transfected with wild-type or mutant GFP-PTOV1 plasmids, shows similar levels of expression of the exogenous PTOV1, as indicated by the GFP antibody signals. Vinculin is shown as protein loading control.

## 5. PTOV1, ALDH1A1 and CCNG2 expression levels are associated with aggressiveness in prostate and colon carcinomas.

To understand the significance of the ability of the oncoprotein PTOV1 to directly bind and activate the expression of *ALDH1A1* and *CCNG2* genes in tumor cells, we interrogated several publicly available databases containing expression data, clinical and pathological information of untreated patients with prostate cancer for the association of expression of these genes. Data derived from micro-dissected untreated prostate tumors specimens show that *PTOV1*, *ALDH1A1* and *CCNG2* transcript levels are significantly increased in patients with high Gleason Score ( $\geq 8$ ) in comparison to patients with low Gleason score ( $\leq 7$ ) (**Figure 38A**) (GSE97284)<sup>287</sup>. The transcript levels of these genes are also significantly higher in prostate adenocarcinomas of patients who developed regional or distal metastasis after radical prostatectomy, suggesting their relationship with metastatic progression<sup>174</sup>. In addition, the expression levels of PTOV1 significantly correlated with the expression of *ALDH1A1* (Spearman 0.46,  $p < 0.0001$ ) and *CCNG2* (Spearman 0.68,  $p < 0.0001$ ) (GSE46691). Moreover, in a cohort of patients with prostate carcinoma including data derived from 10 studies<sup>34,41,55,56,137,185,288-291</sup>, *PTOV1*, *ALDH1A1* and *CCNG2* genes also showed a highly significant co-occurrence of alterations at their DNA (**Table 15**). These observations suggest that the expression of *PTOV1*, *ALDH1A1* and *CCNG2* genes is associated for a coordinated activity in aggressive prostate tumors.

**Table 15.** Co-occurrence of DNA alterations in PCa.

Gene A	Gene B	Log Odds Ratio	Adjusted p-Value	Tendency
<i>PTOV1</i>	<i>ALDH1A1</i>	>3	<0.001	Co-occurrence
<i>PTOV1</i>	<i>CCNG2</i>	2.762	<0.0001	Co-occurrence

Because PTOV1 can strongly and specifically bind to DNA *in vitro* and to chromatin *in vivo*, we searched for PTOV1 association with DNA in mitotic tumors cells using immunohistochemical analysis in different types of tumors. In xenografted mice tumors derived from LNCaP cells, a strong signal for PTOV1 was detected in mitotic cells where the staining appears associated to condensed chromosomes (**Figure 38B**).

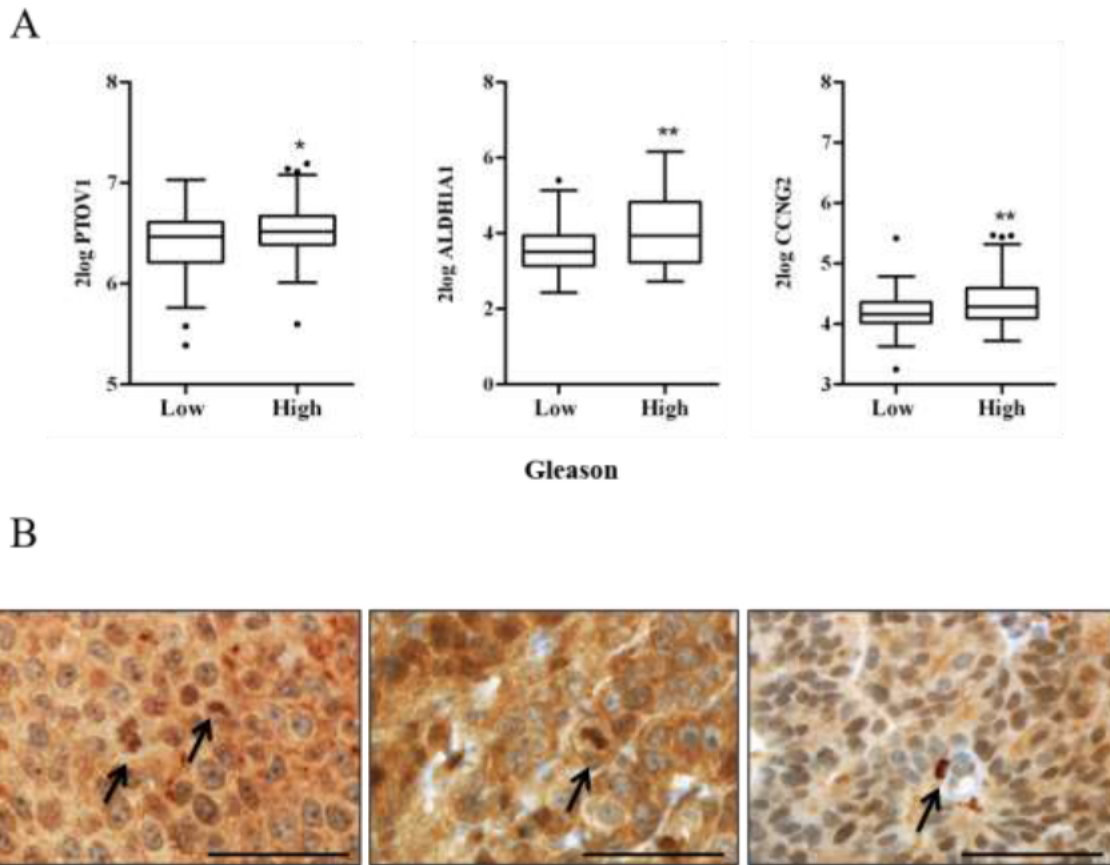


**Figure 38. The expression of PTOV1, ALDH1A1 and CCNG2 is significantly associated with the Gleason score in prostate carcinomas.** (A) Box and whisker plots represent *PTOV1*, *ALDH1A1* and *CCNG2* expression levels in prostate tumors with different Gleason as obtained from published database (GSE 97284). Low grade represents the grade group of  $\leq 7$   $n=83$ ; High grade indicates the grade groups 4 and 5 (Gleason score: 4+4, 3+5, 5+3, 4+5, 5+4, 5+5)  $n=91$ . (B) Immunohistochemical stainings of antibodies to PTOV1 in LNCaP tumors formed in immunosuppressed mice. PTOV1 associates to condensed chromatin in aggressive mitotic cells (arrows). Scale bar: 100  $\mu\text{M}$ . p-value: \*  $<0.05$ ; \*\*  $<0.01$ ; \*\*\*  $<0.001$ .

Similarly, in colon carcinoma tissues immunohistochemical analysis reveals a clear accumulation of PTOV1 in the nuclei of mitotic cells, confirming its strong association with chromatin in aggressive tumor cells (**Figure 39A**). Interrogating publicly available datasets of patients with colon carcinomas (GSE24551, GSE14333), high levels of *PTOV1*, *ALDH1A1* and *CCNG2* expression correlated with poor relapse-free survival and event-free survival, although for *ALDH1A1* the association did not reach significance (**Figure 39B**).



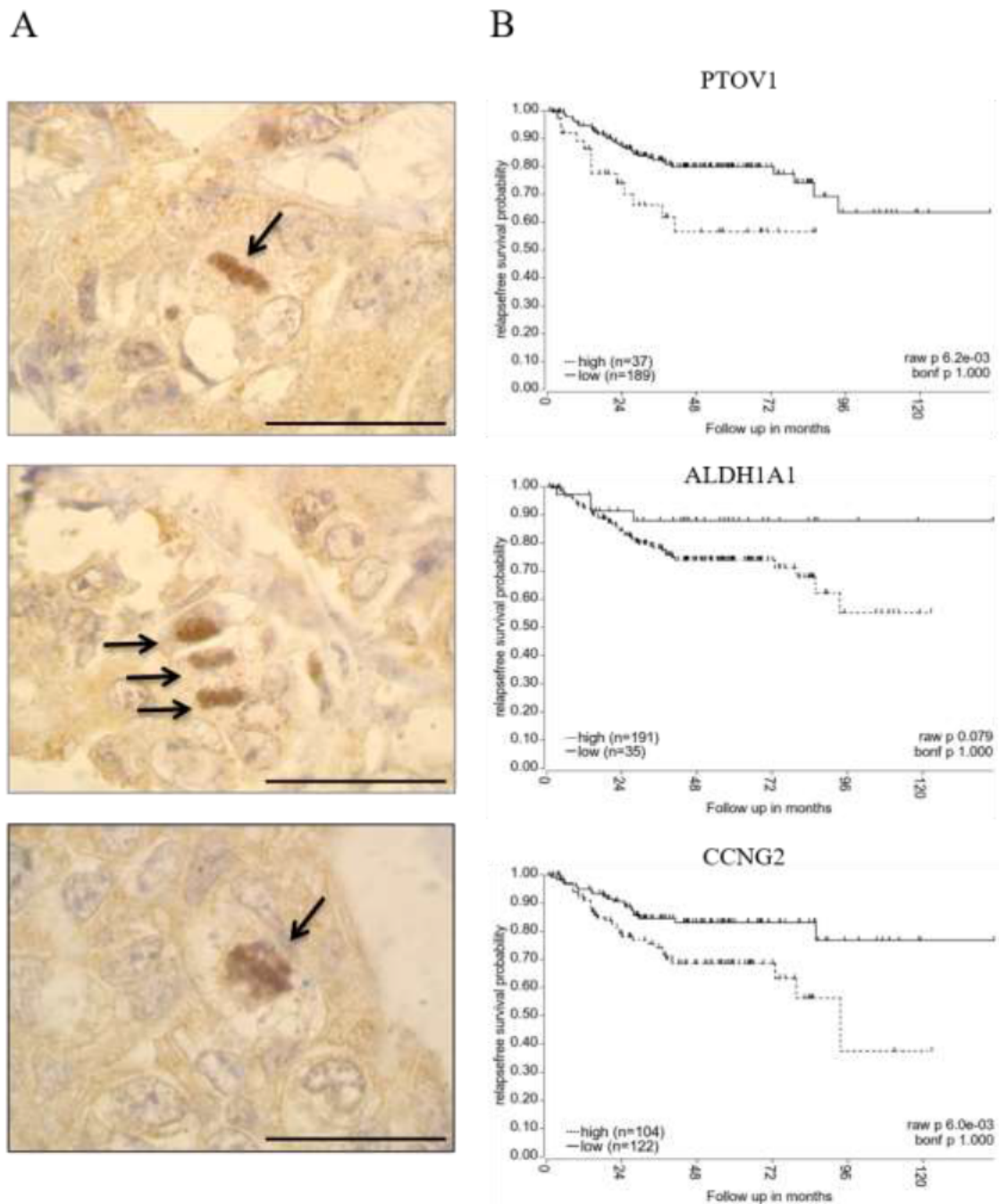


**Figure 39. PTOV1 accumulates in the nuclei of mitotic colon carcinoma cells.** (A) Immunohistochemistry analyses of aggressive colon carcinoma cells show PTOV1 localized in condensed mitotic nuclei (arrows). Scale bar: 100  $\mu$ M. (B) The expression of PTOV1 significantly correlates with poor overall survival in colon tumors. Public datasets (GSE62452, GSE3141, GSE45547, GSE24551, GSE21653, GSE14333) containing information of survival rates in patients with colon cancer were analyzed using R2 platform.

Furthermore, immunohistochemical analyses of high grade urothelial bladder carcinoma and ductal breast carcinoma, previously shown to express high levels of PTOV1<sup>161</sup>, also revealed

a clear association of the protein with condensed mitotic DNA (Figure 40).

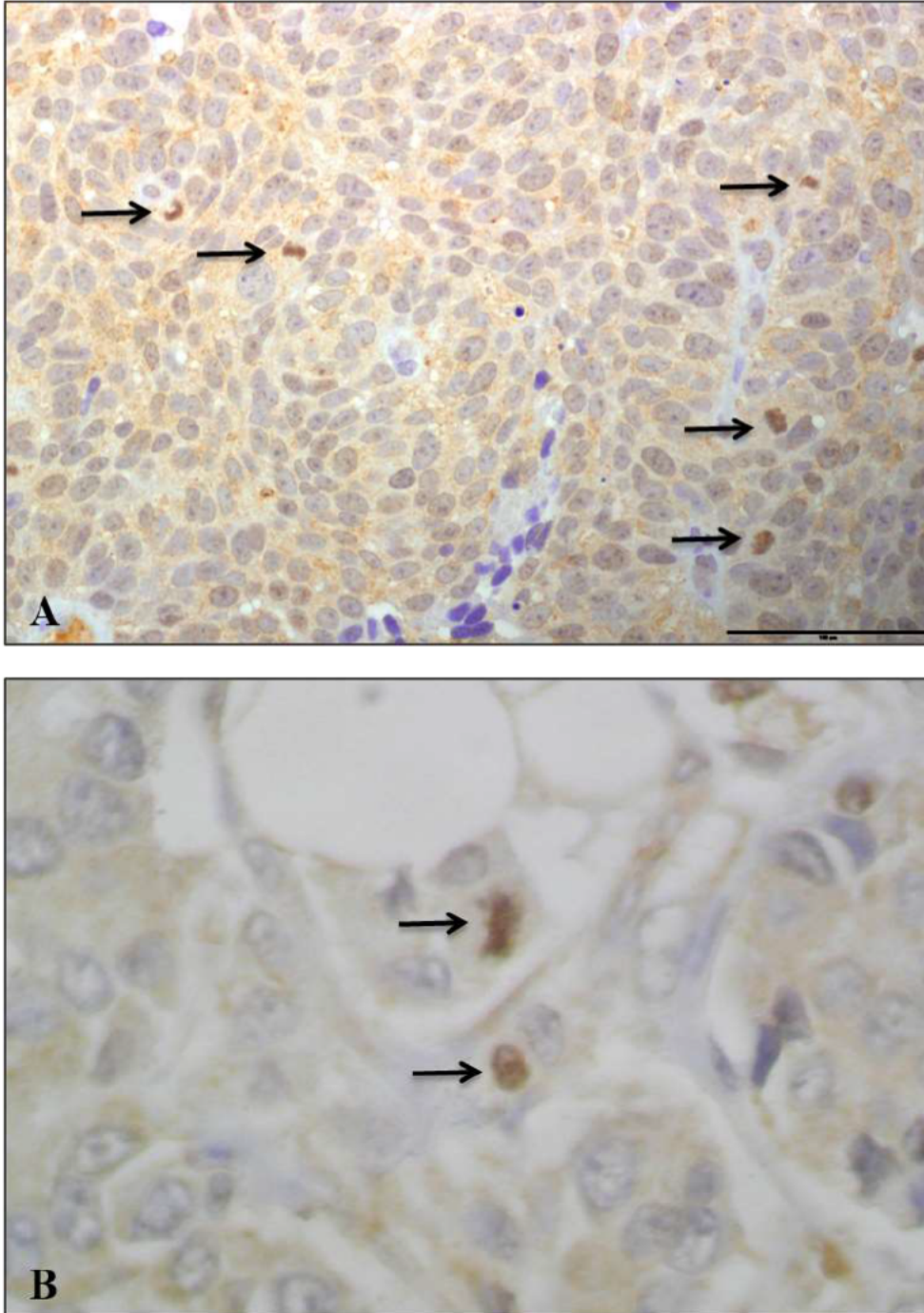


**Figure 40.** PTOV1 accumulates in the nuclei of mitotic bladder carcinoma and breast carcinoma cells. (A) Immunohistochemical staining of antibodies to PTOV1 in high grade bladder carcinoma and breast carcinoma (B) reveal strong staining associated to chromatin of mitotic cells (arrows).

## 6. Discussion

Here, we provide new insights into the mechanisms used by the protein PTOV1 to regulate the expression of *ALDH1A1* and *CCNG2*, relevant factors involved in tumor progression. Specifically, we show that PTOV1 is able to directly bind to the promoter sequences of these

genes through a newly unveiled protein motif localized within the A domain of the protein<sup>168</sup>. This finding impacts on several aspects of the action of PTOV1 in cancer progression.

First, our findings define PTOV1 as a new nucleic acid binding protein containing two distinct motifs: one extended (eAT-hook) at the N-terminal<sup>175</sup> and a second AT-hook-like motif, identified and characterized in this work, within the A domain of PTOV1. The previously described eAT-hook does not bind to any of the DNA sequences tested here, in line with previous results that this motif has a higher affinity for RNA sequences<sup>175</sup>. In contrast, the newly identified AT-hook-like strongly binds to DNA sequences from the *ALDH1A1* and *CCNG2* promoters but not to *ABCB1* promoter or internal *HES1* gene sequences, indicating its specificity. Of note, mutations of the ‘core’ sequence in the AT-hook-like motif, decreases the expression of *ALDH1A1* and *CCNG2* indicating that this motif is functionally relevant for the transcriptional activity of PTOV1. Since PTOV1 was shown to function both at specific promoter sites to regulate transcription<sup>170,171</sup> and at ribosomes<sup>169</sup> to regulate mRNA translation, our present findings reveal potential new ways to selectively mitigate the nuclear or cytoplasmic functions of PTOV1 in cancer cells: the identification of inhibitors of these ‘micro-handles’ in the protein could prevent its specific binding to either DNA or RNA, causing functionally diverse consequences on cell fate.

Secondly, we have shown that the transcriptional activation of *ALDH1A1* and *CCNG2* by PTOV1 is independent of the canonical Wnt or JNK pathways, being instead mechanistically explained by the direct binding of PTOV1 to specific sequences of these promoters. *ALDH1A1* is an established hallmark of CSCs and promoter of drug resistance in different types of cancers, including colon cancer<sup>282,283</sup> and *CCNG2* is an unconventional cyclin whose function in cancer progression remains to be determined. *CCNG2* was first described as a tumor suppressor in several cancer types<sup>292-294</sup>, being significantly upregulated in response diverse growth inhibitory stimuli, contributing to induce G2/M checkpoint and cell cycle arrest in response to doxorubicin<sup>285</sup> and to thiopurine resistance in lymphoblastoid cells<sup>284</sup>. However, it was also reported to modulate invasion in glioblastoma cells<sup>295</sup>. In these tumors, *CCNG2* is remarkably expressed at hypoxic sites, and was shown to cooperate with actin-binding proteins providing flexibility to actin filaments for glioblastoma cell invasion. Consistent with an oncogenic role, we found that *CCNG2* is significantly co-expressed with *PTOV1* and *ALDH1A1* in aggressive prostate tumors and colon carcinomas, where overexpression of these genes is linked to progression and decreased relapse-free survival (**Figure 38A** and **Figure 39B**). The association of *ALDH1A1* with poor survival was very

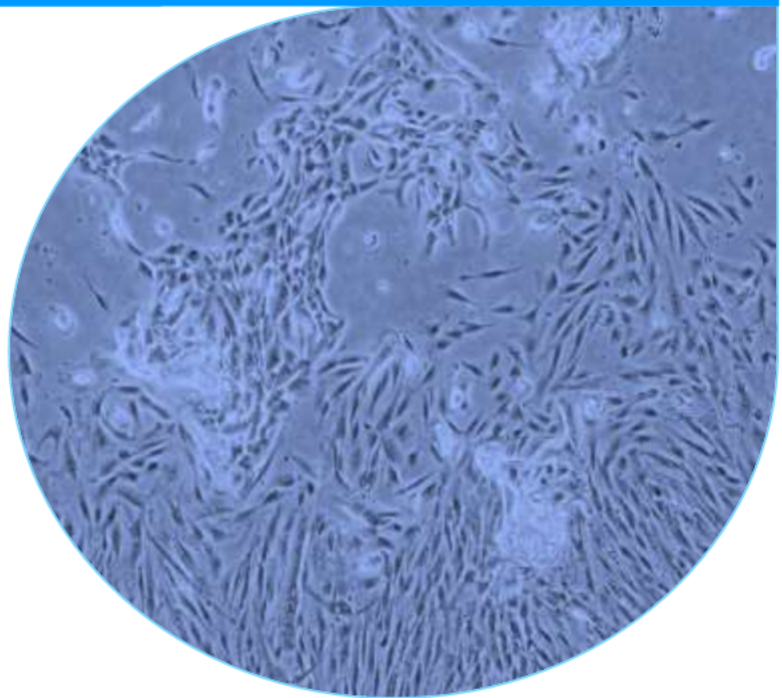
recently confirmed in colon carcinomas<sup>296</sup>. Lastly, the significant co-occurrence of DNA alterations in *PTOV1*, *ALDH1A1* and *CCNG2* in prostate carcinomas (**Table 15**) together with the above mentioned findings, indicate a concerted action of these genes in cancer progression<sup>168,282,284,295</sup>. These observations also suggest that, similarly to HMGA proteins, PTOV1 bound to *ALDH1A1* and *CCNG2* promoters may function as an epigenetic factor that triggers the recruitment of chromatin regulators and transcription factors to activate gene expression. The expression of *CCNG2*, increased at G2-M phase, blocks the cell cycle before mitotic entry and chromosome condensation and is associated to thiopurine and doxorubicin resistance<sup>284,285</sup>. In addition, *ALDH1A1* is one of the most overexpressed gene in Solitary Fibrous Tumors, a rare spindle cell tumor with high mitotic counts<sup>297</sup>. Thus, PTOV1 action on *CCNG2* and *ALDH1A1* promoters might occur at mitotic stages and, conceivably, its binding to chromatin may be detected in condensed chromosomes of tumors cells. In fact, we observed positive PTOV1 staining in mitotic DNA in cells of prostate, colon, bladder and breast carcinomas. In mice tumors from LNCaP cells, numerous mitotic cells had a strong chromatin associated PTOV1 staining, although strong reactivity was also observed in the cytoplasm, suggesting its actions in cytoplasm and nucleus in aggressive tumor stages<sup>172</sup>.

Thirdly, the protein structure of PTOV1 shares similarities with other proteins that interact with nucleic acids, like the  $\beta$ -barrel present in Ku (Ku70/Ku80) heterodimers and the SMRT/HDAC1-associated repressor protein (SHARP)<sup>298,299</sup>. Ku70/Ku80 are the DNA binding subunits of the DNA-PK complex necessary for the assembling of the DNA repair machinery for double strand breaks and are also implicated in transcriptional regulation<sup>300</sup>. SHARP is an important transcriptional regulator of nuclear receptor-mediated responses, Notch-mediated transcription, and X-chromosome silencing during development<sup>299,301</sup>. Besides sharing characteristics like DNA binding abilities and transcription regulatory functions, the two tandem domains in PTOV1 are structurally related to the SPOC domain in Ku and SHARP<sup>298,302</sup>. Similarly to PTOV1, SHARP also contains RNA recognition motifs, but is not known to contain nucleic acid-binding AT-hook-like motifs<sup>299</sup>. Members of the HMGA family of proteins also share structural (presence of several AT-hook motifs) and functional similarities with PTOV1, *e.g.* promote transcription<sup>303-304</sup>, bind directly to gene promoters, are overexpressed in cancer, and are associated to metastasis and therapy resistance<sup>305-307</sup>.

AT-hook variants containing modifications that still allow binding to the DNA minor groove have been discovered, suggesting that the consensus core motif based on the HMGA family might not be so strict<sup>308</sup>. Recently, different unconventional AT-hook motifs were identified in DNA/RNA binding proteins<sup>309,310</sup>. Similar to the unconventional AT-hook-*like* motif reported here for PTOV1, an unconventional AT-hook domain 2 found in MeCP2 with a KRGRK core it is still able to bind AT-rich DNA sequences<sup>311</sup>. Another example of unconventional, AT-hook sequence is the TAF1 protein of *Drosophila melanogaster* that significantly diverges from the HGMA consensus without losing DNA affinity<sup>308</sup>. Moreover, Tip5, a subunit of the nucleolar remodeling complex (NoRC) that provides the link between nucleolar matrix and rDNA, also contains different AT-hook motifs for interaction with nucleic acids<sup>312</sup>, including an *extended*-AT-hook that preferentially binds RNA to modulate the association between NoRC and promoter-associated RNA (pRNA)<sup>313</sup>. Finally, RNA-binding proteins Rrp12 and Srsf10 contain AT-hook motifs, suggesting that similarly to PTOV1 these proteins may have roles in DNA and RNA processes<sup>314</sup>. We propose that the previously identified eAT-hook and the newly unveiled AT-hook-*like* motifs have key roles in the functions of PTOV1 in mRNA translation and transcription, respectively<sup>169-171</sup>.

In summary, we report a novel DNA binding motif in PTOV1 that allows its specific and direct binding to sequences of the *ALDH1A1* and *CCNG2* promoters, genes implicated in self-renewal and drug resistance, and their expression is associated with progression of tumors to aggressive stages and worse patients' outcome. The distinct DNA-RNA-binding AT-hook motifs might direct PTOV1 nuclear and cytoplasmic actions. Noteworthy, these motifs reveal specificities potentially useful to screen for inhibitors of distinct oncogenic functions of PTOV1.

## **CHAPTER 8: GENERAL DISCUSSION**





## 1. Novel tools to study primary prostate cancer

We reported the establishment of primary explant cultures from fresh needle biopsies of patients with aggressive untreated prostate cancer. We overcome the problem of the amount of tissue, setting up a new protocol to culture primary PCa epithelial cells. This protocol opens the possibility to improve the comprehension of several molecular mechanisms still unknown. Indeed, although PCa is the third cause of death in the Western world, the development of new *in vitro* primary prostate tumor models is of utmost important because the actual panorama of tools to study the molecular mechanisms responsible of the resistance and the recurrence is composed of about ten *in vitro* cells lines<sup>15,121,136</sup>. Here, we have provided a partial characterization of ten *ex vivo* primary tumor cultures by analysis of few of the common genes alterations previously described in untreated metastatic tumors, although it is necessary to have a complete genomic vision of the mutations occurred in these cultures<sup>315</sup>. We attempted to conduct similar genetic characterizations in the corresponding original tumor tissues with the aim to confirm the reliability of the *in vitro* culture models<sup>316-318</sup>. One *in vitro* model (*ex vivo* primary culture 1) showed un-functional *PTEN* and *TP53* genes, was composed mostly of luminal epithelial cells, and was able to generate tumors *in vivo*. In addition, we generated *ex vivo* androgen independent (AI) variant cultures with functional differences in comparison to their parental counterparts in their growth, invasion, drug resistance, rate of protein synthesis and alterations in the mTOR pathway. Although these *ex vivo* culture need further characterization in order to be reliable models to study androgen resistance mechanisms in prostate cancer, , they may still provide very useful biological information when analyzed in parallel with cell lines established from metastasis, LNCaP, Du145 and PC3<sup>199,204</sup>. Our studies also found many similarities between AI primary cultures and cancer stem cells, suggesting that the mechanism of androgen resistance might implicate CSCs plasticity<sup>190</sup>. These cells present within the bulk of the tumor have been shown linked to drug resistance mechanisms and recurrence<sup>196</sup>. In fact, we have shown that AI cultures are more quiescent, have a higher resistance to chemotherapeutic drugs, and express several self-renewal markers, features of cancer stem cells<sup>319</sup>. The adaptive response to drugs is different among the *ex vivo* cultures coming from distinct primary tumors. Another study highlights the distinct drug response among tumors but also between the same types of tumors there is heterogeneity in the regulation of the genes target. Our studies suggest that the different adaptation to drugs may explain the difficulties to predict resistance



mechanisms because it may not depend on the tumor type, nor specific genes. For these reasons, more complex prognostic techniques are needed to improve the specificity of therapy<sup>320</sup>.

Based on the results that AI cells were enriched of subpopulations with self-renewal features we developed an additional second *in vitro* model, functionally selected, of cancer stem cells that could be used to study aggressive tumors.

CSCs are supposed to have a key role in tumor initiation, but also in progression and tumor recurrence. In, contrast to other tumor types, PCa lacks a strong marker to identifies prostate CSCs. In contrast to breast CSCs that can be easily purified as the population CD44<sup>+</sup>/CD24<sup>-</sup>, prostate CSCs have irregular levels of several markers during their life<sup>261,262</sup>. For this reason, we established a protocol that functionally enriches populations of CSCs avoiding selecting just for a single CSCs clone (*e.g.* CD133<sup>+</sup> cells) and used different spheres generations to select populations of tumor cells with increased capacity to grow as spheres, using both and established cell lines and *ex vivo* primary tumor cultures. This protocol provides cultures enrichment with CSCs and the possibility to test and validate new drugs. Because targeting CSCs has been suggested as a potential novel therapy to suppress PCa metastasis<sup>249</sup>, our results suggest Galiellalactone (GL), a STAT3 inhibitor, and Bozepinib analogues (MDN-90, MEGR756B) as novel compounds that efficiently target CSCs spheres in PCa cell lines and *ex vivo* primary cultures. Interestingly, docetaxel resistant Du145 cells resulted more sensitive to GL and MDN-90, suggesting that both compounds would be a specific therapy against CRPC. In contrast, primary *ex vivo* AI culture was more affected by the action of MEGR756B, another confirmation of the need for new tools to personalize therapies.

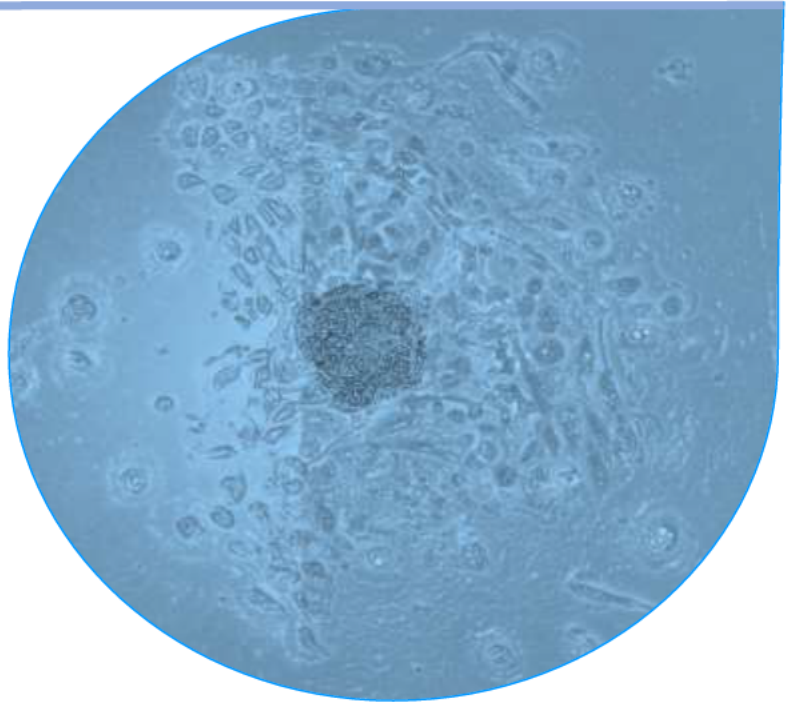
### **2. PTOV1 can directly regulate self-renewal genes like ALDH1A1 and CCNG2**

We provide new insights into the mechanisms used by the protein PTOV1 to regulate the expression of *ALDH1A1* and *CCNG2*, relevant factors involved in tumor progression. Specifically, we show that PTOV1 is able to directly bind to the promoter sequences of these genes through a newly unveiled protein motif localized within the A domain of the protein<sup>168</sup>. This finding impacts on several aspects of the action of PTOV1 in cancer progression. PTOV1 is an oncogenic protein overexpressed and associated to increased proliferation, high malignancy, and unfavorable prognosis in prostate cancer, laryngeal cancer and other

neoplasms. However, low or no expression is detected in normal tissues associated to cancer<sup>174</sup>. In prostate cancer cells, the protein localized in the cytoplasm directly interacts with RACK1 on 40S ribosomes and activates translation of a subset of mRNAs, including the oncogene JUN that amplifies the oncogenic action of PTOV1<sup>169</sup>. In the nucleus, PTOV1 is associated to chromatin and shows repressor activity on HES1 and HEY1 genes, major targets of the receptor Notch, an oncogenic protein in leukemia, but a tumor suppressor in prostate cancer<sup>171</sup>. In addition, our findings define PTOV1 as a new nucleic acid binding protein containing two distinct motifs: one extended (eAT-hook) at the N-terminal<sup>175</sup> and a second AT-hook-like motif, identified and characterized in this work, within the A domain of PTOV1. This novel DNA binding motif in PTOV1 allows its specific and direct binding to sequences of the *ALDH1A1* and *CCNG2* promoters, genes implicated in self-renewal and drug resistance, and their expression is associated with progression of tumors to aggressive stages and worse patients' outcome. *ALDH1A1* is an established hallmark of CSCs and promoter of drug resistance in different types of cancers, including colon cancer<sup>282,283</sup> and *CCNG2* is an unconventional cyclin, found to exert an oncogenic role in glioblastoma through the cooperation with actin-binding proteins providing flexibility to actin filaments for glioblastoma cell invasion. The two AT-hook motifs of PTOV1 may modulate different nuclear and cytoplasmic actions. The above studies suggest a strong pro-oncogenic role for PTOV1 during tumor progression to chemotherapy resistance and support this protein as a suitable therapeutic target for cancer treatment.



## **CHAPTER 9: CONCLUSIONS**



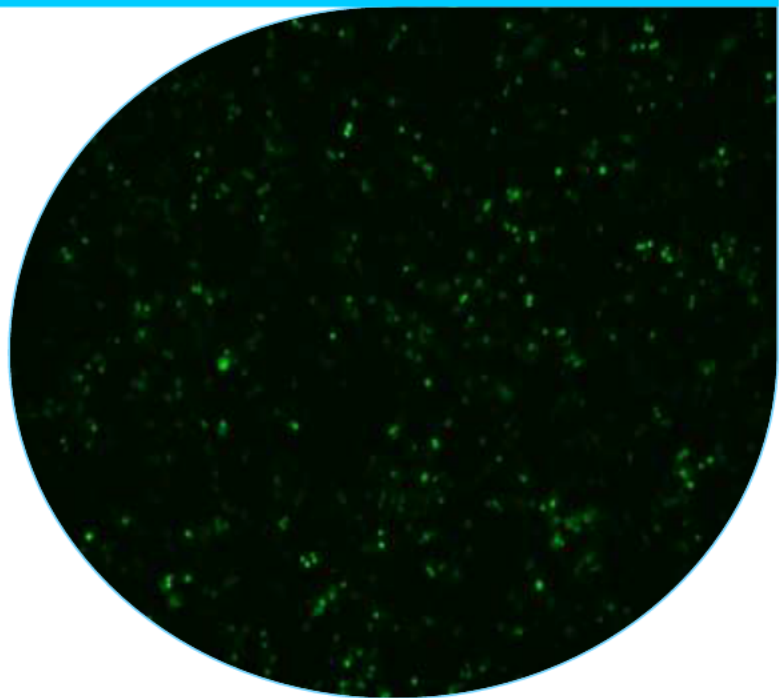


1. A total of 16 *ex vivo* primary tumor cultures were newly established from prostate needle biopsy cores from untreated patients with androgen dependent aggressive prostate cancer.
2. Corresponding Androgen Independent (AI) cultures were derived by growth adaptation of parental androgen dependent cultures in hormone depleted medium. Of note, the treatment of the primary cultures with such medium provoked an increment of expression of self-renewal markers, suggesting an increase of stemness capacities in the resistant AI cell populations.
3. The surviving primary tumor cultures (AI) exhibited in general a reduction of proliferation rate, increase of motility and cross-resistance to chemotherapy, phenomena ligated to the high plasticity of these cultures.
4. CSCs were efficiently selected through a protocol of enrichment in spheres that include different CSCs clones. Spheres were characterized and validated to share many features with CSCs of prostate but also other type of organs. Spheres were applied to perform a small drug screening in order to find new specific targets and personalized therapy based on the patient and the clinical stage of PCa.
5. PTOV1 possesses another AT-hook like motif within the A domain that have more affinity to DNA rather than RNA. Through the AT-hook motif, PTOV1 directly binds to *ALDH1A1* and *CCNG2* promoters to activate their expression in androgen dependent LNCaP cells.
6. PTOV1, *ALDH1A1* and *CCNG2* high levels are correlated with aggressive PCa tumors and worst outcome, suggesting that PTOV1 could be a potential target for the treatment of aggressive androgens responsive prostate cancer



## **CHAPTER 10: BIBLIOGRAPHY**

---







- 1 Kumar, V. L. & Majumder, P. K. Prostate gland: structure, functions and regulation. *Int Urol Nephrol* **27**, 231-243 (1995).
- 2 Lee, C. H., Akin-Olugbade, O. & Kirschenbaum, A. Overview of prostate anatomy, histology, and pathology. *Endocrinol Metab Clin North Am* **40**, 565-575, viii-ix, doi:10.1016/j.ecl.2011.05.012 (2011).
- 3 Aaron, L., Franco, O. E. & Hayward, S. W. Review of Prostate Anatomy and Embryology and the Etiology of Benign Prostatic Hyperplasia. *Urol Clin North Am* **43**, 279-288, doi:10.1016/j.ucl.2016.04.012 (2016).
- 4 Ittmann, M. Anatomy and Histology of the Human and Murine Prostate. *Cold Spring Harb Perspect Med* **8**, doi:10.1101/cshperspect.a030346 (2018).
- 5 Signoretti, S. *et al.* p63 is a prostate basal cell marker and is required for prostate development. *Am J Pathol* **157**, 1769-1775, doi:10.1016/s0002-9440(10)64814-6 (2000).
- 6 Parimi, V., Goyal, R., Poropatich, K. & Yang, X. J. Neuroendocrine differentiation of prostate cancer: a review. *Am J Clin Exp Urol* **2**, 273-285 (2014).
- 7 Szczyrba, J. & Niesen, A. Neuroendocrine Cells of the Prostate Derive from the Neural Crest. **292**, 2021-2031, doi:10.1074/jbc.M116.755082 (2017).
- 8 Beltran, H. *et al.* Molecular characterization of neuroendocrine prostate cancer and identification of new drug targets. *Cancer Discov* **1**, 487-495, doi:10.1158/2159-8290.cd-11-0130 (2011).
- 9 Wang, Y., Hayward, S., Cao, M., Thayer, K. & Cunha, G. Cell differentiation lineage in the prostate. *Differentiation* **68**, 270-279 (2001).
- 10 Wang, X. *et al.* A luminal epithelial stem cell that is a cell of origin for prostate cancer. *Nature* **461**, 495-500, doi:10.1038/nature08361 (2009).
- 11 Taylor, R. A., Toivanen, R. & Risbridger, G. P. Stem cells in prostate cancer: treating the root of the problem. *Endocr Relat Cancer* **17**, R273-285, doi:10.1677/erc-10-0145 (2010).
- 12 Verze, P., Cai, T. & Lorenzetti, S. The role of the prostate in male fertility, health and disease. *Nat Rev Urol* **13**, 379-386, doi:10.1038/nrurol.2016.89 (2016).
- 13 Lamont, K. R. & Tindall, D. J. Androgen regulation of gene expression. *Adv Cancer Res* **107**, 137-162, doi:10.1016/s0065-230x(10)07005-3 (2010).
- 14 Nieto, C. M., Rider, L. C. & Cramer, S. D. Influence of stromal-epithelial interactions on androgen action. *Endocr Relat Cancer* **21**, T147-160, doi:10.1530/erc-14-0138 (2014).
- 15 Siegel, R. L. & Miller, K. D. Cancer statistics, 2019. **69**, 7-34, doi:10.3322/caac.21551 (2019).
- 16 Shen, M. M. & Abate-Shen, C. Molecular genetics of prostate cancer: new prospects for old challenges. *Genes Dev* **24**, 1967-2000, doi:10.1101/gad.1965810 (2010).
- 17 Bostwick, D. G., Liu, L., Brawer, M. K. & Qian, J. High-grade prostatic intraepithelial neoplasia. *Rev Urol* **6**, 171-179 (2004).
- 18 Rybak, A. P., Bristow, R. G. & Kapoor, A. Prostate cancer stem cells: deciphering the origins and pathways involved in prostate tumorigenesis and aggression. *Oncotarget* **6**, 1900-1919, doi:10.18632/oncotarget.2953 (2015).
- 19 Sakr, W. A. & Partin, A. W. Histological markers of risk and the role of high-grade prostatic intraepithelial neoplasia. *Urology* **57**, 115-120 (2001).
- 20 Cheng, L. *et al.* Molecular evidence supporting the precursor nature of atypical adenomatous hyperplasia of the prostate. *Mol Carcinog*, doi:10.1002/mc.23009 (2019).
- 21 Arora, K. & Barbieri, C. E. Molecular Subtypes of Prostate Cancer. *Curr Oncol Rep* **20**, 58, doi:10.1007/s11912-018-0707-9 (2018).
- 22 Tomlins, S. A. *et al.* Recurrent fusion of TMPRSS2 and ETS transcription factor genes in prostate cancer. *Science* **310**, 644-648, doi:10.1126/science.1117679 (2005).
- 23 Shaikhibrahim, Z. & Wernert, N. ETS transcription factors and prostate cancer: the role of the family prototype ETS-1 (review). *Int J Oncol* **40**, 1748-1754, doi:10.3892/ijo.2012.1380 (2012).

- 24 Oikawa, T. & Yamada, T. Molecular biology of the Ets family of transcription factors. *Gene* 303, 11-34 (2003).
- 25 Hsu, T., Trojanowska, M. & Watson, D. K. Ets proteins in biological control and cancer. *J Cell Biochem* 91, 896-903, doi:10.1002/jcb.20012 (2004).
- 26 Hessels, D. *et al.* Detection of TMPRSS2-ERG fusion transcripts and prostate cancer antigen 3 in urinary sediments may improve diagnosis of prostate cancer. *Clin Cancer Res* 13, 5103-5108, doi:10.1158/1078-0432.ccr-07-0700 (2007).
- 27 Wang, J., Cai, Y., Ren, C. & Ittmann, M. Expression of variant TMPRSS2/ERG fusion messenger RNAs is associated with aggressive prostate cancer. *Cancer Res* 66, 8347-8351, doi:10.1158/0008-5472.can-06-1966 (2006).
- 28 Adamo, P. *et al.* The oncogenic transcription factor ERG represses the transcription of the tumour suppressor gene PTEN in prostate cancer cells. *Oncol Lett* 14, 5605-5610, doi:10.3892/ol.2017.6841 (2017).
- 29 Cully, M., You, H., Levine, A. J. & Mak, T. W. Beyond PTEN mutations: the PI3K pathway as an integrator of multiple inputs during tumorigenesis. *Nat Rev Cancer* 6, 184-192, doi:10.1038/nrc1819 (2006).
- 30 Zhou, X. *et al.* Effect of PTEN loss on metabolic reprogramming in prostate cancer cells. *Oncol Lett* 17, 2856-2866, doi:10.3892/ol.2019.9932 (2019).
- 31 Wise, H. M., Hermida, M. A. & Leslie, N. R. Prostate cancer, PI3K, PTEN and prognosis. *Clin Sci (Lond)* 131, 197-210, doi:10.1042/cs20160026 (2017).
- 32 Vivanco, I. *et al.* Identification of the JNK signaling pathway as a functional target of the tumor suppressor PTEN. *Cancer Cell* 11, 555-569, doi:10.1016/j.ccr.2007.04.021 (2007).
- 33 Vidotto, T., Tiezzi, D. G. & Squire, J. A. Distinct subtypes of genomic PTEN deletion size influence the landscape of aneuploidy and outcome in prostate cancer. 11, 1, doi:10.1186/s13039-017-0348-y (2018).
- 34 Taylor, B. S. *et al.* Integrative genomic profiling of human prostate cancer. *Cancer Cell* 18, 11-22, doi:10.1016/j.ccr.2010.05.026 (2010).
- 35 Kaur, H. B. *et al.* TP53 missense mutation is associated with increased tumor-infiltrating T-cells in primary prostate Cancer. *Hum Pathol*, doi:10.1016/j.humpath.2019.02.006 (2019).
- 36 Barbieri, C. E. & Tomlins, S. A. The prostate cancer genome: perspectives and potential. *Urol Oncol* 32, 53.e15-22, doi:10.1016/j.urolonc.2013.08.025 (2014).
- 37 Tomczak, K., Czerwinska, P. & Wiznerowicz, M. The Cancer Genome Atlas (TCGA): an immeasurable source of knowledge. *Contemp Oncol (Pozn)* 19, A68-77, doi:10.5114/wo.2014.47136 (2015).
- 38 Frank, A. K. *et al.* The codon 72 polymorphism of p53 regulates interaction with NF- $\kappa$ B and transactivation of genes involved in immunity and inflammation. *Mol Cell Biol* 31, 1201-1213, doi:10.1128/mcb.01136-10 (2011).
- 39 Kung, C. P. *et al.* The P72R Polymorphism of p53 Predisposes to Obesity and Metabolic Dysfunction. *Cell Rep* 14, 2413-2425, doi:10.1016/j.celrep.2016.02.037 (2016).
- 40 Park, J., Morley, T. S., Kim, M., Clegg, D. J. & Scherer, P. E. Obesity and cancer--mechanisms underlying tumour progression and recurrence. *Nat Rev Endocrinol* 10, 455-465, doi:10.1038/nrendo.2014.94 (2014).
- 41 Barbieri, C. E. *et al.* Exome sequencing identifies recurrent SPOP, FOXA1 and MED12 mutations in prostate cancer. *Nat Genet* 44, 685-689, doi:10.1038/ng.2279 (2012).
- 42 Geng, C. *et al.* Prostate cancer-associated mutations in speckle-type POZ protein (SPOP) regulate steroid receptor coactivator 3 protein turnover. *Proc Natl Acad Sci U S A* 110, 6997-7002, doi:10.1073/pnas.1304502110 (2013).
- 43 Boysen, G. *et al.* SPOP mutation leads to genomic instability in prostate cancer. *Elife* 4, doi:10.7554/eLife.09207 (2015).

- 44 Jin, H. J., Zhao, J. C., Ogden, I., Bergan, R. C. & Yu, J. Androgen receptor-independent function of FoxA1 in prostate cancer metastasis. *Cancer Res* **73**, 3725-3736, doi:10.1158/0008-5472.can-12-3468 (2013).
- 45 Gao, S. *et al.* Forkhead domain mutations in FOXA1 drive prostate cancer progression. *Cell Res*, doi:10.1038/s41422-019-0203-2 (2019).
- 46 Lin, J. J. *et al.* Mediator coordinates PIC assembly with recruitment of CHD1. *Genes Dev* **25**, 2198-2209, doi:10.1101/gad.17554711 (2011).
- 47 Shenoy, T. R. *et al.* CHD1 loss sensitizes prostate cancer to DNA damaging therapy by promoting error-prone double-strand break repair. *Ann Oncol* **28**, 1495-1507, doi:10.1093/annonc/mdx165 (2017).
- 48 Kari, V. *et al.* Loss of CHD1 causes DNA repair defects and enhances prostate cancer therapeutic responsiveness. *EMBO Rep* **17**, 1609-1623, doi:10.15252/embr.201642352 (2016).
- 49 Mehner, C. *et al.* Serine protease inhibitor Kazal type 1 (SPINK1) drives proliferation and anoikis resistance in a subset of ovarian cancers. *Oncotarget* **6**, 35737-35754, doi:10.18632/oncotarget.5927 (2015).
- 50 Rasanen, K., Itkonen, O., Koistinen, H. & Stenman, U. H. Emerging Roles of SPINK1 in Cancer. *Clin Chem* **62**, 449-457, doi:10.1373/clinchem.2015.241513 (2016).
- 51 Wang, C. *et al.* Serine protease inhibitor Kazal type 1 promotes epithelial-mesenchymal transition through EGFR signaling pathway in prostate cancer. *Prostate* **74**, 689-701, doi:10.1002/pros.22787 (2014).
- 52 Johnson, T. E. *et al.* Homeodomain Proteins Directly Regulate ATM Kinase Activity. *Cell Rep* **24**, 1471-1483, doi:10.1016/j.celrep.2018.06.089 (2018).
- 53 Mateo, J. *et al.* DNA-Repair Defects and Olaparib in Metastatic Prostate Cancer. *N Engl J Med* **373**, 1697-1708, doi:10.1056/NEJMoa1506859 (2015).
- 54 Weston, V. J. *et al.* The PARP inhibitor olaparib induces significant killing of ATM-deficient lymphoid tumor cells in vitro and in vivo. *Blood* **116**, 4578-4587, doi:10.1182/blood-2010-01-265769 (2010).
- 55 Robinson, D. *et al.* Integrative clinical genomics of advanced prostate cancer. *Cell* **161**, 1215-1228, doi:10.1016/j.cell.2015.05.001 (2015).
- 56 Grasso, C. S. *et al.* The mutational landscape of lethal castration-resistant prostate cancer. *Nature* **487**, 239-243, doi:10.1038/nature11125 (2012).
- 57 Duff, J. & McEwan, I. J. Mutation of histidine 874 in the androgen receptor ligand-binding domain leads to promiscuous ligand activation and altered p160 coactivator interactions. *Mol Endocrinol* **19**, 2943-2954, doi:10.1210/me.2005-0231 (2005).
- 58 Antonarakis, E. S. *et al.* AR-V7 and resistance to enzalutamide and abiraterone in prostate cancer. *N Engl J Med* **371**, 1028-1038, doi:10.1056/NEJMoa1315815 (2014).
- 59 Gorodetska, I., Lukiyanchuk, V., Peitzsch, C., Kozeretska, I. & Dubrovskaya, A. BRCA1 and EZH2 cooperate in regulation of prostate cancer stem cell phenotype. doi:10.1002/ijc.32323 (2019).
- 60 Miki, J. & Rhim, J. S. Prostate cell cultures as in vitro models for the study of normal stem cells and cancer stem cells. *Prostate Cancer Prostatic Dis* **11**, 32-39, doi:10.1038/sj.pcan.4501018 (2008).
- 61 Mei, W. *et al.* The Contributions of Prostate Cancer Stem Cells in Prostate Cancer Initiation and Metastasis. *Cancers (Basel)* **11**, doi:10.3390/cancers11040434 (2019).
- 62 Al-Hajj, M., Wicha, M. S., Benito-Hernandez, A., Morrison, S. J. & Clarke, M. F. Prospective identification of tumorigenic breast cancer cells. *Proc Natl Acad Sci U S A* **100**, 3983-3988, doi:10.1073/pnas.0530291100 (2003).
- 63 Singh, S. K. *et al.* Identification of human brain tumour initiating cells. *Nature* **432**, 396-401, doi:10.1038/nature03128 (2004).

- 64 Fang, D. *et al.* A tumorigenic subpopulation with stem cell properties in melanomas. *Cancer Res* **65**, 9328-9337, doi:10.1158/0008-5472.can-05-1343 (2005).
- 65 Ricci-Vitiani, L. *et al.* Identification and expansion of human colon-cancer-initiating cells. *Nature* **445**, 111-115, doi:10.1038/nature05384 (2007).
- 66 Prince, M. E. *et al.* Identification of a subpopulation of cells with cancer stem cell properties in head and neck squamous cell carcinoma. *Proc Natl Acad Sci U S A* **104**, 973-978, doi:10.1073/pnas.0610117104 (2007).
- 67 Li, C. *et al.* Identification of pancreatic cancer stem cells. *Cancer Res* **67**, 1030-1037, doi:10.1158/0008-5472.can-06-2030 (2007).
- 68 Eramo, A. *et al.* Identification and expansion of the tumorigenic lung cancer stem cell population. *Cell Death Differ* **15**, 504-514, doi:10.1038/sj.cdd.4402283 (2008).
- 69 She, J. J., Zhang, P. G., Wang, Z. M., Gan, W. M. & Che, X. M. Identification of side population cells from bladder cancer cells by DyeCycle Violet staining. *Cancer Biol Ther* **7**, 1663-1668 (2008).
- 70 Collins, A. T., Berry, P. A., Hyde, C., Stower, M. J. & Maitland, N. J. Prospective identification of tumorigenic prostate cancer stem cells. *Cancer Res* **65**, 10946-10951, doi:10.1158/0008-5472.can-05-2018 (2005).
- 71 Huss, W. J., Gray, D. R., Greenberg, N. M., Mohler, J. L. & Smith, G. J. Breast cancer resistance protein-mediated efflux of androgen in putative benign and malignant prostate stem cells. *Cancer Res* **65**, 6640-6650, doi:10.1158/0008-5472.can-04-2548 (2005).
- 72 Patrawala, L. *et al.* Side population is enriched in tumorigenic, stem-like cancer cells, whereas ABCG2+ and ABCG2- cancer cells are similarly tumorigenic. *Cancer Res* **65**, 6207-6219, doi:10.1158/0008-5472.can-05-0592 (2005).
- 73 Skvortsov, S., Skvortsova, I., Tang, D. G. & Dubrovskaya, A. Concise Review: Prostate Cancer Stem Cells: Current Understanding. **36**, 1457-1474, doi:10.1002/stem.2859 (2018).
- 74 Long, R. M., Morrissey, C., Fitzpatrick, J. M. & Watson, R. W. Prostate epithelial cell differentiation and its relevance to the understanding of prostate cancer therapies. *Clin Sci (Lond)* **108**, 1-11, doi:10.1042/cs20040241 (2005).
- 75 Planz, B., Wang, Q., Kirley, S. D., Lin, C. W. & McDougal, W. S. Androgen responsiveness of stromal cells of the human prostate: regulation of cell proliferation and keratinocyte growth factor by androgen. *J Urol* **160**, 1850-1855, doi:10.1016/s0022-5347(01)62431-5 (1998).
- 76 Sharifi, N., Kawasaki, B. T., Hurt, E. M. & Farrar, W. L. Stem cells in prostate cancer: resolving the castrate-resistant conundrum and implications for hormonal therapy. *Cancer Biol Ther* **5**, 901-906 (2006).
- 77 Schroeder, A. *et al.* Loss of androgen receptor expression promotes a stem-like cell phenotype in prostate cancer through STAT3 signaling. *Cancer Res* **74**, 1227-1237, doi:10.1158/0008-5472.can-13-0594 (2014).
- 78 Bechis, S. K., Carroll, P. R. & Cooperberg, M. R. Impact of age at diagnosis on prostate cancer treatment and survival. *J Clin Oncol* **29**, 235-241, doi:10.1200/jco.2010.30.2075 (2011).
- 79 Perdana, N. R., Mochtar, C. A., Umbas, R. & Hamid, A. R. The Risk Factors of Prostate Cancer and Its Prevention: A Literature Review. *Acta Med Indones* **48**, 228-238 (2016).
- 80 Barber, L. *et al.* Family History of Breast or Prostate Cancer and Prostate Cancer Risk. *Clin Cancer Res* **24**, 5910-5917, doi:10.1158/1078-0432.ccr-18-0370 (2018).
- 81 Board, P. D. Q. C. G. E. in *PDQ Cancer Information Summaries* (National Cancer Institute (US), 2002).
- 82 Islami, F., Moreira, D. M., Boffetta, P. & Freedland, S. J. A systematic review and meta-analysis of tobacco use and prostate cancer mortality and incidence in prospective cohort studies. *Eur Urol* **66**, 1054-1064, doi:10.1016/j.eururo.2014.08.059 (2014).

- 83 Venkateswaran, V. & Klotz, L. H. Diet and prostate cancer: mechanisms of action and implications for chemoprevention. *Nat Rev Urol* **7**, 442-453, doi:10.1038/nrur.2010.102 (2010).
- 84 Allott, E. H., Masko, E. M. & Freedland, S. J. Obesity and prostate cancer: weighing the evidence. *Eur Urol* **63**, 800-809, doi:10.1016/j.eururo.2012.11.013 (2013).
- 85 Zhao, J., Stockwell, T., Roemer, A. & Chikritzhs, T. Is alcohol consumption a risk factor for prostate cancer? A systematic review and meta-analysis. *BMC Cancer* **16**, 845, doi:10.1186/s12885-016-2891-z (2016).
- 86 Gaudreau, P. O., Stagg, J., Soulieres, D. & Saad, F. The Present and Future of Biomarkers in Prostate Cancer: Proteomics, Genomics, and Immunology Advancements. *Biomark Cancer* **8**, 15-33, doi:10.4137/bic.s31802 (2016).
- 87 Peehl, D. M. Prostate specific antigen role and function. *Cancer* **75**, 2021-2026, doi:10.1002/1097-0142(19950401)75:7+<2021::aid-cncr2820751644>3.0.co;2-r (1995).
- 88 Malm, J. & Lilja, H. Biochemistry of prostate specific antigen, PSA. *Scand J Clin Lab Invest Suppl* **221**, 15-22 (1995).
- 89 Mottet, N. *et al.* EAU-ESTRO-SIOG Guidelines on Prostate Cancer. Part 1: Screening, Diagnosis, and Local Treatment with Curative Intent. *Eur Urol* **71**, 618-629, doi:10.1016/j.eururo.2016.08.003 (2017).
- 90 Thompson, I. M. *et al.* First International Conference on Chemoprevention of Prostate Cancer. Overview consensus statement. *J Urol* **171**, S3-4, doi:10.1097/01.ju.0000107100.06725.51 (2004).
- 91 Heidegger, I. *et al.* [-2]proPSA is an early marker for prostate cancer aggressiveness. *Prostate Cancer Prostatic Dis* **17**, 70-74, doi:10.1038/pcan.2013.50 (2014).
- 92 Sokoll, L. J. *et al.* A prospective, multicenter, National Cancer Institute Early Detection Research Network study of [-2]proPSA: improving prostate cancer detection and correlating with cancer aggressiveness. *Cancer Epidemiol Biomarkers Prev* **19**, 1193-1200, doi:10.1158/1055-9965.Epi-10-0007 (2010).
- 93 Press, B., Schulster, M. & Bjurlin, M. A. Differentiating Molecular Risk Assessments for Prostate Cancer. *Rev Urol* **20**, 12-18, doi:10.3909/riu0787 (2018).
- 94 Zappala, S. M., Scardino, P. T., Okrongly, D., Linder, V. & Dong, Y. Clinical performance of the 4Kscore Test to predict high-grade prostate cancer at biopsy: A meta-analysis of us and European clinical validation study results. *Rev Urol* **19**, 149-155, doi:10.3909/riu0776 (2017).
- 95 Vickers, A. J., Eastham, J. A., Scardino, P. T. & Lilja, H. The Memorial Sloan Kettering Cancer Center Recommendations for Prostate Cancer Screening. *Urology* **91**, 12-18, doi:10.1016/j.urology.2015.12.054 (2016).
- 96 Boegemann, M. *et al.* The percentage of prostate-specific antigen (PSA) isoform [-2]proPSA and the Prostate Health Index improve the diagnostic accuracy for clinically relevant prostate cancer at initial and repeat biopsy compared with total PSA and percentage free PSA in men aged <math>\leq 65</math> years. *BJU Int* **117**, 72-79, doi:10.1111/bju.13139 (2016).
- 97 Gomella, L. G. *et al.* Screening for prostate cancer: the current evidence and guidelines controversy. *Can J Urol* **18**, 5875-5883 (2011).
- 98 Scherr, D., Swindle, P. W. & Scardino, P. T. National Comprehensive Cancer Network guidelines for the management of prostate cancer. *Urology* **61**, 14-24 (2003).
- 99 Parker, C., Gillissen, S., Heidenreich, A. & Horwich, A. Cancer of the prostate: ESMO Clinical Practice Guidelines for diagnosis, treatment and follow-up. *Ann Oncol* **26** Suppl 5, v69-77, doi:10.1093/annonc/mdv222 (2015).
- 100 Gittes, R. F. Carcinoma of the prostate. *N Engl J Med* **324**, 236-245, doi:10.1056/nejm199101243240406 (1991).
- 101 Gleason, D. F. & Mellinger, G. T. Prediction of prognosis for prostatic adenocarcinoma by combined histological grading and clinical staging. *J Urol* **111**, 58-64 (1974).

- 102 Epstein, J. I. *et al.* The 2014 International Society of Urological Pathology (ISUP) Consensus Conference on Gleason Grading of Prostatic Carcinoma: Definition of Grading Patterns and Proposal for a New Grading System. *Am J Surg Pathol* **40**, 244-252, doi:10.1097/pas.0000000000000530 (2016).
- 103 Gordetsky, J. & Epstein, J. Grading of prostatic adenocarcinoma: current state and prognostic implications. *Diagn Pathol* **11**, 25, doi:10.1186/s13000-016-0478-2 (2016).
- 104 Wallace, T. J. *et al.* Current approaches, challenges and future directions for monitoring treatment response in prostate cancer. *J Cancer* **5**, 3-24, doi:10.7150/jca.7709 (2014).
- 105 Attard, G. *et al.* Prostate cancer. *Lancet* **387**, 70-82, doi:10.1016/s0140-6736(14)61947-4 (2016).
- 106 Perlmutter, M. A. & Lepor, H. Androgen deprivation therapy in the treatment of advanced prostate cancer. *Rev Urol* **9 Suppl 1**, S3-8 (2007).
- 107 Huggins, C. & Hodges, C. V. Studies on prostatic cancer: I. The effect of castration, of estrogen and of androgen injection on serum phosphatases in metastatic carcinoma of the prostate. 1941. *J Urol* **168**, 9-12 (2002).
- 108 DeVita, V. T., Lawrence, T. S. & Rosenberg, S. A. *DeVita, Hellman, and Rosenberg's Cancer: Principles & Practice of Oncology*. (Wolters Kluwer/Lippincott Williams & Wilkins, 2008).
- 109 Crawford, E. D., Higano, C. S., Shore, N. D., Hussain, M. & Petrylak, D. P. Treating Patients with Metastatic Castration Resistant Prostate Cancer: A Comprehensive Review of Available Therapies. *J Urol* **194**, 1537-1547, doi:10.1016/j.juro.2015.06.106 (2015).
- 110 Stephenson, A. J. *et al.* Defining biochemical recurrence of prostate cancer after radical prostatectomy: a proposal for a standardized definition. *J Clin Oncol* **24**, 3973-3978, doi:10.1200/jco.2005.04.0756 (2006).
- 111 Cooperberg, M. R. *et al.* The contemporary management of prostate cancer in the United States: lessons from the cancer of the prostate strategic urologic research endeavor (CapSURE), a national disease registry. *J Urol* **171**, 1393-1401, doi:10.1097/01.ju.0000107247.81471.06 (2004).
- 112 Shalli, K., Brown, I., Heys, S. D. & Schofield, A. C. Alterations of beta-tubulin isotypes in breast cancer cells resistant to docetaxel. *Faseb j* **19**, 1299-1301, doi:10.1096/fj.04-3178fje (2005).
- 113 Gravis, G. *et al.* Androgen-deprivation therapy alone or with docetaxel in non-castrate metastatic prostate cancer (GETUG-AFU 15): a randomised, open-label, phase 3 trial. *Lancet Oncol* **14**, 149-158, doi:10.1016/s1470-2045(12)70560-0 (2013).
- 114 Paller, C. J. & Antonarakis, E. S. Cabazitaxel: a novel second-line treatment for metastatic castration-resistant prostate cancer. *Drug Des Devel Ther* **5**, 117-124, doi:10.2147/dddtd.s13029 (2011).
- 115 Lombard, A. P. *et al.* ABCB1 Mediates Cabazitaxel-Docetaxel Cross-Resistance in Advanced Prostate Cancer. *Mol Cancer Ther* **16**, 2257-2266, doi:10.1158/1535-7163.Mct-17-0179 (2017).
- 116 Yan, Y. Y. *et al.* Degradation of P-glycoprotein by pristimerin contributes to overcoming ABCB1-mediated chemotherapeutic drug resistance in vitro. *Oncol Rep* **37**, 31-40, doi:10.3892/or.2016.5230 (2017).
- 117 Beltran, H. *et al.* New therapies for castration-resistant prostate cancer: efficacy and safety. *Eur Urol* **60**, 279-290, doi:10.1016/j.eururo.2011.04.038 (2011).
- 118 James, N. D., Spears, M. R. & Sydes, M. R. Abiraterone in Metastatic Prostate Cancer. *N Engl J Med* **377**, 1696-1697, doi:10.1056/NEJMc1711029 (2017).
- 119 Fizazi, K. *et al.* Abiraterone acetate plus prednisone in patients with newly diagnosed high-risk metastatic castration-sensitive prostate cancer (LATITUDE): final overall survival analysis of a randomised, double-blind, phase 3 trial. *Lancet Oncol* **20**, 686-700, doi:10.1016/s1470-2045(19)30082-8 (2019).

- 120 Tucci, M. *et al.* Enzalutamide-resistant castration-resistant prostate cancer: challenges and solutions. *Onco Targets Ther* 11, 7353-7368, doi:10.2147/ott.s153764 (2018).
- 121 Cunningham, D. & You, Z. In vitro and in vivo model systems used in prostate cancer research. *J Biol Methods* 2, doi:10.14440/jbm.2015.63 (2015).
- 122 Suwa, T., Nyska, A., Haseman, J. K., Mahler, J. F. & Maronpot, R. R. Spontaneous lesions in control B6C3F1 mice and recommended sectioning of male accessory sex organs. *Toxicol Pathol* 30, 228-234, doi:10.1080/019262302753559560 (2002).
- 123 Grabowska, M. M. *et al.* Mouse models of prostate cancer: picking the best model for the question. *Cancer Metastasis Rev* 33, 377-397, doi:10.1007/s10555-013-9487-8 (2014).
- 124 Oliveira, D. S. *et al.* The mouse prostate: a basic anatomical and histological guideline. *Bosn J Basic Med Sci* 16, 8-13, doi:10.17305/bjbms.2016.917 (2016).
- 125 Wu, X., Gong, S., Roy-Burman, P., Lee, P. & Culig, Z. Current mouse and cell models in prostate cancer research. *Endocr Relat Cancer* 20, R155-170, doi:10.1530/erc-12-0285 (2013).
- 126 Hensley, P. J. & Kyprianou, N. Modeling prostate cancer in mice: limitations and opportunities. *J Androl* 33, 133-144, doi:10.2164/jandrol.111.013987 (2012).
- 127 McLean, D. T., Strand, D. W. & Ricke, W. A. Prostate cancer xenografts and hormone induced prostate carcinogenesis. *Differentiation* 97, 23-32, doi:10.1016/j.diff.2017.08.005 (2017).
- 128 Park, S. I., Kim, S. J., McCauley, L. K. & Gallick, G. E. Pre-clinical mouse models of human prostate cancer and their utility in drug discovery. *Curr Protoc Pharmacol Chapter 14*, Unit 14.15, doi:10.1002/0471141755.ph1415s51 (2010).
- 129 Wang, Y. *et al.* Development and characterization of efficient xenograft models for benign and malignant human prostate tissue. *Prostate* 64, 149-159, doi:10.1002/pros.20225 (2005).
- 130 Collins, A. T. & Lang, S. H. A systematic review of the validity of patient derived xenograft (PDX) models: the implications for translational research and personalised medicine. *PeerJ* 6, e5981, doi:10.7717/peerj.5981 (2018).
- 131 Petrillo, L. A. *et al.* Xenografts faithfully recapitulate breast cancer-specific gene expression patterns of parent primary breast tumors. *Breast Cancer Res Treat* 135, 913-922, doi:10.1007/s10549-012-2226-y (2012).
- 132 Lee, W. S. *et al.* Genomic profiling of patient-derived colon cancer xenograft models. *Medicine (Baltimore)* 93, e298, doi:10.1097/md.000000000000298 (2014).
- 133 Dobrolecki, L. E. *et al.* Patient-derived xenograft (PDX) models in basic and translational breast cancer research. *Cancer Metastasis Rev* 35, 547-573, doi:10.1007/s10555-016-9653-x (2016).
- 134 Larmour, L. I. *et al.* A patient derived xenograft model of cervical cancer and cervical dysplasia. 13, e0206539, doi:10.1371/journal.pone.0206539 (2018).
- 135 Rea, D. *et al.* Mouse Models in Prostate Cancer Translational Research: From Xenograft to PDX. *Biomed Res Int* 2016, 9750795, doi:10.1155/2016/9750795 (2016).
- 136 Gao, J. *et al.* Integrative analysis of complex cancer genomics and clinical profiles using the cBioPortal. *Sci Signal* 6, pl1, doi:10.1126/scisignal.2004088 (2013).
- 137 Gao, D. *et al.* Organoid cultures derived from patients with advanced prostate cancer. *Cell* 159, 176-187, doi:10.1016/j.cell.2014.08.016 (2014).
- 138 Barretina, J. *et al.* The Cancer Cell Line Encyclopedia enables predictive modelling of anticancer drug sensitivity. *Nature* 483, 603-607, doi:10.1038/nature11003 (2012).
- 139 Horoszewicz, J. S. *et al.* LNCaP model of human prostatic carcinoma. *Cancer Res* 43, 1809-1818 (1983).
- 140 Stone, K. R., Mickey, D. D., Wunderli, H., Mickey, G. H. & Paulson, D. F. Isolation of a human prostate carcinoma cell line (DU 145). *Int J Cancer* 21, 274-281 (1978).



- 141 Kaighn, M. E., Lechner, J. F., Narayan, K. S. & Jones, L. W. Prostate carcinoma: tissue culture cell lines. *Natl Cancer Inst Monogr*, 17-21 (1978).
- 142 Loop, S. M., Rozanski, T. A. & Ostenson, R. C. Human primary prostate tumor cell line, ALVA-31: a new model for studying the hormonal regulation of prostate tumor cell growth. *Prostate* **22**, 93-108 (1993).
- 143 van Helden, P. D., Wiid, I. J., Hoal-van Helden, E. G., Bey, E. & Cohen, R. Detection by DNA fingerprinting of somatic changes during the establishment of a new prostate cell line. *Br J Cancer* **70**, 195-198 (1994).
- 144 MacLeod, R. A. *et al.* Widespread intraspecies cross-contamination of human tumor cell lines arising at source. *Int J Cancer* **83**, 555-563 (1999).
- 145 Narayan, P. & Dahiya, R. Establishment and characterization of a human primary prostatic adenocarcinoma cell line (ND-1). *J Urol* **148**, 1600-1604 (1992).
- 146 Brothman, A. R., Lesho, L. J., Somers, K. D., Wright, G. L., Jr. & Merchant, D. J. Phenotypic and cytogenetic characterization of a cell line derived from primary prostatic carcinoma. *Int J Cancer* **44**, 898-903 (1989).
- 147 Sobel, R. E. & Sadar, M. D. Cell lines used in prostate cancer research: a compendium of old and new lines--part 1. *J Urol* **173**, 342-359, doi:10.1097/01.ju.0000141580.30910.57 (2005).
- 148 Bajgelman, M. C. & Strauss, B. E. The DU145 human prostate carcinoma cell line harbors a temperature-sensitive allele of p53. *Prostate* **66**, 1455-1462, doi:10.1002/pros.20462 (2006).
- 149 Fraser, M. *et al.* PTEN deletion in prostate cancer cells does not associate with loss of RAD51 function: implications for radiotherapy and chemotherapy. *Clin Cancer Res* **18**, 1015-1027, doi:10.1158/1078-0432.Ccr-11-2189 (2012).
- 150 Ikediobi, O. N. *et al.* Mutation analysis of 24 known cancer genes in the NCI-60 cell line set. *Mol Cancer Ther* **5**, 2606-2612, doi:10.1158/1535-7163.Mct-06-0433 (2006).
- 151 Tai, S. *et al.* PC3 is a cell line characteristic of prostatic small cell carcinoma. *Prostate* **71**, 1668-1679, doi:10.1002/pros.21383 (2011).
- 152 Korenchuk, S. *et al.* VCaP, a cell-based model system of human prostate cancer. *In Vivo* **15**, 163-168 (2001).
- 153 Marin-Aguilera, M. *et al.* The influence of treatment sequence in the prognostic value of TMPRSS2-ERG as biomarker of taxane resistance in castration-resistant prostate cancer. *Int J Cancer* **145**, 1970-1981, doi:10.1002/ijc.32238 (2019).
- 154 Yu, J. *et al.* An integrated network of androgen receptor, polycomb, and TMPRSS2-ERG gene fusions in prostate cancer progression. *Cancer Cell* **17**, 443-454, doi:10.1016/j.ccr.2010.03.018 (2010).
- 155 Blee, A. M. *et al.* TMPRSS2-ERG Controls Luminal Epithelial Lineage and Antiandrogen Sensitivity in PTEN and TP53-Mutated Prostate Cancer. *Clin Cancer Res* **24**, 4551-4565, doi:10.1158/1078-0432.Ccr-18-0653 (2018).
- 156 Mertz, K. D. *et al.* Molecular characterization of TMPRSS2-ERG gene fusion in the NCI-H660 prostate cancer cell line: a new perspective for an old model. *Neoplasia* **9**, 200-206 (2007).
- 157 Navone, N. M. *et al.* Establishment of two human prostate cancer cell lines derived from a single bone metastasis. *Clin Cancer Res* **3**, 2493-2500 (1997).
- 158 Sramkoski, R. M. *et al.* A new human prostate carcinoma cell line, 22Rv1. *In Vitro Cell Dev Biol Anim* **35**, 403-409, doi:10.1007/s11626-999-0115-4 (1999).
- 159 Benedict, P. *et al.* PTOV1, a novel protein overexpressed in prostate cancer containing a new class of protein homology blocks. *Oncogene* **20**, 1455-1464, doi:10.1038/sj.onc.1204233 (2001).
- 160 Morote, J. *et al.* PTOV1 expression predicts prostate cancer in men with isolated high-grade prostatic intraepithelial neoplasia in needle biopsy. *Clin Cancer Res* **14**, 2617-2622, doi:10.1158/1078-0432.ccr-07-4987 (2008).

- 161 Fernandez, S. *et al.* PTOV1 is overexpressed in human high-grade malignant tumors. *Virchows Arch* **458**, 323-330, doi:10.1007/s00428-010-1018-1 (2011).
- 162 Lei, F. *et al.* Overexpression of prostate tumor overexpressed 1 correlates with tumor progression and predicts poor prognosis in breast cancer. *BMC Cancer* **14**, 457, doi:10.1186/1471-2407-14-457 (2014).
- 163 Chen, S. P. *et al.* Prostate tumor overexpressed 1 is a novel prognostic marker for hepatocellular carcinoma progression and overall patient survival. *Medicine (Baltimore)* **94**, e423, doi:10.1097/md.0000000000000423 (2015).
- 164 Yang, L. *et al.* Prostate tumor overexpressed-1, in conjunction with human papillomavirus status, predicts outcome in early-stage human laryngeal squamous cell carcinoma. *Oncotarget* **7**, 31878-31891, doi:10.18632/oncotarget.8103 (2016).
- 165 Rausch, S. *et al.* Prostate tumor overexpressed 1 expression in invasive urothelial carcinoma. *J Cancer Res Clin Oncol* **142**, 937-947, doi:10.1007/s00432-015-2107-y (2016).
- 166 Guo, F. *et al.* Increased PTOV1 expression is related to poor prognosis in epithelial ovarian cancer. *Tumour Biol* **36**, 453-458, doi:10.1007/s13277-014-2662-x (2015).
- 167 Maggio, V. *et al.* A novel DNA-binding motif in prostate tumor overexpressed-1 (PTOV1) required for the expression of ALDH1A1 and CCNG2 in cancer cells. *Cancer Lett* **452**, 158-167, doi:10.1016/j.canlet.2019.03.019 (2019).
- 168 Canovas, V., Lleonart, M., Morote, J. & Paciucci, R. The role of prostate tumor overexpressed 1 in cancer progression. *Oncotarget* **8**, 12451-12471, doi:10.18632/oncotarget.14104 (2017).
- 169 Marques, N. *et al.* Regulation of protein translation and c-Jun expression by prostate tumor overexpressed 1. *Oncogene* **33**, 1124-1134, doi:10.1038/onc.2013.51 (2014).
- 170 Cui, Y. *et al.* Prostate tumour overexpressed-1 promotes tumorigenicity in human breast cancer via activation of Wnt/beta-catenin signalling. *J Pathol* **239**, 297-308, doi:10.1002/path.4725 (2016).
- 171 Alana, L. *et al.* Prostate tumor Overexpressed-1 (PTOV1) down-regulates HES1 and HEY1 notch targets genes and promotes prostate cancer progression. *Mol Cancer* **13**, 74, doi:10.1186/1476-4598-13-74 (2014).
- 172 Santamaria, A. *et al.* PTOV-1, a novel protein overexpressed in prostate cancer, shuttles between the cytoplasm and the nucleus and promotes entry into the S phase of the cell division cycle. *Am J Pathol* **162**, 897-905, doi:10.1016/s0002-9440(10)63885-0 (2003).
- 173 Santamaria, A. *et al.* PTOV1 enables the nuclear translocation and mitogenic activity of flotillin-1, a major protein of lipid rafts. *Mol Cell Biol* **25**, 1900-1911, doi:10.1128/mcb.25.5.1900-1911.2005 (2005).
- 174 Canovas, V. *et al.* Prostate Tumor Overexpressed-1 (PTOV1) promotes docetaxel-resistance and survival of castration resistant prostate cancer cells. *Oncotarget* **8**, 59165-59180, doi:10.18632/oncotarget.19467 (2017).
- 175 Filarsky, M. *et al.* The extended AT-hook is a novel RNA binding motif. *RNA Biol* **12**, 864-876, doi:10.1080/15476286.2015.1060394 (2015).
- 176 Abidi, A. Cabazitaxel: A novel taxane for metastatic castration-resistant prostate cancer-current implications and future prospects. *Journal of pharmacology & pharmacotherapeutics* **4**, 230-237, doi:10.4103/0976-500x.119704 (2013).
- 177 Jones, J. C. Reduction of contamination of epithelial cultures by fibroblasts. *CSH Protoc* **2008**, pdb.prot4478, doi:10.1101/pdb.prot4478 (2008).
- 178 Sanger, F., Nicklen, S. & Coulson, A. R. DNA sequencing with chain-terminating inhibitors. *Proc Natl Acad Sci U S A* **74**, 5463-5467, doi:10.1073/pnas.74.12.5463 (1977).
- 179 Schmidt, E. K., Clavarino, G., Ceppi, M. & Pierre, P. SUNSET, a nonradioactive method to monitor protein synthesis. *Nat Methods* **6**, 275-277, doi:10.1038/nmeth.1314 (2009).

- 180 Cerami, E. *et al.* The cBio Cancer Genomics Portal: An Open Platform for Exploring Multidimensional Cancer Genomics Data. *Cancer Discovery* **2**, 401-404, doi:10.1158/2159-8290.cd-12-0095 (2012).
- 181 Sachs, N. & Clevers, H. Organoid cultures for the analysis of cancer phenotypes. *Current opinion in genetics & development* **24**, 68-73, doi:10.1016/j.gde.2013.11.012 (2014).
- 182 Gao, D. & Chen, Y. Organoid development in cancer genome discovery. *Current opinion in genetics & development* **30**, 42-48, doi:10.1016/j.gde.2015.02.007 (2015).
- 183 Shariat, S. F. & Roehrborn, C. G. Using biopsy to detect prostate cancer. *Rev Urol* **10**, 262-280 (2008).
- 184 McGraw, K. L. *et al.* The relationship of TP53 R72P polymorphism to disease outcome and TP53 mutation in myelodysplastic syndromes. *Blood Cancer J* **5**, e291, doi:10.1038/bcj.2015.11 (2015).
- 185 Fraser, M. *et al.* Genomic hallmarks of localized, non-indolent prostate cancer. *Nature* **541**, 359-364, doi:10.1038/nature20788 (2017).
- 186 Huggins, C. & Hodges, C. V. Studies on prostatic cancer. I. The effect of castration, of estrogen and androgen injection on serum phosphatases in metastatic carcinoma of the prostate. *CA Cancer J Clin* **22**, 232-240 (1972).
- 187 Guo, S. *et al.* A Single Glycan at the 99-Loop of Human Kallikrein-related Peptidase 2 Regulates Activation and Enzymatic Activity. *J Biol Chem* **291**, 593-604, doi:10.1074/jbc.M115.691097 (2016).
- 188 Scher, H. I., Buchanan, G., Gerald, W., Butler, L. M. & Tilley, W. D. Targeting the androgen receptor: improving outcomes for castration-resistant prostate cancer. *Endocr Relat Cancer* **11**, 459-476 (2004).
- 189 Zhang, R. *et al.* Volume doubling time of lung adenocarcinomas considering epidermal growth factor receptor mutation status of exon 19 and 21: three-dimensional volumetric evaluation. *J Thorac Dis* **9**, 4387-4397, doi:10.21037/jtd.2017.10.58 (2017).
- 190 Ku, S. Y. *et al.* Rb1 and Trp53 cooperate to suppress prostate cancer lineage plasticity, metastasis, and antiandrogen resistance. *Science* **355**, 78-83, doi:10.1126/science.aah4199 (2017).
- 191 Bhat, M. *et al.* Targeting the translation machinery in cancer. *Nature Reviews Drug Discovery* **14**, 261, doi:10.1038/nrd4505  
<https://www.nature.com/articles/nrd4505#supplementary-information> (2015).
- 192 Pierobon, M. *et al.* Enrichment of PI3K-AKT-mTOR Pathway Activation in Hepatic Metastases from Breast Cancer. *Clin Cancer Res* **23**, 4919-4928, doi:10.1158/1078-0432.Ccr-16-2656 (2017).
- 193 Blanco, S. *et al.* Stem cell function and stress response are controlled by protein synthesis. *Nature* **534**, 335-340, doi:10.1038/nature18282 (2016).
- 194 Luongo, F. *et al.* PTEN Tumor-Suppressor: The Dam of Stemness in Cancer. *Cancers (Basel)* **11**, doi:10.3390/cancers11081076 (2019).
- 195 Truitt, M. L. & Ruggero, D. New frontiers in translational control of the cancer genome. *Nat Rev Cancer* **16**, 288-304, doi:10.1038/nrc.2016.27 (2016).
- 196 De Angelis, M. L., Francescangeli, F., La Torre, F. & Zeuner, A. Stem Cell Plasticity and Dormancy in the Development of Cancer Therapy Resistance. *Front Oncol* **9**, 626, doi:10.3389/fonc.2019.00626 (2019).
- 197 Gupta, P. B. *et al.* Stochastic state transitions give rise to phenotypic equilibrium in populations of cancer cells. *Cell* **146**, 633-644, doi:10.1016/j.cell.2011.07.026 (2011).
- 198 Sharma, S. V. *et al.* A chromatin-mediated reversible drug-tolerant state in cancer cell subpopulations. *Cell* **141**, 69-80, doi:10.1016/j.cell.2010.02.027 (2010).
- 199 Peehl, D. M. Primary cell cultures as models of prostate cancer development. *Endocr Relat Cancer* **12**, 19-47, doi:10.1677/erc.1.00795 (2005).

- 200 van Bokhoven, A., Varella-Garcia, M., Korch, C., Hessels, D. & Miller, G. J. Widely used prostate carcinoma cell lines share common origins. *Prostate* **47**, 36-51, doi:10.1002/pros.1045 (2001).
- 201 Theodore, S. *et al.* Establishment and characterization of a pair of non-malignant and malignant tumor derived cell lines from an African American prostate cancer patient. *Int J Oncol* **37**, 1477-1482, doi:10.3892/ijo\_00000800 (2010).
- 202 Namekawa, T., Ikeda, K., Horie-Inoue, K. & Inoue, S. Application of Prostate Cancer Models for Preclinical Study: Advantages and Limitations of Cell Lines, Patient-Derived Xenografts, and Three-Dimensional Culture of Patient-Derived Cells. *Cells* **8**, doi:10.3390/cells8010074 (2019).
- 203 Koochekpour S, Maresh GA, Katner A, Parker-Johnson K, Lee TJ, Hebert FE, Kao YS, Skinner J, Rayford W. Establishment and characterization of a primary androgen-responsive African-American prostate cancer cell line, E006AA. *Prostate* 2004;60(2):141-152. *Prostate* **79**, 815, doi:10.1002/pros.23800 (2019).
- 204 Peehl, D. M. Are primary cultures realistic models of prostate cancer? *J Cell Biochem* **91**, 185-195, doi:10.1002/jcb.10691 (2004).
- 205 Pasquali, D. *et al.* Loss of estrogen receptor beta expression in malignant human prostate cells in primary cultures and in prostate cancer tissues. *J Clin Endocrinol Metab* **86**, 2051-2055, doi:10.1210/jcem.86.5.7441 (2001).
- 206 Chander, A. C. *et al.* Rapid and Short-term Extracellular Matrix-mediated In Vitro Culturing of Tumor and Nontumor Human Primary Prostate Cells From Fresh Radical Prostatectomy Tissue. *Urology* **105**, 91-100, doi:10.1016/j.urology.2017.03.029 (2017).
- 207 Prabhu, V., Lee, T., McClintock, T. R. & Lepor, H. Short-, Intermediate-, and Long-term Quality of Life Outcomes Following Radical Prostatectomy for Clinically Localized Prostate Cancer. *Rev Urol* **15**, 161-177 (2013).
- 208 Walton, T. J., McCulloch, T. A., Rees, R. C. & Bishop, M. C. Obtaining fresh prostate cancer tissue for research: a novel biopsy needle and sampling technique for radical prostatectomy specimens. *Prostate* **64**, 382-386, doi:10.1002/pros.20264 (2005).
- 209 Wang, S. *et al.* Enrichment of prostate cancer stem cells from primary prostate cancer cultures of biopsy samples. *Int J Clin Exp Pathol* **7**, 184-193 (2014).
- 210 Castillo, V., Valenzuela, R., Huidobro, C., Contreras, H. R. & Castellon, E. A. Functional characteristics of cancer stem cells and their role in drug resistance of prostate cancer. *Int J Oncol* **45**, 985-994, doi:10.3892/ijo.2014.2529 (2014).
- 211 Buhler, P. *et al.* Primary prostate cancer cultures are models for androgen-independent transit amplifying cells. *Oncol Rep* **23**, 465-470 (2010).
- 212 van Bokhoven, A. *et al.* Molecular characterization of human prostate carcinoma cell lines. *Prostate* **57**, 205-225, doi:10.1002/pros.10290 (2003).
- 213 Sowalsky, A. G. *et al.* Neoadjuvant-Intensive Androgen Deprivation Therapy Selects for Prostate Tumor Foci with Diverse Subclonal Oncogenic Alterations. *Cancer Res* **78**, 4716-4730, doi:10.1158/0008-5472.Can-18-0610 (2018).
- 214 Puca, L. *et al.* Patient derived organoids to model rare prostate cancer phenotypes. *Nat Commun* **9**, 2404, doi:10.1038/s41467-018-04495-z (2018).
- 215 Kamoun, A. *et al.* Comprehensive molecular classification of localized prostate adenocarcinoma reveals a tumour subtype predictive of non-aggressive disease. *Ann Oncol* **29**, 1814-1821, doi:10.1093/annonc/mdy224 (2018).
- 216 Demichelis, F. *et al.* TMPRSS2:ERG gene fusion associated with lethal prostate cancer in a watchful waiting cohort. *Oncogene* **26**, 4596-4599, doi:10.1038/sj.onc.1210237 (2007).
- 217 Tomlins, S. A. *et al.* Role of the TMPRSS2-ERG gene fusion in prostate cancer. *Neoplasia* **10**, 177-188, doi:10.1593/neo.07822 (2008).

- 218 Garraway, I. P. *et al.* Human prostate sphere-forming cells represent a subset of basal epithelial cells capable of glandular regeneration in vivo. *Prostate* **70**, 491-501, doi:10.1002/pros.21083 (2010).
- 219 Litvinov, I. V. *et al.* Low-calcium serum-free defined medium selects for growth of normal prostatic epithelial stem cells. *Cancer Res* **66**, 8598-8607, doi:10.1158/0008-5472.Can-06-1228 (2006).
- 220 The Molecular Taxonomy of Primary Prostate Cancer. *Cell* **163**, 1011-1025, doi:10.1016/j.cell.2015.10.025 (2015).
- 221 Carracedo, A., Alimonti, A. & Pandolfi, P. P. PTEN level in tumor suppression: how much is too little? *Cancer Res* **71**, 629-633, doi:10.1158/0008-5472.Can-10-2488 (2011).
- 222 Correia, N. C., Girio, A., Antunes, I., Martins, L. R. & Barata, J. T. The multiple layers of non-genetic regulation of PTEN tumour suppressor activity. *Eur J Cancer* **50**, 216-225, doi:10.1016/j.ejca.2013.08.017 (2014).
- 223 Wang, X. *et al.* Clinical Significance of PTEN Deletion, Mutation, and Loss of PTEN Expression in De Novo Diffuse Large B-Cell Lymphoma. *Neoplasia* **20**, 574-593, doi:10.1016/j.neo.2018.03.002 (2018).
- 224 Dumont, P., Leu, J. I., Della Pietra, A. C., 3rd, George, D. L. & Murphy, M. The codon 72 polymorphic variants of p53 have markedly different apoptotic potential. *Nat Genet* **33**, 357-365, doi:10.1038/ng1093 (2003).
- 225 Xu, Y. *et al.* p53 Codon 72 polymorphism predicts the pathologic response to neoadjuvant chemotherapy in patients with breast cancer. *Clin Cancer Res* **11**, 7328-7333, doi:10.1158/1078-0432.Ccr-05-0507 (2005).
- 226 Sullivan, A. *et al.* Polymorphism in wild-type p53 modulates response to chemotherapy in vitro and in vivo. *Oncogene* **23**, 3328-3337, doi:10.1038/sj.onc.1207428 (2004).
- 227 Vikhanskaya, F., Siddique, M. M., Kei Lee, M., Broggini, M. & Sabapathy, K. Evaluation of the combined effect of p53 codon 72 polymorphism and hotspot mutations in response to anticancer drugs. *Clin Cancer Res* **11**, 4348-4356, doi:10.1158/1078-0432.Ccr-04-1547 (2005).
- 228 Kung, C. P., Liu, Q. & Murphy, M. E. The codon 72 polymorphism of p53 influences cell fate following nutrient deprivation. *Cancer Biol Ther* **18**, 484-491, doi:10.1080/15384047.2017.1323595 (2017).
- 229 Burgdorf, K. S. *et al.* Studies of the association of Arg72Pro of tumor suppressor protein p53 with type 2 diabetes in a combined analysis of 55,521 Europeans. *PLoS One* **6**, e15813, doi:10.1371/journal.pone.0015813 (2011).
- 230 Marin, M. C. *et al.* A common polymorphism acts as an intragenic modifier of mutant p53 behaviour. *Nat Genet* **25**, 47-54, doi:10.1038/75586 (2000).
- 231 Papadakis, E. D., Soultzis, N. & Spandidos, D. A. Association of p53 codon 72 polymorphism with advanced lung cancer: the Arg allele is preferentially retained in tumours arising in Arg/Pro germline heterozygotes. *Br J Cancer* **87**, 1013-1018, doi:10.1038/sj.bjc.6600595 (2002).
- 232 Gravis, G. *et al.* Androgen Deprivation Therapy (ADT) Plus Docetaxel Versus ADT Alone in Metastatic Non castrate Prostate Cancer: Impact of Metastatic Burden and Long-term Survival Analysis of the Randomized Phase 3 GETUG-AFU15 Trial. *Eur Urol* **70**, 256-262, doi:10.1016/j.eururo.2015.11.005 (2016).
- 233 Perner, S. *et al.* Adaptive responses of androgen receptor signaling in castration-resistant prostate cancer. *Oncotarget* **6**, 35542-35555, doi:10.18632/oncotarget.4689 (2015).
- 234 Oskarsson, T., Batlle, E. & Massague, J. Metastatic stem cells: sources, niches, and vital pathways. *Cell Stem Cell* **14**, 306-321, doi:10.1016/j.stem.2014.02.002 (2014).
- 235 Wang, Z. A. & Shen, M. M. Revisiting the concept of cancer stem cells in prostate cancer. *Oncogene* **30**, 1261-1271, doi:10.1038/onc.2010.530 (2011).

- 236 Dean, M., Fojo, T. & Bates, S. Tumour stem cells and drug resistance. *Nat Rev Cancer* **5**, 275-284, doi:10.1038/nrc1590 (2005).
- 237 Sun, Y. *et al.* Androgen deprivation causes epithelial-mesenchymal transition in the prostate: implications for androgen-deprivation therapy. *Cancer Res* **72**, 527-536, doi:10.1158/0008-5472.Can-11-3004 (2012).
- 238 Kahn, B., Collazo, J. & Kyprianou, N. Androgen receptor as a driver of therapeutic resistance in advanced prostate cancer. *Int J Biol Sci* **10**, 588-595, doi:10.7150/ijbs.8671 (2014).
- 239 Shiota, M. *et al.* Interaction between docetaxel resistance and castration resistance in prostate cancer: implications of Twist1, YB-1, and androgen receptor. *Prostate* **73**, 1336-1344, doi:10.1002/pros.22681 (2013).
- 240 Millican-Slater, R. A., Sayers, C. D., Hanby, A. M. & Hughes, T. A. Expression of phosphorylated eIF4E-binding protein 1, but not of eIF4E itself, predicts survival in male breast cancer. *Br J Cancer* **115**, 339-345, doi:10.1038/bjc.2016.178 (2016).
- 241 Chen, L. C. & Casadevall, A. Labeling of proteins with [35S]methionine and/or [35S]cysteine in the absence of cells. *Anal Biochem* **269**, 179-188, doi:10.1006/abio.1999.4023 (1999).
- 242 Ingolia, N. T., Ghaemmaghami, S., Newman, J. R. & Weissman, J. S. Genome-wide analysis in vivo of translation with nucleotide resolution using ribosome profiling. *Science* **324**, 218-223, doi:10.1126/science.1168978 (2009).
- 243 Yu, P. *et al.* Androgen-independent LNCaP cells are a subline of LNCaP cells with a more aggressive phenotype and androgen suppresses their growth by inducing cell cycle arrest at the G1 phase. *Int J Mol Med* **40**, 1426-1434, doi:10.3892/ijmm.2017.3125 (2017).
- 244 Cheng, H., Snoek, R., Ghaidi, F., Cox, M. E. & Rennie, P. S. Short hairpin RNA knockdown of the androgen receptor attenuates ligand-independent activation and delays tumor progression. *Cancer Res* **66**, 10613-10620, doi:10.1158/0008-5472.Can-06-0028 (2006).
- 245 Butler, D. E. *et al.* Inhibition of the PI3K/AKT/mTOR pathway activates autophagy and compensatory Ras/Raf/MEK/ERK signalling in prostate cancer. *Oncotarget* **8**, 56698-56713, doi:10.18632/oncotarget.18082 (2017).
- 246 Ulukaya, E. *et al.* Differential cytotoxic activity of a novel palladium-based compound on prostate cell lines, primary prostate epithelial cells and prostate stem cells. *PLoS One* **8**, e64278, doi:10.1371/journal.pone.0064278 (2013).
- 247 Colak, S. & Medema, J. P. Cancer stem cells--important players in tumor therapy resistance. *Febs j* **281**, 4779-4791, doi:10.1111/febs.13023 (2014).
- 248 Harris, K. S. & Kerr, B. A. Prostate Cancer Stem Cell Markers Drive Progression, Therapeutic Resistance, and Bone Metastasis. *Stem Cells Int* **2017**, 8629234, doi:10.1155/2017/8629234 (2017).
- 249 Dawood, S., Austin, L. & Cristofanilli, M. Cancer stem cells: implications for cancer therapy. *Oncology (Williston Park)* **28**, 1101-1107, 1110 (2014).
- 250 Kroon, P. *et al.* JAK-STAT blockade inhibits tumor initiation and clonogenic recovery of prostate cancer stem-like cells. *Cancer research* **73**, 5288-5298, doi:10.1158/0008-5472.can-13-0874 (2013).
- 251 Don-Doncow, N. *et al.* Galiellalactone is a direct inhibitor of the transcription factor STAT3 in prostate cancer cells. *J Biol Chem* **289**, 15969-15978, doi:10.1074/jbc.M114.564252 (2014).
- 252 Hellsten, R., Johansson, M., Dahlman, A., Sterner, O. & Bjartell, A. Galiellalactone inhibits stem cell-like ALDH-positive prostate cancer cells. *PLoS One* **6**, e22118, doi:10.1371/journal.pone.0022118 (2011).
- 253 Canesin, G. *et al.* The STAT3 Inhibitor Galiellalactone Effectively Reduces Tumor Growth and Metastatic Spread in an Orthotopic Xenograft Mouse Model of Prostate Cancer. *Eur Urol* **69**, 400-404, doi:10.1016/j.eururo.2015.06.016 (2016).
- 254 Lopez-Cara, L. C. *et al.* New (RS)-benzoxazepin-purines with antitumour activity: The chiral switch from (RS)-2,6-dichloro-9-[1-(p-nitrobenzenesulfonyl)-1,2,3,5-tetrahydro-4,1-

- benzoxazep in-3-yl]-9H-purine. *Eur J Med Chem* **46**, 249-258, doi:10.1016/j.ejmech.2010.11.011 (2011).
- 255 Ramirez, A. *et al.* HER2-signaling pathway, JNK and ERKs kinases, and cancer stem-like cells are targets of Bozopinib small compound. *Oncotarget* **5**, 3590-3606, doi:10.18632/oncotarget.1962 (2014).
- 256 Derynck, R. & Weinberg, R. A. EMT and Cancer: More Than Meets the Eye. *Dev Cell* **49**, 313-316, doi:10.1016/j.devcel.2019.04.026 (2019).
- 257 Baulida, J. & Garcia de Herreros, A. Snail1-driven plasticity of epithelial and mesenchymal cells sustains cancer malignancy. *Biochim Biophys Acta* **1856**, 55-61, doi:10.1016/j.bbcan.2015.05.005 (2015).
- 258 Chen, X., Rycaj, K., Liu, X. & Tang, D. G. New insights into prostate cancer stem cells. *Cell Cycle* **12**, 579-586, doi:10.4161/cc.23721 (2013).
- 259 Skvortsov, S., Skvortsova, I., Tang, D. G. & Dubrovskaya, A. Concise Review: Prostate Cancer Stem Cells: Current Understanding. *Stem Cells* **36**, 1457-1474, doi:10.1002/stem.2859 (2018).
- 260 Pellacani, D., Oldridge, E. E., Collins, A. T. & Maitland, N. J. Prominin-1 (CD133) Expression in the Prostate and Prostate Cancer: A Marker for Quiescent Stem Cells. *Adv Exp Med Biol* **777**, 167-184, doi:10.1007/978-1-4614-5894-4\_11 (2013).
- 261 Wei, X., Orjalo, A. V. & Xin, L. CD133 does not enrich for the stem cell activity in vivo in adult mouse prostates. *Stem Cell Res* **16**, 597-606, doi:10.1016/j.scr.2016.03.003 (2016).
- 262 Duhagon, M. A., Hurt, E. M., Sotelo-Silveira, J. R., Zhang, X. & Farrar, W. L. Genomic profiling of tumor initiating prostatospheres. *BMC Genomics* **11**, 324, doi:10.1186/1471-2164-11-324 (2010).
- 263 Sato, T. *et al.* Long-term expansion of epithelial organoids from human colon, adenoma, adenocarcinoma, and Barrett's epithelium. *Gastroenterology* **141**, 1762-1772, doi:10.1053/j.gastro.2011.07.050 (2011).
- 264 Wang, L. *et al.* Enrichment of prostate cancer stem-like cells from human prostate cancer cell lines by culture in serum-free medium and chemoradiotherapy. *Int J Biol Sci* **9**, 472-479, doi:10.7150/ijbs.5855 (2013).
- 265 Collins, A. T., Habib, F. K., Maitland, N. J. & Neal, D. E. Identification and isolation of human prostate epithelial stem cells based on alpha(2)beta(1)-integrin expression. *J Cell Sci* **114**, 3865-3872 (2001).
- 266 Richichi, C. *et al.* Tumor-initiating cell frequency is relevant for glioblastoma aggressiveness. *Oncotarget* **7**, 71491-71503, doi:10.18632/oncotarget.11600 (2016).
- 267 Qureshi-Baig, K., Ullmann, P., Haan, S. & Letellier, E. Tumor-Initiating Cells: a criTICal review of isolation approaches and new challenges in targeting strategies. *Mol Cancer* **16**, 40, doi:10.1186/s12943-017-0602-2 (2017).
- 268 Shmelkov, S. V. *et al.* CD133 expression is not restricted to stem cells, and both CD133+ and CD133- metastatic colon cancer cells initiate tumors. *J Clin Invest* **118**, 2111-2120, doi:10.1172/jci34401 (2008).
- 269 Quintana, E. *et al.* Efficient tumour formation by single human melanoma cells. *Nature* **456**, 593-598, doi:10.1038/nature07567 (2008).
- 270 Qureshi-Baig, K. *et al.* What Do We Learn from Spheroid Culture Systems? Insights from Tumorspheres Derived from Primary Colon Cancer Tissue. *PLoS One* **11**, e0146052, doi:10.1371/journal.pone.0146052 (2016).
- 271 O'Brien, C. A. *et al.* ID1 and ID3 regulate the self-renewal capacity of human colon cancer-initiating cells through p21. *Cancer Cell* **21**, 777-792, doi:10.1016/j.ccr.2012.04.036 (2012).
- 272 Hou, G. X. *et al.* Elimination of stem-like cancer cell side-population by auranofin through modulation of ROS and glycolysis. *Cell Death Dis* **9**, 89, doi:10.1038/s41419-017-0159-4 (2018).

- 273 Kuhlmann, J. D., Hein, L., Kurth, I., Wimberger, P. & Dubrovskaya, A. Targeting Cancer Stem Cells: Promises and Challenges. *Anticancer Agents Med Chem* 16, 38-58 (2016).
- 274 Nwani, N. G. *et al.* A Novel ALDH1A1 Inhibitor Targets Cells with Stem Cell Characteristics in Ovarian Cancer. *Cancers (Basel)* 11, doi:10.3390/cancers11040502 (2019).
- 275 Kawai, N. *et al.* ABCG2 expression is related to low 5-ALA photodynamic diagnosis (PDD) efficacy and cancer stem cell phenotype, and suppression of ABCG2 improves the efficacy of PDD. *PLoS One* 14, e0216503, doi:10.1371/journal.pone.0216503 (2019).
- 276 Zinzi, L. *et al.* ABC transporters in CSCs membranes as a novel target for treating tumor relapse. *Front Pharmacol* 5, 163, doi:10.3389/fphar.2014.00163 (2014).
- 277 Thaper, D. *et al.* Galiellalactone inhibits the STAT3/AR signaling axis and suppresses Enzalutamide-resistant Prostate Cancer. *Sci Rep* 8, 17307, doi:10.1038/s41598-018-35612-z (2018).
- 278 Tomida, C. *et al.* VEGF pathway-targeting drugs induce evasive adaptation by activation of neuropilin-1/cMet in colon cancer cells. *Int J Oncol* 52, 1350-1362, doi:10.3892/ijo.2018.4291 (2018).
- 279 Roberts, E., Cossigny, D. A. & Quan, G. M. The role of vascular endothelial growth factor in metastatic prostate cancer to the skeleton. *Prostate Cancer* 2013, 418340, doi:10.1155/2013/418340 (2013).
- 280 Jeppesen, M. *et al.* Short-term spheroid culture of primary colorectal cancer cells as an in vitro model for personalizing cancer medicine. *PLoS One* 12, e0183074, doi:10.1371/journal.pone.0183074 (2017).
- 281 Bellot, G. L., Tan, W. H., Tay, L. L., Koh, D. & Wang, X. Reliability of tumor primary cultures as a model for drug response prediction: expression profiles comparison of tissues versus primary cultures from colorectal cancer patients. *J Cancer Res Clin Oncol* 138, 463-482, doi:10.1007/s00432-011-1115-9 (2012).
- 282 Li, T. *et al.* ALDH1A1 is a marker for malignant prostate stem cells and predictor of prostate cancer patients' outcome. *Laboratory investigation; a journal of technical methods and pathology* 90, 234-244, doi:10.1038/labinvest.2009.127 (2010).
- 283 Ma, I. & Allan, A. L. The role of human aldehyde dehydrogenase in normal and cancer stem cells. *Stem cell reviews* 7, 292-306, doi:10.1007/s12015-010-9208-4 (2011).
- 284 Chouchana, L. *et al.* Molecular insight into thiopurine resistance: transcriptomic signature in lymphoblastoid cell lines. *Genome medicine* 7, 37, doi:10.1186/s13073-015-0150-6 (2015).
- 285 Zimmermann, M. *et al.* Elevated cyclin G2 expression intersects with DNA damage checkpoint signaling and is required for a potent G2/M checkpoint arrest response to doxorubicin. *The Journal of biological chemistry* 287, 22838-22853, doi:10.1074/jbc.M112.376855 (2012).
- 286 Reeves, R. & Nissen, M. S. The A.T-DNA-binding domain of mammalian high mobility group I chromosomal proteins. A novel peptide motif for recognizing DNA structure. *The Journal of biological chemistry* 265, 8573-8582 (1990).
- 287 Tyekucheva, S. *et al.* Stromal and epithelial transcriptional map of initiation progression and metastatic potential of human prostate cancer. 8, 420, doi:10.1038/s41467-017-00460-4 (2017).
- 288 Beltran, H. *et al.* Divergent clonal evolution of castration-resistant neuroendocrine prostate cancer. 22, 298-305, doi:10.1038/nm.4045 (2016).
- 289 Baca, S. C. *et al.* Punctuated evolution of prostate cancer genomes. *Cell* 153, 666-677, doi:10.1016/j.cell.2013.03.021 (2013).
- 290 Kumar, A. *et al.* Substantial interindividual and limited intraindividual genomic diversity among tumors from men with metastatic prostate cancer. 22, 369-378, doi:10.1038/nm.4053 (2016).



- 291 Hieronymus, H. *et al.* Copy number alteration burden predicts prostate cancer relapse. *Proceedings of the National Academy of Sciences of the United States of America* **111**, 11139-11144, doi:10.1073/pnas.1411446111 (2014).
- 292 Cui, D. W., Sun, G. G. & Cheng, Y. J. Change in expression of cyclin G2 in kidney cancer cell and its significance. *Tumour biology : the journal of the International Society for Oncodevelopmental Biology and Medicine* **35**, 3177-3183, doi:10.1007/s13277-013-1415-6 (2014).
- 293 Sun, G. G., Hu, W. N., Cui, D. W. & Zhang, J. Decreased expression of CCNG2 is significantly linked to the malignant transformation of gastric carcinoma. *Tumour biology : the journal of the International Society for Oncodevelopmental Biology and Medicine* **35**, 2631-2639, doi:10.1007/s13277-013-1346-2 (2014).
- 294 Sun, G. G., Zhang, J. & Hu, W. N. CCNG2 expression is downregulated in colorectal carcinoma and its clinical significance. *Tumour biology : the journal of the International Society for Oncodevelopmental Biology and Medicine* **35**, 3339-3346, doi:10.1007/s13277-013-1440-5 (2014).
- 295 Fujimura, A. *et al.* Cyclin G2 promotes hypoxia-driven local invasion of glioblastoma by orchestrating cytoskeletal dynamics. *Neoplasia (New York, N.Y.)* **15**, 1272-1281 (2013).
- 296 van der Waals, L. M., Borel Rinkes, I. H. M. & Kranenburg, O. ALDH1A1 expression is associated with poor differentiation, 'right-sidedness' and poor survival in human colorectal cancer. *PloS one* **13**, e0205536, doi:10.1371/journal.pone.0205536 (2018).
- 297 Bertucci, F. *et al.* Gene expression profiling of solitary fibrous tumors. *PloS one* **8**, e64497, doi:10.1371/journal.pone.0064497 (2013).
- 298 Vojnic, E. *et al.* Structure and VP16 binding of the Mediator Med25 activator interaction domain. *Nature structural & molecular biology* **18**, 404-409, doi:10.1038/nsmb.1997 (2011).
- 299 Oswald, F. *et al.* RBP-Jkappa/SHARP recruits CtIP/CtBP corepressors to silence Notch target genes. *Molecular and cellular biology* **25**, 10379-10390, doi:10.1128/mcb.25.23.10379-10390.2005 (2005).
- 300 Fell, V. L. & Schild-Poulter, C. The Ku heterodimer: function in DNA repair and beyond. *Mutation research. Reviews in mutation research* **763**, 15-29, doi:10.1016/j.mrrev.2014.06.002 (2015).
- 301 McHugh, C. A. *et al.* The Xist lncRNA interacts directly with SHARP to silence transcription through HDAC3. *Nature* **521**, 232-236, doi:10.1038/nature14443 (2015).
- 302 Bontems, F. *et al.* NMR structure of the human Mediator MED25 ACID domain. *Journal of structural biology* **174**, 245-251, doi:10.1016/j.jsb.2010.10.011 (2011).
- 303 Benecke, A. G. & Eilebrecht, S. RNA-Mediated Regulation of HMGA1 Function. *Biomolecules* **5**, 943-957 (2015).
- 304 Shah, S. N. & Resar, L. M. High mobility group A1 and cancer: potential biomarker and therapeutic target. *Histology and histopathology* **27**, 567-579, doi:10.14670/hh-27.567 (2012).
- 305 Mendez, O. & Peg, V. Extracellular HMGA1 promotes tumor invasion and metastasis in Triple-Negative Breast Cancer. doi:10.1158/1078-0432.ccr-18-0517 (2018).
- 306 Liao, S. S., Rocha, F., Matros, E., Redston, M. & Whang, E. High mobility group AT-hook 1 (HMGA1) is an independent prognostic factor and novel therapeutic target in pancreatic adenocarcinoma. *Cancer* **113**, 302-314, doi:10.1002/cncr.23560 (2008).
- 307 Wood, L. J. *et al.* HMG-I/Y, a new c-Myc target gene and potential oncogene. *Molecular and cellular biology* **20**, 5490-5502 (2000).
- 308 Metcalf, C. E. & Wassarman, D. A. DNA binding properties of TAF1 isoforms with two AT-hooks. *The Journal of biological chemistry* **281**, 30015-30023, doi:10.1074/jbc.M606289200 (2006).

- 309 Blokken, J., De Rijck, J., Christ, F. & Debyser, Z. Protein-protein and protein-chromatin interactions of LEDGF/p75 as novel drug targets. *Drug discovery today. Technologies* **24**, 25-31, doi:10.1016/j.ddtec.2017.11.002 (2017).
- 310 Garabedian, A., Bolufer, A. & Leng, F. Peptide Sequence Influence on the Conformational Dynamics and DNA binding of the Intrinsically Disordered AT-Hook 3 Peptide. **8**, 10783, doi:10.1038/s41598-018-28956-z (2018).
- 311 Lyst, M. J., Connelly, J., Merusi, C. & Bird, A. Sequence-specific DNA binding by AT-hook motifs in MeCP2. *FEBS letters* **590**, 2927-2933, doi:10.1002/1873-3468.12328 (2016).
- 312 Zillner, K. *et al.* Large-scale organization of ribosomal DNA chromatin is regulated by Tip5. *Nucleic acids research* **41**, 5251-5262, doi:10.1093/nar/gkt218 (2013).
- 313 Zhou, Y. *et al.* Reversible acetylation of the chromatin remodelling complex NoRC is required for non-coding RNA-dependent silencing. *Nature cell biology* **11**, 1010-1016, doi:10.1038/ncb1914 (2009).
- 314 Gerstberger, S., Hafner, M. & Tuschl, T. A census of human RNA-binding proteins. *Nature reviews. Genetics* **15**, 829-845, doi:10.1038/nrg3813 (2014).
- 315 Bailey, M. H. *et al.* Comprehensive Characterization of Cancer Driver Genes and Mutations. *Cell* **174**, 1034-1035, doi:10.1016/j.cell.2018.07.034 (2018).
- 316 Cifola, I. *et al.* Renal cell carcinoma primary cultures maintain genomic and phenotypic profile of parental tumor tissues. *BMC Cancer* **11**, 244, doi:10.1186/1471-2407-11-244 (2011).
- 317 Jiguet Jiglaire, C. *et al.* Ex vivo cultures of glioblastoma in three-dimensional hydrogel maintain the original tumor growth behavior and are suitable for preclinical drug and radiation sensitivity screening. *Exp Cell Res* **321**, 99-108, doi:10.1016/j.yexcr.2013.12.010 (2014).
- 318 Masuch, A. *et al.* Microglia replenished OHSC: A culture system to study in vivo like adult microglia. *Glia* **64**, 1285-1297, doi:10.1002/glia.23002 (2016).
- 319 Reya, T., Morrison, S. J., Clarke, M. F. & Weissman, I. L. Stem cells, cancer, and cancer stem cells. *Nature* **414**, 105-111, doi:10.1038/35102167 (2001).
- 320 Di Nicolantonio, F. *et al.* Cancer cell adaptation to chemotherapy. *BMC Cancer* **5**, 78, doi:10.1186/1471-2407-5-78 (2005).



## ANNEX 1: PUBLICATIONS

- 1 **STAT3 inhibition with Galiellalactone effectively targets the prostate cancer stem-like cell population.**  
Canesin G., **Maggio V.**, Collins A. T., Contreras H.R., Castellón E.A., Morote J., Paciucci R., Maitland N. J., Bjartell A. and Hellsten R. Submitted June 2019.
- 2 **Autophagy inhibition as a promising therapeutic target for laryngeal cancer.**  
Garcia-Mayea Y., Mir C., Muñoz L., Benavente S., Castellvi J., Temprana J., **Maggio V.**, Lorente J., Paciucci R. and Leonart ME. Carcinogenesis, 2019 May 3.
- 3 **A novel DNA-binding motif in prostate tumor overexpressed-1 (PTOV1) required for the expression of ALDH1A1 and CCNG2 in cancer cells.**  
**Maggio V.\***, Cánovas V.\*, Félix AJ., Gómez V., de Torres I., Semidey ME., Morote J., Noé V., Ciudad CJ. and Paciucci R. Cancer Letters 2019 Jun 28; 452:158-167.
- 4 **Prostate Tumor Overexpressed-1 (PTOV1) promotes docetaxel-resistance and survival of castration resistant prostate cancer cells.**  
Cánovas V., Puñal Y., **Maggio V.**, Redondo E., Marín M., Mellado B., Olivan M., Leonart ME., Planas J., Morote J. and Paciucci R. Oncotarget. 2017 Jul 22;8(35):59165-59180.

\*(Equal contribution)

